New Materials from Renewable Sources in the Development of a Non-Stick Coating for Bakeware

By

Andrew Henry Ross

A Thesis Submitted for the Degree of

Doctor of Philosophy

Supervised by **Dr Andrew Clark** and **Professor Stefan Bon**

Department of Chemistry

University of Warwick

September 2015

Contents

List of Figures

List of Tables

Acknowledgements

Firstly I would like to thank my academic supervisors Dr Andrew Clark and Professor Stefan Bon for their guidance and advice during my study at Warwick. And a thank you to Cooper Coated Coil for part funding of this research. I'd also like to extend my thanks to the technical staff at the NMR service, mass spectrometry suite and thermal analysis for any help during this project

On a personal note I'd like to thank members of the Clark group Collette, Lauren and Deborah for their advice on laboratory work and techniques and welcoming me into the group when I first started. And thanks to Andy Sellars (aka 2) who's been a good friend during my time at Warwick. In more recent times thanks goes to Paul, Jess, Nikki and Helen for creating a most banterous workplace

Finally I would like to thank my Mum, Dad and family for their encouragement and support throughout my life, and one last thanks to my best mates who are always up for a laugh and few beers to keep me sane.

Right, now time for a pint or two…

Andy '3' Ross

Declaration

The work presented in this thesis is the original work of the author. Reference to previous related results and ideas has been fully acknowledged. All work has been performed in the Department of Chemistry at the University of Warwick unless otherwise stated between October 2011 and September 2015 and has not been submitted for a degree at any other institution.

Andrew Henry Ross

Abstract

The work presented in this thesis reports the development of a non-stick coating for bakeware from renewable materials. Also investigated is the use of epoxidised vegetable oils for renewable polyesters and nanocomposites. Chapter 1 provides a brief introduction to materials from renewable sources leading to a more detailed overview of triglyceride chemistry and finishes with a brief background of non-stick coatings.

Chapter 2 presents the development of the non-stick coating. Current commercial coatings were analysed identifying the key components that could be replaced with more environmentally friendly alternatives. Thermal and photo-initiated curing regimes were studied on a range of epoxidised vegetable oil monomers for use as a polymer binder. Thermally cured epoxy soybean oil using a sulfonic acid catalyst was deemed superior. Additives to this resin such as silica, pigments and solvents were investigated to produce a coating formulation which was analysed by TGA and industry standard surface tests including pencil hardness, flexibility and cross-hatching.

Chapter 3 reports the hydrosilylation reaction on vegetable oils. A model system with fatty acids and triethylsilane was proposed which lead to the formation of crosslinked silicone rubbers using di- and polyfunctional silanes and vegetable triglycerides. Epoxy fatty acid – silicone hybrids were used as release agents in the non-stick coating formulation described above.

Chapter 4 focuses on the ring opening polymerisation of epoxidised vegetable oils with cyclic anhydrides forming crosslinked polyesters. Mechanical properties such as tensile strength, elasticity and Young's modulus were measured as well as thermal

analysis (TGA, DSC and DMTA). It was found that the physical properties were related to the crosslinking density with a higher density lead to strong but brittle polymers whereas lower crosslinking density samples were soft and elastic. The crosslinking density could be controlled by the choice of the vegetable oil type, anhydride type and the epoxide : anhydride ratio.

Chapter 5 uses these polyester resins in the formation of nanocomposites. Nanocomposites were created using hollow silica shells and polyaromatic hydrocarbons and the mechanical properties measured and compared to the vegetable oils resins alone and other work in this area. This was followed by the copolymerisation of epoxy vegetable oils and styrene oxide and blends of grapessed and euphorbia oils with different epoxide functionality. It was found that blends could achieve properties of both oils such as high strength and elasticity in the same polymer sample.

Chapter 6 describes the experimental procedures and chemical analysis of reactions performed in this thesis.

Abbreviations

BADGE	Bisphenol A diglycidyl ether
br	Broad
$CDCl_3$	Deuterated Chloroform
$CHCl_3$	Chloroform
CSA	Camphor sulfonic acid
d	Doublet
DBSA	Dodecylbenzene sulfonic acid
DCM	Dichloromethane
dd	Doublet of doublets
DMF	Dimethylformamide
DSC	Dynamic Scanning Calorimetry
EB	Elongation at break
ECB	Epoxidised cocoa butter
EEuO	Epoxidised euphorbia oil
EHOSO	Epoxidised high oleic sunflower oil
ELA	Epoxidised linoleic acid
EPO	Epoxidised palm oil
ER	Erichsen test
ERSO	Epoxidised rapeseed oil
ESBO	Epoxidised soybean oil
ESI	Electrospray Ionisation
Et_2O	Diethyl ether
Flex	Flexibility test
GPa	Giga Pascal
GPC	Gel Permeation Chromatography
h	Hours
H_2O_2	Hydrogen Peroxide
Hz	Hertz
IR	Infrara-Red
m	Multiplet
min	Minutes

Mn	Number average Molecular weight
MNA	Methyl Nadic Anhydride
MPa	Mega Pascal
Mw	Weight average Molecular weight
N_2	Nitrogen
NMR	Nuclear Magnetic Resonance
OH	Hydroxyl
OSA	Octadecenyl Succinic Acid
PAH	Polyaromatic Hydrocarbon
PDi	Polydispersity Index
PET	Polyethylene Terephthalate
PH	Pencil Hardness test
ppm	Parts per million
q	Quartet
s	Singlet
s	Second
t	Triplet
TAS	Triarylsulfonium hexafluoroantimonate salts
T_g	Glass Transition Temperature
TGA	Thermo Gravimetric Analysis
THF	Tetrahydrofuran
UTS	Ultimate Tensile Stress
YM	Young's Modulus

1 Introduction

In the modern world demand for materials is ever increasing, however as supplies of crude oil are becoming limited[1] the use of renewable feed-stocks become ever more attractive. Typically renewable materials are sourced from living organisms, most commonly plant matter biomass not used as human or animal feed, which can include vegetable oils and fats,[2] carbohydrates,[3] wood and agricultural waste.[4] Biomass can be used for the production of a number of environmentally friendly products which typically occupy two areas, energy[5] and materials.[6] Biomass for energy can be solid biofuels for heating or electricity generation, liquid biodiesel used as transport fuel and natural gas from landfill sites for household heating and cooking. In the materials industry, biomass can be used for building materials[7] or bioplastics such as polymers and composites.[8]

In recent years polymers from renewable sources have generated much interest as alternatives to petrochemical products. A very brief review is given of recent advances in this area but will be mainly focused on the use of plant oils in polymer synthesis. Most renewable sources undergo chemical modification before they can be used effectively in materials applications, and we will mainly focus on the chemical modification of vegetable oils although one or two modern examples of applications of other plant materials will be illustrated.

1.1 Wood and Agricultural Waste

A wide range of materials can be obtained as by-products from agricultural or wood processing industries. The structural properties of plants are determined by the components of the cell wall such as cellulose and lignin, these materials can be isolated and used to produce polymers or materials from renewable sources.[9]

1.1.1 Materials from Cellulose

Cellulose, as the main structural component of cell walls in green plants is the most abundant organic polymer on earth. The polysaccharide cellulose is a semi-crystalline linear chain of D-glucose building blocks, it is hydrophilic, biodegradable and has broad potential for chemical modification through the 3 hydroxyl groups per repeat unit (Figure 1.1). Cellulose has a variety of uses in paper manufacture,[10] cotton clothing[11] and cellophane packaging.[12]

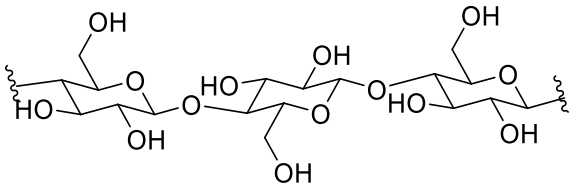

Figure 1.1. Chemical structure of cellulose.

Cellulose has been used in polymeric materials for many years, in 1995 Gatenholm *et al*[13] produced composites with cellulose fibres in a low density polyethylene (LDPE) and polystyrene (PS) matrix. It was found that a fibre content of 30 wt% increased the tensile strength from 9.8 MPa of the base polymer to 11.3 MPa of the composite. The tensile strength was further increased to 17.4 MPa by first functionalising cellulose with a maleic anhydride. The increased strength was thought to arise from greater bonding between the polymer and fibre chains. This highlights that it is often neccessary to chemically modify biomass to obtain the optimum properties for any application.

Cellulose has high strength due to the strong hydrogen bonds between hydroxyl groups on the 2-, 3- and 6- positions (Figure 1.1). These intermolecular bonds are not broken easily by heat, which means that cellulose degrades below its theoretical melting temperature. In 1998 Simon *et al* functionalised cellulose with ε-

caprolactone and cyclic anhydrides such as maleic and phthalic anhydride. The pendant ester groups reduced the level of hydrogen bonding allowing for a reduced melting point (Figure 1.2). This work shows the potential of a melt processable polymer from renewable sources.

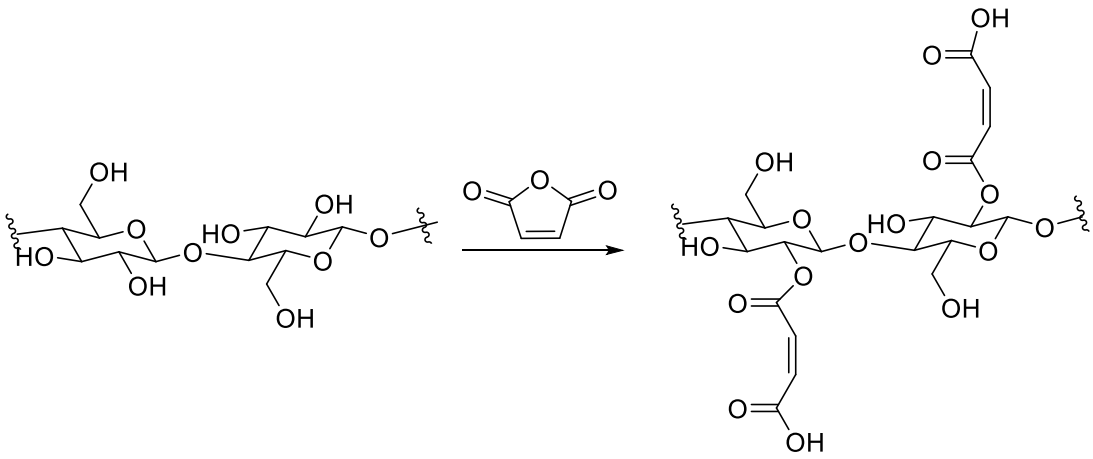

Figure 1.2. Functionalization of cellulose with maleic anhydride.

More recently in 2011 Oksman *et al*[14] used nano scale cellulose fibres to create composites with cellulose acetate butyrate (Figure 1.3). Nanofibres were mixed with the cellulose resin at 3, 6, 9 and 12 wt%. It was found that 9 wt% gave the greatest improvements in tensile strength and Young's modulus giving a 95% increase in tensile strength from 29.3 MPa to 57.1 MPa and a 73% increase in Young's modulus from 1260 MPa to 2180 MPa compared to the base resin. No significant change in elasticity was observed by increasing fibre content. This work shows an interesting concept for composite manufacture where both polymer resin and filler components are both derived from the same renewable source.

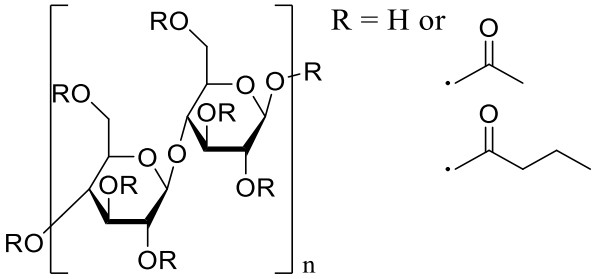

Figure 1.3. Cellulose acetate butyrate, can be strengthened significantly with the addition of cellulose nanofibres.

1.1.2 Materials from Hemicellulose

Cellulose is a linear crystalline polymer purely of glucose, whereas hemicellulose contains a mixture of sugars including xylose, mannose and galactose which varies by plant source. Hemicellulose has shorter chains than cellulose (500-3000 units) and has a branched structure making it an amorphous polymer (Figure 1.4). Hemicellulose can be obtained from a wide variety of plant material, such as straw from cereal crops in agriculture or sawdust from timber production, and is isolated by extraction with alkaline solutions[15] or pyrolysis.[16] In recent years hemicellulose has shown use as a cheap green component in food additives,[17] films[18] and wound dressings.[19]

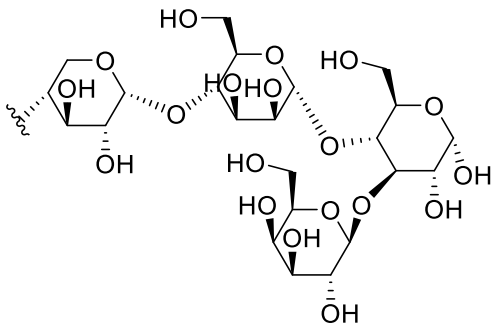

Figure 1.4. Basic structure of hemicellulose.

In 2010 Sun *et al*[20] functionalized hemicellulose with maleic anhydride (in1-butyl-3-methylimidazolium chloride) with LiOH as a catalyst. The degree of substitution

of hydroxyl groups could be controlled by varying the reaction conditions. Maleic anhydride (MA) in a 4:1 excess (relative to sugar content) was found to give highest functionalization of 0.26 (MA per sugar). This work produced a novel biopolymer with C=C double bonds and pendant carboxyl groups to increase the functionality of hemi-cellulose for a wider range of applications.

In 2015 Xiao *et all*[21] produced hydrogels that show high water absorption from hemicellulose. The hemicellulose polymers (HC) are functionalised with acrylic acid (AA) and acrylamide (AM) and crosslinked with *N*,*N*-methylenebisacrylamide (Figure 1.5). It was found that an increase of acrylic acid in the formulation (AA:AM:HC = 6:3.5:1 to 15:3.5:1) increased water absorption by 122% attributed to the increase of hydrophilic groups promoting water take up. Conversely increasing the hemicellulose content from AA:AM:HC = 15:3.5:1 to 15:3.5:2.5 per sample decreased water absorption by 60% thought to be due to formation of a tighter network.

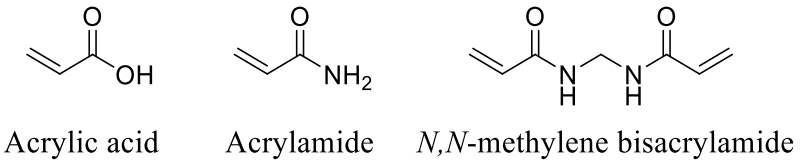

Acrylic acid Acrylamide *N,N*-methylene bisacrylamide

Figure 1.5. Functionalization of hemicellulose for hydrogels

1.1.3 Materials from Lignin

Lignin is a more complex polymer than cellulose or hemicellulose and is a crosslinked network of aromatic and oxygen containing groups.[22] Representing between 20 and 35% of wood based vegetation, lignin provides an increased strength to cell walls. The total lignin availability is around 300 billion tonnes which represents 30% of all non-fossil carbon in the biosphere.[23] Lignin can be isolated from wood waste in biorefineries and is considered waste from the paper industry.

The aromatic nature of lignin and the oxygen functional groups make this an attractive renewable raw material (Figure 1.6).

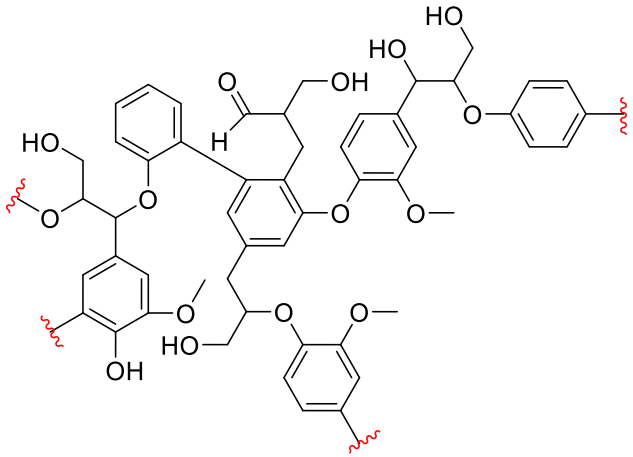

Figure 1.6. Basic structure of lignin.

In 2015 Sixta[24] investigated extraction of lignin from 'black liquor' a waste product from paper processing. It was found that extraction at different pH levels affected the size of the lignin isolated. Higher pH (10.5) extracted larger lignin samples (1508 – 1347 $gmol^{-1}$) than extraction at low pH (2.5, 798 – 787 $gmol^{-1}$) and had a higher purity (lower sulphur content). Polymeric blends of these lignin samples and high density polyethylene (HDPE) 50:50 by weight showed that materials from lower molecular weight lignin had a greater tensile strength and Young's modulus due to a better distribution of lignin in the HDPE matrix. There was insignificant difference in elongation between various sized lignin samples. This investigation shows that different extraction techniques of biomass (in this case lignin) can have an effect on physical properties of the composites produced.

1.2 Carbohydrates

Carbohydrates are a term for a group of materials consisting of sugars, starch or cellulose, they can be divided into four groups monosaccharides, disaccharides,

oligosaccharides and polysaccharides. Carbohydrates are important in all living organisms as an energy source (starch or glycogen) or structural (chitin in anthropoids or cellulose in plants) but are also useful in polymer/materials chemistry such as catalysts,[25] adhesives[26,27] and composites[28]

In 2014 Zhang[27] investigated the use of expanded corn starch in polyvinyl alcohol (PVOH) in the formation of hot melt adhesives. Expanded starch was esterified with propionate anhydride to increase thermal stability and hydrophobicity. Thermal degradation temperatures were increased with an increased degree of substitution (DS) from 0.38 to 2.54, however T_g and melting point were largely unaffected (0 °C and 160 °C respectively). Expanded starch with no pendant ester groups showed the greatest adhesive strength (2.0 MPa) which was stronger than unexpanded starch due to larger surface area (176 m^2g^{-1} compared with <5 m^2g^{-1}) leading to greater availability of hydroxyl groups promoting greater non-covalent interaction with PVOH. Adhesive strength decreased with increasing ester substitution and a degree of substitution of 1.46 -1.82 was similar to unexpanded corn starch. This work shows use of starch is effective in bio-based hot melt adhesives, which may be beneficial to our work on coatings where adhesion strength is an integral property of a formulation.

Recently there has been keen interest in polyalkanoates (PHA) as biodegradable polymers as a replacement for petrochemical based materials.[29,30,31] A common PHA is polyhydroxyl butyrate (PHB) it has similar mechanical properties to polypropylene (tensile strength = 19 – 40 MPa),[32] however PHB can be costly to produce. One route to PHB is to use modified *E. coli* bacteria with a PHB polymerase gene using glucose solution as a feedstock, the process itself is not expensive however the glucose feed stock can account for around 45% of total

production costs. Yang *et al*[33] investigated the further modification of *E. coli* with plasmids containing genes for starch hydrolysis and PHB polymerase so cheap starch can be used as feedstock. This shows how modifying the organisms that produce the biomass to be used can lead to cheaper feedstocks.

In 2015 Karak *et al*[34] described a 1-pot synthesis of hyperbranched starch based epoxy resins. The reaction mixture consisted of bisphenol-A, 5, 10 or 20% starch and epichlorohydrin (3 eq relative to amount of OH). At first epichlorohydrin reacts with bisphenol-A forming bisphenol-A digylcidylether (BADGE, a common epoxy resin) which is then grafted to the starch backbone. This order is due to the greater reactivity of primary hydroxyl groups compared to the secondary hydroxyls of starch any that didn't react with BADGE reacted with epichlorohydrin forming the hyperbranched epoxy resin (Figure 1.7). Polymerisation with poly(amido amine)(PAA) led to a highly crosslinked material with a tensile strength of 29 MPa (10% starch sample) which was lower than BADGE/PAA alone at 62 MPa. However the starch based polymer had greater impact resistance (>1 m compared to 0.65 m) and adhesive strength (2906 MPa vs 598 MPa) than purely BADGE. There was no significant change in thermal properties with any amount of starch (0 – 20%) with onset degradation at 262 – 287 °C.

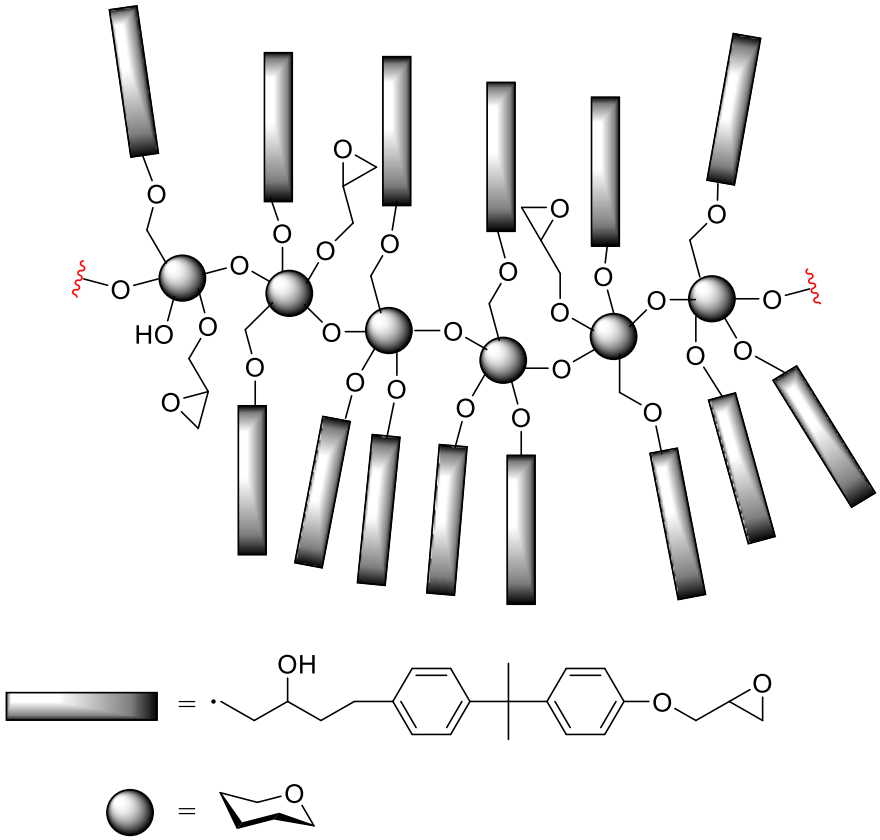

Figure 1.7. Hyperbrached epoxy resin formed in 1-pot reaction of bisphenol-A, starch and epichlorohydrin.

In 2014 Thakore[35] investigated polyurethanes crosslinked with carbohydrates for drug delivery. Using lamotrigine as a model it was found that release properties could be tailored by changing the crosslinker type or the polyol/crosslinker ratio. The polyurethanes were synthesised from polypropylene glycol, diethylene glycol and 2,4-toluene diisocyanate (2,4-TDI, Figure 1.8) and crosslinked with either glucose, cellulose or starch.

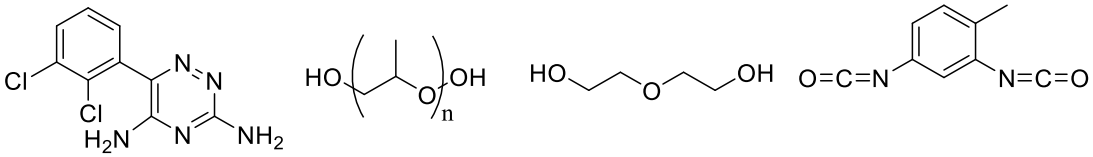

Lamotrigine | polypropylene glycol | diethylene glycol | 2,4-toluene diisocyanate

Figure 1.8. Reagents use in carbohydrate crosslinked polyurethanes.

The results show that release rates increased with an increase in 'soft segment' which was achieved with a lower isocyanate/OH ratio or higher polyol/crosslinker ratio. It was also found the type of crosslink affected release rates cellulose>glucose>starch. This work outlines bio-based polymers as a useful material for drug delivery and the release properties can be tailored increasing the range of applications.

1.3 Vegetable Oils

This thesis describes work undertaken with vegetable oil based polymers and consequently, we will focus on the chemistry and applications of these materials. Fats and oils (known as lipids) and are an integral part of cell membranes present in all living organisms. Vegetable oil is the common name given for triglycerides derived from plant sources which are often liquids at room temperature (solid triglycerides are known at fats). A triglyceride is an ester of glycerol and three fatty acid chains which can vary depending on the organism in which they are found (Figure 1.9).

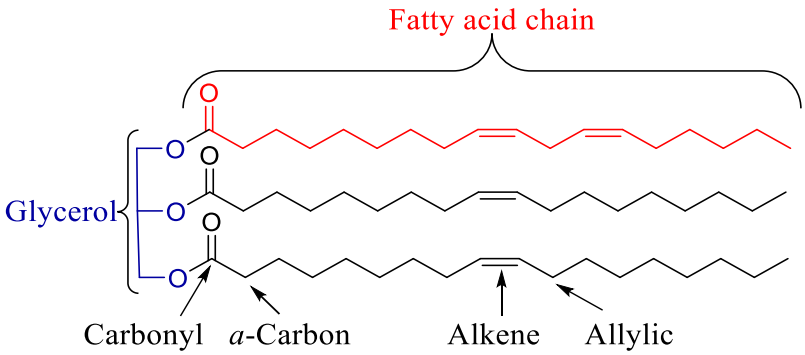

Figure 1.9. Triglyceride showing constituent parts and areas for chemical modification.

The variation in fatty acids is typically in chain length or level of unsaturation often denoted with a number (18:1 for oleic acid) (Figure 1.10). Warm blooded organisms generally have lipids that contain shorter saturated chains (14:0 myristic acid), while marine organisms (which exist at lower temperatures) have longer polyunsaturated chains (22:4 adrenic acid). Plant lipds are moderately unsaturated (18:2 linoleic acid). The composition of a variety of common vegetable oils, determined by fatty acid methyl ester (FAME) analysis are shown in Table 1.1.

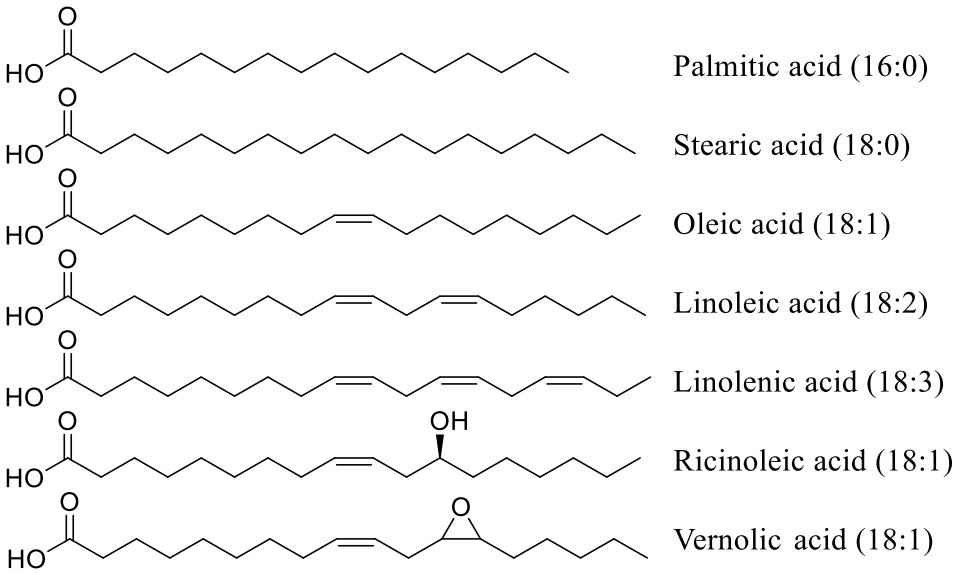

Figure 1.10. Common fatty acids present in vegetable oils.

Plant Oil	Fatty acid composition /%				
	C16:0	**C18:0**	**C18:1**	**C18:2**	**C18:3**
Cocoa Butter	26	34	35	-	-
Corn	13	3	31	52	1
Cottonseed	23	2	17	56	-
Linseed	6	3	17	14	60
Olive	10	2	78	7	2
Palm	44	4	39	11	-
Rapeseed	4	2	62	22	10
Safflower	7	3	14	75	-
Soybean	11	4	23	53	-
Sunflower	6	5	65	26	-

Table 1.1. Typical fatty acid composition of some common plant oils.[36]

Vegetable oils offer various reactive sites for chemical modification, such as alkenes and their allylic positions, the carbonyl groups or in some cases hydroxyls and epoxide functionality (Figure 1.10). Consequently, plant oils are widely used in industry, for example as biofuels (carbonyl modification),[37,38] hydrogenation for margarine (alkene modification),[39,40] and polyurethanes (reaction at hydroxyl sites).[41,42] World production of plant oils in 2014 was 166 million metric tonnes[43] making triglycerides an attractive feedstock from which to synthesise renewable materials. A brief review of chemistry of triglycerides is presented to give the reader an overview of the subject.

1.3.1 Reactions at the allylic carbon

The allylic carbon in a fatty acid chain is susceptible to oxidation, even more reactive is the allylic carbon between two alkene groups such as in linoleic acid and it is oxidation at these positions which occurs in the autoxidation of fatty acids.[44] Hydroxyl groups are attractive functionality to incorporate into renewable feedstocks as they can be used to make polyurethane and polyesters. Znothe *et al*[45] investigated hydroxylation of some monounsaturated fatty acids at the allylic

positions using SeO_2 and *t*-BuOOH to give a mixture of mono and dihydroxy compounds.

The allylic bromination of methyloleate and methylerucate (C22:1) was investigated by Winker *et al* in 2014. The reaction of a fatty acid methyl ester with *N*-bromosuccinimide (NBS) and AIBN at 60 – 100 °C in solvent or bulk yielded monobrominated fatty esters (Figure 1.11). These brominated fatty esters could be used as initiators for the atom transfer radical polymerisation (ATRP) of methyl methacrylate (MMA). At 80 °C PMMA was produced in 15 min with Mn = 11500 – 34600 Da and a PDi of 1.05 – 1.35. using [M]:[I] of 50:1 – 300:1 This work shows the potential of plant oil based compounds as useful renewable initiators for radical polymerisation.

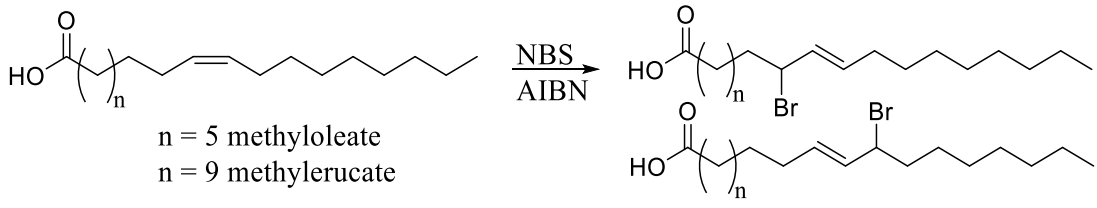

Figure 1.11. Bromination of the allylic carbon of fatty acid methyl esters.

1.3.2 Reactions at the Carbonyl

1.3.2.1 Aminolysis

Reactions at the carbonyl position are one of the most common procedures in triglyceride chemistry. Aminolysis is the splitting of an ester linkage with amines which produces amides, this reaction can be achieved by sodium methoxide,[46] microwave irradiation[47,48,49] or enzymes.[50,51]

In 2012 Lligdas[52] investigated the use of fatty acid based amides for tissue engineering scaffolds. A polyurethane derived from methyloleate and 10-

undecanoate diols were subjected to aminolysis by 1,6-hexamethylene diamine. The pendant amide groups increased the non-covalent interaction of chondroitin sulfate (CS) a major component of cartilage, CS immobilization is a promising way to enhance biological activity of fatty acid-derived PUs.

Hyaric *et al*[53] in 2013 investigated aminolysis of a triglyceride from *Passiflora edulis* which contains linoleic (69%), oleic (14%), palmitic (10%) and stearic (3%) fatty acids.[54] Aminolysis was performed with ethanolamine and a range of metal catalysts and the amide product was achieved in good yields, for $ZnO.La_2CO_5.LaOOH$ a yield of 100% was achieved after 8h at 100 °C. A year later More[55] also produced fatty amides from ethanolamine but with *Jatropha* oil (linoleic 80%, palmitic 15%, strearic 5%).[56] The fatty amides were mixed with bis(2-hydroxyethyl) terephthalate (PET monomer Figure 1.12) from recycled polyethylene terephthalate (PET) and cured with isocyanate to form renewable/recycled coatings. The coatings showed excellent balance of flexibility and hardness due to the structural differences between PET and the fatty amide, adhesion was also increased compared to PET alone due to non-covalent interactions from the amide linkage.

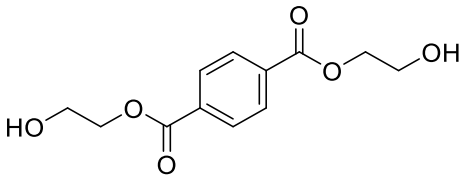

bis(2-hydroxy ethyl) terephthalate

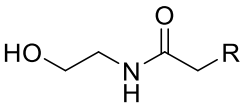

fatty amide from *Jatropha* oil

Figure 1.12. Hydroxyl terminated fatty amide and bis(2-hydroxyl ethyl)terephthalate for polyurethane coatings.

1.3.2.2 Transesterification

One of the most common reactions at the carbonyl site is transesterification. Glycerolysis involves the breaking of an ester link of triglycerides with glycerol forming a mixture of mono- and diglycerides.[57] The increased OH functionality can be used for further modification or the mono- and di-glycerides are often used as food additives.[58,59]

The most common application of transesterification is in the production of biofuels, which have received a lot of attention recently due to the depletion of fossil fuel reserves.[60] Biodiesel is typically manufactured from triglycerides from plant sources rather than animal fats. Standard diesel engines cannot run on standard plant oils as they are too viscous and have low volatility. Modification of triglycerides by transesterification by short chain alcohols produces methyl or ethyl esters of fatty acids which have properties closer to conventional diesel fuel (Figure 1.13). Branched alcohols such as isopropyl alcohol are also used in biodiesel to lower crystallisation temperature important for use in colder climates.[61] Alkali catalysts are most common for transesterification due to increased yields but other methods are used such as lipase enzymes[62,63] and microwave irradiation[64] if continuous processing is required.

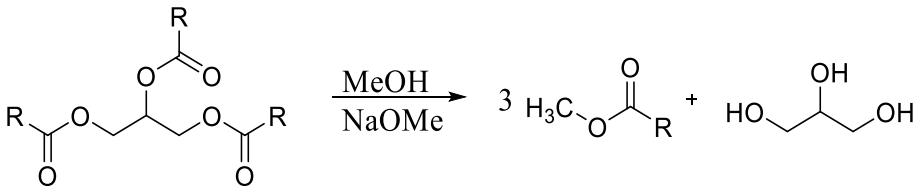

Figure 1.13.Synthesis of fatty acid methyl esters for biodiesel.

1.3.3 Reactions at the Alkene

1.3.3.1 Hydrogenation

Conversion of C=C double bonds of an unsaturated oil to fully saturated oils can be achieved by hydrogenation. A large scale application of this reaction is in the processing of polyunsaturated oils in the manufacture of margarine. Hydrogenation of most of the C=C bonds in an oil increases the melting range, converting a liquid oil to a semi-solid or solid fat or wax this process is also known as hardening. This process commonly used in the food industry was first proposed in 1902[65] and has been used widely ever since.[66,67] Other uses for hydrogenated oils are in cosmetics[68] and substitutes for paraffin wax in candles.[69]

Most common procedures use high pressure hydrogen gas and a metal catalyst such as platinum,[70,71] palladium[72,73] or nickel[74] a standard process would be heating the oil to 80 – 120 °C in the presence of a nickel catalyst under 200 – 300 bar of H_2 gas depending if full or partial hydrogenation is desired.[75]

One of the side effects of using partially hydrogenated vegetable oils in food use is the formation of *trans* fatty acids. Nearly all naturally occurring unsaturated oils have *cis* C=C bonds but during partial hydrogenation these can isomerise to the *trans* isomer which is favoured due to being a lower energy (thermodynamic product). *Trans* fatty acids are linked to circularity problems such as heart disease.[76,77] A method proposed by Singh in 2009[78] used mild conditions to partially hydrogenate soybean oil with minimal *trans* fat production. The reaction was performed at 70 °C under only 65 psi (4.5 bar) H_2 and catalysed by platinum immobilised by a porous polyetherimide membrane. The products contained 4% *trans* fatty acid compared to ~10% for conventional Pt based systems.

1.3.3.2 Crosslinking and Metathesis

Triglycerides with a high level of unsaturation are often called drying oils as they have the ability to polymerise *via* radical polymerisation with ambient oxygen.[79] The process is shown in Figure 1.14 and starts with the removal of a hydrogen atom from the allylic position most commonly the methylene carbon between a diene of a polyunsaturated fatty acid (C11). The energy to remove a hydrogen atom from C11 is 50 kcal/mol compared with 75 kcal/mol at C8 or C14. This accounts for the reactivity order of fatty acids of linolenic>linoleic>oleic.[80] The double bond adjacent to the carbon radical in linoleic/linolenic acids shifts to give the more stable isomer **1.3** and to conjugation of the double bonds. The fatty acid radical **1.3** then reacts with oxygen from the air to form a peroxy radical **1.4** which can abstract a hydrogen from another triglyceride forming a hydroperoxide **1.5** and propagating the chain reaction. Thermal degradation of the hydroperoxide leads to oligomerisation of fatty acid chains creating ether links **1.6**, if two alkyl radicals react in a termination step alkyl linkages can be produced. However the reaction of alkyl radicals with oxygen at ambient pressures occurs very quickly, consequently the concentration of alkyl radicals is much lower than peroxy radicals so alkyl oligomers are not often observed.[81]

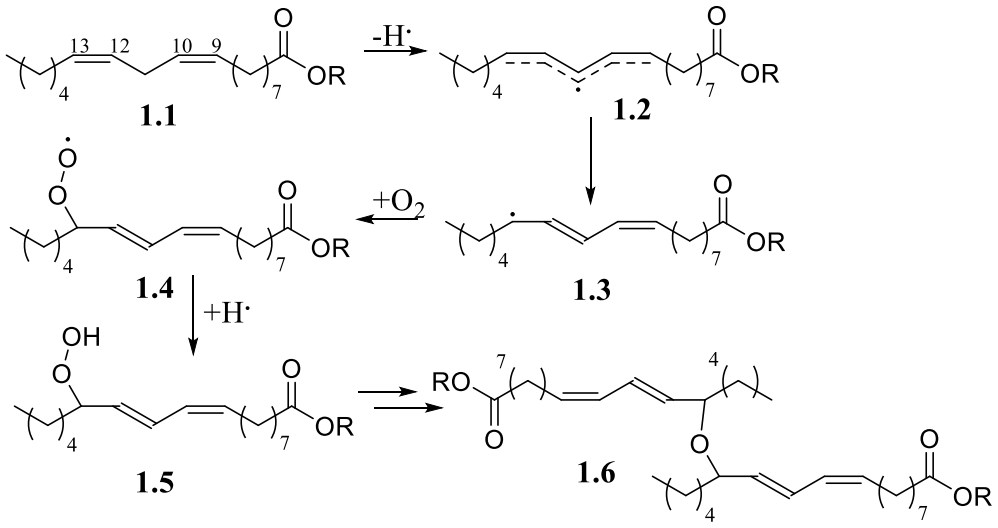

Figure 1.14. Autoxidation of polyunsaturated oils (drying oils).[80,82]

The ability to crosslink *via* autoxidation makes these oils useful as film formers in paints and coating formulations.[83,84] Typically in film formation, drying agents such as cobalt 2-ethylhexanoate or manganese catalysts, are added to enhance degradation of hydroperoxides hence increasing drying rate.[85] However, in thicker films rapid drying can form an oxygen impermeable barrier on top of the coating while the remaining compound is liquid underneath. Autoxidation rates can also be increased with gamma and infra-red irradiation inducing free radical formation.[86,87]

Olefin metathesis is a reaction involving redistribution of alkenes by the scission and regeneration of C=C bonds.[88] Olefin metathesis of vegetable oils is a useful technique for producing materials with improved drying properties. An inclusion of 5% self-metathesized soybean oil into unmodified soybean showed reduced drying times from 312 min to 182 min.[89] Standard metathesis conditions use a WCl_6 and Me_4Sn catalyst system, however this has some disadvantages such as the use of halogenated solvents, large catalyst loadings and sensitivity to oxygen and moisture.[90] The use of Grubbs second generation ruthenium carbene catalysts allow

the metathesis reaction to be tolerant of oxygen and even works in water (Figure 1.15).[91,92]

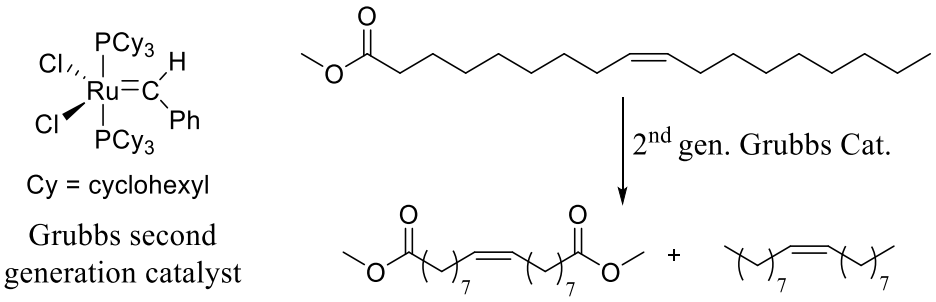

Figure 1.15 Self metathesis of methyl oleate using Grubbs second generation catalyst.[93]

Acyclic diene metathesis (ADMET) is a type of olefin metathesis to polymerise molecules with two alkene groups. ADMET is a step growth condensation polymerisation forming linear chains with an unsaturated backbone. Typically terminal alkenes are polymerised liberating ethylene gas as the driving force.[94]

In 2002 Larock *et al*[95] investigated ADMET polymerisation of soybean oil using Grubbs second generation catalyst. The reactions were performed between room temperature and 55 °C using 0.1 to 1.5 mol % catalyst loading and produced a range of polymers from sticky oils to soft rubbers. In 2010 Meier further investigated triene metathesis with high oleic sunflower oil and proposed ATMET[96] where hyperbranched/crosslinked polymers were formed. The molecular weight of these polymers could be controlled with the addition of methyl acrylate as a chain stopper, with greater acrylate concentrations producing smaller polymers. Using only sunflower oil the molecular weight was 4695 $gmol^{-1}$ compared to 1547 $gmol^{-1}$ using a 1:7 ratio of oil:acrylate.

1.3.4 Epoxidation of Vegetable Oils

One of the most important reactions in oleochemisty is the epoxidation of unsaturated fatty acids of a triglyceride.[97] These reactions add value to the oils as the epoxides allow a wide range of possibilities for further modification in many applications. There are many methods of epoxidation involving peroxides/peracids,[98] metal catalysts[99] or enzymes.[100] One of the most common procedures is the reaction of double bonds with peracids such as *meta*-chloro perbenzoic acid (mCPBA) known as the Prilezhaev reaction. This reaction follows a concerted step known as the 'butterfly mechanism' (Figure 1.16).[101]

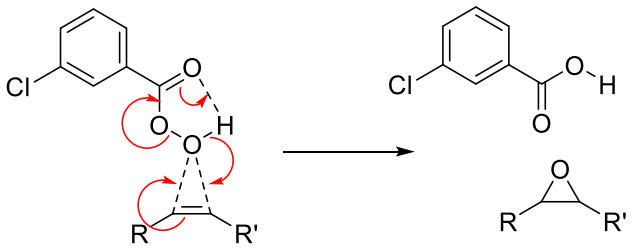

Figure 1.16. Epoxidation of an alkene by mCPBA showing the 'butterfly mechanism'.

However this process is not suitable for an industrial scale due to the production of benzoic acid which is costly to remove. For commercial applications more volatile peracids (such peracetic acid or performic acid) are used which can be generated *in situ*.

The most widely used process for epoxidation of vegetable oils used in industry utilises concentrated hydrogen peroxide (30 - 50%) and carboxylic acids with an acid catalyst (which generates peracid in *situ*).[102] In 2008 Dinda[103] investigated a range of inorganic acid catalysts along with acetic and formic acids in the epoxidation of cottonseed oil. The reactions were performed at 60 °C with 0.5 equivalents of carboxylic acid and 2 wt% acid catalyst, an increase of acid concentration lead to epoxide ring opening. It was found that acetic acid was superior to formic acid and

the reactivity of inorganic acids was H_2SO_4 > H_3PO_4 > HNO_3 > HCl. The same year Meyer[104] used formic acid and H_2O_2 to epoxidise soybean and jatropa oils and achieved a conversion of 83 and 87% respectively.

However the presence of inorganic acids leads to unwanted side reactions such as ring opening of epoxides, hydrolysis of the ester linkage and oligomerisation (Figure 1.17), which is not ideal industrially due to expensive purification required.[105]

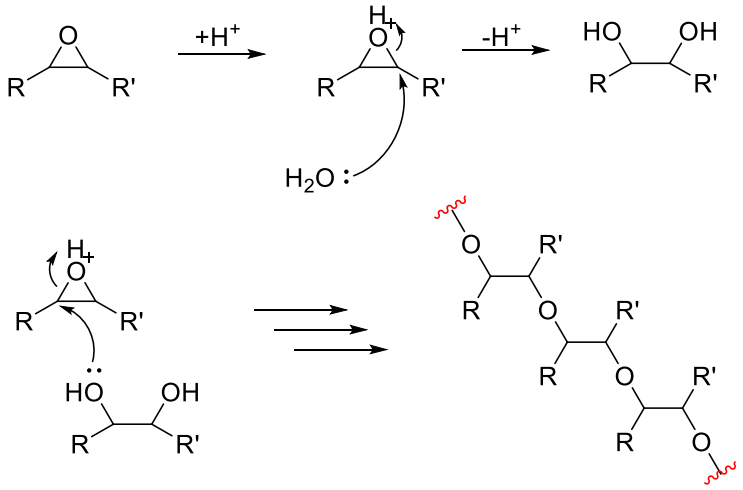

Figure 1.17. Ring opening of an epoxide forming a diol and leading to oligomerisation.

Acidic ion exchange resins (AIER) are insoluble gels or polymer beads impregnated with inorganic acids such as H_2SO_4 and are often used to minimise side reactions during epoxidation. Peracids are formed between H_2O_2 and carboxylic acids in the conventional way but inside the AIER, this minimises side reactions as triglycerides cannot enter the pores of the resin so are not exposed to strong acids.[106] Investigation into fatty acid epoxidation using formic and acetic acids with an AIER showed different conversion rates depending on the type of vegetable oil. With soybean oil Petrović[107] showed formic acid was more efficient than acetic acid possibly due to smaller molecule having easier access through pores in the resin. This approach also led supressed acid catalysed ring opening or ester hydrolysis and

<2% higher weight oligomers were obtained. In 2006 Goud[108] optimised this reaction and found a

That the temperature of 55 – 65 °C, with 0.5 equivalents of carboxylic acid and 1.5 equivalents of H_2O_2 (per C=C number) was optimal.

There are several drawbacks of the peracid method of epoxidation which could be improved;

i) Conversion is limited by competing acid catalysed oxirane ring opening.

ii) Removal of the acidic oxygen carrier whose presence may be detrimental to final application.

iii) Safe handling of concentrated hydrogen peroxide and strong acids.

To address these issues Campanella[109] investigated the epoxidation of soybean oil and soybean methyl esters using a titanium catalyst, dilute hydrogen peroxide (6% v/v) and *t*-BuOH. Only a small excess of peroxide was required (with anything over 1.1 mol equivalent compared to C=C bonds having no effect on conversion) and no epoxide ring opening was observed. This process negates the need for concentrated peroxide or strong acids. Other metal catalysts have been investigated and can be based on Mo, W, Re, Rh, Pt or Pd.[110,111]

A more environmentally friendly method of epoxidation is *via* an enzymatic route and is a good alternative to the peroxide/peracid method as the need for strong acids is reduced. Enzymes such as *Candida Antarctica* can be used to form the percarboxylic acid in place of inorganic acids. The peracids then donate oxygen to the C=C double bonds as mentioned above, however the peracid does not have to be

synthesised from acetic or formic acids as fatty acids themselves can be used or created *in situ* from ester cleavage of triglycerides (Figure 1.18).[112]

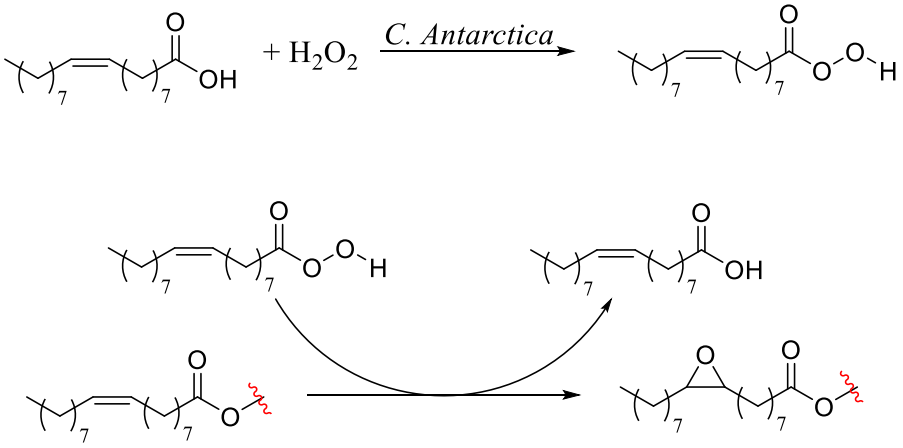

Figure 1.18. Enzymatic route to epoxidation of vegetable oils.

Enzyme catalysed epoxidation is a useful technique when the substrates are fatty acids, however with triglycerides some ester hydrolysis is required to form the peracid intermediate. Enzymes are also sensitive to reaction conditions such as temperature or H_2O_2 concentration which needs to be considered if used on industrial scales. Sun *et al* showed that the addition of 14 wt% stearic acid to the epoxidation of *Sapindus Mukorossi* oil as an efficient oxygen carrier suppressed ester hydrolysis.[113] It was also shown that using free fatty acids, from the same source as the triglyceride to be epoxidised, hydrolysis was suppressed at only 5 wt% of fatty acid.[114] The use of octanoic acid in the epoxidation of sunflower oil methyl esters increased conversion to 99% with *C. Antarctica*.[115]

1.3.5 Polymers from Epoxidised Oils

Vegetable oil epoxides are strained due to their small ring size and as a result are relatively reactive readily undergoing nucleophilic ring opening by a variety of nucleophiles including amines, alcohols or halogens (Figure 1.19).[116,117,118,119,120] Ring opening of vegetable oil epoxides can add functionalization such as hydroxyl

groups which can then be used for polyurethane synthesis.[121] Alternatively ring opening polymerisation of epoxides themselves can lead to polyethers,[123] or copolymerisation with diacids or anhydrides leads to polyesters.[122]

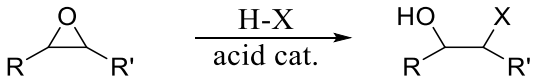

X = H, OH, OR, SR, NR_2, Cl or Br

Figure 1.19. Ring opening of epoxides with nucleophiles.

1.3.5.1 Polyethers

The reaction of epoxides with Lewis acids initiates cationic ring opening polymerisation leading to polyethers, this process has been known for a number of years. In 1992 Crivello *et al*[123] investigated cationic ring opening polymerisation of epoxidised plant oils for the formation of polyether films. The catalysts were diaryliodium and triarylsulfonium salts (3 wt%) and the polymerisations were initiated by UV light (300 W). It was found that coatings from oils with higher epoxide functionality had a harder surface but were less resistant to impact due to brittleness caused by greater crosslinking. The work suggests that due to the wide variety of oils with varied levels of unsaturation the final properties of the films could be tailored for any application. In 2004 Park *et al*[124] reported cationic ring opening polymerisation of epoxidised castor oil using *N*-benzylpyrazinium hexafluoroantimonate as a catalyst. The thermally latent catalyst showed no signs of polymerisation at temperatures below 60 °C. This system showed potential for pre-mixed polymer formulations with a stable pot life that could be activated when required. In 2006 Lligdas[125] investigated ring opening polymerisation of epoxidised methyl oleate using hexafluoroantimonic acid ($HSbF_6$) producing methyl oleate polyethers (961 - 1235 $gmol^{-1}$). Reduction of the esters with $LiAlH_4$ increased the

number of hydroxyl groups which were then crosslinked with MDI to form polyurethanes ranging from rubbery to hard plastics (Figure 1.20).

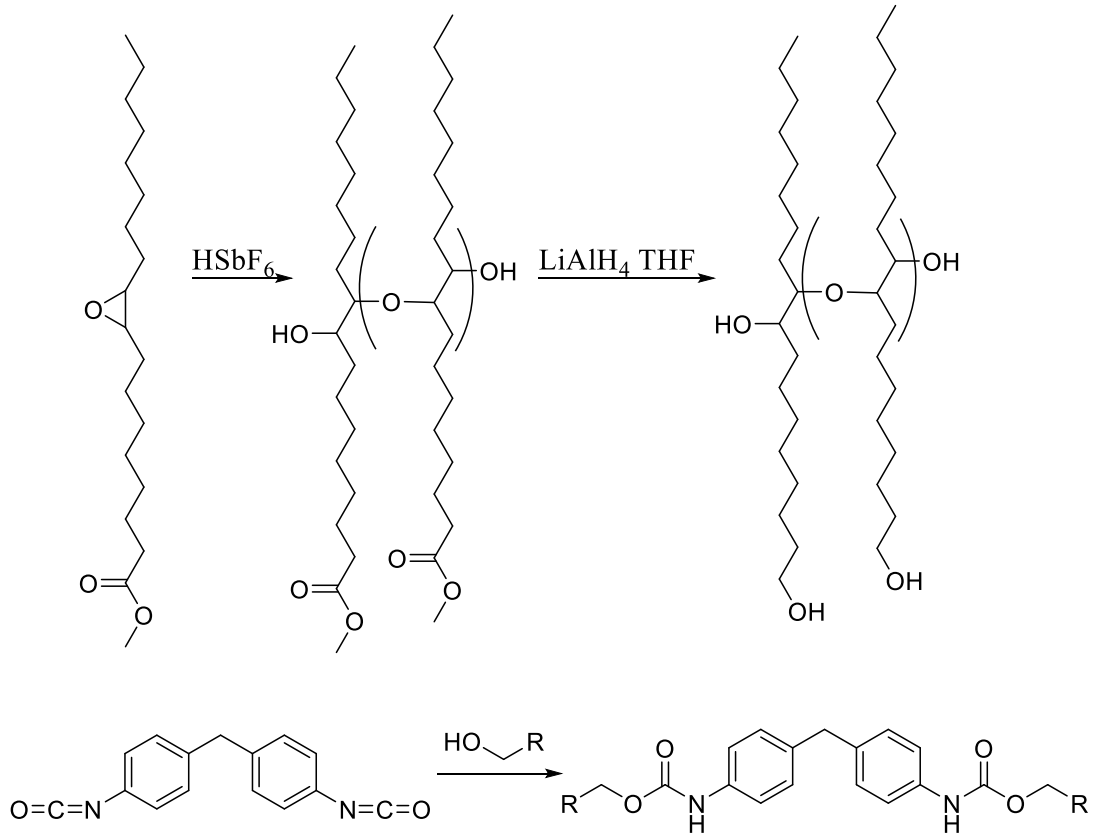

Figure 1.20. Synthesis of polyurethanes from epoxidised methyl oleate.

Ring opening can also be achieved with Lewis acids, such as $BF_3.OEt_2$ as shown by Liu *et al*[126] in 2010. The polymerisation of epoxy soybean oil with 1wt% $BF_3.OEt_2$ at 0 °C produced crosslinked polyethers insoluble in common solvents. These polymers could be converted to hydrogels by saponification of the ester linkage which could be used in the healthcare or cosmetic industries. Recently Clark[127] reported the ring opening polymerisation of plant oils in THF producing copolyethers. Polymers from epoxy methyl oleate, cocoa butter and palm oil showed molecular weights ranging from 8000-56000 with palm oil giving larger weights due to higher epoxide functionality (Figure 1.21). Polyurethanes produced from these

copolymers showed superior mechanical properties compared to polyurethanes from purely vegetable oils with little effect on thermal stability.

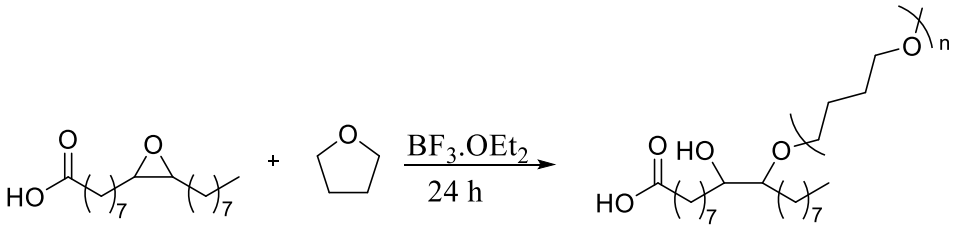

Figure 1.21. Copolymerisation of THF and epoxidised vegetable oil.[127]

1.3.5.2 Polyurethanes

Polyurethanes are most commonly synthesised from polyols and di- or polyisocyanates such as hexamethylene diisocyantate (HDI), 2,4-toluene diisocyanate (TDI), or methylene bis(phenylisocyanate) (MDI) (Figure 1.22). Polyurethanes (PU's) have excellent structural properties owing to a balance between a hard section (urethane link) providing high strength and a soft section from the polyol increasing flexibility and impact resistance. The physical properties of PU's can be tailored to meet the application demands, for flexibility, longer polyols (3000-6000 Da) with lower hydroxyl functionality (2 – 3) are used. Using shorter chain polyols or increasing hydroxyl functionality increases crosslinking density forming a more rigid material.

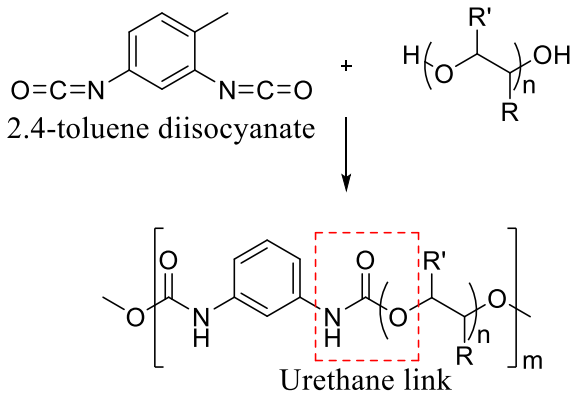

Figure 1.22. Polyurethane synthesis from TDI and a polyol showing the urethane linkage.

Petrović *et al*[128] investigated the preparation of polyurethane foams from polyols derived from epoxidised soybean oil. The foams were created by blowing agents hydrochlorofluorocarbon and pentane. The soybean oil based foams were found to have mechanical and insulating properties comparable with commercially available polypropylene oxide (PPO) foams. It was also reported the soybean oil polyurethanes had greater thermal degradation temperatures thought to be from a reduced number of ether links in soybean oil compared to PPO. The Petrović group[129] also studied polyurethanes from polyols formed by hydroformylation. Hydroformylation is an important industrial process which can be used to prepare aldehydes from alkenes. The reaction involves addition of a formyl group (CHO) and a hydrogen across a C=C double bond. The alkenes of soybean oil were converted to aldehydes using rhodium or cobalt catalysts, the aldehydes were then reduced to alcohols forming polyols. Polyols from the rhodium catalysed reaction (95% conversion) resulted in rigid PU's whereas the cobalt reaction (67%) produced rubbery materials with lower tensile strength. Polyurethanes were produced from a range of isocyanates 2,4-TDI, MDI and Desmodur N-3300 (a triisocyanate from 3 HDI molecules). It was reported that PU's from triisocyanates showed higher density, higher T_g and greater tensile strength than diisocyanate PU's.

Wang *et al*[130] synthesised polyurethanes using polyols from epoxidised soybean oil ring opened with methanol, ethylene glycol and 1,2-propanediol. Hydroxyl functionality ranged from 2.6 – 4.9 and PU's were synthesised using 2,4-TDI. Increased hydroxyl functionality produced PU's with increased crosslinking density which gave greater tensile strength, glass transition temperatures but lower thermal degradation temperatures.

1.3.5.3 Polyesters

Thermosetting plastics are a family of polymers formed from a starting liquid that irreversibly leads to a solid material upon curing. The most common thermosets are derived from epoxide monomers and cyclic anhydrides and copolymerise *via* ring opening, they are often called epoxy resins but are crosslinked polyesters. Epoxy monomers typically contain more than one epoxide group to allow crosslinking. Consequently, epoxidised triglycerides with high epoxy functionality should make ideal candidates for crosslinked polyesters. Ruseckaile *et al*[131] investigated epoxidised soybean oil (ESBO) and bisphenol-A based epoxy resin (BADGE) blends cured with methyl tetrahydrophthalic anhydride (MTHPA). Epoxy soybean oil was blended at 20, 40, 60, 80 and 100% of BADGE weight. It was found that with increased ESBO content glass transition temperature decreased (108 for 20% to 57 at 100%). Tensile strength decreased linearly from 110 MPa to 40 MPa with increasing ESBO content. The greatest impact strength was from a sample with 40% ESBO content at 0.4KJ/m^2 this was due to slight phase separation between the oil and BADGE which created hard and soft regions. The interface between the regions absorbs the impact energy and dissipates fractures. A high impact strength was also found for blends by Drzal[132] using a bisphenol-F epoxy and ESBO with 30% ESBO being the toughest sample, the phase separation regions were visible in SEM.

In 2006 White *et al*[133] synthesised a triglyceride with terminal alkenes which were epoxidised by peracetic acid and crosslinked with phthalic anhydride. The properties of this polymer were compared to BADGE and epoxidised linseed oil (ELO) samples. The terminal epoxides were more labile to nucleophilic attack than the more hindered ELO, DSC analysis showed a similar onset (100 °C) and peak (141 °C) curing profile to BADGE. Tensile strength was greater for BADGE (184 MPa)

and ELO (56 MPa) than the synthetic triglyceride (36 MPa), Young's modulus followed the same pattern (2.4, 1.5, 1.1 GPa). The terminal epoxide triglyceride offered no advantages in terms of mechanical properties over linseed oil, but being more reactive may be advantageous if a lower cure temperature is required. In 2007 Takahashi[134] synthesised a cyclic anhydride from α-pinene and maleic anhydride (Figure 1.23).

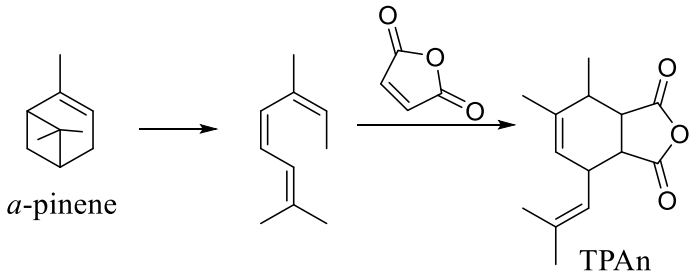

Figure 1.23. Synthesis of a cyclic anhydride from α-pinene.

The terpene based anhydride (TPAn) was used to crosslink ESBO and the properties compared with hexahydrophthalic anhydride (HPAn) and antimonite salts producing a polyether. The T_g was higher for TPAn (67.2 °C) than HPAn (59 °C) derivatives and much higher than the polyether compound (10 °C). The terpene based polymer also showed greater tensile strength 22 MPa than the other polymers (15 MPa and 2 MPa). All polymers showed similar levels of biodegradability losing about 10% mass after 45 days. Biocomposites were produced with the TPAn resin system and with cellulose fibres, tensile strength increased with fibre content up to 65 MPa at 75% loading. This work shows an attractive route to degradable biobased composite materials where all the components are from a renewable source.

1.3.6 Vegetable Oils in Coatings

In section 1.3.3.2 it was shown that polyunsaturated oils can undergo autooxidation and polymerise to form crosslinked polymer films, this reaction has been exploited

for 1000's of years without true understanding of the chemistry. Early oil based coatings were used as preservatives for wood, they were made from resins such as pine sap mixed with a drying oil like linseed or tung oil. Additon of pigments and turpentine as a solvent created what we know today as the early oil paints which have been used since the Middle Ages and were commonplace for artists during the renaissance era. The slow drying nature of these oil paints was well suited to artwork as they could be manipulated hours after first application. However the long drying times were not suited for commercial aspects such as in construction or protection of metals which became more widely used during the industrial revolution.

The need for a quicker drying paint led to the formation of alkyd resin based paints. The term alkyd was coined many years ago, the *AL* from the polyhydric *AL*cohols and the *KYD* (originally *CID*) from acid. Chemically the terms alkyd and polyester are synonymous.[135] Typical alkyd resins are formed by heating natural oils such as linseed with diacids like *ortho*-phthalic acid (often as an anhydride) and glycerol to from fatty acid containing polyesters (Figure 1.24).[136,137]

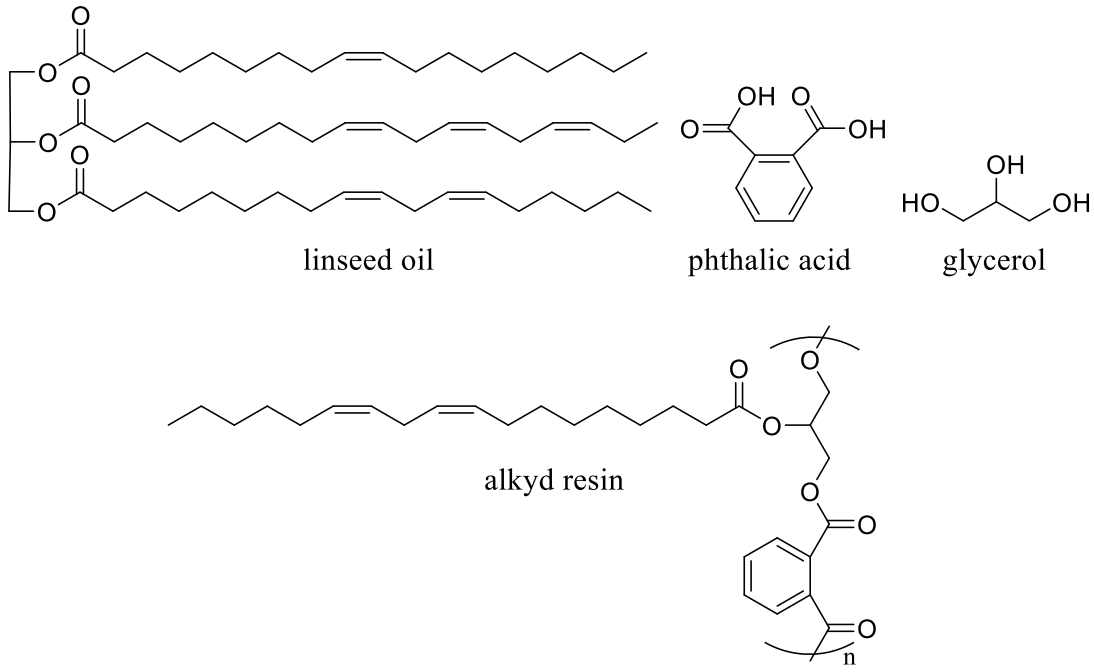

Figure 1.24. Schematic impression of an alkyd resin used as a binder compound in alkyd paint. The fatty acid chain shown is linoleic acid.

Alkyds fall into two cateories - drying (made from poly unsaturated oils) and non-drying (from saturated oils). Non-drying alkyds rely on solvent evapouration to form a film whereas drying alkyds ungergo autoxidation (section 1.3.3.2) and from a crosslinked film. To speed up drying times alkyd resins generally contain a drying agent that promotes the free radical autoxidation. Typical drying agents are derived from a metal centre usually cobalt, manganese or iron and formed into ‘salts’ with olephillic lignads such as octanoates and naphthalates to aid solubility in the oil.[138]

Alkyd resisn show excellent properties for use in coatings as the crosslinked nature provides good weatherability and chemical inertness, wheras the oil content allows for flexibitly preventing craking of the coating. However alkyds are not without drawbacks such as the need for metal catalysts and volatile organic compounds (VOC’s) as solvents.

Recently for environmental reasons there has been increased demand for waterborne coatings to decrease the use of VOC's and alkyd resins are no exeption. Ongoing research into the development of hybrid alkyd-acrylate latexs shows promise as a viable water based binder to replace solvent based systems. Hybrid alkyd-acrylate coatings have benefits of both systems, high gloss, water/chemical resistance and auto-oxidative crosslinking of alkyds and fast drying, weatherability and low VOC content of acrylate latexs. In 2015 Assanvo and Baruah[139] synthesised alkyd-acrylate hybrids from ricinodendro oil, phthalic and maleic anhydrides and methylmethacrylate (MA) and butylacrylate (BA).

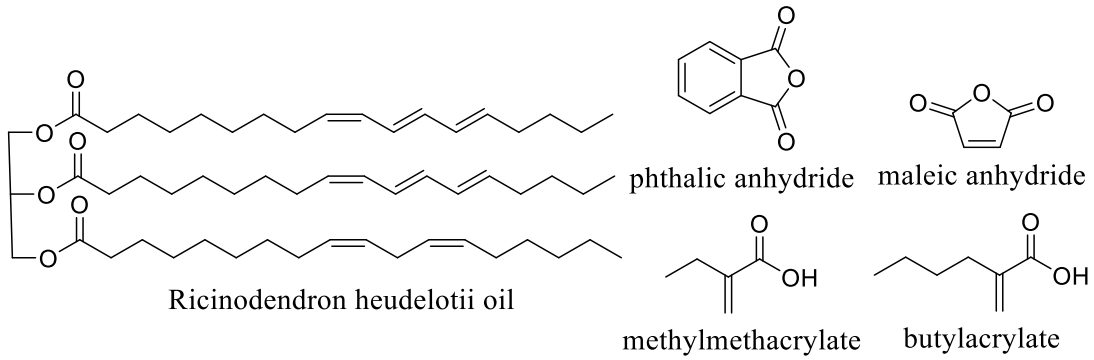

Figure 1.25. Ricinodendro oil, anhydrides and acrylates used in the formation of hybrid alkyd-acylate waterborne coatings.

Ricinodendro oil was first converted to monoglycerides with glycerol and LiOH followed by poly-transesterification with different ratios of phthalic anhydride and maleic anhydride (100:0, 75:25, 50:50 and 25:75 respectively). The ricinodendro alkyd resin was converted to a hybrid latex my miniemulsion polymerisation using a 50:50 mixture of MMA and BA. It was thought the acrylates bond to residual COOH of maleic anhydride rather than phthalic anhydride as increased maleic content increased monomer conversion from 89% to 96% (25 – 75% maleic) and only 14% conversion was achuieved with phthalic anhydride alone.

Films formed from these latexs showed contact angles 64 - 89°, T_g -41 to -24 and tensile strength 2.34 – 7.75 MPa with the higher amount of maleic showing the greater properties. It was shown that greater maleic anhydride content led to greater crosslinking by FTIR as C=C bonds were still present with 0 and 25% samples but not in 50 and 75%. After UV exposure the tensile properties of 0 and 25% increased due to further crosslinking but not with 50 and 75% samples thought to be due to bond scission. This study shows waterborne alkyd-acrylate hybrid systems as a viable and useful replacement for sovent based coatings.

Alkyds also suffer some drawbacks such as low mechanical strength, low hardness and low thermal stability. To overcome this alkyds can be blended with resins such as epoxy which can increase mechanical properties by increasing crosslinking. In 2015 Dolvi[140] *et al* produced alkyd resins from non-edible Jatropha oil (JO) and blended with epoxidised JO (EJO). The alkyd resin was synthesised by alcoholysis of JO with glycerol forming monogylcerides followed by esterification by phthalic anhydride. The alkyd resin wa then epoxidised with formic acid and hydrogen peroxide and the resulting epoxidised resins was blended with EJO at 20, 30 ,40 and 50 wt%. Crosslinking of the epoxidised oil and resin was initiated by citric acid and cured at 120°C. Increasing EJO content from 0 to 50% decreased cure times from 9 to 6.45 h, increased tensile strength from 0.72 to 3.18 MPa and inmproved thermal stability from 280 to 322°C. A post cure at 160°C further increased these properties due to OH generated from epoxide ring opening reactin with residual COOH of the anhydrides further increasing crosslinking. This work shows a useful method to improve the mechanical properties of alkyds with biobased, environmentally friendly components in a catalyst and solvent free system. This presents an interesting step towards a fully renewable based coating.

1.4 Non-stick Surfaces

One of the main aims of this project is the development of a renewable non-stick coating incorporating vegetable oils. There are many routes to achieving a non-stick surface using a number of different compounds. A brief overview of non-stick surfaces follows to provide the reader with some background information in this area.

Possibly the most well know non-stick surface is the non-stick pan, a house hold item since the 1950's, this technology relies on Teflon and is described in more detail in section 2.1.

One application of non-stick technology is self-cleaning surfaces. These are typically on glass and used in construction materials,[141] skyscraper windows[142] and photovoltaic cells.[143] Self-cleaning ability is achieved through one of two methods, a hydrophobic route or a hydrophilic route and both use different technologies. The hydrophobic approach incorporates a microscopic roughness to the surface and is normally coated with a silicone polymer. The low surface energy and hydrophobicity of silicone prevents attachment of organic matter. When water is applied, or during rain, the water has a large contact angle with the surface so forms droplets which roll across the surface taking dirt particles with it. In 2006 Wang *et al*[144] investigated hydrophobic glass. First the glass substrate was cleaned with a plasma treatment to remove any containments and increase the surface roughness. The glass was then coated with polydimethylsiloxane (PDMS) oil and exposed to further plasma treatment to chemically bond the silicone to the glass. This procedure increased the contact angle with water from 69° to 105° and was effective as a self-cleaning surface. The hydrophilic method works on a different principle utilising a photocatalytic reaction.[145] A thin transparent film of TiO_2 is deposited onto the

surface which is activated over 5 – 7 days by UV light during daytime. During UV irradiation TiO_2 reacts with oxygen and water forming hydroxyl radicals. When dirt or dust attach to the glass they are oxidised by the radicals and degraded.[146] Another theory is the UV light excites TiO_2 creating free electrons and holes, the electrons reduce O_2 to water and the holes oxidise the organic matter. It is not yet clear which mechanism is correct or if a combination of both is active.[147] Since UV light is present even on cloudy days this process works continually during daytime hours. The organic material is removed by water which upon contact with the surface forms thin sheets due to the hydrophilic nature of the surface and the dirt is removed by gravity.

In the marine industry non-stick coatings are essential in preventing bio-fouling, defined as the accumulation of plant or animal species on a surface below the waterline. In the case of ships this can cause severe problems;[148]

- Decreased efficiency through increased roughness and weight of ships hulls leading to greater fuel consumption and emissions.
- Increased ‘dry docking’ frequency to remove fouling incurring costs and decreasing usage time.
- Deterioration of coating leading to corrosion of the underlying metals.
- Introduction of species to environments they are not naturally present.

Traditionally antifouling coatings are based on trialkyl tin species such as tributyltin acrylate – methacrylate copolymers (TBT, Figure 1.26).

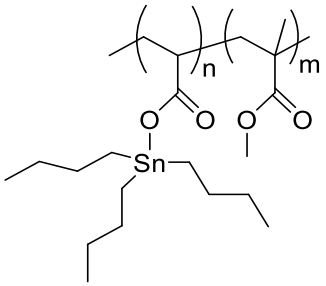

Figure 1.26. Tributyltin tin acrylate - methacrylate copolymer used in antifouling marine paints.

The TBT coatings reduce fouling by providing a hydrophobic surface minimising adhesion but also by poisoning any organisms that do adhere.[149] Under the slight alkali environment of seawater, hydrolysis of the polymer contributes to leaching of the tin species from the coating causing environmental issues. Consequently the use of TBT coatings is now banned. Recent research has focused on non-toxic coatings as environmentally benign systems providing low friction ultra-smooth surfaces to prevent adhesion.[150] The main types of antifouling coatings are based on fluoropolymers or silicones. Fluoropolymers form non-porous low surface energy coatings, the close packing of CF_3 groups locked in position by crosslinking form a smooth surface on the molecular level preventing mechanical adhesion. The inertness of the C-F bonds prevents chemical bonding.[151] Silicones are also non-porous, but the molecules are more mobile presenting moving targets for any functional group of a marine bio-adhesive minimising interactions. Mechanical adhesion is reduced due to the flexible nature of silicones.[152] Consequently, to have a successful non-stick coating there is a need to address different types of adhesion such as chemical bonding and mechanical ‘locking’.

Release properties are an important part of some industries such as resin transfer moulding (RTM) where a monomer or prepolymer liquid is injected into a heated mould and cured. The mould needs to have excellent release properties so the

polymer sample can be removed without damage. Critchlow *et al*[153] reviewed types of release agent used in this industry and found they fall into two main component types – fluoropolymers and silicones. Silicones are effective due to their low surface energy but the thin coatings conform to the mould topography and some adhesion is observed though mechanical interlocking. Fluoropolymers tend to have thicker coatings so are smoother and also have low surface energy. However the thick coatings lead to cracks and fissures which allow resin penetration at higher pressures leading to some mechanical adhesion.

It appears that in most applications non-stick coatings utilise either fluoropolymer or silicones, for this reason both will be considered in our investigation. The following report describes the development of a non-stick coating employing renewable components and technologies using the knowledge gained in this section about non-stick surfaces and vegetable oil chemistry.

2 Development of a Renewable Binder for Non-Stick Coating for Bakeware

2.1 Introduction

The properties of a surface can be modified by coating with thin films. In this way the surface properties can be improved while keeping the bulk properties of the substrate. Coatings can be added for various reasons the most common are;

- Protection – corrosion resistance, abrasion resistance or UV protection.
- Aesthetic – colour, patterns or texture.
- Functional – increase adhesion (paint primers), self-cleaning or non-stick.

Some of the earliest forms of coatings were used to prevent oxidation of metals,[154] metals have been a commonly used material for thousands of years. In recent times more sophisticated coatings have become a reality, such as titanium dioxide in self-cleaning glass.[155] Other industries using non-stick surface are; telecommunications preventing ice build-up on masts/lines,[156] aeronautical for similar reasons as ice can reduce fuel efficiency[157] and the marine industry preventing organisms growing on ships hulls.[158]

There are a number of ways a coating can be applied to substrates such as spray coating,[159] curtain coating[160] or coil coating.[161]

- Spray coating – widely used, ideal for complex structures, however coating can be wasted or areas missed.
- Curtain coating – passing the substrate through a ‘waterfall’ of the coating formulation, achieves uniform coating but over thickness at the edges can lead to cracking or bubbling during curing.

- Coil coating – most accurate and cost effective, large rolls of sheet metal (coil) is unwound, the coating is applied by rollers on one or both sides then substrate rewound after curing. This is a continuous process that provides a smooth even coat.

Possibly the most ubiquitous non-stick surface found in the home is the non-stick frying pan, first marketed by Tefal® in 1956 it used Teflon as the active component (Figure 2.1).

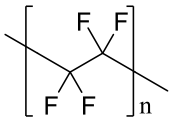

Figure 2.1. Chemical structure of Teflon (PTFE).

Traditional cast iron cookware had no coating, they were vulnerable to corrosion and iron could be leached from the surface increasing a person's intake above recommended levels.[162,163] Most modern cookware does have an inert coating based either on baked enamel or polymer films. Enamel surfaces are typically titanium[164] or zirconium nitride,[165] polymer films are either silicone or Teflon based. Silicones are hydrophobic and have low surface energy (20 mJ m^{-2}) but can be sensitive to high temperatures.[166] Teflon (accidently discovered in 1938[167]) is ideal for cookware, it has low friction coefficient (0.05 – 0.1) low surface energy (20 mJ m^{-2}) inert to nearly all chemicals and a melting point of 327 °C.[168] However excess heating can liberate the toxic gas perfluorooctanoic acid[169] and it is also relatively soft (50 – 60 HB)[168] making it susceptible to damage by metal utensils or vigorous cleaning. To overcome this PTFE coatings often contain inorganic particles or fillers.

Coating formulations are commonly comprised of a polymer binder, a release agent, solid particles and solvents. The binders are typically epoxy resins or polysulfones

both from petrochemical sources. A common epoxy adhesive is bisphenol-A diglycidyl ether (BADGE), it is formed by the reaction of bisphenol-A with epichlorohydrin (Figure 2.2).

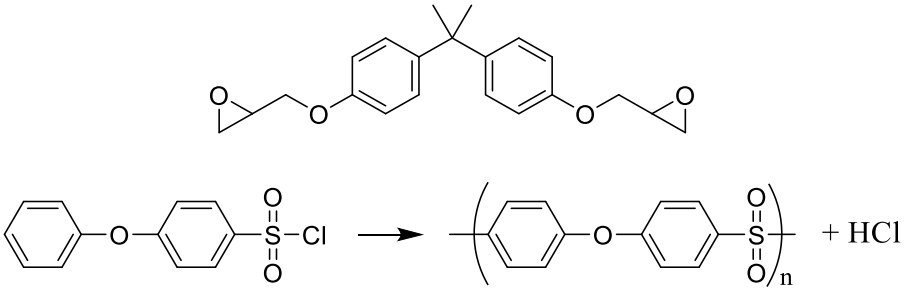

Figure 2.2. Bisphenol-A diglycidyl ether and poly(arylene ether sulfone) commonly used binder in coating formulations.

A typical polysulfone binder, poly (arylene ether sulfone) can be formed by polysulphonylation[170] (Figure 2.2). Epoxy resins achieve strong adhesion through two methods, polymerised resins have pendant hydroxyl groups (-OH) which can from strong polar attractions to oxides on the surface or if epoxides are polymerised on a surface any hydroxyl groups present can covalently bond to the polymer. ***One aspect of this work will be developing novel RENEWABLE binders (e.g. epoxy resins from vegetable oils). The new binders will need to be compatible with common particles/fillers, stable up to 260 °C and pass regulative legislation.***

Solid particles added to formulations are often silica or alumina to provide abrasion resistance.[171,172] To improve the 'look' of coatings, pigments are added. These are often dark as not to discolour at high temperatures, a popular one being carbon black. Aluminium particles are sometimes added to give a sparkle effect.[173] ***Another aspect of this work will be developing fillers to impart toughness and other properties.***

In recent years demand for materials from non-petrochemical sources has increased dramatically, the coating industry is no exemption. Vegetable oils are an important renewable raw material in the chemical industry and functionalization of their fatty acid chains can provide a wide range of compounds[174] including diols[175] and epoxides.[176] Epoxy resins have a wide range of uses due to their thermal and chemical resistance and excellent adhesion to many substrates. Epoxides can be polymerised either thermally[177] or photoinitiated[178] further increasing their appeal. ***An epoxy resin produced from a vegetable oil raw material has the potential to be a renewable polymer binder for use in non-stick coatings.***

2.2 Background of Industrial Sponsors

This section of work was sponsored by Cooper Coated Coil (CCC) a coatings company based in the Midlands, UK. CCC specialise in coil coating[161] for the bakeware, homeware and domestic appliance industries.

The procedure at CCC involves roll of sheet metal, which can be aluminium, cold rolled steel or electrolytic chrome coated steel (ECCS), up to 1 m wide weighing up to 2 ton (Figure 2.3) in a continuous process it is unwound, washed in surfactants and dried under hot air. Then the material is coated, the liquid formulations are transferred from a reservoir to the metal via a series of rollers, after which the coated substrate is cured by passing through an oven at 400 °C for 60 s. One or both sides can be coated in this way and the material is then rewound and sold as a coil of

coated material. The most common material used by the sponsors is ECCS which may become subject to change as the hexavalent chromium used during plating is to be phased out by European REACH regulations,[179] however a trivalent process is possible.[180]

Figure 2.3. A new coil ready for loading onto the start of the coil coating line.

2.3 Analysis of Coatings

Before any advances in non-stick coatings could be achieved, the commercial products were analysed to determine their chemical and physical properties in order to improve them. We investigated the chemical structure, composition, thickness, thermal stability and hydrophobicity of four coatings. The sponsors provided 4 liquid non-stick coating samples; a budget coating ***Easy Clean***, a single coat application ***Single Coat*** in the mid-price range, and the most expensive a two part coating ***Base Coat*** and ***Top Coat***. The formulations were used in the coating coil process and had not been fully analysed. Our ultimate aim was to replace as much of the formulations with renewable and sustainable components and to prepare anon-stick coating that retained the thermal and hydrophobicity profiles of the commercial materials. The initial aim was therefore to identify their chemical composition, the first step was splitting all of the samples into 3 separate parts, solid particles, polymer binders and solvents.

2.3.1 Solid Particles

Solid particles suspended in the formulations were removed by centrifugation, washed and dried to constant weight.

Easy Clean – 30.9% solid content.

Single Coat – 33.0% solid content.

Base Coat– 47.2% solid content.

Top Coat – 39.4% solid content.

The solid particles were analysed by TGA/DSC which showed the presence of PTFE in all but the Base Coat sample as there was a sharp peak in the DSC corresponding to the melting point of PTFE (327 °C) and a degradation temperature of 550 °C in the TGA.[168] Based on the wt % decrease during TGA ***Easy Clean*** contained the greatest amount of PTFE followed by ***Single Coat*** and ***Top Coat*** with a negligible amount present on ***Base Coat*** (Figure 2.4). PTFE is a semi crystalline polymer, below 19 °C it has a highly ordered hexagonal structure, at 19 °C it undergoes some thermal expansion (0.4%) and becomes partially ordered (not shown in our results). It is in this stable pseudo hexagonal structure up to the melting point ~330 °C. The PTFE in these samples was in the same semi crystalline state throughout its usage temperature range (25 – 260 °C).[181]

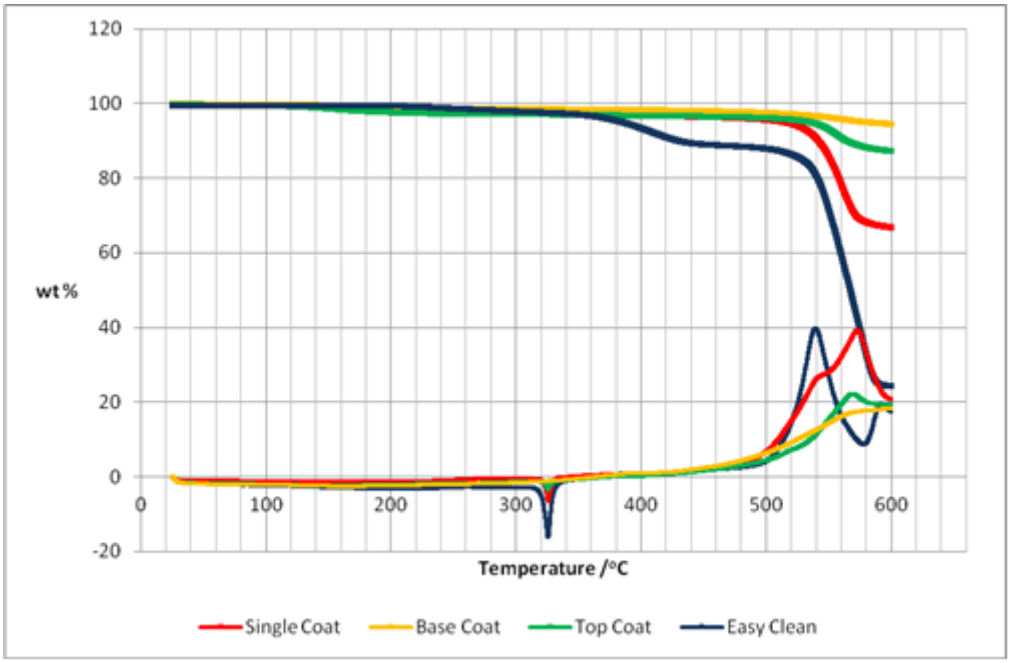

Figure 2.4. TGA/DSC of the solid components of commercial samples provided by the sponsors. Heating rate was 10 °C min^{-1} from 25 – 600 °C in an ambient atmosphere.

The solid components were also analysed by Energy Dispersive X-ray spectroscopy (EDAX) a technique used to identify the elemental composition of a sample (Figure 2.5). An EDAX probe is mounted on an SEM and uses the electron beam for analysis, when atoms are excited by the electron beam secondary electrons are released leaving ‘holes’ where electrons used to be. If the ‘holes’ are in an inner shell the atom is not stable so to regain stability an electron from an outer shell can move to fill the hole. As the outer electrons are in a higher energy state than they would be in the inner shell some energy must be lost which is emitted in the form of x-rays. The emitted x-rays are characteristic in terms of energy and wavelength to the parent atom and the shell that lost an electron.

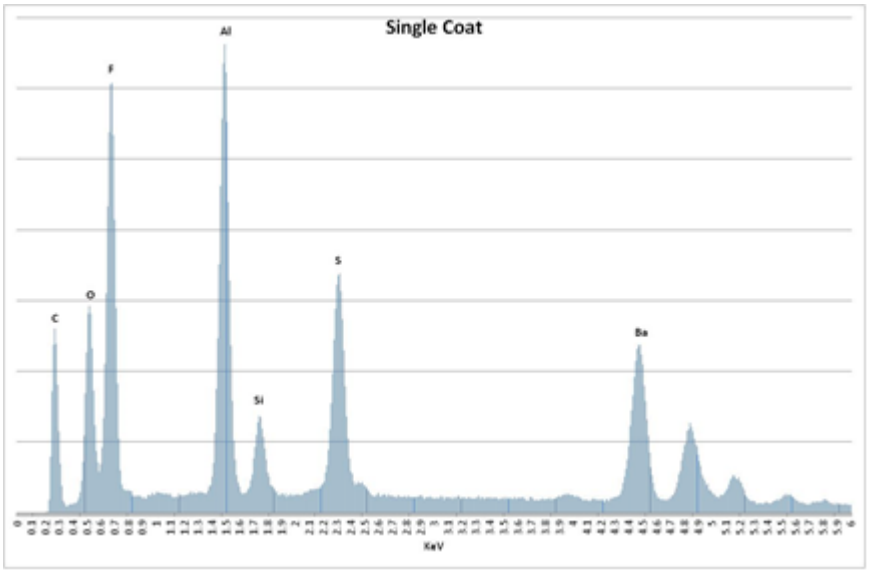

Figure 2.5. EDAX (Zeiss Supra 55-VP) spectrum of the solids in the Single Coat formulation.

Typical elements found in the samples were carbon and fluorine (from PTFE), oxygen, aluminium and silicon (silica/alumina or aluminium flake) and barium and sulphur (barium sulphate a common filler).

2.3.2 Polymer Binder

The supernatant from centrifugation contained a polymer binder and a mixture of solvents which were removed by vacuum distillation. ^{1}H NMR analysis was performed on each polymer, it was known that ***Easy Clean*** was an epoxy based binder and ***Single Coat***, ***Base Coat*** and ***Top Coat*** were polysulfone based, the NMR spectra confirmed their structure.

Easy Clean. After distillation a brown solid was observed which was insoluble in common laboratory solvents; acetone, chloroform, DCM, diethyl ether, ethanol, ethyl acetate, hexane and methanol. The heat from distillation had polymerised the binder forming an insoluble crosslinked network. However when cleaning the centrifuge tubes it was observed a white solid precipitated from the supernatant upon

addition of acetone this solid was soluble in $CDCl_3$ and ^1H NMR analysis shows it was an epoxy monomer based on bisphenol-A (Figure 2.6).

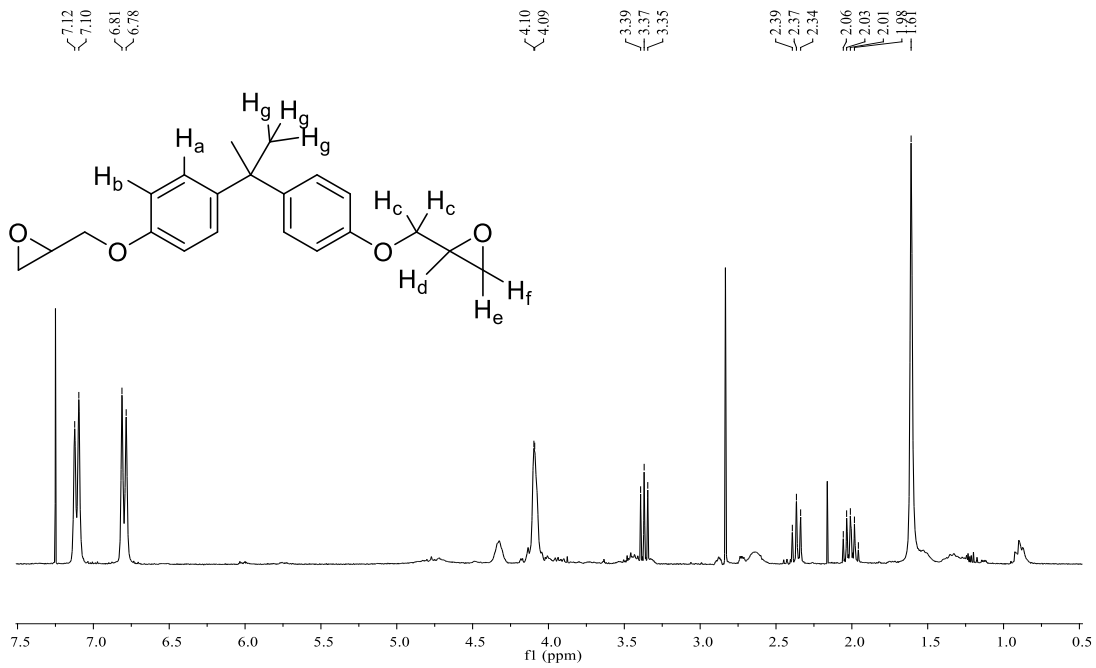

Figure 2.6. ^1H NMR (300MHz, $CDCl_3$) analysis of epoxy monomer used as the binder in ***Easy Clean***.

Single Coat.

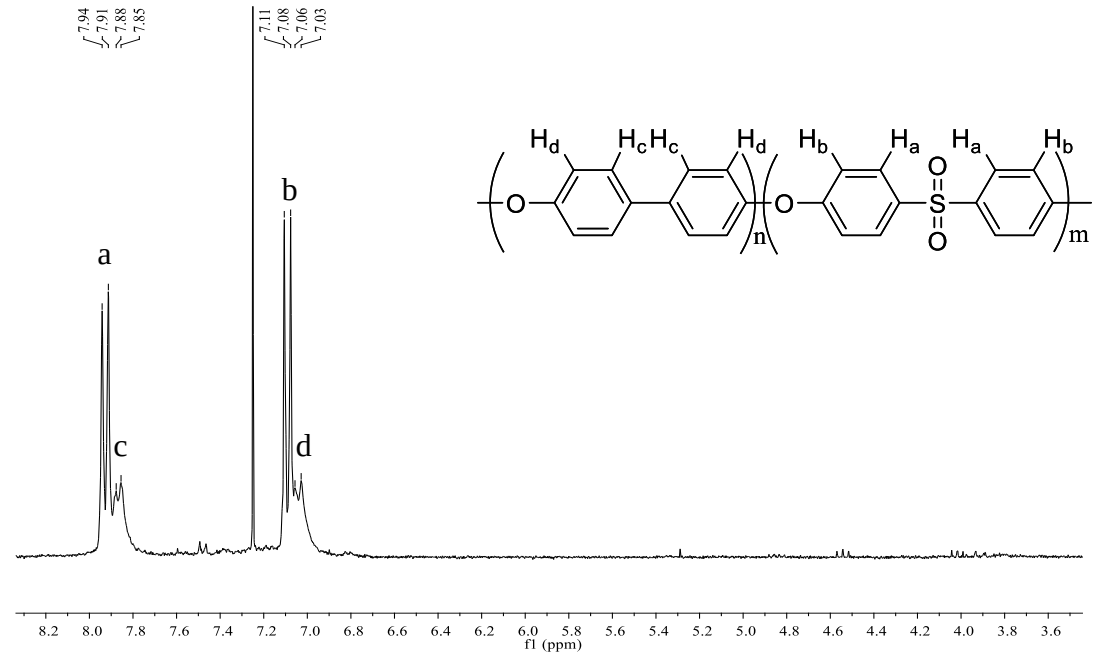

Figure 2.7. ^1H NMR (300MHz, $CDCl_3$) analysis of polymer binder from ***Single Coat***.

A colourless polymer was isolated by distillation of ***Single Coat***, ^{1}H NMR analysis shows it was poly(ether ether sulfone)(Figure 2.7).

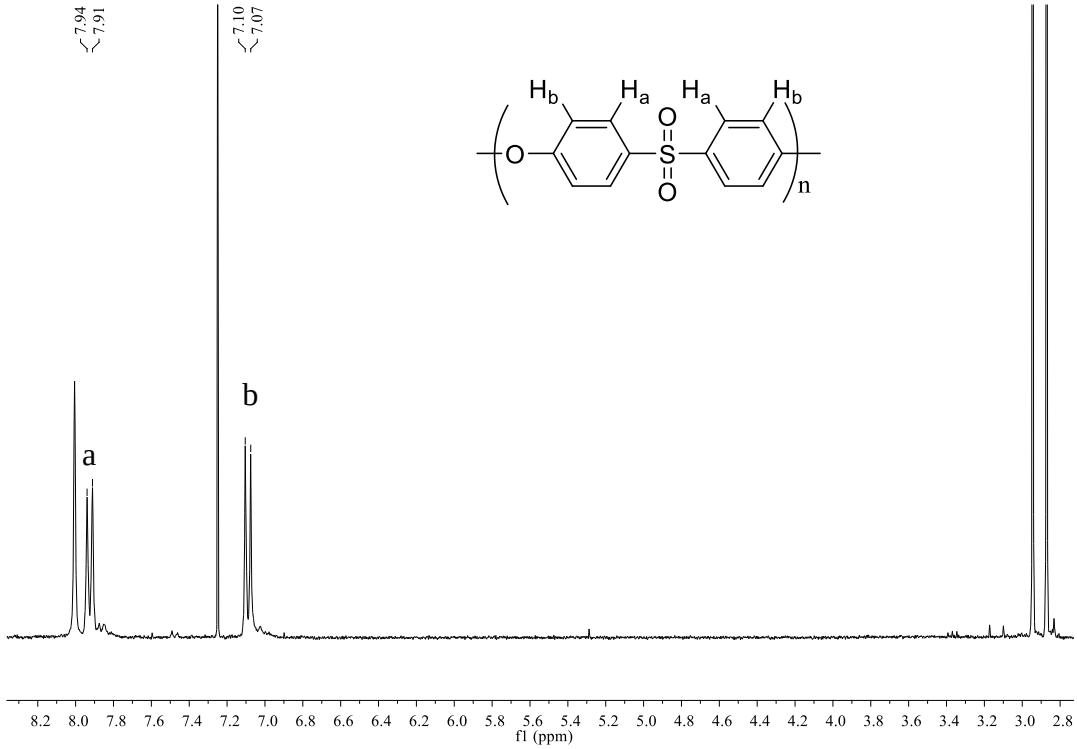

Figure 2.8. ^{1}H NMR (300MHz, $CDCl_3$) analysis of polymer binder used in ***Base Coat*** and ***Top Coat***.

Base Coat and ***Top Coat***. After distillation a colourless solid was observed which was dissolved in DMF to disperse any residual solvents such as NMP trapped in the polymer network and distillation was performed again. NMR analysis shows the binder was poly(ether sulfone), some residual DMF still present (Figure 2.8).

A polymer binder provides adhesion to a surface via two main mechanisms, chemical and mechanical adhesion. Chemical adhesion is bonding on a molecular level such as covalent bonds between substrate and polymer, or intermolecular attraction e.g. hydrogen bonds, dipole interaction or van der Waals forces.

In the case of epoxy binders, a polymerised sample has ether linkages in the backbone and pendant hydroxyls groups which can provide strong polar attraction to metal oxides on a substrate. If an epoxide coating is polymerised on the substrate

hydroxyl groups on the metal surface can covalently bond to the polymer by ring opening of epoxides. It is also important for a binder to wet the surface it is coating, firstly it must have low enough viscosity to flow easily. Secondly the substrate must have a higher surface energy than the coating so a low contact angle is achieved allowing the formulation to flow into crevices and pores on the surface. As polymerisation occurs the viscosity increases and the binder is locked in these voids creating a strong mechanical bond.

In the case of polysulfones adhesion is achieved through hydrogen bonds between the sulfone group and surface hydroxyls, polar interactions form the ether linkage and mechanical adhesion.

2.3.3 Solvents

Solvents are an important factor in coil coating as the viscosity controls the wet film weights which governs the dry thickness once cured. MSDS information was provided with each sample which identified the solvents present and NMR analysis was used to calculate the relative amounts.

2.3.4 Final Composition of Commercial Formulations

Combining the data from analysis of each constituent part of the liquid coatings it was possible to state the composition of the formulations (Table 2.1).

Easy Clean		***Single Coat***		***Base Coat***	
Teflon	25%	Teflon	10%	Barium Sulfate	40%
Epoxy Polymer	25%	Barium Sulfate	15%	Silica	2%
Alumina	2%	Silica	2%	Carbon Black	5%
Carbon Black	2%	Aluminium	4%	PES	7%
Aluminium	2%	Carbon Black	2%	NMP	26%
PGMEA	24%	PES Copolymer	10%	Naphtha (L)	20%
NMP	6%	Naphtha (H)	4%	***Top Coat***	
Xylene	6%	NMP	24%	Barium Sulfate	28%
Ethyl Benzene	2%	Cyclohexane	1%	Teflon	3%
Butan-1-ol	6%	Naphtha (L)	12%	Carbon Black	2%
		Propylene Carbonate	4%	Aluminium Silicate	1%
		4-Hydroxy Butyric Acid Lactone	12%	Magnesium Silicate	6%
				PES	8%
				NMP	30%
				Naphtha (L)	23%

Table 2.1. Chemical composition of liquid coating samples used by industrial sponsors.

Some of the components have apparent uses within the formulation, Teflon is the release agent and provides the non-stick properties, the epoxy polymer and polysulfone are binders and adhere all other components to the surface, the carbon black pigment is for aesthetics. But some components have less obvious uses, aluminium particles provide a sparkle effect to the finish. Barium sulfate is a common filler in coatings it can increase adhesion to a substrate by creating a roughness that improves mechanical adhesion.[182] It is interesting to note that the coatings that contain a higher amount of barium sulfate also contain a lower amount of Teflon, Top Coat has 28% barium sulfate but only 3% Teflon whereas ***Easy Clean*** has no barium sulfate and 25% Teflon. A hydrophobic surface increases in hydrophobicity with surface roughness.[183] It seems that the ***Top Coat*** and ***Single Coat*** gain extra hydrophobicity though surface roughness reducing the need for Teflon so a lower % is used.

2.3.5 Cured Coating Samples

The industrial sponsors also provided four samples of their coatings cured on electrolytically chromium coated steel (ECCS) these samples were ***Easy Clean***, ***Single Coat***, ***2 Coat***, (Base and Top Coat) and ***Top Coat*** (Top Coat can also be used as a 1 layer coating) a competitor product was also tested; ***Spray Coat***.

Coating thickness was analysed by SEM and profilometry, a profilometer is a type of microscope where a beam of light is split, one path is to the test piece and the other to a reference panel, then both are reflected and combined at a detector. Where the difference between the two beam lengths differ, interference is observed. The reference panel is at a known distance and because it is near perfectly flat any interference comes from the sample distance, this allows a 3D picture of a surface to be built up.

A scratch was introduced along the surface exposing the bare metal the height difference between the top of the coating and where the coating meets the metal could be observed (Figure 2.9) and thickness calculated. It was found that the cured coatings had film thicknesses within the ranges stated by the manufacturers; ***Easy Clean*** – 6-8 μm, ***Single Coat*** – 9 ±1 μm, ***2 Coat*** – 8 μm, ***Top Coat*** - 4 μm. It was also found the competitors coating ***Spray Coat*** was 12 μm.

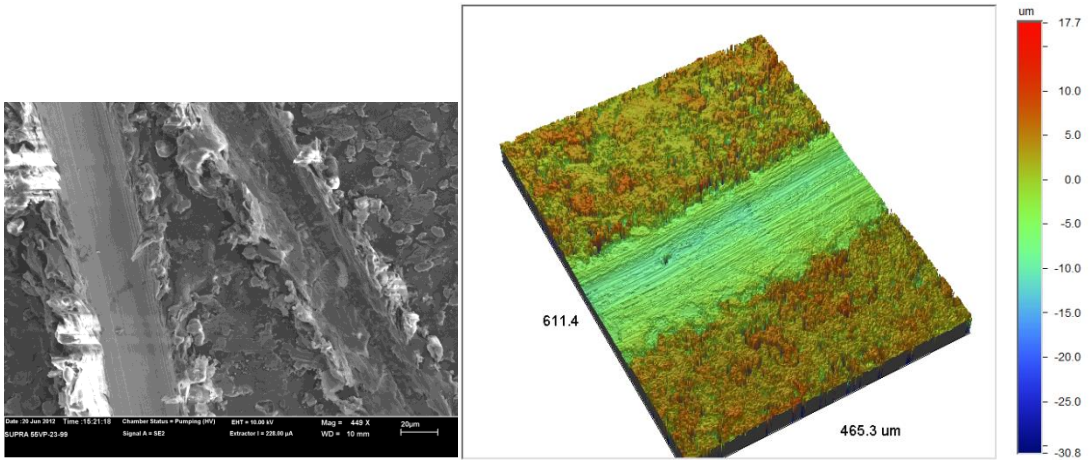

Figure 2.9. SEM (Zeiss Supra 55-VP, 440x magnification) and Profilometry (Wyko, Vision 4.1 software) of scratched ***Easy Clean*** coating.

Non-Stick bakeware must perform and be stable at high temperatures so the 5 surfaces were analysed by TGA (Figure 2.10), the 3 polysulfone based coatings were stable up to 450 °C whereas the epoxy base ***Easy Clean*** was stable up to around 250 °C but this was still above the manufacturers stated usage temperature of 215 °C. The competitors ***Spray Coat*** is stated by manufacturers as safe up to 240 °C but began degrading below 200 °C. The ***Easy Clean*** coating displays a two stage degradation process one starts around 250 °C and the second at 400 °C. Thermal degradation is based on bond energies the lower energy bonds degrade at lower temperatures eg C-C and C-O (346 and 358 $kJmol^{-1}$ respectively). The first stage of the epoxy binder degradation is attributed to the C-C and C-O bonds of the ring opened epoxide, the second stage is from degradation of the aromatic C=C (518 $kJmol^{-1}$). The degradation of aromatic C=C bonds is also observed in the polysulfone samples starting at 450 °C with a second stage at 550 ° due to sulfone degradation (522 $kJmol^{-1}$).

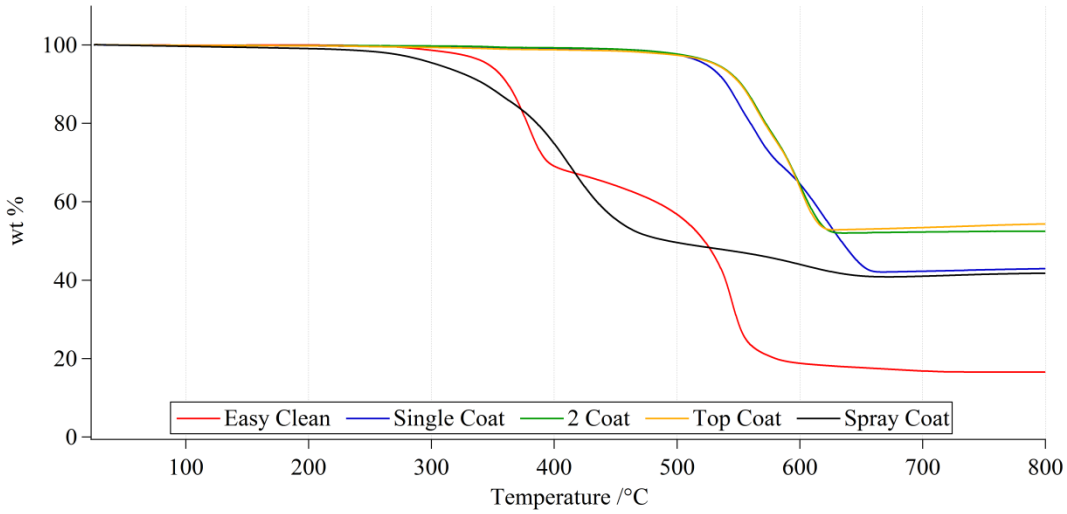

Figure 2.10. TGA analysis of cured coating samples. Heating rate was 10 °C min^{-1} from 50 – 800 °C in an ambient atmosphere.

2.3.6 Non-stick Properties of Commercial Samples

The non-stick properties of these samples was tested by drop shape analysis using water and rapeseed oil to mimic cooking conditions, various sized droplets were used and an average was calculated.

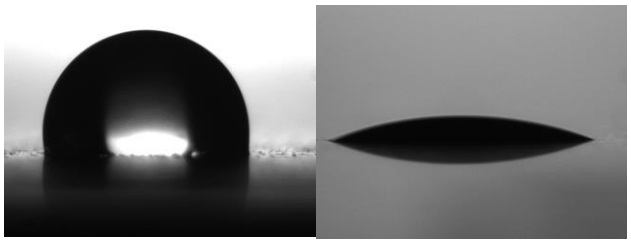

Surface		
	Water	**Rapeseed Oil**
Easy Clean	90.9 ±4.7	35.0 ±3.6
Single Coat	88.3 ±6.7	26.1 ±5.7
2 Coat	89.1 ±3.3	21.9 ±3.5
Top Coat	87.9 ±3.0	17.5 ±2.9
Spray Coat	88.3 ±12.2	44.1 ±0.5

Table 2.2. Contact angles of CCC coated samples and a competitors spray coating. Errors are reported as one standard eviation away from the mean.

These results show the surfaces are moderately hydrophobic but are also olephillic this is useful for cookware as the hydrophobicity allows for a non-stick surface but

the oleophillic nature allows for complete wetting when cooking oil is used creating a barrier between surface and food.

2.3.7 Summary and Aims for Making More Sustainable Formulation

The coatings based upon a polysulfone binder (***2 Coat*** and ***Top Coat***) showed greater thermal stability and greater control of film weights as tolerances were lower, but there was not a great difference in hydrophobicity between the coatings. The epoxy based coating (***Easy Clean***) was less oleophilic possibly due to the pendant hydroxyl groups increasing polarity.

In order to provide a formulation that contains more renewable and sustainable components we initially needed to focus on a renewable binder to replace the epoxy or sulfone binders. Despite the epoxy based coating (***Easy Clean***) being less oleophilic and having lower thermal stability than the other analysed materials, it may be beneficial to produce a binder based on epoxides as they can be easily produced from renewable feedstocks. Epoxides can be polymerised through UV curing which may reduce energy costs (current commercial process 400 °C / 60s). The thermal stability of materials from epoxide polymerisation may not be as high as polysulfones but for cookware the maximum user temperature is stipulated to be 260 °C so the benefits of a renewable coating outweigh the need of a coating stable to 400 °C.

Another area of concern for making the manufacturing process more environmentally friendly is the use of solvents. Epoxides from plant oils are typically a liquid at room temperature (with the exception of less unsaturated oils such as palm oil) which reduces the amount of solvent required for a coiling manufacturing process. Thus solvents whenever possible should be from renewable sources such as

glycerol a by-product from biodiesel manufacture or solvents derived from carbohydrates or lactic acid.

Leading on from the general aims of the project and the information obtained from currently available formulations we can proposed a definitive list of aims to prepare a more sustainable non-stick formulation and coating process;

- To produce a polymer binder from renewable sources. This green binder must provide good adhesion to ECCS and be thermally stable up to 260 °C.
- Investigate solid fillers to provide abrasion resistance and to achieve a contact angle with water greater than 90°.
- Create a more environmentally friendly process which can be achieved by use of lower amounts of solvents, green solvents, lower cure temperatures or UV cure to save energy.

2.4 Renewable Polymer Binder

One of the aims of this project was to synthesise a non-petrochemical based polymer binder. Recent work in the group using vegetable oils as a feedstock for renewable polymers has shown some interesting properties that would make them suitable for a binder.[176,184] Vegetable oils can be easily functionalised at the double bond, such as epoxidation with hydrogen peroxide and a tungsten catalyst in good yield (> 90%). The epoxidised oils can then undergo cationic ring opening polymerisation using BF_3.OEt under solvent free conditions at room temperature and in the case of polyunsaturated oils form an insoluble crosslinked gel.[185] Solvent free polymerisation would provide a step towards a more environmentally friendly binder and room temperature polymerisation would reduce energy costs.

Polymers from plant oil sources are suited to use in non-stick cookware as the parent oils are naturally hydrophobic, have high thermal stability >260 °C and are designated food safe as they are already used in cooking.

2.4.1 Epoxidation of Plant Oils

A range of vegetable oils were chosen with varied levels of unsaturation which would provide different levels of epoxide functionality. The oils used in this study were soybean oil (epoxide number = 4.4), rapeseed oil (3.8), high oleic sunflower oil (3.0) palm oil (1.8) and linoleic acid (2.0). All oils are commercially available on a large scale, worldwide production in the 2012/13 season for soybean, rapeseed, palm and sunflower combined was 160 mT.[186]

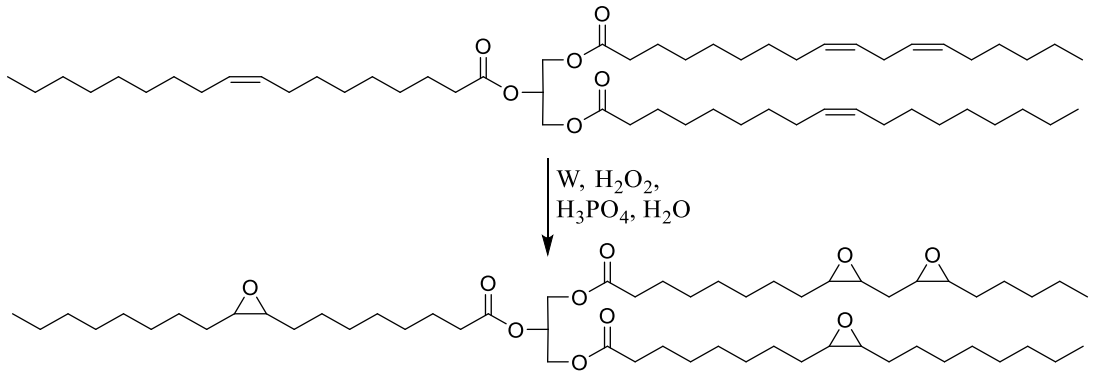

Figure 2.11. Epoxidation of rapeseed oil

The oils were epoxidised using hydrogen peroxide and phosphoric acid with a tungsten powder catalyst at 60 °C and the reaction were performed on 250 g scale (Figure 2.11). Epoxidation was monitored by ^{1}H NMR observing the disappearance of alkene peaks (~ 5.3 ppm) and appearance of epoxide peaks (~ 2.8) the reaction was complete in less than 6 h. Yields were generally high; epoxy soybean oil (yield 91%), epoxy rapeseed oil (94%), epoxy high oleic sunflower oil (96%), epoxy palm oil (95%) and epoxy linoleic acid (86%).

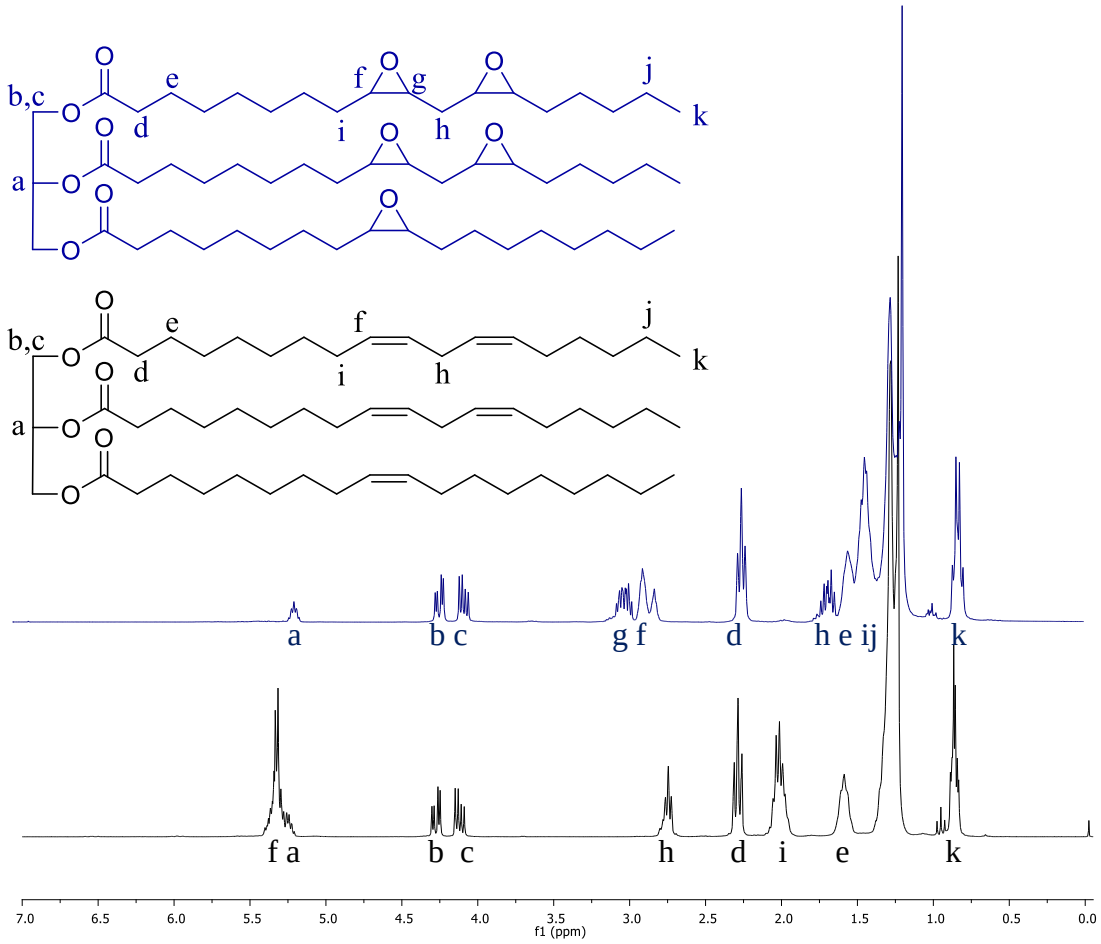

Figure 2.12. ^{1}H NMR (300MHz, $CDCl_3$) analysis of epoxidation of soybean oil.

This method of epoxidation is a useful reaction, epoxides are produced in good yield (86 – 96%) with high purity and in a relatively short reaction time (~ 6 h). The reaction has the potential to be scaled up for industrial quantities as the solvent is water allowing for easy isolation of products by separation as epoxidised oils and water are not miscible so minimal organic solvents were required. Epoxidised palm oil and linoleic acid were waxy solids so more solvent was required for these epoxidations.

2.4.2 Ring Opening Polymerisation - Catalyst

Previous work in this research group has highlighted useful materials can be produced from epoxides created from vegetable oils,[184] Epoxides can undergo

cationic ring opening polymerisation in the presence of strong Lewis acids (BF_3, SbF_5) or strong Brønsted acids (FSO_3H, $CF_3SO_2OSO_2CF_3$)[187] and our work has shown $BF_3.Et_2O$ to be highly efficient. Plant oils with a lower epoxide functionality (palm oil and methyl oleate) were shown to produce polyols upon reaction with 0.15 mol equivalent of $BF_3.Et_2O$ with molecular weights of 6100 and 1800 respectively, whereas higher epoxide functional oils formed an insoluble crosslinked gel.[185] The insoluble polymer would be of more use as a binder in coating formulations due to the increased chemical resistance. However the use of BF_3 would not be suitable for use in cookware applications due to high toxicity. As use in a general coating it would also not be suitable for this application as it is too active, polymerisation of epoxidised plant oils with $BF_3.Et_2O$ occurs at 20 °C in less than 24 h which would give a very short pot life for any formulation created with these reagents. Small batch mixing of formulations may be possible but would not be suitable for the continuous nature of coil coating.

An efficient catalyst for cationic ring opening polymerisation are triarylsulfonium hexafluoroantimonate salts (TAS, Figure 2.13).[177,178]

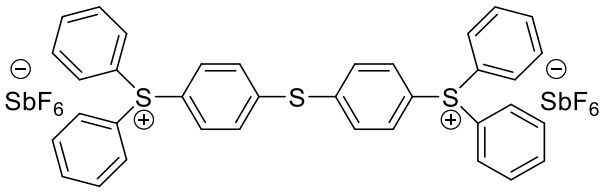

Figure 2.13. Triarylsulfonium hexafluoroantimonate salts (TAS) a thermally and UV active catalyst

Sulfonium salts are more suitable catalysts as they would not react with plant oil epoxides at room temperature without activation allowing the coating to be stored in liquid form for greater periods. Although this class of initiator has not been approved for food contact use and ultimately therefore could not be utilised in any renewable

formulation the ability of TAS to lie dormant in the formulation until activated was of interest for initial preparation of materials to test the hypothesis that renewable epoxide binders would provide appropriate material properties for non-stick applications. TAS is a photo acid generator, meaning it releases H^+ ions upon excitation with light, typically UV light is used for initiation. The mechanism is generally accepted as upon illumination the sulfonium salt becomes a cation radical and undergoes electronic rearrangement to produce H^+ which is balanced by the salts anion in solution (Figure 2.14).

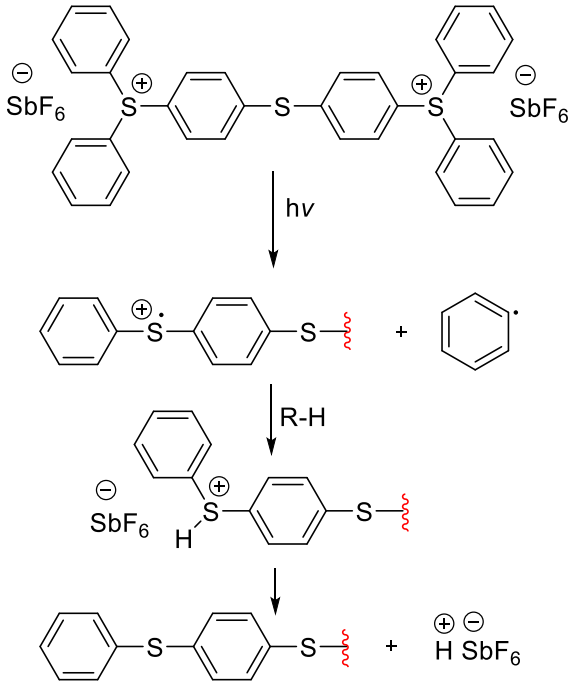

Figure 2.14. Triarylsulfonium hexafluoroantimonate salt a photoacid generator producing aicd upon exposure to UV light.

Typically after activation by UV irradiation polymerisation can be performed either at room temperature or at elevated temperature, which made it an attractive possibility as a catalyst in this formulation. The ability to use UV light for polymerisation would reduce energy costs associated with high temperature thermal curing increasing the green credentials and satisfying our aims of a more environmentally friendly coating. Polymerisation by heat may also occur at a lower

temperature then previously used (400 °C) if we are able to create a solvent free system.

Crivello[177] has shown the ability of TAS as a dual cure system in the polymerisation of bisphenol based epoxides. Firstly, the reaction is initiated by UV for 20 – 60 s which achieves a prepolymer of 22 – 30 % conversion, then upon heating at 100 °C for 30 min conversion reaches 83 – 91 %. Decker[178] has also shown UV to be a rapid method for epoxy polymerisation. In bisphenol- epoxy soybean oil blends UV irradiation (520 $mWcm^{-2}$) produced polymers with 96% conversion after only 5 second irradiation. UV induced polymerisation of epoxy plant oils appears to be an effective curing method for a renewable polymer binder.

2.4.3 Ring Opening Polymerisation – UV initiated

Triarylsulfonium hexafluoroantimonate salts (TAS) can be initiated by UV light allowing ring opening polymerisation to occur at room temperature. A UV cured system would be beneficial in terms of improving the environmental impact of the coating as energy costs would be reduced. A range of epoxidised vegetable oils were mixed with 3 wt% of TAS and coated onto an electrolytic chrome coated steel (ECCS) substrate using a wire wound coating bar producing a film 12 μm thick. The samples were initiated by a UV weather station, typically used to accelerate degradation of paints, at a power of 0.45 W/m^2. The samples were irradiated at 5 minute intervals until the coating was dry to the touch (Figure 2.15, Table 2.3).

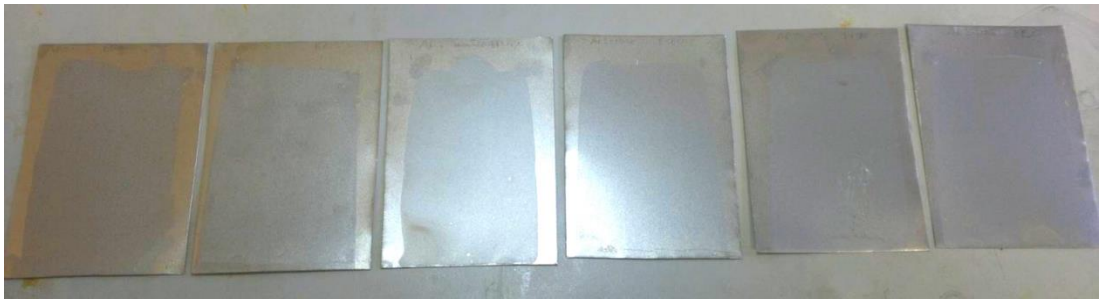

Figure 2.15. UV cured epoxy plant oil coatings on ECCS.

The samples were sent to the sponsors where a series of industry standard tests were performed, these tests are;

Cross-Hatch, BS EN ISO 2409:2013 – Examines adhesion of coating to the substrate. A grid of 100 squares 1 mm x 1 mm is scribed through the coating exposing the substrate. Adhesive tape is applied to the grid and removed sharply and the test piece is inspected for any removal of coating.

Flexibility, BS EN 13523-7:2001 – Determines flexibility of the coating film. The test piece is bent through 180° and tape is applied on the bend and removed sharply. The test piece is inspected for any removal of coating. The first fold is classed as 0T, if a coating fails this test the sample is folded again the thickness is double so fold radius is greater this is 1T and inspected again for coating removal.

Pencil Hardness, BS EN 13523-4:2001 – Measures hardness of the coatings surface, conforms to EN 13523-4:2001. Pencils of different lead hardness's are pushed across the surface at a 45° angle. The hardest lead that doesn't damage the surface determines the degree of hardness e.g. 2H.

Coating	Cure time /m	Comments	X-Hatch	Flexibility	Hardness
CCC PES coating	N/A	Reference panel	100%	Pass	>5H
Epoxy Linoleic Acid	30	Tacky	100%	Pass	F
Epoxy Palm Oil	15	Slightly tacky	80%	Pass	F
Epoxy Sunflower Oil	5	Slightly tacky	100%	Pass	HB
Epoxy Rapeseed Oil	25	Very tacky	100%	Pass	HB
Epoxy Soybean Oil	10	Dry to touch	25%	Fail	F-H
Epoxy Euphorbia Oil	5	Dry to touch	Fail	Fail	2H-3H

Table 2.3. Industry tests on UV cured epoxy plant oil coatings.

The coatings derived from less unsaturated oils (linoleic acid, palm, sunflower and rapeseed oils) have good adhesion and flexibility but they are tacky to the touch and lack sufficient hardness for a useable product, current coatings have hardness greater than 5H. The higher unsaturated oils (soybean and euphorbia) provided coatings showing greater hardness (H and 2-3H) possibly due to more crosslinking through an increased number of epoxides. However the harder coatings fail in terms of adhesion and flexibility due to being more brittle.

The work by Crivello[188] has shown that a natural product curcumin can act as a photosensitzer to triarylsulfonium salts (TAS). Curcumin is excited at around 427 nm and initiates sulfonium salts by electron transfer, the broader absorption band allowed for polymerisation to be performed between 340 and 535 nm, presenting the possibility of polymerisation by daylight. Curcumin was isolated from supermarket bought turmeric powder by Soxhlet extraction using DCM (Figure 2.16).

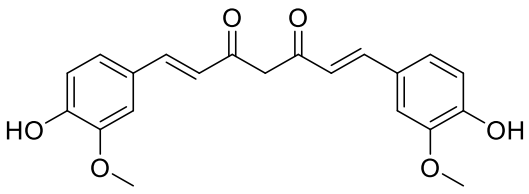

Figure 2.16. Curcumin a photosensitizer extracted from turmeric.

Addition of 0.1 wt% curcumin allowed for a reduced amount of catalyst to be used (1 wt% instead of 3 wt%) and also decreased curing times to below 5 min. The

yellow tinted coatings were harder possibly due to a greater degree of polymerisation, but lacked flexibility and adhesion (Table 2.4).

Coating	Comments	X-Hatch	Flexibility	Hardness
CCC PES coating	Reference panel	100%	Pass	>5H
Epoxy Sunflower Oil	Slightly tacky	100%	Patchy	4H
Epoxy Soybean Oil	Dry to touch	30%	Fail	5H
Epoxy Euphorbia Oil	Dry to touch	90%	Fail	3H

Table 2.4. Industry standard tests of UV cured coatings with the addition of curcumin.

Consequently, epoxidised plant oils polymerised by UV using this system would not be suitable for use as binders in non-stick coating formulations required for bakeware.

2.4.4 Ring Opening Polymerisation – Thermally initiated

While UV curing may look like an attractive proposition due to energy considerations, in reality heat was still required during the curing to remove any solvents present in the liquid formulation. From a commercial viewpoint the cost of installing a UV system may not outweigh the benefits of reduced energy costs in any case.

Ring opening polymerisation catalysed by TAS by thermal initiation was explored next. A range of epoxidised vegetable oils were mixed with 3 wt% of TAS and coated onto an ECCS substrate using a 12 μm coating bar. Initially we chose to perform the polymerisation using the same regime already in use by the sponsors, samples were polymerised by heating at 400 °C for 60 s. The coatings showed some discolouration due to the high temperature (Figure 2.17) but this can be masked with the use of pigments (see section 2.5.2). The surfaces were soft to the touch possibly due to incomplete polymerisation.

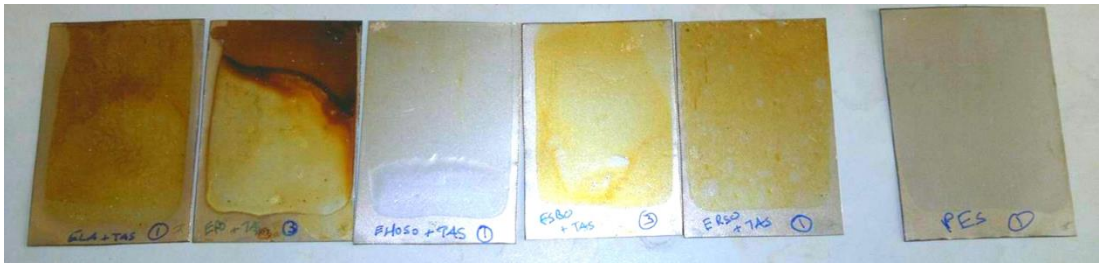

Figure 2.17. Thermally cured epoxy plant oil coatings on ECCS.

These samples were analysed by the sponsors by cross hatch, flexibility and pencil hardness (Table 2.5).

Coating	Epoxides	Comments	X-Hatch	Flexibility	Hardness
CCC PES coating	N/A	Reference	100%	Pass	>5H
PES	N/A	Dry to touch	100%	Pass	>5H
Epoxy Linoleic Acid	2	Very slightly tacky	100%	Pass	<HB
Epoxy Palm Oil	2	Tacky	100%	Pass	<HB
Epoxy Sunflower Oil	3	Very slightly tacky	100%	Pass	HB-F
Epoxy Rapeseed Oil	3.8	Tacky	100%	Pass	<F
Epoxy Soybean Oil	4.4	Very slightly tacky	100%	Pass	<F

Table 2.5. Industry tests performed on thermally cured epoxidised oil coatings.

All the heat cured coatings passed the industry tests in terms flexibility, presumably either due to the soft nature of vegetable oil polymers or the samples were not fully cured, which is consistent with the tacky surface. However, heat cured samples did show sufficient adhesion to the substrate (unlike the UV cured samples), this may be because the higher temperature allows the metal surface hydroxyl groups to ring open some epoxides creating covalent bonds between the polymer and metal. The higher temperatures also reduced the viscosity of the epoxidised oils allowing greater flow into surface voids thus creating increased mechanical adhesion upon polymerisation. However, the epoxidised plant oils polymerised by thermal initiation would not be suitable for a polymer binder in this state due to soft nature of the coating, the surface would be damaged easily. However, because the heat cured

coatings showed more encouraging properties than the UV cured coatings our industrial partners wished to pusue thermal curing methods only.

2.5 Addition of Solid Particles

2.5.1 Fumed Silica

To overcome the soft nature of the heat cured vegetable oil polymers solid fillers could be added. The four commercial samples analysed (see section 2.3.4) contained particles of alumina, silica and barium sulphate, and silica and alumina are well known coating additives.[189,190] It has been shown that silica can hydrogen bond to the polymer matrix in epoxy resin-silica nanocomposites, this is shown by a decrease in vibrational frequency of C=O and SiO-H bonds in FT-IR spectroscopy.[191] Consequently, we chose to explore the use of added silica to increase the toughness of our coatings.

Fumed silica, also known as pyrogenic silica, is produced in a flame or an electric arc from silicon tetrachloride, the particles are large 3-dimentional aggregates. Fumed silica has a very large surface area and low density it is often used in coatings, used in cosmetics and an abrasive in toothpaste, so it is food safe. The silica used for this study was supplied by Wacker Chemie AG, a hydrophobic grade (HDK H20) was supplied which was functionalised with dimethylsiloxane.[192]

For the remainder of this investigation coating formulations will be based on epoxidised soybean oil as it showed the best properties of all of the heat cured plant oils. Epoxidised soybean oil is also commercially available and produced on a large scale as it is used as a plasticizer in PVC manufacture.[193]

Epoxidised soybean oil was mixed with fumed silica in volume ratios of 10:1, 5:1, 2:1 and 1:1 and 3 wt% TAS used as catalyst. The mixtures were coated onto ECCS with a 12 μm coating bar and cured at 400 °C for 60 s (Figure 2.18).

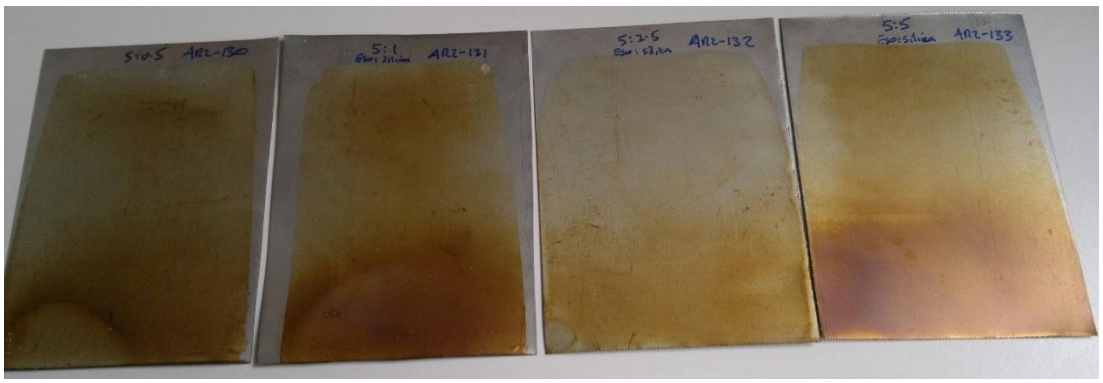

Figure 2.18. ESBO and fumed silica coatings on ECCS.

The addition of silica provided a great improvement to the surface properties, the samples were non tacky, were not damaged by a 5H pencil in hardness testing and passed adhesion and flexibility tests (Table 2.6). At this point a further adhesion test was used to screen the coatings, the Erichsen test;

Erichsen test, BS EN ISO 1520:2006 - measures adhesion to a substrate. The area where a cross hatch test has been performed is deformed into a dome 8 mm in height and tape is used to inspect for any removal of coating.

Volume ratio					
Epoxy Soybean Oil	**Silica**	**X-Hatch**	**Flexibility**	**Hardness**	**Erichsen**
10	1	100%	Pass	4H	100%
5	1	100%	Pass	>5H	100%
2	1	100%	Pass	>5H	100%
1	1	100%	Pass	>5H	100%

Table 2.6. Industry tests of silica containing coatings.

In conclusion, the addition of fumed silica particles to the thermal improved the hardness and theother surface properties. A volume ratio of 5:1 (epoxidised oil: silica) produced a coating with sufficient hardness for a commercial coating, and

consequently, increasing the amount of silica would gain no advantage but increase the overall cost.

2.5.2 Addition of Pigments

Thermally cured samples are prone to discolouration (see 2.5.1 above), this is unattractive for a commercial product, so formulations often contain pigments. A common pigment used in cookware is carbon black, it is relatively cheap, safe for food use (recorded as E153 on food labelling)[194] and the dark colour disguises discolouration from repeated uses.

Carbon black was added to a formulation of epoxy soybean oil, fumed silica and TAS in amounts of 1, 2, 3, 4, 5 and 10 wt%, each mixture was coated onto an ECCS substrate, cured at 400 °C for 60 s, and then subjected to X-hatch, hardness, flexibility and Erichsen tests to evaluate their properties (Figure 2.19).

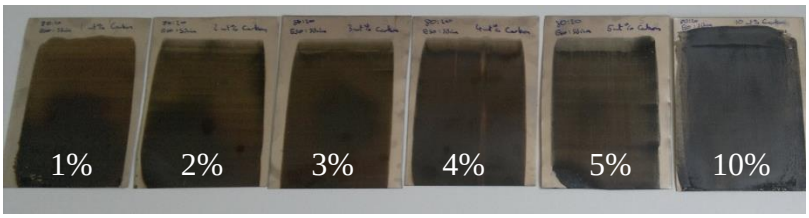

Figure 2.19. Coating formulations containing ESBO, fumed silica, carbon black and TAS.

The addition of carbon pigment did not affect surface hardness or adhesion properties until 10 wt% was included, where some coating is removed in the Erichsen test. However, the flexibility of the coatings were reduced significantly.

Carbon wt%	Hardness	Flexibility	X-Hatch	Erichsen
1	>5H	Fail	100%	100%
2	>5H	Pass	100%	100%
3	>5H	Patchy	100%	100%
4	>5H	Fail	100%	100%
5	>5H	Fail	100%	100%
10	>5H	Fail	100%	< 100%

Table 2.7. Surface tests of coating formulation containing carbon black pigment.

Flexibility was adequate when 2 and 3 wt% of pigment was present, but a small amount of pigment was removed from the 3 wt% sample when folded through 180 °C, when folded again to give a 1T fold no coating was removed. In terms of aesthetics the 3 wt% coating performed better than 2 wt% as discolouration was less apparent and coating was more opaque. Thus the optimum amount of carbon black for this coating formulation would be ~3 wt% as more than this affects physical properties to much and any less does not give enough colouration.

2.5.3 Addition of PTFE

The optimum formulation so far (containing 5:1 epoxy soybean oil (ESBO):silica and 3 wt% carbon black) had a contact angle with water of 72° which was too hydrophilic for non-stick applications, (the commercial samples were around 90°). To increase this contact angle, the surface energy needed to be reduced, through the use of a release agent such as Teflon (PTFE).

PTFE is chemically inert due to the strength of the C-F bonds, this bond is highly polarised from the high electronegativity of fluorine. The polarisation adds some ionic character which shortens and strengthens the bond (C-F, length = 1.35 Å energy = 544 $kJmol^{-1}$).[195] The chemical inertness and resistance to intermolecular forces gives a low coefficient of friction which creates non-stick behaviour.

Coating formulations of 5:1 volume ratios of ESBO and silica with 3 wt% carbon black were combined with 1, 2, 3, 4, 5, 10 and 20 wt% of PTFE powder. The formulations were coated with a 12 μm bar onto ECCS and cured at 400 °C for 60 s.

For all samples there was failure of adhesion, the surface was rough with a powdery residue, which was easily removed exposing bare metal. It would appear that Teflon was not bonding to the ESBO binder which caused lack of adhesion between the binder and the surface. In commercial samples it is thought PTFE particles sinter together and create mechanical adhesion with the binder. The same curing process was used in our system so the particles should sinter together. It is possible that this failure might be due to either incompatibility between Teflon and epoxidised vegetable oils, or the oils are affecting the particle sizes of Teflon produced. More work and analysis would have to be undertaken to fully explain the reasons for the lack of adhesion, but at this point attention was turned elsewhere and not further work was undertaken

2.6 Alternative Catalysts: Food Safe Sulfonic Acids

The use of TAS has proven to be a useful catalyst for the ring opening polymerisation of the ESBO binder, however to be efficient it had to be used at 3 wt% which is not a problem for lab scale coatings (~ 2 g) but scaled up to industrial sized formulations would become prohibitively costly. In addition, TAS was not food safe..

Sulfonic acids have been shown to catalyse ring opening polymerisations of epoxides at low concentrations.[196] Two sulfonic acids, camphor sulfonic acid (CSA)[197] and 4-dodecylbenzene sulfonic acid (DBSA)[198] (Figure 2.20) have previously been reported to be efficient catalysts, in addition, 4-dodecylbenzene

sulfonic acid is approved for food contact use[199] and is produced in large quantities as the sodium salt as a common surfactant used in detergents (SDBS).[200]

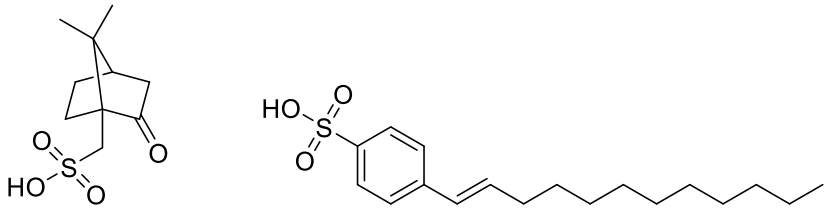

Camphor sulfonic acid
CSA

4-Dodecylbenzene sulfonic acid
DBSA

Figure 2.20. Sulfonic acids used as catalysts for ring opening polymerisation of ESBO coatings

2.6.1 Curing Characteristics of Polymerisation of ESBO with Sulfonic Acids

In order to determine the optimum temperature for curing of ESBO with DBSA, DSC analysis was performed on mixtures with varying amounts of DBSA catalyst (1, 2, 3, 5 and 10 wt%), (Figure 2.21). As the amount of DBSA is increased the peak cure temperature is reduced, at 1 wt% of DBSA, peak activity is at 239 °C which decreases to 187 °C at 10 wt% catalyst. The use of camphor sulfonic acid (CSA) as an alternative catalyst exhibited higher cure temperatures (compare 1 wt% DBSA = 239 °C, 1 wt% CSA = 252 °C).

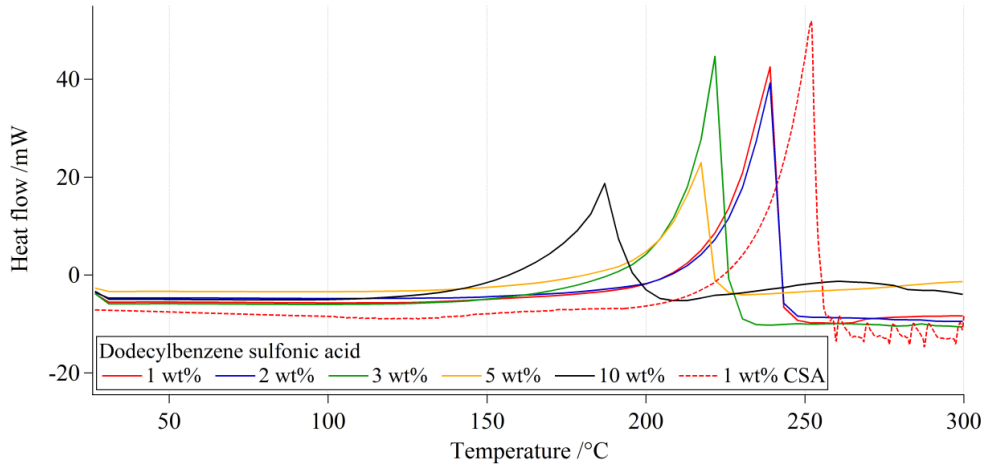

Figure 2.21. DSC analysis of ESBO curing with sulfonic acid catalysts. Heating rate 10 °C min^{-1} from 25 – 300 °C under ambient atmosphere.

The nature of the sulfonic acid initiator may change the physical properties of the polymer produced from ESBO, which in turn would affect the coating surface. In addition, the required amount of silica required to create an appropriate abrasive resistant coating may be different than the previous formulations with TAS. Consequently, we investigated the effect of both the catalyst (CSA verse DBSA, 1 wt%) and the amount of added silica (0.5-5 wt%) in 10 different formulations, Table 6). ESBO and a sulfonic acid (1 wt%) were mixed with hydrophobic fumed silica using 0.5, 0.88 (same as 5:1 vol ratio used previously), 2, 3, 4 and 5 wt%, coated as a 12 µm film on ECCS and cured at 400 °C for 60 s (Table 2.8, Figure 2.22). The previous cure temperature of 400 °C was used for comparison, and to give rapid polymerisation.

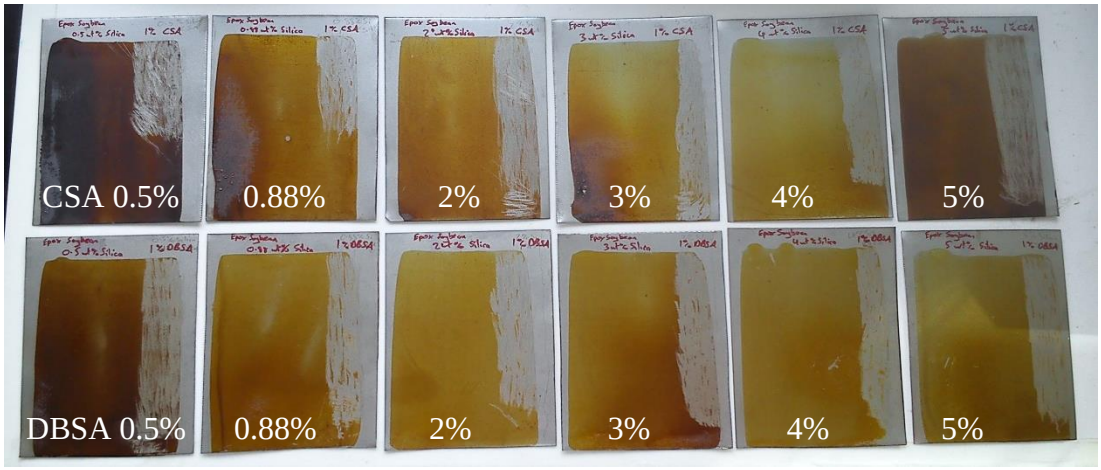

Figure 2.22. Fumed silica ESBO coatings cured with sulfonic acids.

Coating Reference						
Catalyst	**Silica wt%**	**Comments**	**Flexibility**	**Pencil Hardness**	**X-Hatch**	**Erichsen**
CSA	0.5	Dry	Pass	>5H	100%	100%
	0.88	Dry	Pass	>5H	100%	100%
	2	Dry	Pass	>5H	100%	100%
	3	Tacky	Pass	4H	90%	100%
	4	Tacky	Patchy	H	100%	100%
	5	Dry	Pass	>5H	100%	100%
DBSA	0.5	Tacky	Pass	3H	100%	100%
	0.88	Tacky	Patchy	H	100%	100%
	2	Dry	Pass	3H	100%	100%
	3	Dry	Pass	3H	100%	100%
	4	Tacky	Pass	H	95%	100%
	5	Dry	Patchy	2H	100%	100%

Table 2.8 Coating tests of sulfoninc acid catalysed formulations

The results show that polymerisation with CSA produced a coating that was generally harder than when DBSA was used, (0.5% CSA >5H verses DBSA 3H, 0.88 wt% CSA >5H verses DBSA 1H etc). The softer coatings with DBSA maybe due to it acting as a plasticizer (long hydrocarbon chain), or because of the different molecular weight of the initiators (DBSA = 326.5 $gmol^{-1}$, CSA = 232.3 $gmol^{-1}$). The intiators were used in terms of weight percent NOT mol% relative to ESBO and so 71% less DBSA compared to CSA was used in each run .

2.6.2 Thermal and Dropshape Analysis of Coatings

An important aspect of a coating for cookware is the ability to withstand high temperatures, consequently, TGA analysis was performed to investigate the thermal stability of the sulfonic acid catalysed coatings (Figure 2.23). All samples showed good thermal stability with most having $T_{1\%}$ >260 °C needed for cookware. There was no significant difference in thermal stability between the two initiators below 300 °C however, in general the $T_{50\%}$ for those materials derived from CSA were higher than DBSA.

There appers to be a considerable amount of sample remaining at 600 °C, up to 70% for CSA cured with 5% silica. It may be posible the silca is protecting the organic matter from thermal stress, however this should show a tend where the greater the silica content in the sample the more material remains at 600 °C. But there is no general trend relating silica content to remaining organic matter. It is unclear why such a residue is obtained.

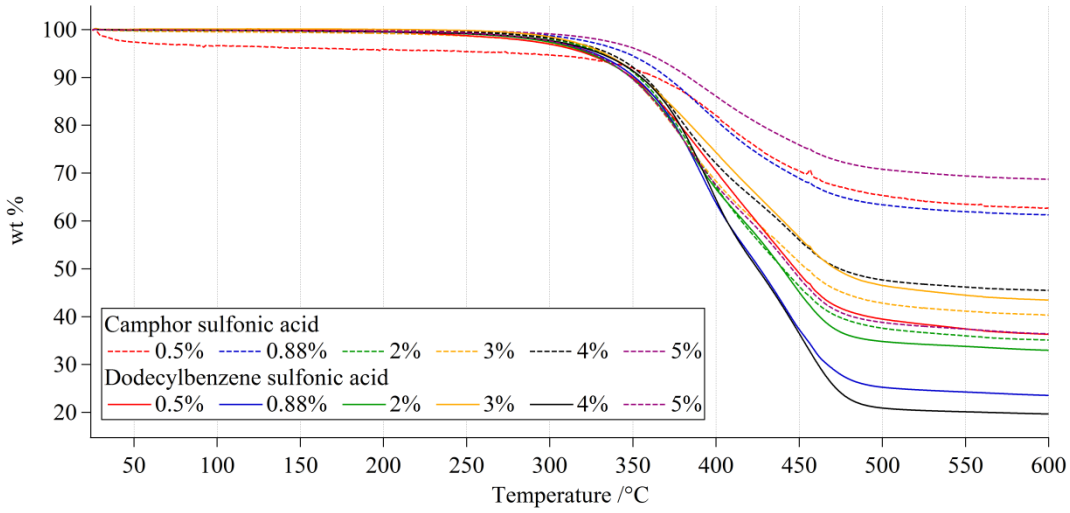

Figure 2.23. TGA analysis of sulfonic acid cured ESBO coatings containing silica. Heating rate 10 °C min^{-1} from 25 – 600 °C under ambient atmosphere.

Drop shape analysis was performed on the 10 coatings, the commercial samples analysed previously had contact angles with water between 87.9° and 90.9° which is classed as borderline hydrophobic. The sulfonic acid cured coatings contained no release agent, such as Teflon, so the contact angle would be a product of the hydrophobicity of ESBO and hydrophobic silica. Contact angles varied between 71-86% for CSA derived coatings and 74-96% for DBSA coatings (Figure 2.24).

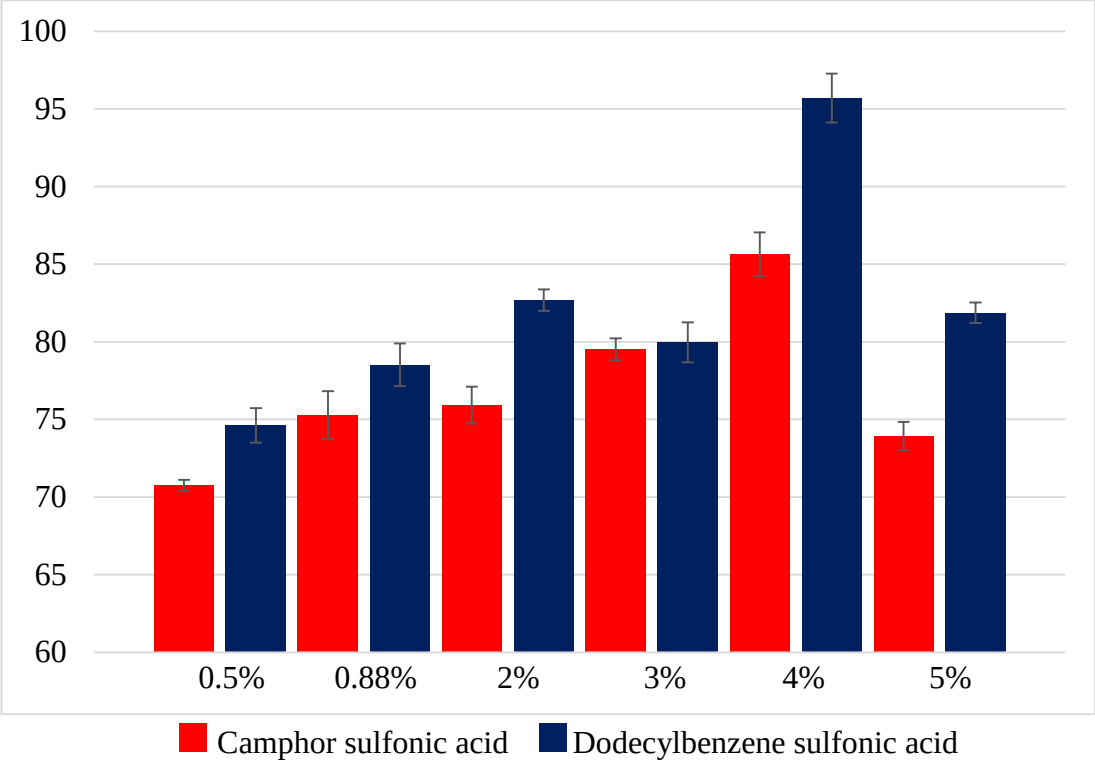

Figure 2.24 Drop shape analysis of sulfonic acid cured coatings, CSA shown in red and DBSA in blue. Contact angles are from water droplets and error bars are from the standard deviation about the mean.

Within error the general trend for both CSA and DBSA initiated polymers showed an increase in contact angle with the amount of silica added to the formulation. Increasing the amounts of silica gave a higher contact angle as expected up until 5 wt% where the contact angle sharply decreased. The grade of fumed silica used (Wacker HDK H20) has on average 50% surface coverage of hydroxyl groups, (the other half is functionalised with methyl groups). Some of the hydroxyl groups would

have covalently bonded with ESBO during curing as previously mentioned, however it may be possible that this silica-ESBO bonding does not increase linearly with increasing wt% of silica and a plateau is reached. After a point (e.g. 5 wt%) the residue –OH groups on the silica may not react with ESBO suggesting that the surface polarity may be increasing and decreasing the water contact angle accordingly. The DBSA cured coatings showed a greater contact angle than the corresponding CSA cured samples due to long alky chain increasing the hydrophobic nature of the material.

Consequently, it was decided to use DBSA as the catalyst for future formulations as it produced coatings with greater hydrophobicity. Despite the fact that it did not exhibit a pencil hardness as great as the CSA cured samples, it was felt hardness should be able to be controlled by the addition of carbon black. In addition DBSA is approved for food contact use[201] and is commercially available in large quantities. For further research, we decided to use formulations that contained 2 wt% fumed silica, as coatings containing this amount passed the industrial tests, although pencil hardness was low, and had relatively high contact angle with water (82.7°).

2.7 Addition of Solvents

A potential formulation was proposed which contained ESBO polymerised by 1 wt% of DBSA as the binder, 2 wt% hydrophobic fumed silica for surface hardening and 3 wt% carbon black as pigment. When combined this formulation did not mix readily and formed a viscous paste unsuitable for coating, a solvent was required to evenly disperse the solid particles and reduce viscosity. The industrial sponsors had strict guidelines governing the use of solvents in any future coatings. The guidelines ruled out any solvents that are;

- Carcinogenic, mutagenic or reprotoxic – which includes NMP
- Aromatic hydrocarbons
- Chlorinated solvents

It was decided to exclude alcohols as solvents due to their reactivity towards epoxides particularly in the presence of sulfonic acid catalysts.[202] During the coating process any formulation used is exposed to the air for extended periods, therefore a relatively non-volatile solvent is necessary so as not to evaporate and alter coating viscosity over time. Propyl acetate (Figure 2.25) was chosen, as it food safe (often used as pear flavour in food), and is considered a 'green' solvent with a boiling point of 102 °C.[203]

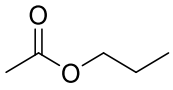

Figure 2.25. Propyl acetate

Viscosity is a significant factor in coil coating as this governs the amount of liquid transferred by the rollers to the surface, it is therefore important that any formulation has the same viscosity as currently used coatings.

Simple fluids such a air or water are known as Newtonian fluids which means viscosity is contant as the shear stress experienced by the liquid is linearly proportional to the shear force applied to it. More complex fluids such as polymer solutions, slurries or suspensions are non-Newtonian and cannot be described by one value of viscosity. The relationship beteween applied shear and stress is variable and can even be time dependant. For example a suspension of corn flour in water is shear thickening were viscosity is increased by an increased shear rate (eg faster stirring). Other fluids such as polymer solutions including paints/coatings exhibit shear

thinning (pseudoplastic) where viscoaity decreases upon increased shear rate. Shear thinning is common in modern paints as the sheer force of a brush or roller allows the paint to wet the surface, once applied high viscosity returns preventing drips or runs. The proposed formulation of this chapter would exhibit shear thinning.

For non-Newtonian fluids the measure of viscosity requires more parameters than simple liquids so the rheometry is measured which is the relationship between shear rate and shear stress. A rheometer applies a range of shear rates to a sample and measures the experienced stress is measured. The machine in this study is a cone and plate plate device where the sample is placed on a horizontal plate and a shallow cone is lowered into it. The cone rotates at increasing speed, increasing sheer force and the resistant force from the sample is measured. Newtonian fluids have viscosity independent of sheer rate substance like gasses and water, more complex solutions/suspensions do not behave this way. The rheometry data from the proposed formulation shows they exhibit a sheer thinning behaviour where viscosity decreases with increased sheer rate (Figure 2.26).

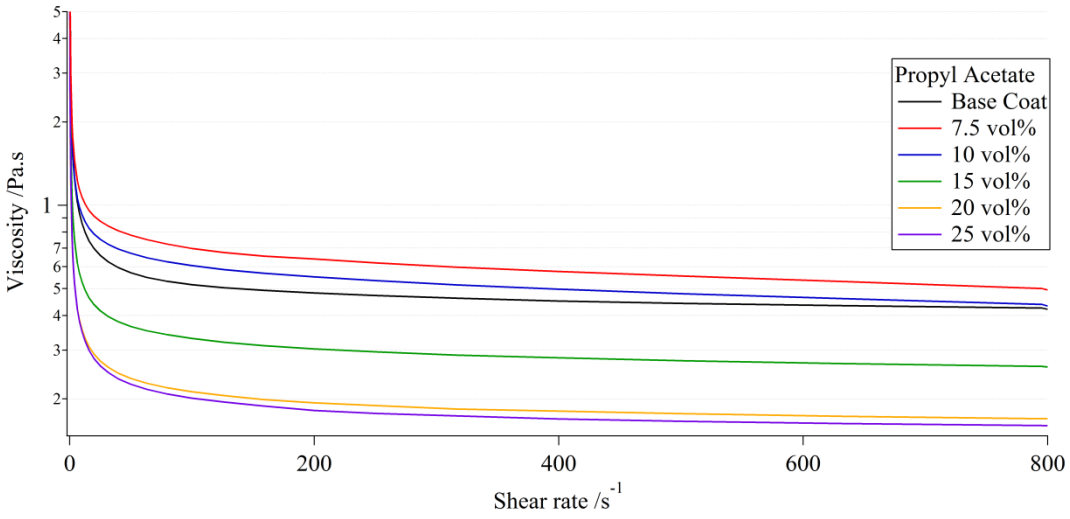

Figure 2.26. Rheometry measurements of ESBO based formulations with varied amounts of solvent. Shear rate varied from 0 to 800 revolutions per second at 25 °C under ambient atmosphere.

Coating formulations were produced with varied amounts of propyl acetate and the dynamic viscosity measured against a sample of ***Base Coat***. The coil coating used by the sponsors is a reverse roller coating, where the application rollers spin in the opposite direction to the coil, this is a high sheer process around 1000 s^{-1}.[204] The limit of our analysis was 800 s^{-1} (in order to keep the material on the plate), however it can be seen that 10 vol% of propyl acetate closely matches the commercial sample viscosity at high shear (Figure 2.26). ESBO is a liquid at room temperature, therefore a reduced amount of solvent is required compared to the commercial products (10 vol% vs 53-70 wt%) this is useful to reduce the environmental impact of the coating process.

2.8 Real World Product Testing

The industrial sponsors were interested in the optimum current formulation described above and wanted to perform further tests including some that mimicked 'real world' use. The formulation was produced on a larger scale (150g) and compromised of the following;

Component	Amount
ESBO	94 wt%
DBSA	1 wt%
Hydrophobic fumed silica	2 wt%
Carbon Black	3 wt%
Propyl acetate	10 vol%

Table 2.9. Composition of coating for product testing.

The formulation was coated onto an A4 sized sample of ECCS with a film thickness of 12 µ and cured at 400 °C for 60 s. The coating tests described earlier were performed (pencil hardness, X-hatch, Erichsen, flexibility) and this sample passed them all. However the coating was not even and the sample contained defects on the surface known as 'fish eyes' small crater like voids where no coating was present.

These defects are due to incomplete wetting of the substrate and can occur when the surface energy of the substrate is lower than the coating, and the coating has stronger attractive forces within itself than to the surface. These defects could have arisen from contamination or as a product of scale up as they were not observed on lab scale samples.

The sponsors wanted to perform some further tests involving cooking on and cleaning the test piece to mimic product use by the consumer. These tests were subjective, but it gave an idea of product performance. For the cooking test a piece of steak was placed on the sample coating and placed in a domestic oven at 200 °C for 1 h. Once removed the coating is assessed on food release and if any deposits remain. The food was easily removed however trace amounts, a thin layer in the shape of the meat sample, remained stuck to the surface.

For the cleaning test the sample is immersed in detergent for 20 min followed by cleaning with a scouring pad, the coating is assessed for ease of cleaning and integrity of the surface. The sample is then cleaned in a domestic dishwasher and assessed for any defects appearing or removal of coating. The epoxy soybean coating showed no signs of damage by the cleaning methods, but some evidence of food was still present on the surface indicating a fail on this test.

2.8.1 Removal of Fish Eye Defect

It is known that fatty acids can adsorb to a metal surface.[205] Metallic surfaces (in the case of ECCS a layer of chromium) are partially covered in oxides and hydroxides due to ambient air and moisture, as carboxylic acids come in contact with such a surface, hydrogen bonds can form. At elevated temperatures the physisorbed molecules can chemisorb with covalent bonds (Figure 2.27). To combat the ‘fish

eye' defects present in the formulation discussed above, epoxidised linoleic acid was added to the formulation (1, 2 and 5 wt%) to replace some of the ESBO content. Linoleic acid acts as a surfactant and the carboxylic group would increase attraction with the metallic surface and increase wetting. Once chemisorbed the epoxidised linoleic fatty chain would copolymerise with the ESBO binder.

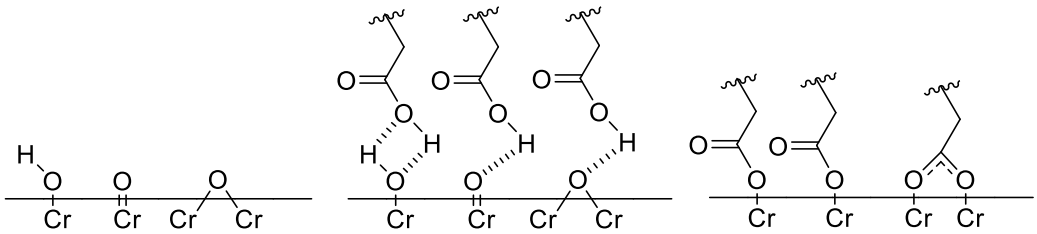

Figure 2.27. Adsorption of fatty acids to an ECCS surface.

In each of the coatings (1, 2, and 5wt% of epoxidised linoleic acid) on a lab scale, no fish eye defect was observed, possibly due to the increased wetting by surfactant behaviour. However, a fish eye defect was not observed in any of the previous lab scale coatings but only on the larger samples prepared at the sponsor's laboratory, further testing of this latest formulation on a larger scale is required to fully assess if the fish eye problem had been solved.

2.9 Conclusion and future work

In this chapter we have prepared a range of non-stick coatings for bakeware and produced a formulation based on an epoxy binder from renewable sources.

Firstly, analysis of the existing commercial formulations currently in use was performed. Anaylsis showed that in budget coatings, binders were based on bisphenol epoxides, but that higher performance coatings utilised polysulfone binders. The higher performance coatings had similar non-stick properties to the budget ones (~90° contact angle with water) but were significantly more thermally

stable. The commercial coatings were found to contain solid particles, such as silica and alumina for abrasion resistance, carbon black pigments and barium sulfate to modify roughness and reducing the amount of Teflon required.

In order to prepare a more sustainable non-stick coating it was necessary to replace the existing binders with a renewable binder as well as lowering the levels and toxicity of any solvents utilised. Lowering the curing temperatures of the existing commercial processes was also an aim. It was decided to pursue the use of renewable vegetable oil based epoxy binders as they had previously been shown to have high thermal stability, hydrophobicity and were safe for food contact. Modification of a range of plant oils by epoxidation was simple and produced epoxy monomers in good yield (~90%). Polymerisation was achieved by two methods, photoinitiation and thermal curing with TAS. With UV polymerisation adhesion was poor, while thermal polymerisation was more successful and allowed a range of coatings to be tested. Epoxidised soybean oil (ESBO) was chosen as the binder, but hardness of the coatings was poor for commercial applications. The addition of fumed silica (5 wt%) allowed for a tailored increase in hardness of the coatings, while the addition of carbon black (3 wt%) provided a cosmetically acceptable product. However, the contact angles (water) of the materials were too low and incorporation of Teflon into the formulation failed due to incompatability (phase separation) with the binder.

The use of sulfonic acids as replacements to TAS for thermal polymerisation of ESBO was examined and food safe DBSA produced materials that were more flexible (due to the plasticizing effect) than those produced from CSA. Addition of solid particles provided improvements to the blank polymer, fumed silica increased surface hardness potentially through increased crosslinking between the epoxides

and the OH groups on the silica, with 2 wt% being the most effective. As with the TAS coatings, carbon black pigment was successful at disguising discolouration of the thermal cured polymers. The viscosity of the formulation was optimised for roller coating applications by the addition of 10% propyl acetate solvent. The optimised formulation produced a coating that had a contact angle with water of 85°C, however this was without any release agents. Preparing coatings on a large scale for industry tests led to a fish eye defect which could be removed using an additional amount (1-3%) of epoxidised linoleic acid. Industry tests to mimic real world use in the kitchen also identified the requirement for a release agent.

Due to the incompatibly of our renewable formulation with Teflon, it was decided to investigate the use of other release agents in the formulation. The next chapter will investigate the use of silicones and novel silicone / vegetable oil epoxide hybrid polymers as release agents to increase the hydrophobicity of the coatings.

3 Investigation into a Silicone Containing Additive Produced by Hydrosilylation for use in Non-stick Coatings

3.1 Introduction

In the previous chapter we described how a renewable binder, based upon thermal or UV initiated polymerisation of epoxidised soybean oil, could be used in a new coating formulation. While epoxidised soybean oil proved to be effective as a binder when combined with silica particles, it failed when Teflon particles were added, due to inefficient adhesion of the Teflon to the renewable binder. The properties of the silica coating passed the industry standard surface hardness, adhesion and flexibility tests but failed when it came to its non-stick ability, this was mainly due to relying on the hydrophobicity of the oil based binder as there was no other release agent present in the formulation. Silicone polymers have been reported to exhibit non-stick and release characteristics and could be used as a replacement to Teflon.[206,207,208] Industrially silicones are used in paints and coatings where the low surface energy promotes wetting of the substrate.[206] Polysiloxanes can also be used due to their low surface energy, high thermal stability and smooth texture. Polysiloxanes are used in pressure sensitive adhesives as they have good release properties without leaving adhesive residue[207] and are also widely used in mould making where the non-stick ability allows the product to be easily removed.[208] Short chain silicone oils are used as a release sprays on aluminium moulds during injection moulding. Another advantage for utilising a silicone as a non-stick component in our coatings, is that they are low taint non-toxic materials, widely where food contact is required. In the food processing industry silicones are used as

antifoam agents. Domestically silicones are used in cookware, where modern utensils are often coated in silicone rubber, and silicone rubber cake tins are available. But the main use is in non-stick coatings, silicones due to their high temperature stability and low surface energy are a viable alternative to Teflon based coatings.

Consequently we decided to investigate the use of a compatible silicone additive to the coating as a release agent. Consequently, we decided to investigate the synthesis and application of hybrid fatty acid / silicone material.

3.1.1 Hydrosilylation

Hydrosilylation is the addition of a Si-H bond across an unsaturated bond and was first documented in 1947.[209] The typical substrates for hydrosilylation are alkenes, forming alkyl silanes, alkynes creating vinyl silanes,[210] and aldehydes[211] or ketones[212] producing silyl ethers. The reaction requires a metal catalyst usually rhodium[213] (such as Wilkinson catalyst),[214] ruthenium[215] (in some cases Grubb's 1st generation can be employed)[216] or more often platinum, the most commonly used platinum complexes are Spier's[217] or Karstedt's[218] catalysts (Figure 3.1).

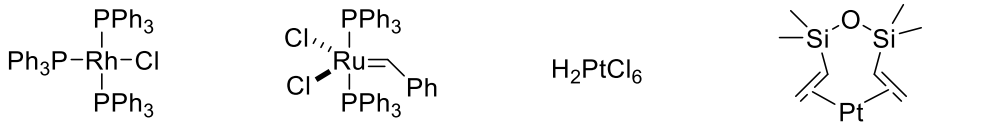

Figure 3.1. Structures of commonly used catalysts for hydrosilylation.

One of the most common uses of hydrosilylation in industry is to create Si-C bonds in the manufacture of silicone monomers with hydrocarbon functionality.[219] The

monomers can then undergo condensation polymerisation to form polysiloxanes, such as in mould making kits or bathroom sealants.

Another use for hydrosilylation is for vulcanising silicone rubbers, which is the crosslinking of polysiloxane (silicone) chains. Crosslinking occurs between silicone chains functionalised with vinyl groups and silicones containing silicon hydride bonds[220]

Hydrosilylation which is an effective choice for making carbon-silicon bonds has previously been explored with fatty acid and ester based compounds. The work by Saghian and Gertner[221] involved the hydrosilylation of methyl oleate, methyl linoleate and methyl 10-undeanoate with various chlorine containing silanes using chloroplatinic acid as the catalyst, however the reactions had to be performed in a pressurised vessel at 90 °C. Studies by Kadib *et al*[222] show that triglycerides are suitable substrates for hydrosilylation, however internal C=C bonds required harsh conditions. For methyl linoleate a mixture of radical initiators at 150 °C for 60 h was required and for triglycerides the use of a Carrius tube under pressure for 72 h was needed. Only chlorine containing silanes were active as the reaction with triethoxy silane was shown to be ineffective. Ronda and Cádiz[223] have shown Karstedt's catalyst to be an effective catalyst under mild conditions for hydrosilylation of the terminal alkene in methyl 10-undecanoate for the production of silicon containing polyols. The reactions were performed at 65 °C for only 2 h, however no work on internal C=C bonds were investigated under these conditions. Arno Behr[224] showed a range of platinum catalysts to give average to good yields for hydrosilylation of methyl 10-undecanoate and methyl linoleate respectively using mild conditions. The reactions were performed at 40 °C and took 4 h for methyl linoleate and only 10 min for methyl 10-undecanote. Again only chlorine containing silanes were used and it

was found that after 45 minutes of reacting some high boiling point products had formed, possibly dimers due to the reactive Si-Cl bond. In a subsequent paper[225] it was shown that hydrosilylation using chlorine free silanes was unsuccessful. *Consequently, for further exploitation of fatty acids there is a need for a mild method of hydrosilylation of vegetable oil derivatives.*

3.2 Aims

In this study we initially chose to investigate the hydrosilylation, using Karstedt's catalyst and mild conditions, on internal C=C bonds of fatty acids, fatty esters and triglycerides. We chose three silanes, the monofunctional triethyl silane, the difunctional PDMS and a polyfuntional polysiloxane (Figure 3.2).

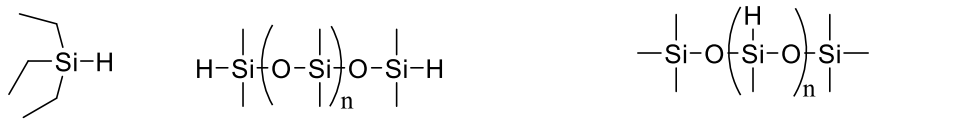

Triethyl silane | DMS-H11 Mn = 1,100 g/mol; DMS-H25 Mn = 17,200 g/mol | HMS-991 Mn = 1400 g/mol

Figure 3.2. Silanes used in this study

The use of triethyl silane would allow us to determine reactivity, regioselectivity and effectiveness in a simple model, while the difunctional and polyfunctional siloxanes would allow us to prepare cross-linked silicone rubbers with a renewable content. By changing the type of plant oil and polysiloxane the level of crosslinking will be affected, which would alter the properties of the rubber. We would then use the results obtained in these first studies to design a hybrid epoxidised fatty acid siloxane for use as a binder and release agent for a renewable non-stick coating. In this case, the new material should exhibit the same standard surface hardness, adhesion and flexibility of those obtained in chapter 2 but with an increased non-stick ability.

3.3 Results and Discussion

3.3.1 Hydrosilylation of Oleic and Linoleic Acids with Triethyl Silane

Our collaborators felt it was important industrially to develop a solvent free approach to hydrosilylation. In this study a modified version of the solvent free method used by Behr[224] was followed. Our approach was to combine the silane and unsaturated oil in an inert atmosphere with a catalyst at 40 °C for 4 h. However, while the published procedure utilised hexachloroplatinic acid (Spier's catalyst) as a catalyst we investigated the alternative Karstedt's catalyst.

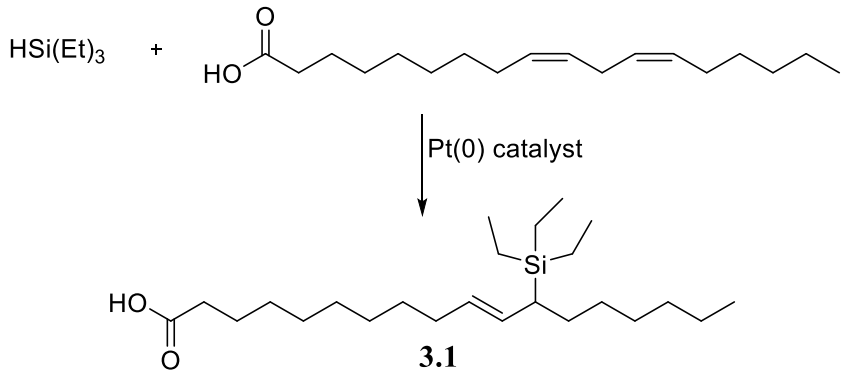

Figure 3.3. Hydrosilylation of linoleic acid with triethyl silane.

We chose to initially investigate the addition of triethyl silane to three fatty acid derivatives, notably linoleic acid (Figure 3.3), oleic acid and methyl oleate under the conditions stated above. The reactions were monitored with ^{1}H NMR (Figure 3.4) seeking the disappearance of alkene protons (5.3 ppm) and silicone hydride peak at 3.5 ppm to assess conversion.

For oleic acid and methyl oleate no reaction had occurred after 4 h. Repeating the reaction with methyl oleate but for 20 h only showed a 10% conversion by ^{1}H NMR but a peak corresponding to the product was visible in the ESI-MS ($[M+H]^{+}$ = 413.2). While this was disappointing, much better results were obtained for the reaction with linoleic acid.

For linoleic acid complete loss of Si-H was observed along with 50% of the alkene peaks which is consistent with work by Behr for silyl chlorides.[224] This suggests that only one alkene had reacted and migration of the remaining C=C bond to the α-position relative to the silanyl substituted carbon had occurred and was confirmed by ^{1}H NMR (Figure 3.4). The loss of the peak at 2.75 ppm, (representing the allylic protons of the skipped diene) but the retention of the other allylic protons at 2.00 ppm confirms this. FT-IR analysis showed an absence of the Si-H bond indicating complete reaction of the silane. While the ESI-MS data showed peaks consistent with the sodium and potassium adducts of compound **3.1** it also indicated a small amount of oleic acid present. This may have arisen from a hydrogenation reaction using triethylsilane as the hydrogen source, this has been observed in literature for related structures.[224]

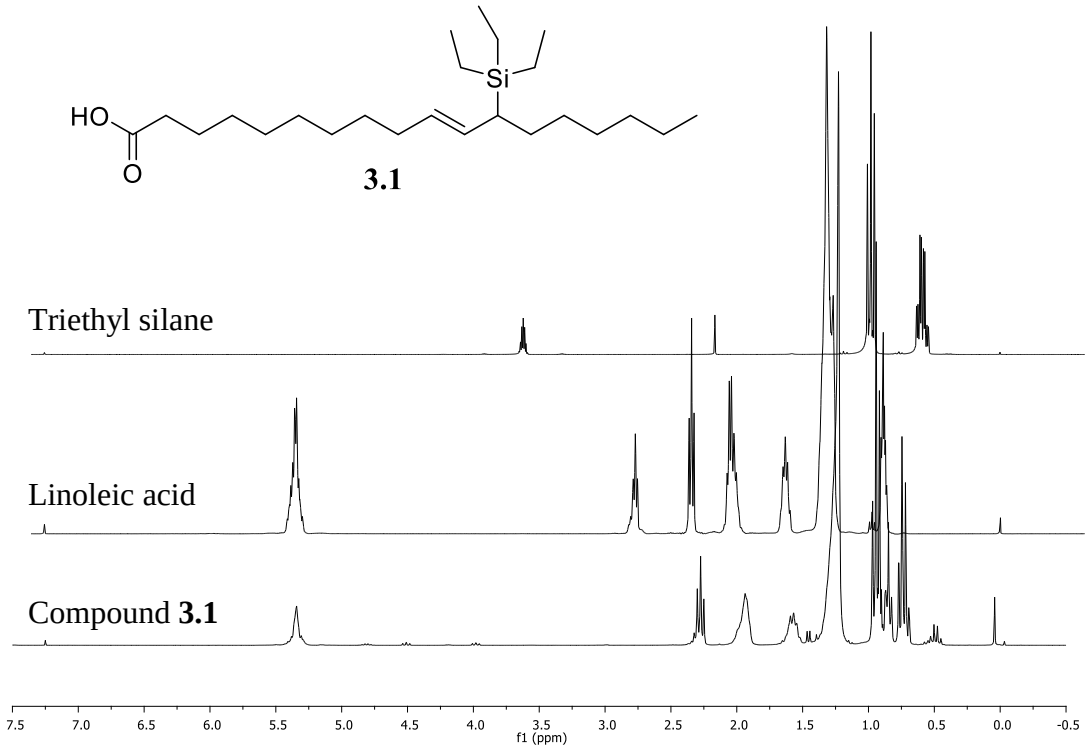

Figure 3.4. ^{1}H NMR (300MHz, $CDCl_3$) of triethyl silane, linoleic acid and the hydrosilylation product **3.1**.

3.3.2 Hydrosilylation with Polysiloxane

Having found appropriate conditions for hydrosilylation with triethyl silane we next examined the reactions with the polysiloxanes (as before without solvent). A polysiloxane was provided by Gelest Inc with a PDMS backbone and terminal Si-H bonds and a molecular weight of 1000 – 1100 Da (the product code was DMS-H11). This silane was reacted with linoleic acid in a 1:1 ratio under the same conditions as above. However linoleic acid and DMS-H11 did not readily mix so rapid stirring was used to create an emulsion. If both alkenes of the linoleic acid reacted then the equal numbers of C=C and Si-H bonds should form a long chain polymer. However, in light of the results obtained in section 3.3.1 it was not surprising that this was not the case. Only one alkene per molecule reacted and migration of the other double bond occurred in a similar manner to the previous reaction. This was confirmed in the ^{1}H and ^{13}C NMR spectra showing the presence of C=C and Si-H (Figure 3.5) **3.2.**

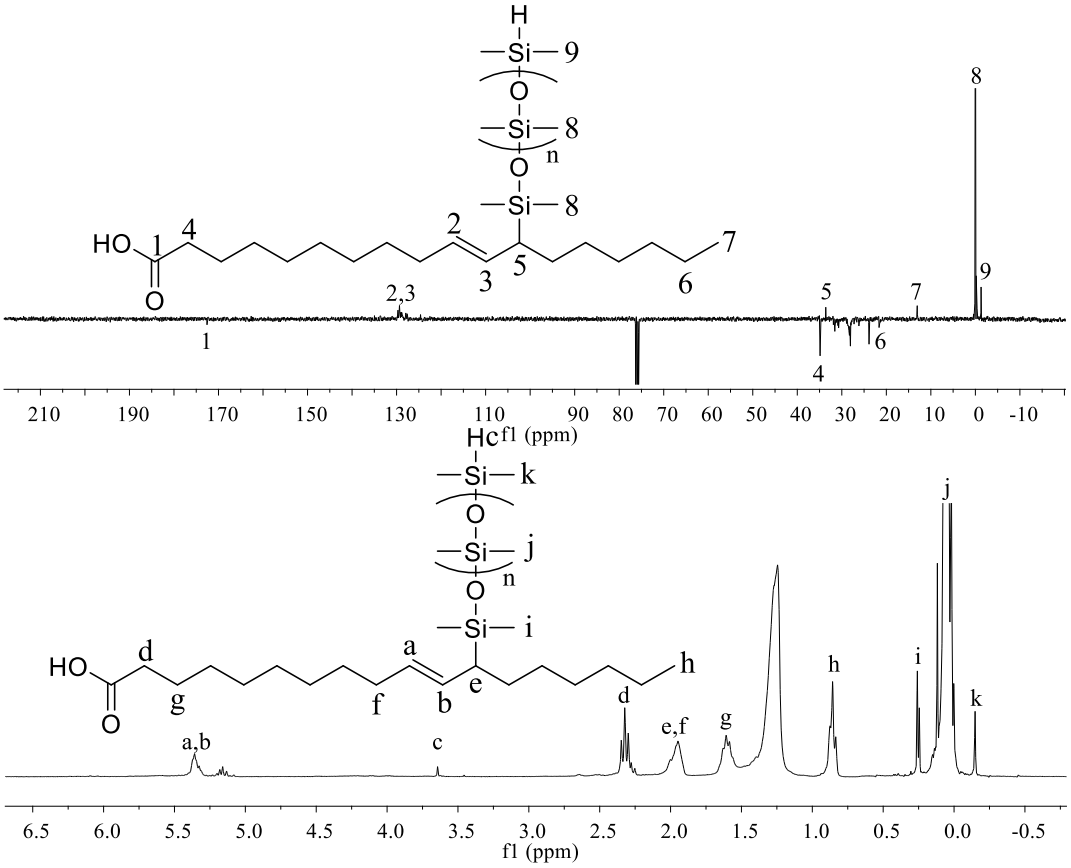

Figure 3.5. NMR (400MHz, $CDCl_3$) analysis of compound **3.2**.

This reaction was repeated with a 2:1 ratio of linoleic acid to siloxane in order to fully react the terminal hydride bonds and make the dimeric derivative **3.3.** (Figure 3.6). Interestingly, this novel derivative retains alkene functionality that could be further epoxidised to make a silylated monomer containing two epoxide groups (Figure 3.7).

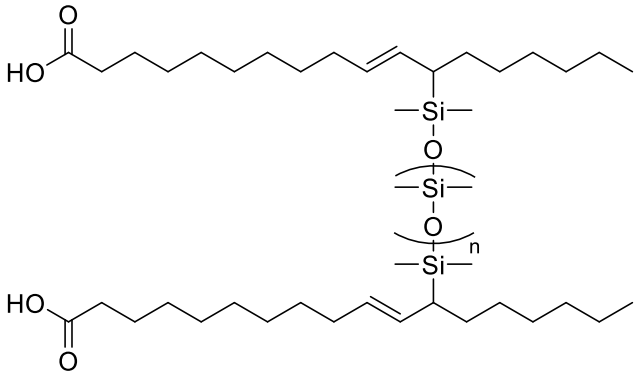

Figure 3.6. NMR (400MHz, $CDCl_3$) analysis of compound **3.3** two linoleic acid molecules joined by a PDMS chain

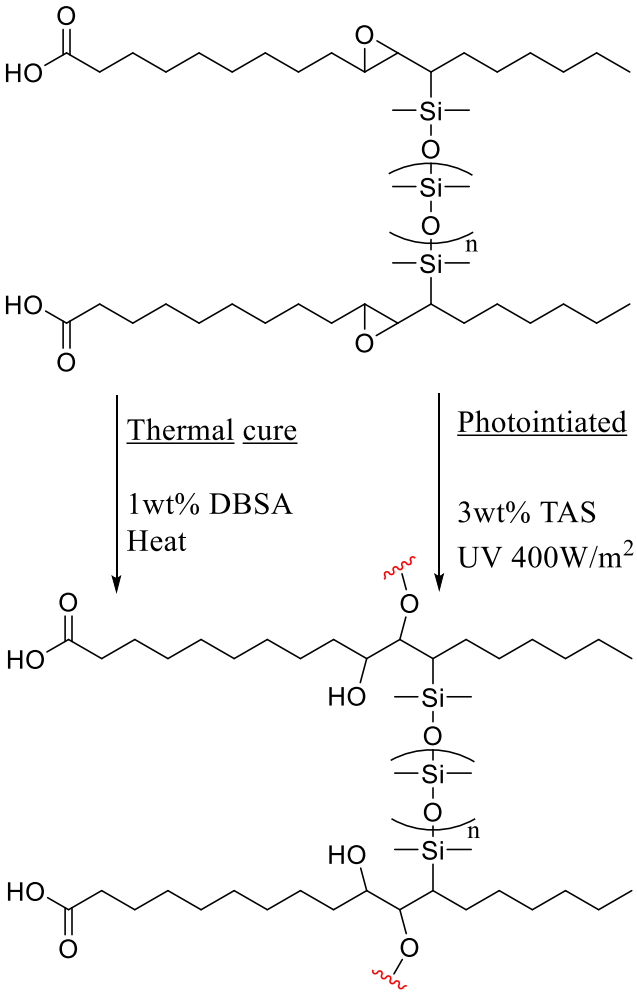

Figure 3.7. Potential route for silicone containing epoxy polymers.

^{1}H NMR and FT-IR analysis of the obtained monomer **3.3** showed no presence of any remaining Si-H bond and a 50% reduction in C=C proton signals as observed before. GPC results indicated a large molecule with a Mn of 2209 and Mw of 2833 (although the GPC was calibrated with PMMA standards and so these results should be taken as approximate).

In order to make a cross-linked derivative we required a starting material that contained more than two linoleic side-chains. The fatty acid content of grapeseed oil is around 70% linoleic (average 2.2 chains per molecule available for hydrosilylation). The aim was to react grapeseed oil with DMS-H11 in order to form a crosslinked network of PDMS and fatty acids, the crosslinks would be formed by

the hydrosilyated double bonds and glycerol of the vegetable oil. Grapeseed and DMS-H11 were mixed in a 1:1 ratio and reacted at 40 °C for 4h as previously, after this time a green tinted oil was observed, the ^{1}H HMR data showed about a 50% reduction in C=C bonds as before but the FT-IR still indicated the presence of Si-H bonds. The GPC results showed the presence of unreacted silane or grapeseed oil (1176), hydrosilated grapeseed oil (2167) and peak at 5098 indicating dimerisation may have started (Figure 3.8).

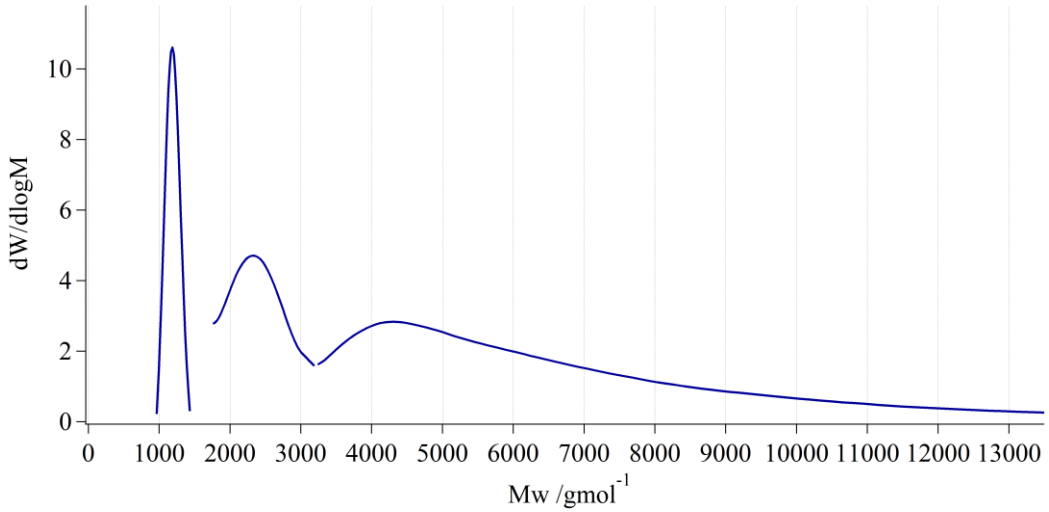

Figure 3.8. GPC analysis of hydrosilylation of grapeseed oil with DMS-H11. Detected by refractive index, calibrated against a polystyrene standard, eluent was chloroform.

With evidence suggesting onset of polymerisation the reaction was repeated and left at 40 °C for 5 days, after which time a soft gel had formed (**3.4**) insoluble in a range of common solvents; acetone, chloroform, dichloromethane, diethyl ether, ethanol, ethyl acetate, hexane, methanol and toluene which suggests crosslinking or possibly hyperbranching. The reaction was repeated at 100 °C to decrease reaction times, polymerisation was apparent after 1 hour, but the reaction was left overnight to ensure complete curing (18 h, **3.5**).

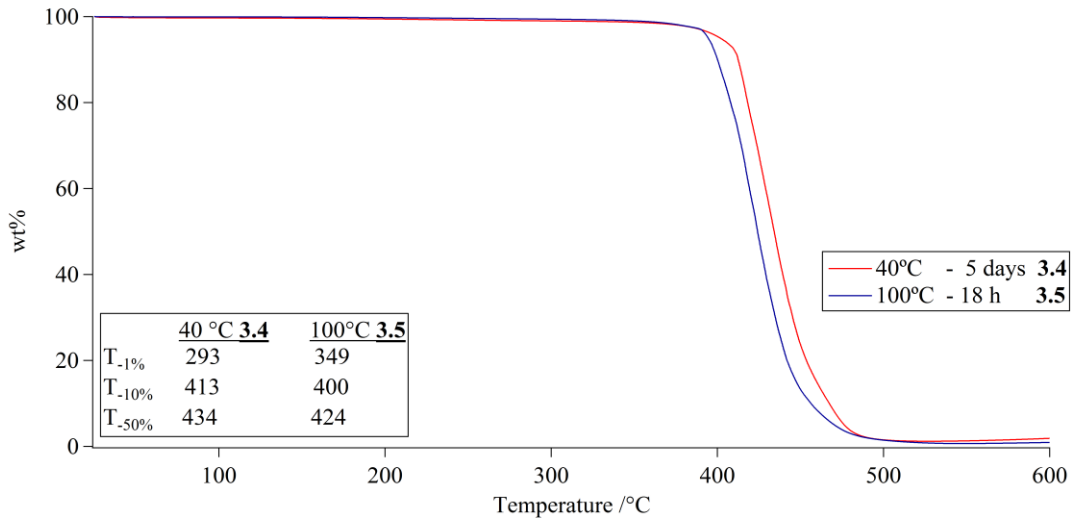

Figure 3.9. TGA analysis of grapeseed oil hydrosilylation by DMS-H11 at 40 °C and 100 °C. Heating rate was 10 °C min^{-1} from 0 – 600 °C under ambient atmosphere.

TGA analysis shows polymer **3.4** has a onset degradation temperature of 290 °C (cured over 5 days at 40 °C) while polymer **3.5** had a much higher onset degradation temperature of 349 °C (cured over 18 h at 100 °C)(Figure 3.9). This is consistent with other work showing PDMS degradation temperatures ~290 °C.[226] Faster curing at higher temperature has increased onset thermal degradation by 50 °C, presumably due to more complete polymerisation and increased cross-linking. High temperature curing initiates chemical reactions even at the most hindered areas and provide enough mobility to fully network. These hybrid grapeseed oil / siloxanes contain 46% renewable content by weight. We next investigated the effect of a range of different renewable oils and silanes to prepare a range of silicone rubbers.

3.3.3 Silicone Rubbers

It is well known silicones are an important material for uses as adhesives and sealants. Taking into account our preliminary results we briefly studied creating silicone rubbers with renewable content. By using the reactions investigated above using plant oils instead of fatty acids (which contain a greater number of C=C double

bonds per molecule) a crosslinked network would be possible. Due to the success of the previous reactions with linoleic acid, oils that contained significant quantities of polyunsaturated side-chains were chosen. In this study we compared grapeseed (containing 72.5% of linoleic acid chains), with soybean (61.6%) and rapeseed oils (30.5%). We chose to hydrosilylate each of these oils with three different polysiloxanes, supplied by Gelest. We chose DMS-H11 and DMS-H25, both PDMS chains with terminal silicon hydrides and molecular weights of 1000-1100 g/mol and 17200 g/mol respectively and HMS-991 a siloxane with multiple Si-H bonds along the backbone of the chain and mass of 1400-1800 g/mol (Figure 3.10).

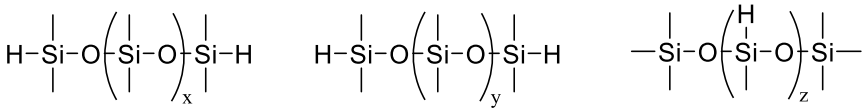

DMS-H11 Mw = 1000-1100 g/mol | DMS-H25 Mw = 17200 g/mol | HMS-H11 Mw = 1400 - 1800 g/mol

Figure 3.10. Structure of the reactive silicones used in this study.

Each oil was combined with the difunctional silanes in a 1:1 mol ratio, the multifunctional silane HMS-H11 was calculated to have roughly 24 repeat units so was combined with the oils in a 12:1 ratio of oil to silane. The reaction mixtures were heated in a nitrogen atmosphere to 100 °C, a gel typically formed after 1-2 h but the reactions were left overnight to ensure complete curing. This produced 9 samples varying in physical appearance (Table 3.1).

Polymer		Appearance
GSO-H11	**3.6**	Dry to touch, brittle, green tint
GSO-H25	**3.7**	Dry to touch, flexible, green tint
GSO-991	**3.8**	Dry to touch, brittle, green tint
SBO-H11	**3.9**	Dry to touch, brittle, green/yellow
SBO-H25	**3.10**	Dry to touch, elastic, green/yellow
SBO-991	**3.11**	Dry, to touch, brittle, green/yellow
RSO-H11	**3.12**	Tacky, flexible, yellow/brown
RSO-H25	**3.13**	Sticky, v. elastic, yellow/brown
RSO-991	**3.14**	Tacky, elastic, yellow/brown

Table 3.1. Physical appearance of silicone- plant oil polymers.

The colour of the samples were governed by the colour of the starting oil and were unaffected by heating. Higher unsaturated oil based polymers were dry to the touch and were brittle (e.g. grapeseed based **3.6** – **3.8**). Lower unsaturated samples (rapeseed **3.12 – 3.14**) had greater elasticity and were tacky. Polymers with DMS-H25 silane (**3.7**, **3.10** and **3.13**) were also more flexible than the other silanes.

The physical properties can be attributed to the level crosslinking, the crosslinking density can be calculated using the Flory-Rehner equation[227]

$$M_c = \frac{\nu_s \, \rho_p \left(V_p^{\frac{1}{3}} - V_p/2 \right)}{\ln(1 - V_p) + V_p + \chi V_p^2} \quad \text{and} \quad \upsilon_c = \frac{\rho_P}{M_c}$$

Where $1 + Q = \frac{1}{Vp}$ and $Q = \frac{(\omega_0 - \omega_1)\rho_p}{\omega_0 \rho_s}$

The crosslinking density υ_c is stated as the moles of crosslinks per cm^3 and is calculated from the relationship between polymer density ρ_p and the molar mass between crosslinks M_c. For these equations measurements of polymer density ρ_p, initial weight of sample ω_o and weight of swelled sample ω_1 were required. Polymer density was calculated by weight divided by volume (from water displacement). For

swelling, samples of ~0.5 g were immersed in 15 mL of toluene at room temperature for 1 week, with gentle swirling daily.

Polymer		Cosslinking Density x 10^{-4} mol/cm^3
GSO-H11	**3.6**	0.21
GSO-H25	**3.7**	0.15
GSO-991	**3.8**	11.80
SBO-H11	**3.9**	0.20
SBO-H25	**3.10**	0.17
SBO-991	**3.11**	10.68
RSO-H11	**3.12**	-
RSO-H25	**3.13**	0.09
RSO-991	**3.14**	-

Table 3.2. Crosslinking density of plant oil silicone rubbers.

The trend in crosslinking data (Table 3.2) between different oils loosely follows the level unsaturation e.g. for DMS-H25; GSO (0.15), SBO (0.17) and RSO (0.09 x 10^{-4} mol/cm^3). The higher unsaturated oils (GSO, SBO) had greater crosslinking density than the more saturated oil (RSO) which accounts for the difference in flexibility. The type of silane also had an effect on crosslinking, longer chain silanes produced rubbers of a lower crosslink density e.g. GSO - H11 (0.21) and H25 (0.15), and the multifunctional silane as expected had a much greater density (11.8 x 10^{-4-} mol/cm^3), this is also observed in the physical properties.

Interestingly two of the rapeseed oils had dissolved during this experiment. One reason for dissolution could be that rapeseed oil only has ~30% polyunsaturated chains, roughly one per molecule, so is unlikely to propagate polymerisation. Rapeseed oil is more likely to end cap the difunctional silanes and attach as pendant groups on the multifunctional silane HMS-991. It is presently unclear as to why RSO-H25 did not dissolve.

Silicone rubbers are well known for their thermal stability[226] and their chemical inertness and are often used in cooking utensils for this reason. Decomposition of the alkyl chains in the triglycerides would be expected to occur at a slightly lower temperature (380-440 °C) than the siloxane portion (>420°C) of any polymer and incorporation of a longer siloxane chain (HMS11 →HMS25) should lead to higher thermal stability. This expected trend was observed and can be seen when these silicones were examined using TGA (Figure 3.11).

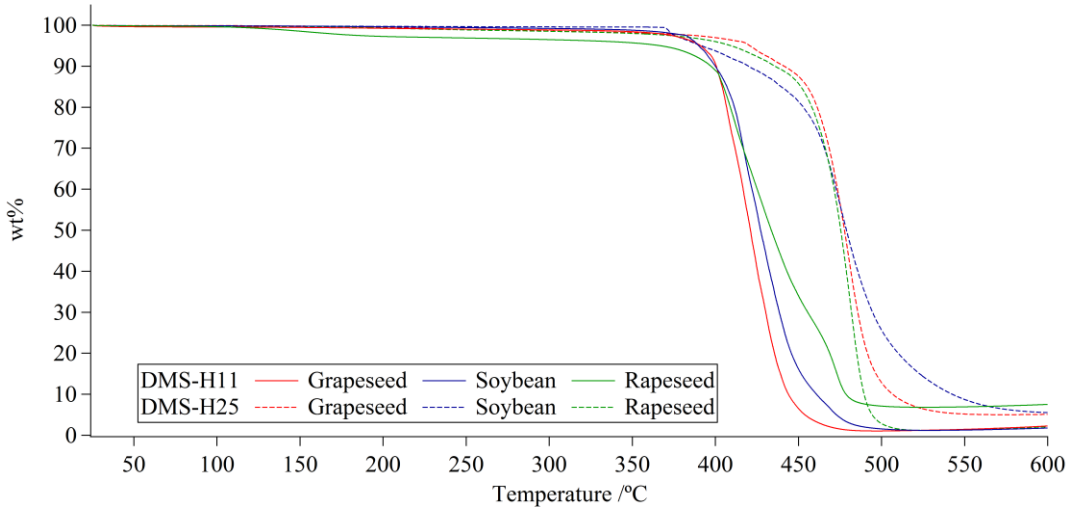

Figure 3.11. TGA of DMS-H11 and DMS-H25 copolymerised plant oil silicone rubbers. Heating rate was 10 °C min^{-1} from 25 – 600 °C under ambient atmosphere.

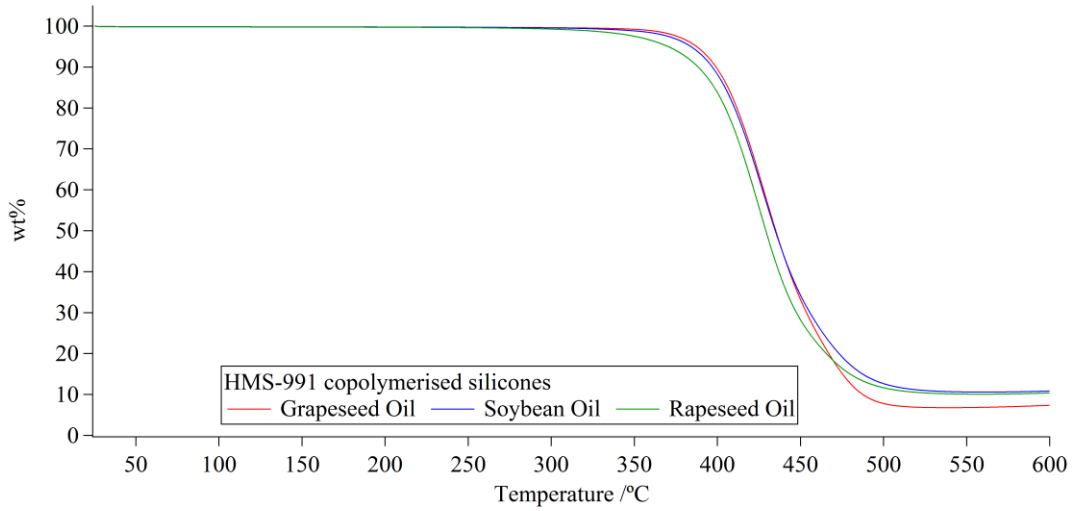

Figure 3.12. TGA of grapeseed, soybean and rapeseed oil and HMS-991 copolymer gels. Heating rate was 10 °C min^{-1} from 25 – 600 °C under ambient atmosphere.

The results in Table 3.3 show there is little difference between the oils for a particular silane, a subtle trend is present of GSO>SBO>RSO which matches the crosslinking density reported above.

Between silanes the trend is that long silicone chains result in higher degradation temperatures e.g. soybean polymers at $T_{-10\%}$ DMS-H11 (400 °C), DMS-H25 (420 °C) and HMS-991 (397 °C), this trend remains true at 50% degradation. Silicones are more thermally stable than alkyl chains due to a stronger bond energy (S-O = 452 $kJmol^{-1}$ and C-C = 346 $kJml^{-1}$), longer chains contain more silicone by weight in the polymer (1:1 ***mol*** ratio used). Silicones have also shown to create an inorganic silica layer on the surface upon heating in air which protects the under layers from heat,[228] further increasing their thermal stability.

Polymer		$T_{-1\%}$ /°C	$T_{-10\%}$ /°C	$T_{-50\%}$ /°C
GSO-H11	**3.6**	259	401	421
GSO-H25	**3.7**	251	442	478
GSO-991	**3.8**	359	399	435
SBO-H11	**3.9**	332	400	427
SBO-H25	**3.10**	371	420	479
SBO-991	**3.11**	344	397	435
RSO-H11	**3.12**	135	397	434
RSO-H25	**3.13**	232	436	476
RSO-991	**3.14**	316	389	429

Table 3.3. TGA results of plant oil - silicone polymers.

Polymerisation with the polysiloxane HMS-991 leads to three materials with similar thermal profiles (see Figure 3.12). From our hydrosilylation results earlier in this chapter hydrosilylation only occurs on polyunsaturated chains, therefore the level of unsaturation in each oils should be similar after hydrosilylation roughly 1 C=C per chain. This may account for their similar degradation temperatures.

In conclusion, we have reported a range of silicone rubbers formed by hydrosilylation of three different plant oils. Alkene functionality and silane choice can govern crosslink density which in turn determines physical properties. Thermal degradation is largely unaffected by varying plant oils, but can be altered by siloxane content with more silicone giving a higher degradation temperature.

We next further studied the relationship between plant oil – silicone based materials through hydrosilylation for their application in non-stick coatings.

3.3.4 Silicone Containing Coating Additive

Polysiloxanes have been widely used to prevent adhesion to a surface, they can be applied externally, such as silicone release sprays used in injection moulding, or as part of the coating on the surface as used in the bakeware industry. As discovered earlier in section 3.3.2 vegetable oils and polysiloxanes do not mix readily and an emulsion will phase separate fairly quickly, consequently, the use of a silicone

would not be beneficial for a non-stick coating where the main component is based on a vegetable oil epoxide such as the coating formulations reported in earlier chapters. However, if the silicone was able to be covalently linked to the vegetable oil epoxide (such as structures **3.18** and **3.20** Figure 3.13) then this may overcome these problems.

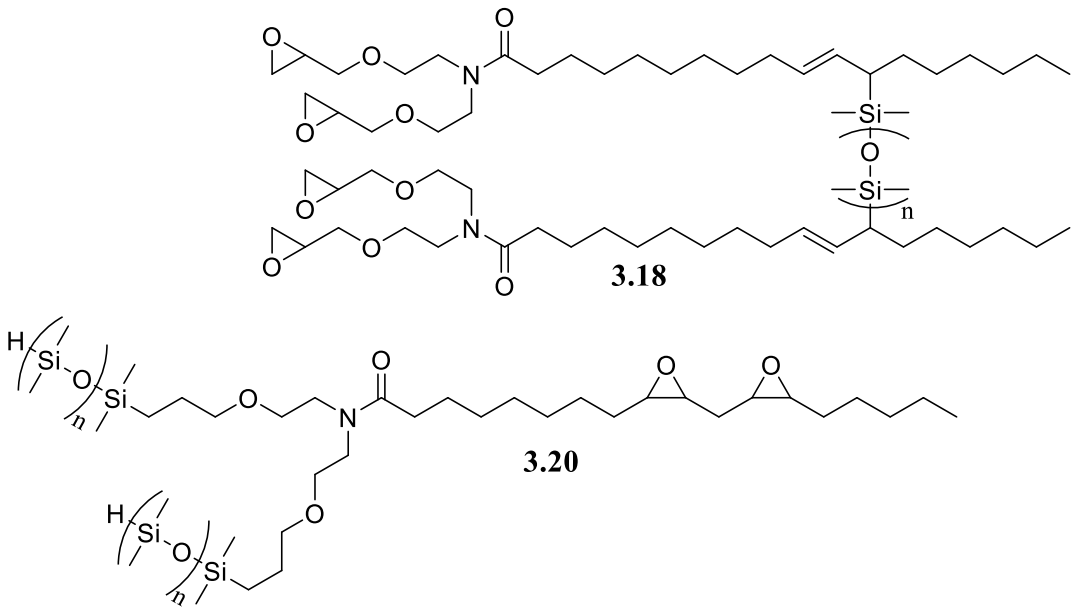

Figure 3.13. Potential silicone containing epoxide monomers for non-stick coating formulations.

*Consequently, it was decided to look at the possibility of using hydrosilylation to covalently bond a polysiloxane to an epoxidised fatty acid derivative **3.18** in order to produce a release agent that would co-polymerise with the epoxy soybean oil binder (Figure 3.14).*

3.3.5 Synthesis of Silicone / Epoxy Fatty Acid Hybrids

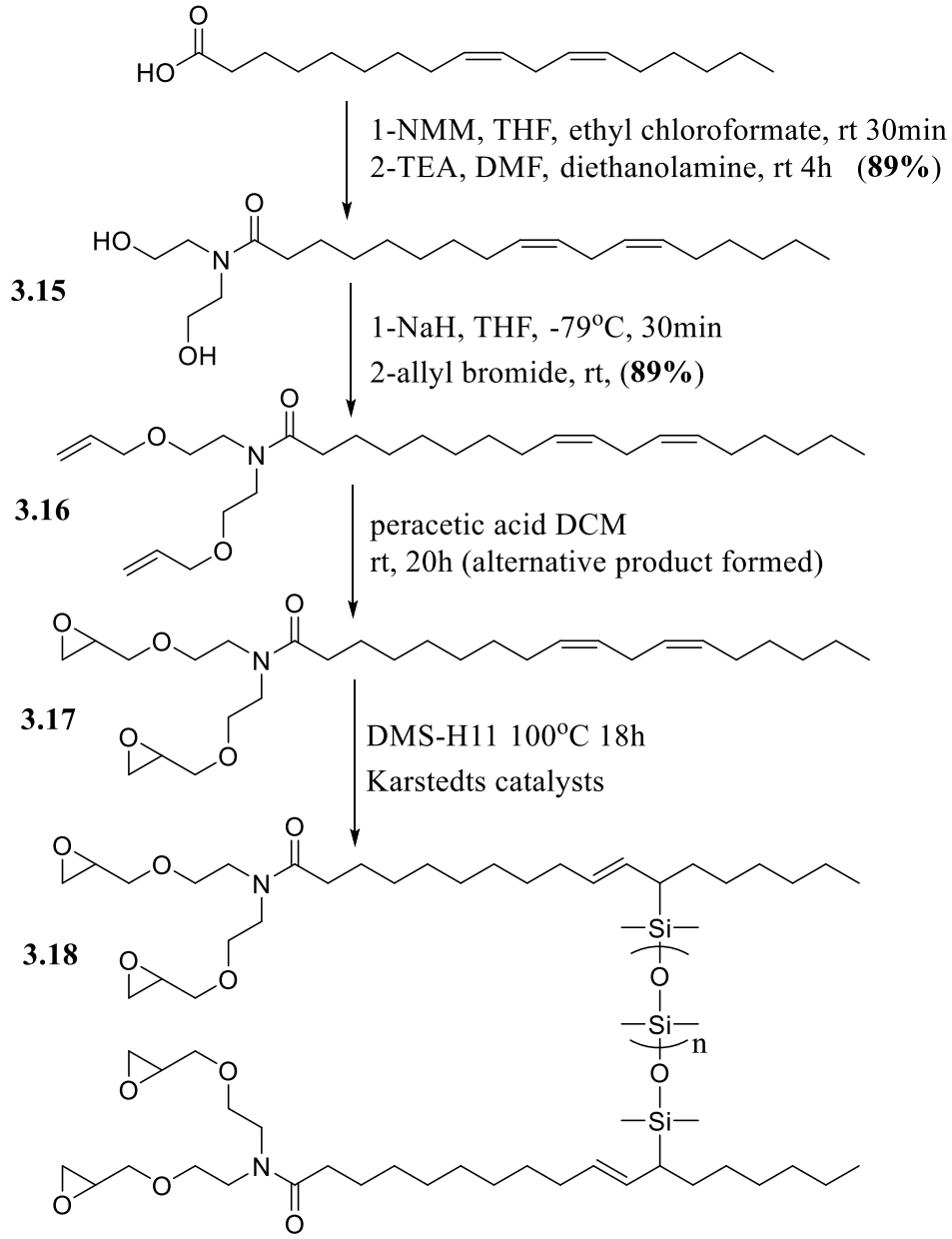

Figure 3.14. Proposed route to fatty acid containing silicone release agent.

Synthesis of siloxane / epoxy hybrid fatty acid monomers

Our initial approach towards monomer **3.18** is shown below. Hence, amidation followed by allylation would provide the difunctionalised molecule **3.16** which after selective epoxidation and hydrosilylation would provide a hybrid monomer 3.18 suitable for incorporation into the non-stick coating formulation. Amide **3.15** was

prepared by the method of Rho *et al.*[229] Hence, reaction of linoleic acid with ethylchloroformate produced a mixed anhydride intermediate that was then subjected to substitution by diethanolamine. Washing with copious amounts of water to remove traces of DMF furnished **3.15** in 89% yield which was used without further purification. No *O*-substituted or *N,O*-disubstituted by-products were observed. This reaction provides a useful general method for synthesising amides from fatty acids as it requires mild conditions, is rapid (~5 h) and produces products with high yield (89%) and purity.

In order to prepare terminal epoxides it was first necessary to functionalise the hydroxyl groups with alkene substituents. Hence amide **3.15** was deprotonated with NaH at -78 °C followed by the addition of allyl bromide. The reaction was warmed to room temperature and stirred overnight to give **3.16** in 89% yield after purification. The next step required epoxidation of the terminal alkenes. Consequently, epoxidation was carried out using the standard conditions previously described, peracetic acid in DCM. However, analysis of the product from this reaction confirmed that the fatty acid alkenes had been preferentially epoxidised over the terminal alkenes producing compound **3.19** (Figure 3.15). This is presumably because the internal alkenes are more electron rich (disubstituted) than the terminal ones (monosubstituted) and hence react faster with the electron poor peracids.

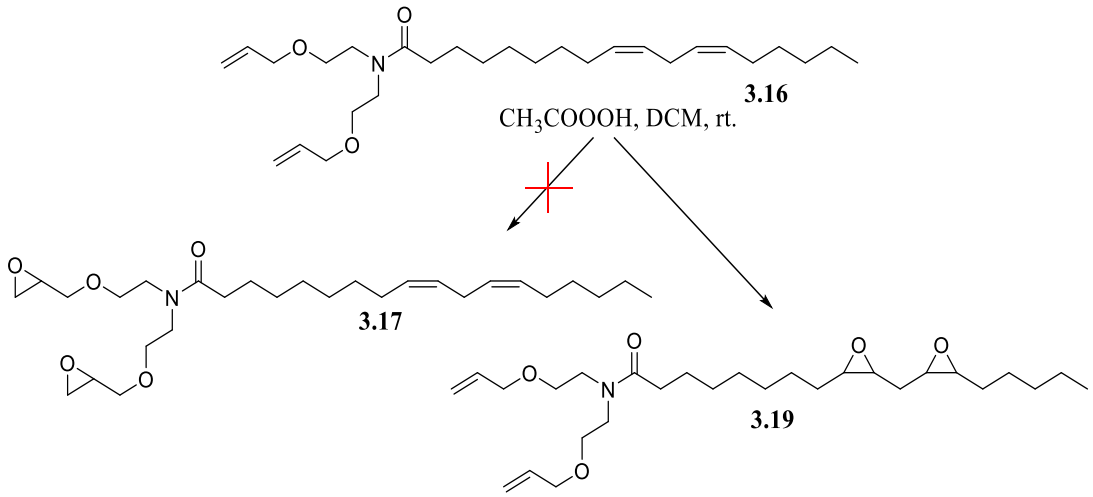

Figure 3.15. Epoxidation of vinyl fatty amide **3.16** showing nearly 100% selectivity towards internal C=C bonds (**3.19**).

Monitoring the epoxidation by ^{1}H NMR indicated that the reaction was complete after 20 hours (97%). The conversion was obtained by measuring the ratio of the disappearance of the alkene protons at 5.4 ppm and the appearance of epoxide protons at 2.9 – 3.1 ppm (Figure 3.3.16). It was found that after 30 min the conversion was 62% which rose to 86 % after 4 h (Figure 3.3.17). This has commercial implications as it may be more economically viable to sacrifice some epoxy content to gain shorter reaction times.

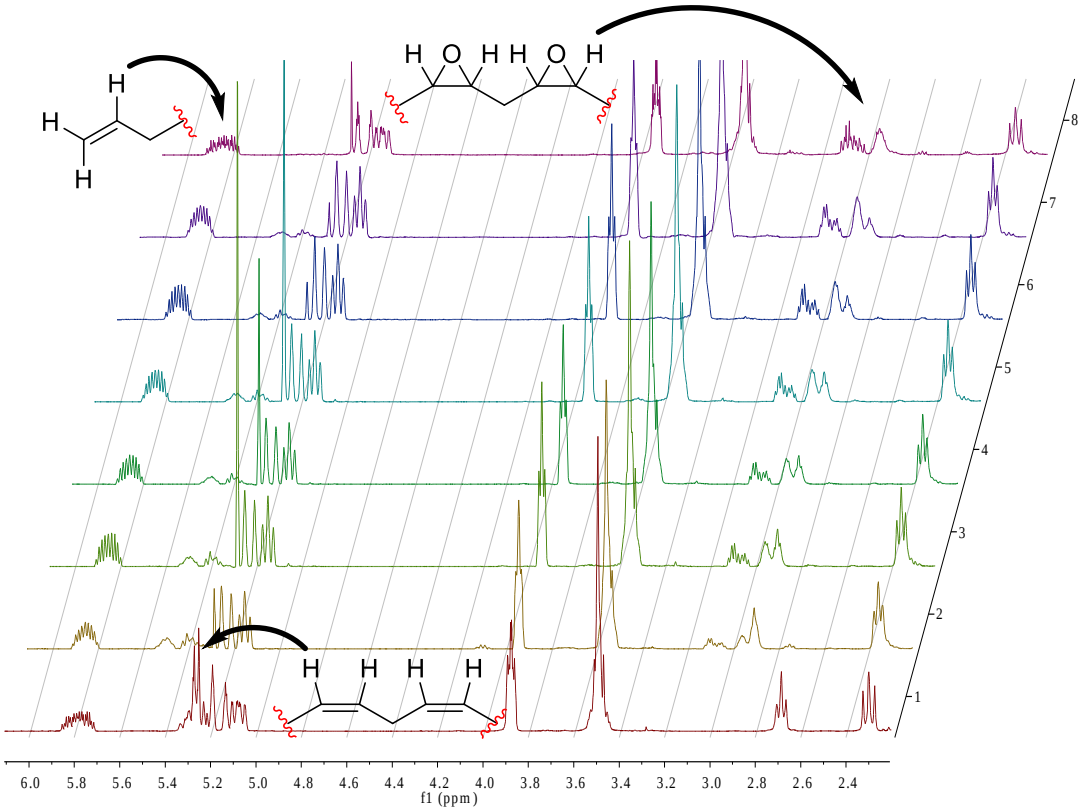

Figure 3.3.16. ^{1}H NMR (300 MHz, $CDCl_3$) monitoring of **3.16** epoxidation by peracetic acid.

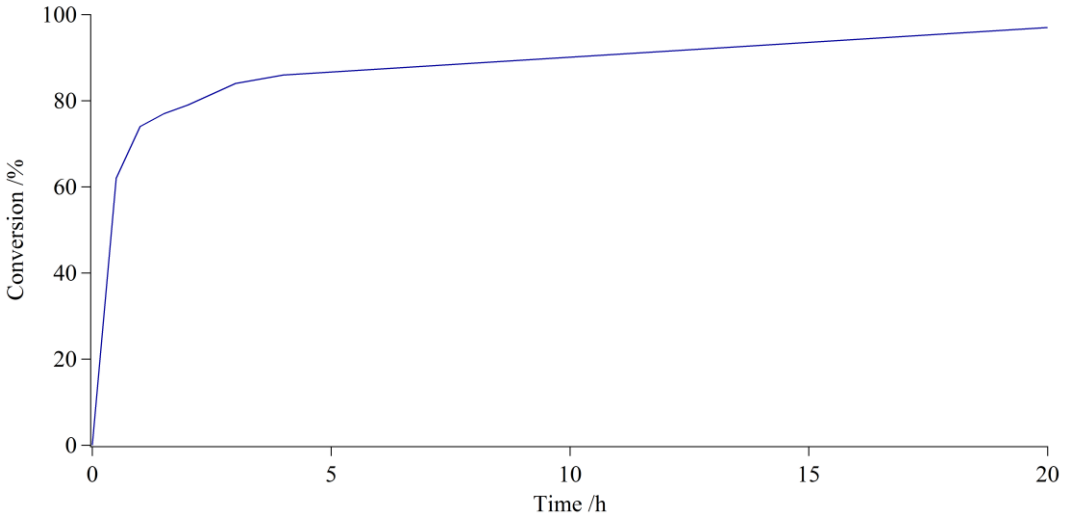

Figure 3.3.17. Conversion to 3.19 with time.

Consequently in order to prepare **3.18** an alternative strategy was required. One approach towards **3.18** was to perform the hydrosilylation before epoxidation on compound **3.16**, however previous work by Behr[224] and Gertner[221] showed that

terminal alkenes were more reactive than internal alkenes in hydrosilyation. This was confirmed in our system by reaction of **3.16** with DMS-H11 under our standard hydrosilylation conditions. The ^{1}H NMR showed loss of terminal vinyl protons but not the internal ones (Figure 3.18).

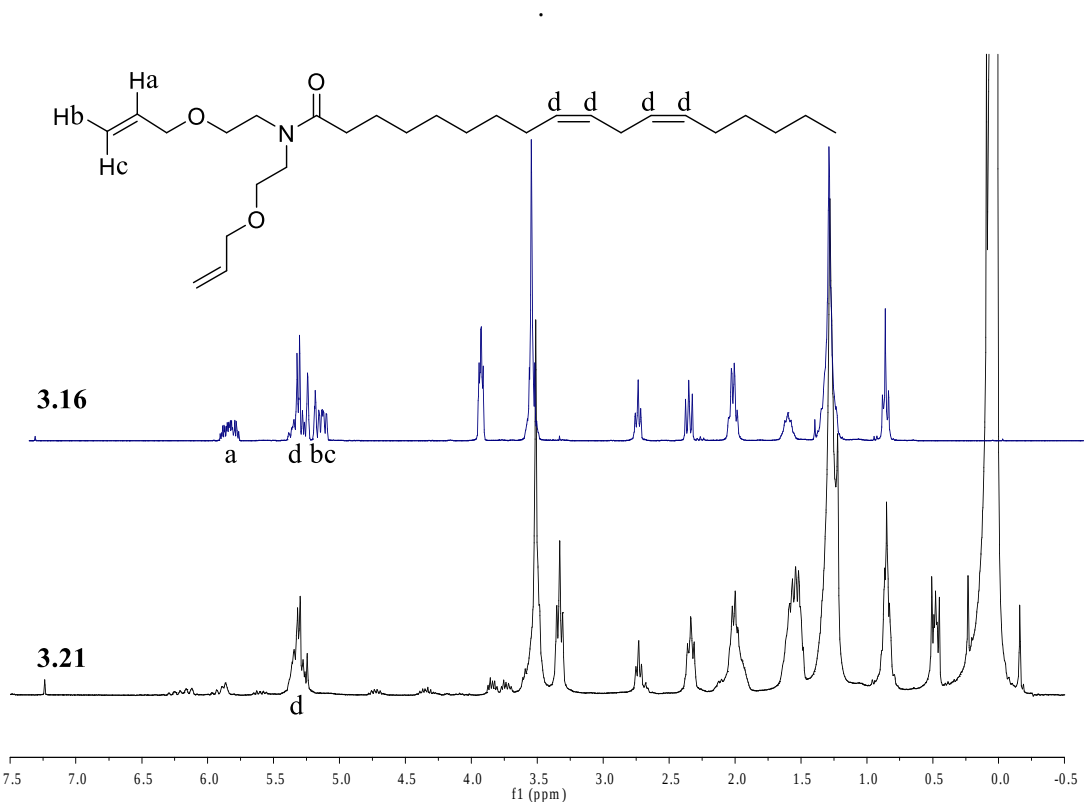

Figure 3.18. ^{1}H NMR (300 MHz, $CDCl_3$) showing selectivity of hydrosilylation towards vinyl groups over internal C=C bonds.

Alternatively, we could prepare **3.17** (Figure 3.19) by the addition of epichlorohydrin to the diol **3.15**.

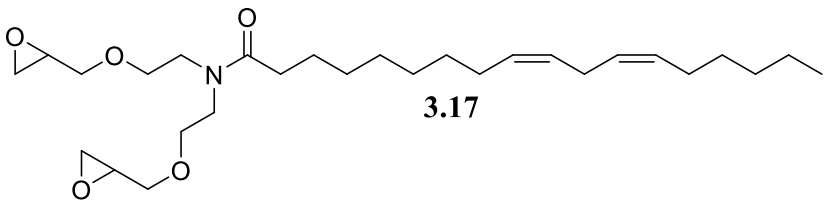

Figure 3.19. Fatty amide **3.17** with terminal epoxides.

Hence, reaction of **5.15** with 6 equivalents of epichlorohydrin and 6 equivalents of NaOH at 40 °C furnished **3.17** is 61% yield after 4 hours, excess epichlorohydrin

was removed by distillation. Hydrosilylation at 100 °C in inert atmosphere with Karstedt's catalyst using DMS-H11 for 1 h led to an insoluble gel. Infra-red analysis indicated only a trace of silane remaining but interestingly suggested a severe loss of epoxide content. The insoluble gel may have formed by polymerisation of the epoxides as well as hydrosilylation resulting in a crosslinked network. This may have been caused by the high temperature and the fact that terminal epoxides are more reactive than internal epoxides. Immersion of the gel overnight in chloroform allowed some soluble material to be isolated, GPC analysis of this material indicated a polymer with an Mn of 35600, Mw of 38900 and PD = 1.1, this is much larger than the ~2000 Da expected for two fatty amides linked by a polysiloxane. To test the theory that cross-linking was occurring via reaction at the terminal epoxides due to excessive temperature, the reaction was repeated at a lower temperature 40 °C and left for 5 days. This time the resulting oil was soluble and ^{1}H NMR data confirmed that the epoxide functional groups were intact although a trace of silicone hydride was still visible (Figure 3.20).

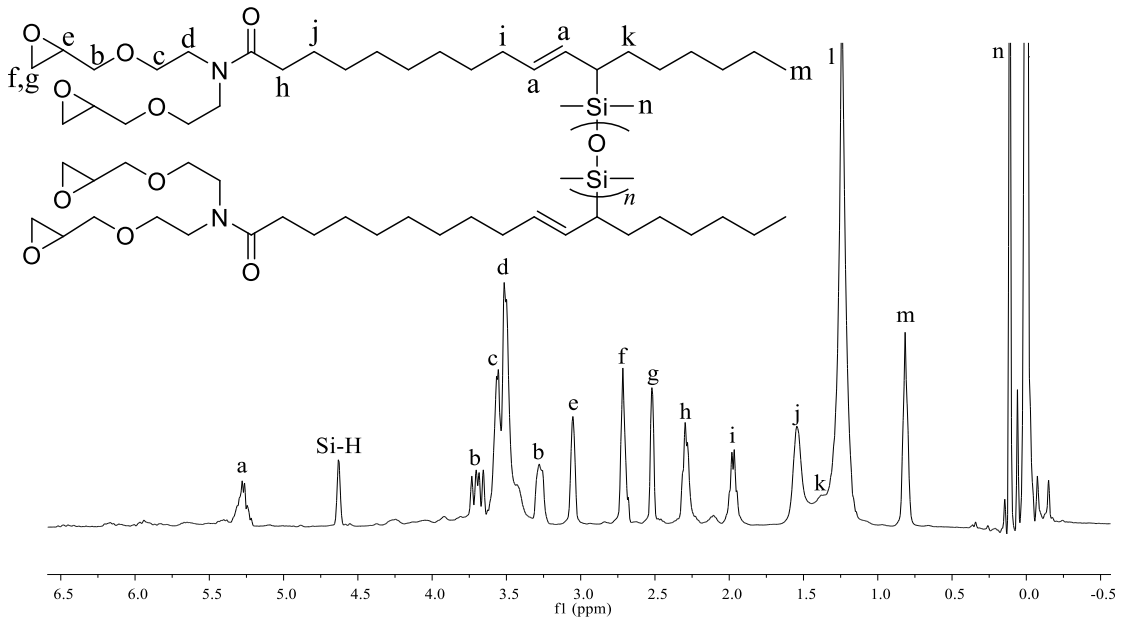

Figure 3.20. ^{1}H NMR (300 MHz, $CDCl_3$) of **3.18** showing epoxide groups intact after hydrosilylation of the alkenes

With one monomer in hand we next turned our attention to the synthesis of **3.20** (Figure 3.21) as the internal epoxide would still be suitable in the coating. In addition as the epoxidised fatty acid chain is similar in structure to epoxidised soybean oil used as the renewable binder, incorporation of the silane into the growing polymer chains should be better controlled.

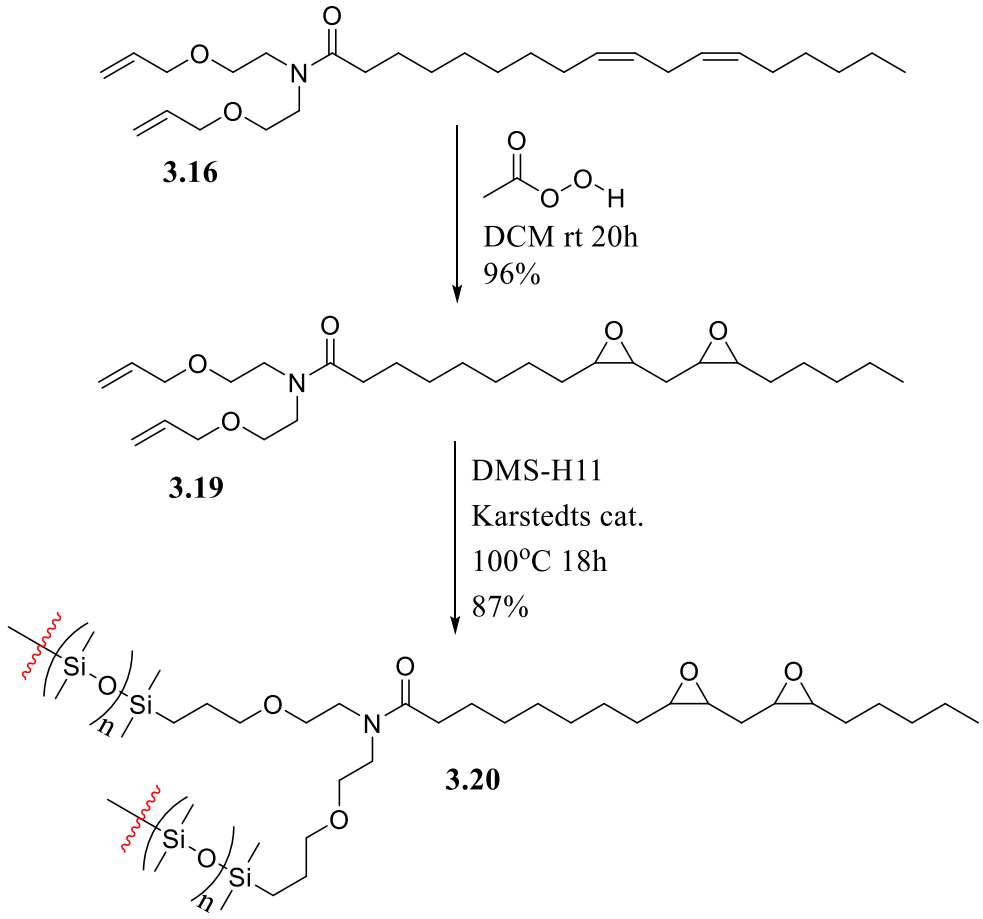

Figure 3.21. Synthetic route to **3.20**.

To incorporate silicone to the epoxy monomer **3.19**, the terminal alkenes were hydrosilyated with DMS-H11 and Karstedt's catalyst using the identical conditions to those reported in section 3.3.2. Initial mixing of the reagents produced an emulsion, which cleared after 1 h to give a golden solution. The reaction was left overnight to ensure complete reaction. The crude ^{1}H NMR data shows significant loss of the terminal vinyl protons (5.4, 5.5 and 5.8 ppm) and the Si-H peak (4.6 ppm), but small traces of each were still visible. Integration ratios between remaining vinyl protons and former allylic protons ('g' 3.34 ppm Figure 3.22) indicated 87% conversion.

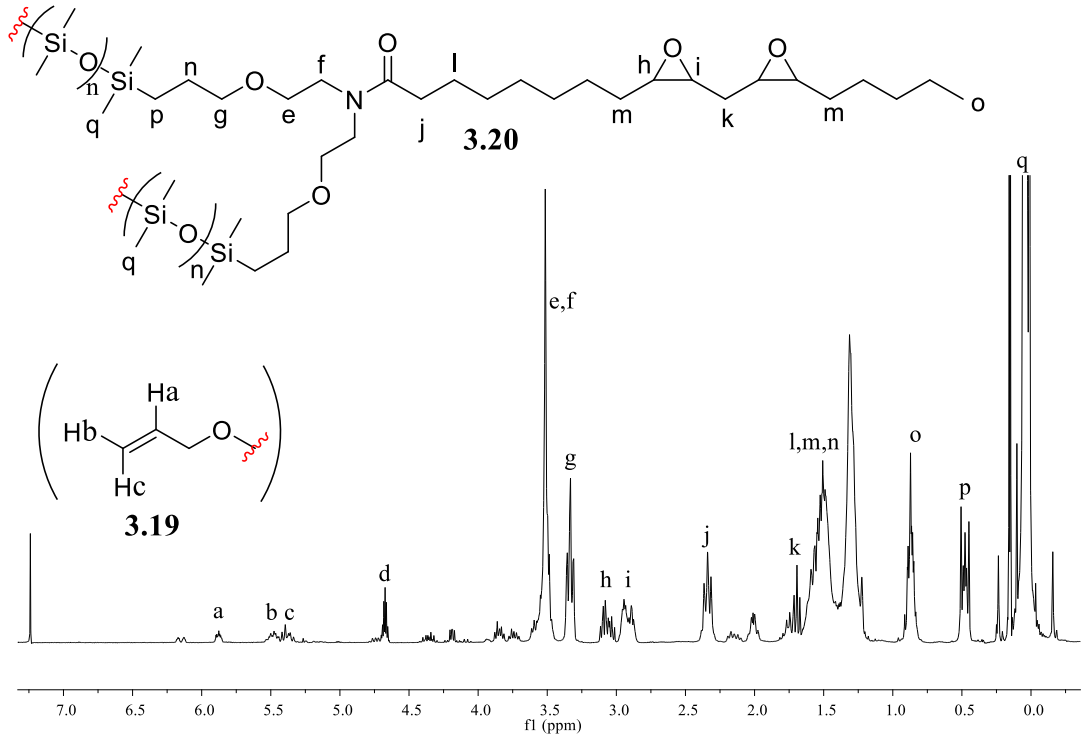

Figure 3.22. ^{1}H NMR (300 MHz, $CDCl_3$) analysis of compound **3.20**.

Purification of the mixture proved difficult, although the catalyst was easily removed by passing the crude mixture through a silica plug, the three organic materials could not be fully separated by column chromatography. The purified NMR spectra still showed trace amounts of staring material. The GPC data indicated the product had a Mn of 5930 g mol^{-1} , Mw of 8370 g mol^{-1} and a PD = 1.41. This silicone and fatty acid pre-polymer should be suitable to copolymerise with the epoxy soybean binder and increase the non-stick properties of the coating.

In conclusion, we prepared two different silicone containing epoxide monomers for potential incorporation into a non-stick coating, **3.18** and **3.20** (Figure 3.23). The latter contains internal epoxides, while the former, more reactive terminal ones. While the synthesis of **3.18** was less efficient it was easier to produce purer materials than **3.20**.

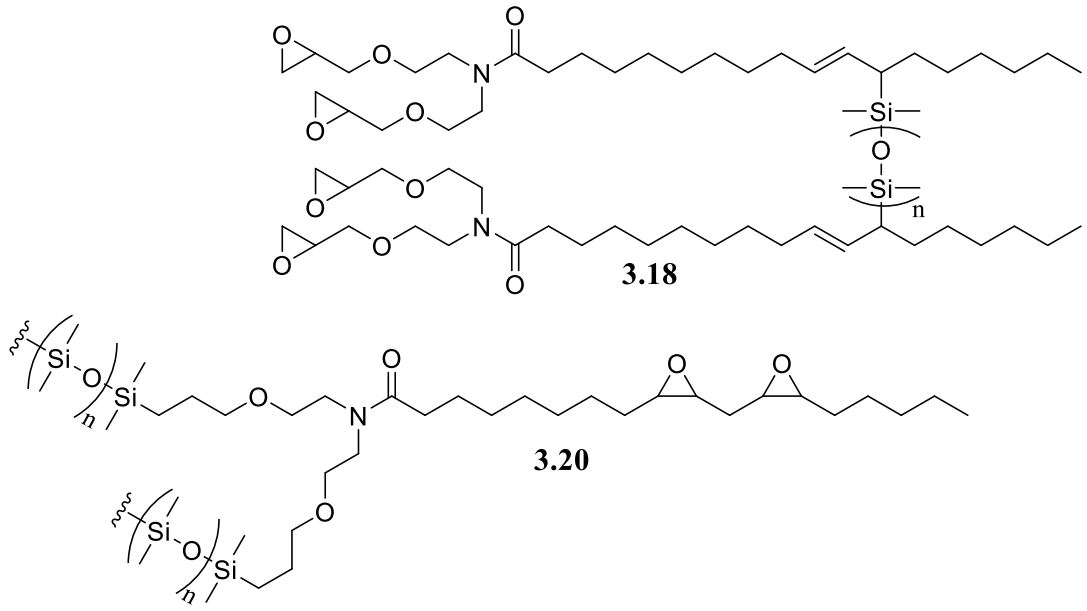

Figure 3.23. Silicone containing additive for ESBO based coatings.

3.3.6 Thermal properties of silicone additives

The thermal properties of the two silicone containing additives **3.18** and **3.20** were compared, due to their required use in bakeware high temperature stability was vital, coating samples need a degradation temperature >260 °C. TGA analysis shows degradation begins at 210 °C and 255 °C (**3.20** and **3.18** respectively). Although these monomers are below the required degradation temperature, polymerised samples of DMS-H11 with soybean oil in section 3.3.3 show onset of degradation at ~330 °C. When polymerised in a coating these silicone-epoxy monomers are expected to achieve a similar level of stability. Polymerisation of the coating formulations in the current process occurs at 400 °C as shown in chapter 2 which is above thermal stability of both monomers, however short curing times (60 s) ensure degradation is minimal. Alternatively, curing temperatures could be lowered if the materials produced were commercially viable.

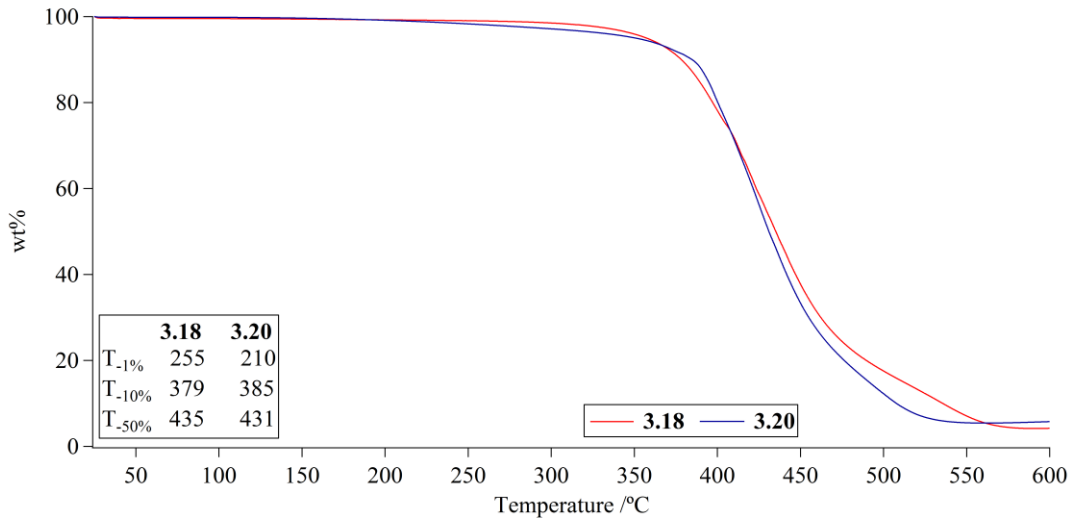

Figure 3.24. TGA analysis of silicone containing epoxy monomers for non-stick coatings. Heating rate 10 °C min^{-1} from 25 – 600 °C in an ambient atmosphere.

TGA analysis shows that both materials have similar degradation profiles (Figure 3.24). Both show a two stage decomposition, with the last stage (>450 °C) presumably being the residual polysiloxane decomposition. That **3.18** has a higher onset degradation temperature possibly due to the terminal epoxides polymerising forming a highly crosslinked material and increasing stability as higher crosslinking gives higher stability as seen in section 3.3.3. The internal epoxides of **3.20** are not as reactive as seen during hydrosilylation of **3.19** in section 3.3.4 where they epoxides remain intact after 18h at 100 °C. However it is possible that the internal epoxides of **3.20** begin to react at higher temperatures leading to a higher degradation temperature at $T_{-10\%}$ than **3.18** (385 °C compared to 379 °C). At higher temperatures both samples are similar in structure both as crosslinked network of PDMS and fatty amides which is shown in the similar degradation temperatures at $T_{-50\%}$ of 431 (**3.20**) and 435 (**3.18**).

3.3.7 Silicone additives in non-stick coating

The two additives **3.18** and **3.20** were designed to lower the surface energy of any coating, but had to be compatible with the epoxy soybean oil binder. To test their suitability, both of the additives **3.18** and **3.20** were mixed with the most successful ESBO/carbon/silica formulation described in the chapter 2. Incorporation of the additives were carried out at 1, 2 and 5 wt% replacing some of the ESBO binder to keep weight percentage of solids constant, formulations were produced on a 2g scale. A 0% formulation was prepared as a control. The formulations were coated onto ECCS (75 mm x 100 mm) using a 12 μm wire wound bar coater (K-bar) and cured in an oven at 400℃ for 60s. The samples produced were of even consistency with no phase separation and dry to the touch.

		Pencil Hardness	X-Hatch	Flexibility
0 wt% silicone	**3.22**	6H	100%	1T Pass
1 wt% **3.18**	**3.23**	6H	100%	0T Pass
2 wt% **3.18**	**3.24**	6H	100%	0T Pass
5 wt% **3.18**	**3.25**	5H	100%	1T Pass
1 wt% **3.20**	**3.26**	6H	100%	0T Pass
2 wt% **3.20**	**3.27**	6H	100%	0T Pass
5 wt% **3.20**	**3.28**	5H	95%	1T Pass

Table 3.4. Industry coating tests of surface properties of silicone monomers in non-stick coatings.

Generally all the coating samples were of sufficient hardness for commercial use (>5H). At higher silicone content pencil hardness was reduced (5%, 5H), the increase in silicon content can decrease crosslinking density and produce softer polymers which was observed in section 3.3.3. Adhesion was successful as no coating was removed during the cross hatch test (except a small amount removed from **3.28**). As silicone content increased epoxy soybean binder decreased resulting in a lower amount of pendant OH groups to form polar attractions to the surface which accounts for some loss of adhesion at 5% **3.20**. This type of process has been

reported in the literature where small amounts of silicone oil can reduce adhesion of commercial epoxy adhesives.[230] Flexibility was generally acceptable, as the control (0% silicone) showed a failure from the first fold (0T) but not with the second larger radius fold (1T). Interestingly, for both monomers at 5% silicone content some coating was removed during the first fold, this would not be a result of less flexibility as in theory flexibility would increase with increasing amounts of silicone consistent with decreased hardness as explained above, but can be attributed to decreased adhesion from increased silicone.

To test the hydrophobicity of each coating, drop shape analysis was used, various sized droplets of water were placed on the surface of the sample at random locations and the contact angle was measured as an average of >5 results (**Error! Reference source not found.**).

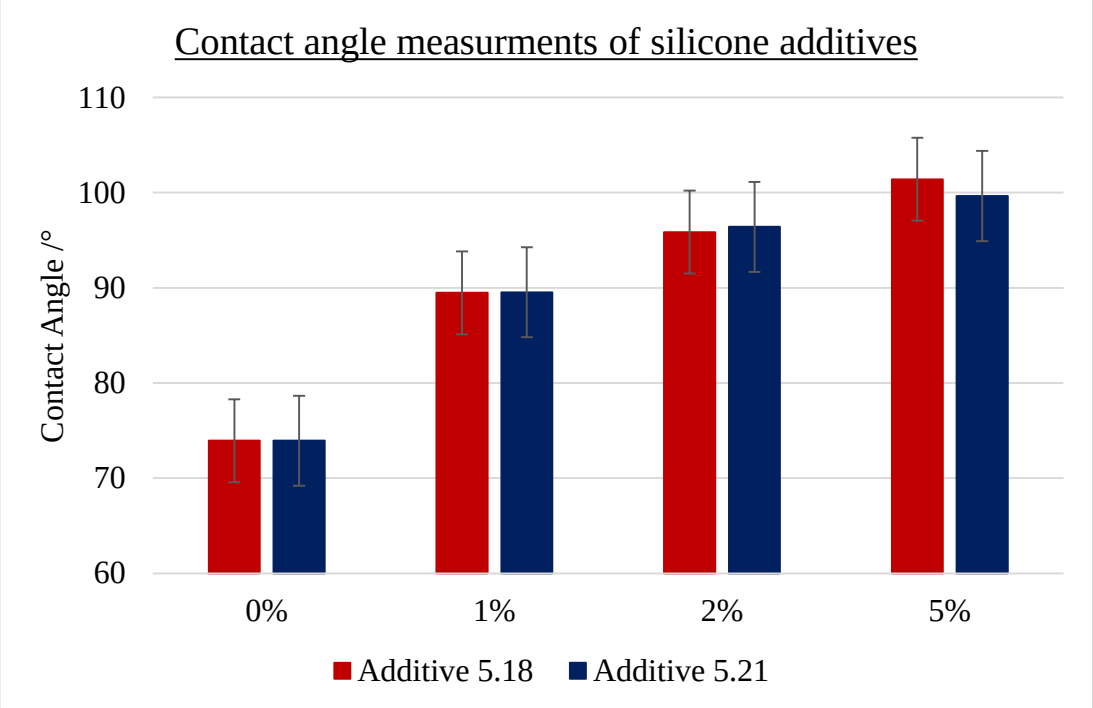

Figure 3.25 Contact angle measurements of silicone additives at various wt%. Compound 5.18 shown in red and compound 5.20 in blue, error bars are the standard deviation about the mean.

As expected an increase in the silicone content leads to a decrease in the surface energy of the coating resulting in greater hydrophobicity as indicated by an increased contact angle. The greater the percentage of silicone additive used the greater the contact angle, the assumption is that this trend will plateau giving a maximum value with this type of silicone. Commercially cost will become a factor and it may be commercially viable to sacrifice some hydrophobicity to save costs. Within error there is little difference in contact angle between the two types of additive used so the recommendation would be to use **3.20** as the reactions to prepare it are simpler and it can be produced in greater yield than **3.18**.

Using information from this chapter and chapter 2 a new more sustainable coating formulation can be proposed, in a typical 2g sample the formulation contains;

Component	**wt /g**
Epoxy soybean oil	1.8
Silicone monomer **3.20**	0.04
Epoxy Linoleic acid	0.04
DBSA cataylst	0.02
Fumed silica	0.04
Carbon black	0.06
Propyl acetate	0.2 mL

3.4 Conclusion and Future Work

In this study we have demonstrated hydrosilylation to be an effective method for introducing silicone content to plant oils based materials. Hydrosilylation is shown to readily react with polyunsaturated fatty acid chains leading to a migration of a C=C bond, but no reaction with a monounsaturated fatty acid was observed. It was shown that epoxidation with peracetic acids provides nearly 100% selectivity

towards the more electron rich internal alkenes, however hydrosilylation favours reaction with vinyl C=C bonds.

It was shown that crosslinked silicone rubbers with renewable plant oils content can be prepared and the physical properties can be tailored by altering crosslinking density through the use of different oils or silanes. A lower alkene functionality or longer silicones produced less crosslinked polymers that were more elastic.

The ability to covalently bond a silicone to an epoxy fatty acid was shown to be an effective method of introducing silicone into non-stick coatings which were compatible and readily polymerised with an epoxy plant oil binder. The resulting coting formulations had desirable properties in terms of physical surface properties, thermal stability and hydrophobicity.

Our studies from this and the previous chapter have led to produce a coating with ~85% by weight renewable content, compatible fillers and additives and more environmentally friendly solvents. The coating process and curing regimes have not been changed allowing direct substitution of currently used formulations if required. However further tests are required to assess their usefulness as a non-stick coating in real world conditions.

4 Renewable Polyesters from Ring Opening Polymerisation of Epoxidised Vegetable Oils and Cyclic Anhydrides. Comparison of Grapeseed and Soybean Oils.

4.1 Introduction and Aims

4.1.1 Background.

In the previous chapters it was described how epoxidised soybean oil proved to be an effective component for a binder when combined with silica particles. They exhibited excellent surface hardness, adhesion and flexibility upon coating on ECCS but failed in non-stick applications. This led to the development of two hybrid renewable epoxy-silicone monomers that could be copolymerised with the epoxidised soybean oil binder. The hydrophobicity of the coatings increased with the level of silicone monomer added in the formulation. While this new formulation was analysed by the same industry tests as before and was found to be successful as just a black coating, unfortunately its effectiveness as a non-stick coating could not be evaluated by our industrial sponsors after their company underwent liquidation. At this point we decided to continue to investigate the chemistry of renewable oils, in particular epoxidised vegetable oils. Epoxidised soybean oil (Figure 4.1) is the most common vegetable oil used in industry, traditionally it is used as a plasticizer for PVC, but it is also used for producing polyesters from cyclic anhydrides,[231,232] such as maleic anhydride.[233]

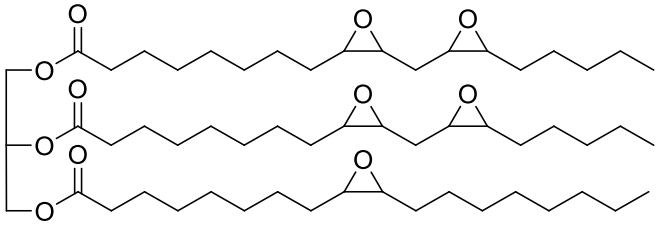

Figure 4.1. Epoxidised Soybean Oil.

Grapeseed oil has a similar structure to soybean oil with the most abundant fatty acid being linoleic (72%[234] for grapeseed and 55%[235] for soybean) followed by oleic acid (16[234] and 23%[235**Error! Bookmark not defined.**] respectively). Grapeseed oil can be extracted from the residue left over after wine making, the pomace, containing the skin, stems and seeds. From 100 Kg of grapes it is possible to extract 400g of oil[236] and with worldwide production of grapes at 67 million tonnes in 2012[237] this gives a potential of 268,000 tonnes of grapeseed oil per year. The estimated production of epoxidised soybean oil is 200,000 tonnes per year,[238] so in terms of volume the waste product grapeseed oil has the potential to replace the food crop soybean oil. Chemically, the slight increase in unsaturation in grapeseed over soybean would lead to increased cross-linking in polyesters and potentially harder materials. On the other hand oils with less unsaturation should lead to softer, more elastic materials.

Palm oil is a triglyceride with low levels of unsaturation and is widely used in the food and cosmetic industry, however palm oil has recently shown interest as a feedstock for renewable materials such as polyurethanes,[239] epoxy resins[240] and polyesters.[241] Worldwide production of palm oil was 53 million tonnes in 2014 and estimated to rise to 68 million by 2020 and 1 tonne requires around 0.26 hectares of land.[242] The clearing of land for plantations is presently blamed for severe deforestation so the increased use of palm oil is a contentious one.

Euphorbia oil from the plant *Euphorbia tirucalli* is a relatively underutilised plant oil, its use is appealing because of the ability of *E. tirucalli* to grow on land that is not suitable for most other crops. The chemistry is also of interest as it is moderately unsaturated and has naturally occurring epoxide groups.

Cocoa butter is a triglyceride from cocoa beans, it has on average 64% saturated content, the high level of saturated chains allows closer packing so it is a solid at room temperature. Ground cocoa beans are pressed into cocoa butter (54%) and cocoa mass (46%) with a worldwide production of cocoa beans in 2014 at 4.2 million tonnes (mT) this gives a yield of 2.3 mT of cocoa butter.[243] Cocoa butter accounts for about 20% of the mass of chocolate which has a yearly production of 7.2 mT requiring only 1.4 mT of cocoa butter.[244] This leaves a surplus of 0.9 mT some of which is used in cosmetics or pharmacology but the majority is discarded as waste. Cocoa butter could be a potential feed-stock for renewable polymers with less environmental impact.

4.1.2 Aims

We embarked on a study on how the properties of renewable polyesters could be controlled utilising different epoxidised oils and different hardeners (including food safe hardeners). In particular to determine if epoxidised grapeseed oil could be used as a replacement to epoxidised soybean oil. The new materials may have potential use in coatings, resins or adhesives.

4.2. Results and Discussion

4.2.1. Composition of vegetable oils

The vegetable oils used in this investigation are listed in Table 4.1 with their fatty acid compositions and the average number of double bonds per molecule. These oils are mainly formed from palmitic (16:0), stearic (18:0), oleic (18:1), linoleic (18:2) and linolenic (18:3) acids.

Oil	C=C Number[a]	% Fatty acids[b] (Chain length:Double bond)						
		(14:0)	(16:0)	(18:0)	(18:1)	(18:2)	(18:3)	(20:0)
Cocoa butter **CB**	0.9	-	25.8	37.9	32.2	2.9	-	0.9
Euphorbia **EuO**	3.2	-	6.8	2.0	81.5[c]	3.71	2.87	-
Palm **PO**	1.8	1.1	44.0	4.5	39.2	10.1	0.4	0.4
Rapeseed **RSO**	3.8	0.2	4.1	1.8	60.9	21.0	8.8	0.7
Soybean **SBO**	4.4	0.1	10.6	4.0	23.3	53.7	7.6	0.3
Grapeseed **GSO**	4.8	0.1	7.4	3.9	15.6	72.2	0.3	-

Table 4.1. Fatty acid composition and double bond number of vegetable oils used in this study.
[a]Calculated from ^{1}H NMR analysis. [b]From references [245, 246, 247] [c]includes vernolic acid[248]

The oils are listed in order of unsaturation expressed as the average number of C=C double bonds per molecule. The C=C number was calculated by ^{1}H NMR analysis, the peaks at 5.35 ppm represent alkene protons, but they often overlap with C-H of the glycerol. The alkene/glycerol peak is integrated relative to the methyl peaks of the chain end at 0.9 ppm which has an integration ratio of 9, for example (Figure 4.2) the integration of grapeseed oil is 10.5 which gives (10.5-1)/2 = 4.75 alkene groups.

The level of unsaturation increases from 0.9 for CB to 4.75 for GSO, this is important as the level of unsaturation indicates how many epoxide groups will be

present after epoxidation. The number of epoxide groups per molecule will govern the level of crosslinking, which will ultimately affect the physical properties of polyesters formed form these oils.

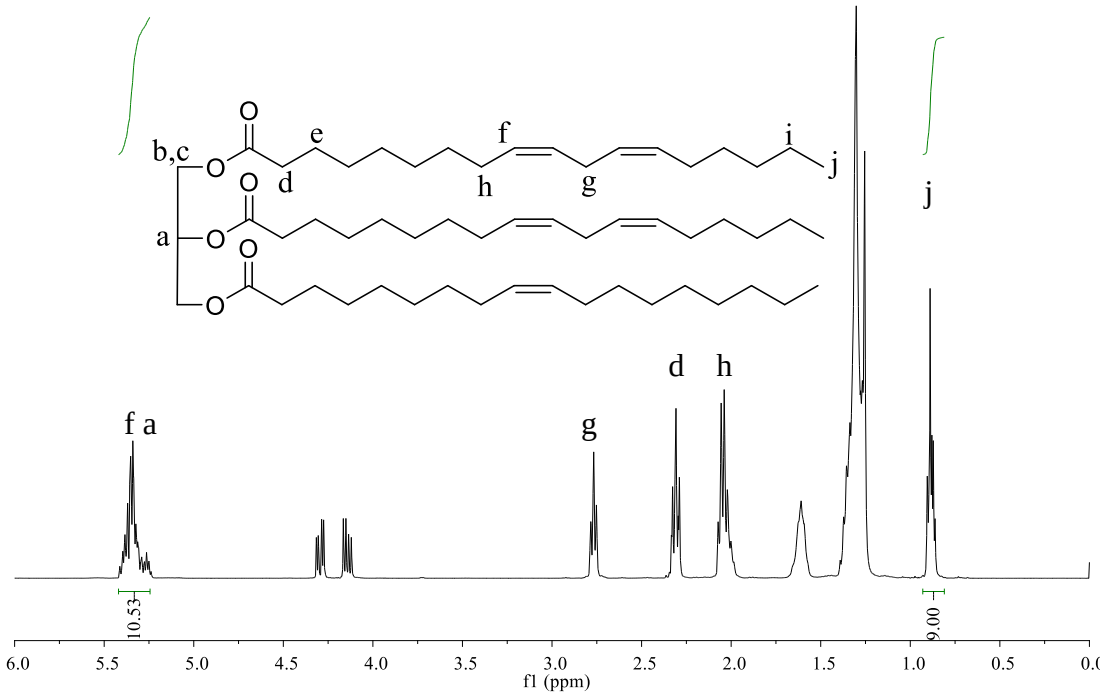

Figure 4.2. ^{1}H NMR (400 MHz, $CDCl_3$) spectrum of grapeseed oil.

It is also worth noting that the composition of individual oils may vary batch to batch, depending on the climate conditions, soil type and plant maturity as well as isolation and purification methods for each batch.[245]

4.2.2. Epoxidation of vegetable oils

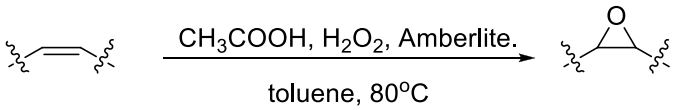

Figure 4.3. Epoxidation of unsaturated vegetable oils.

The vegetable oils were epoxidised following the method by Petrovic,[249] using acetic acid, an ion exchange resin (Amberlite®) and hydrogen peroxide in toluene (Figure 4.3). The reactions were performed at 80°C and were monitored by ^{1}H NMR looking for disappearance of alkene peaks at around 5.35 ppm and appearance of epoxide peaks at 2.8 – 3.1 ppm (Figure 4.4).

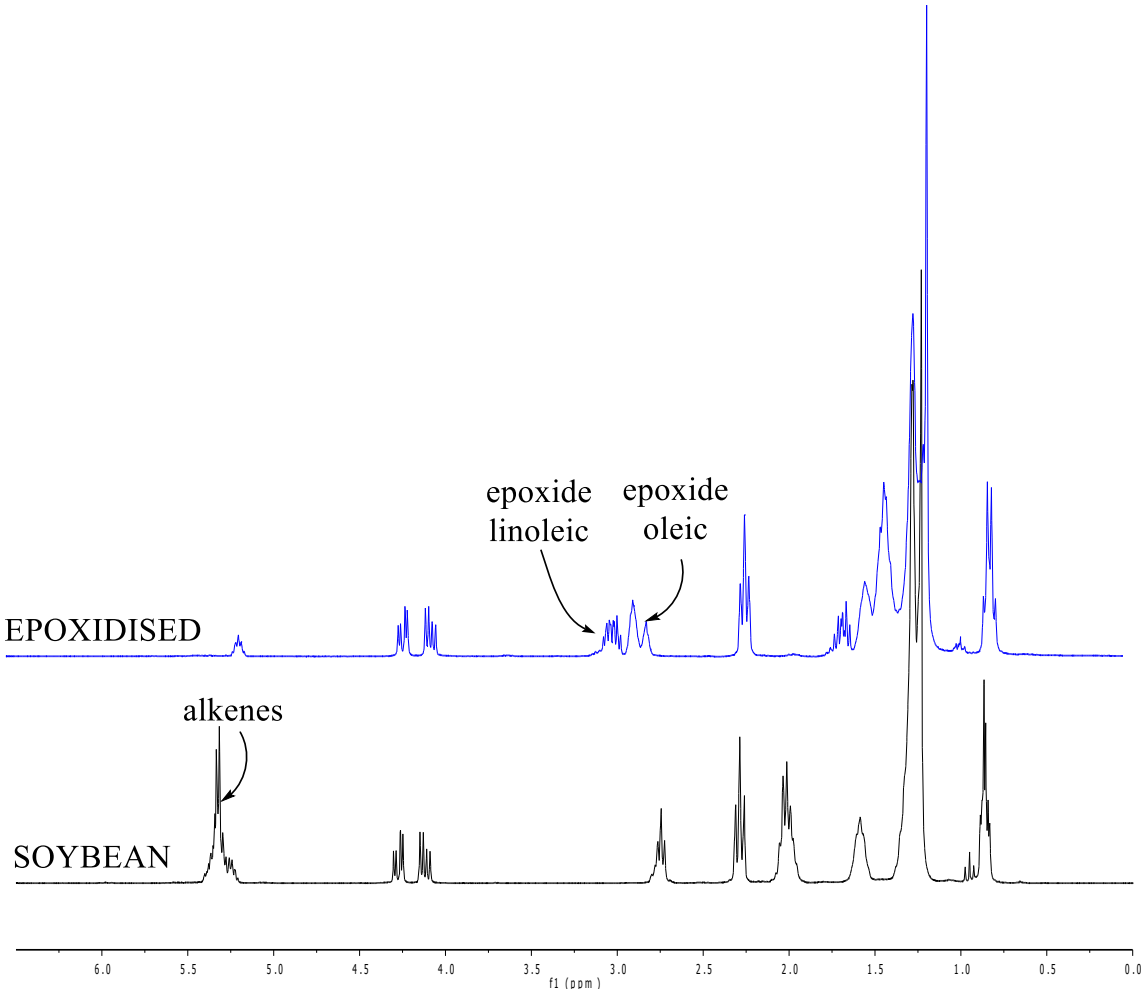

Figure 4.4. ^{1}H NMR (300 MHz, $CDCl_3$) spectra of soybean oil (black) and epoxidised soybean oil (blue).

The epoxidised plant oils were epoxidised cocoa butter (ECB), epoxidised palm oil (EPO), epoxidised rapeseed oil (ERSO), epoxidised soybean oil (ESBO) and epoxidised grapeseed oil (EGSO), (Figure 4.5).

The epoxidation reaction produced epoxy oils with a high yield (95 – 97%) and purity, they were used without any further purification. Euphorbia oil is a naturally occurring epoxidised oil comprised of around 60% vernolic acid[250] which also contains a C=C double bond (Figure 4.5), by ^{1}H NMR analysis this was shown to be on average 1.6 epoxide groups per molecule.

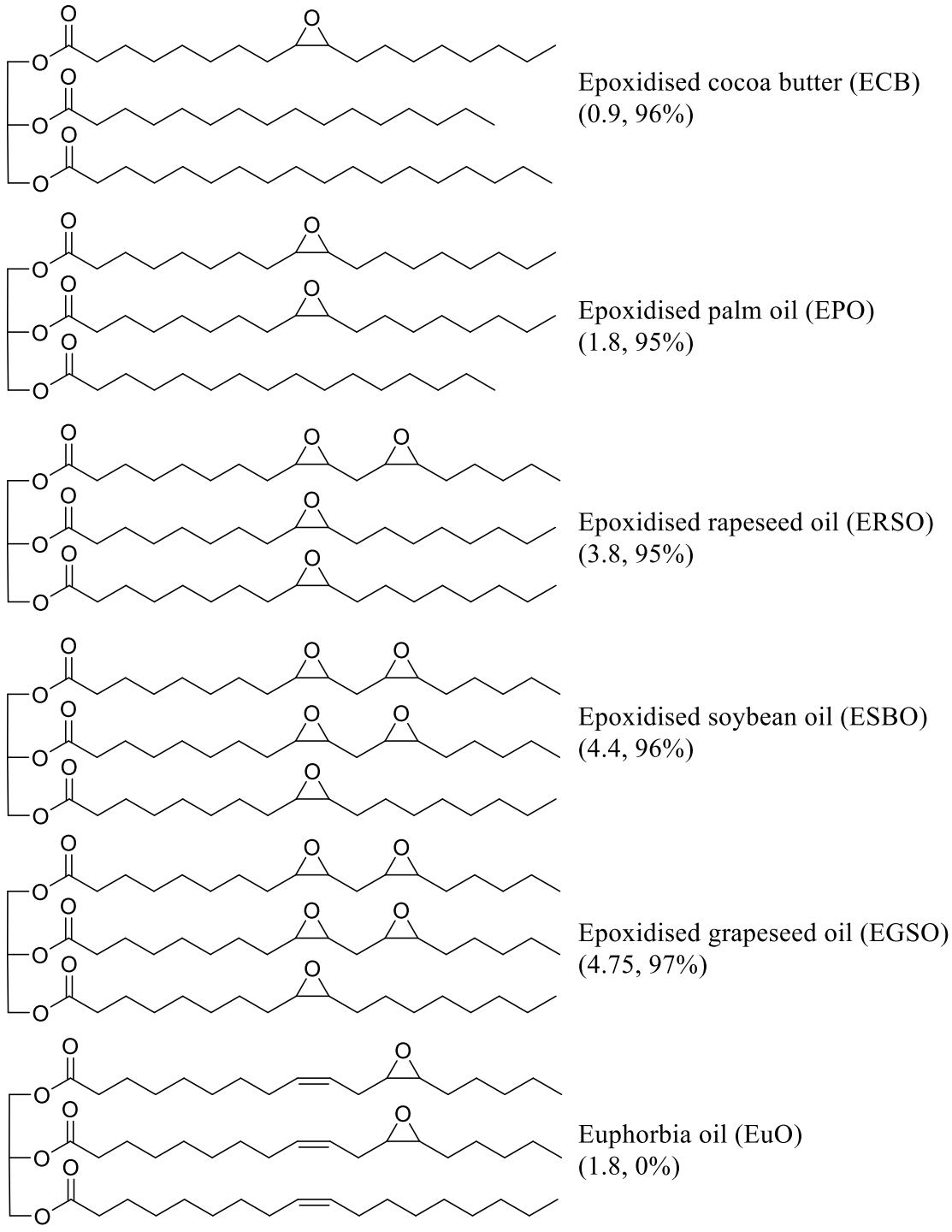

Figure 4.5. Epoxidised vegetable oils, average number of epoxides and % yield in brackets

4.2.3 Copolymerisation of epoxidised oils with a commercial anhydride hardener Aradur® 917

A well-known hardener for copolymerisation with epoxides is biodegradable methyl tetrahydrophthalic anhydride,[251,252] it is marketed by Huntsman Corporation as Aradur® 917 (Figure 4.6). This anhydride was polymerised with the epoxidised plant oils using 4-methyl imidazole as a catalyst to form polyesters.

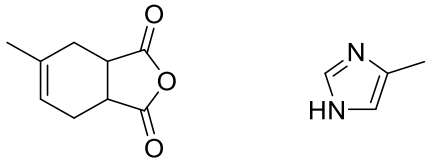

Figure 4.6. Methyl tetrahydrophthalic anhydride commercially available as Aradur® 917 and 4-methyl imidazole used as a catalyst.

The epoxidised oils and anhydrides were combined to give epoxide:anhydride ratios of 1:1 and 2:1, and for rapeseed, soybean and grapeseed a 1:1 ratio of triglyceride to anhydride was also chosen. 4-Methyl imidazole was added at 1 wt% relative to the total weight of oil and anhydride.

To determine the cure characteristics, small samples (~ 10 mg) of the monomer mixture were analysed by DSC with a heating rate of 10°C per min in air (Figure 4.7). The results show that a temperature of 170°C and curing for 1 h would be sufficient for complete polymerisation for all oils. However, the peak cure temperature was found to increase inversely to the epoxide number of the reacting oil. Interestingly, the peak cure temperature for ESO with Aradur®917 was found

(151°C) to be only 1°C different to that previously reported with maleic anhydride (150°C).[253]

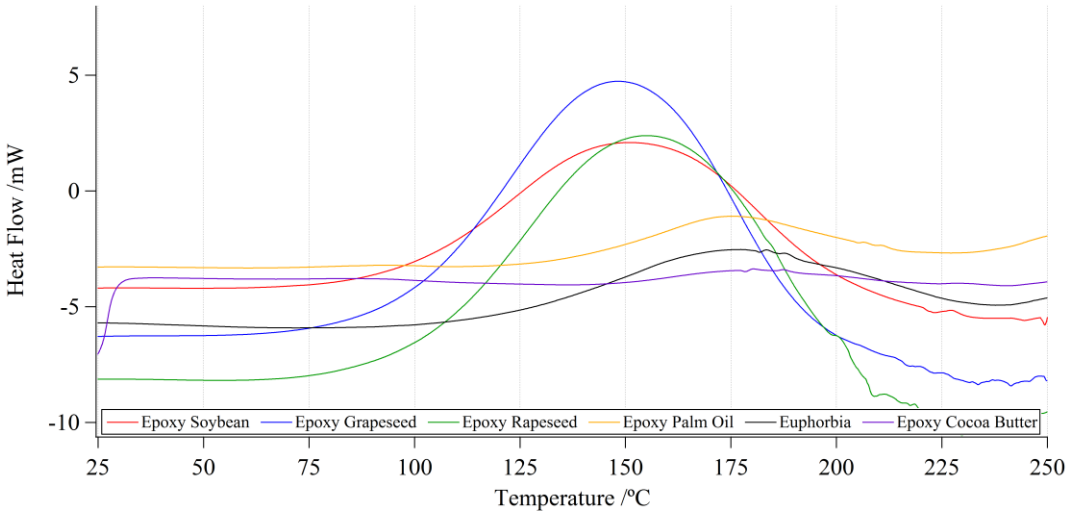

Figure 4.7. DSC analysis of curing of plant oils with Aradur® 917. Heating rate was 10 °C min^{-1} in ambient atmosphere.

It is also possible from this data to determine the energy released by polymerisation, $\Delta H_{polymerisation}$, by integrating the area under the peaks (Table 4.2).

Polymer			$\Delta H_{polymerisation}$ /Jg^{-1}	Peak Cure Temp /°C
Anhydride	**Epoxide**	**E:A**		
Aradur 917(R)	Epoxy Grapeseed Oil	1:1	218	148
	Epoxy Soybean Oil	1:1	201	151
	Epoxy Rapeseed Oil	1:1	176	155
	Epoxy Palm Oil	1:1	58	175
	Euphorbia Oil	1:1	66	175
	Epoxy Cocoa Butter	1:1	19	180

Table 4.2. DSC data from polymerisation of epoxidised plant oils and Aradur 917®.

As the polymerisation occurs through the epoxide groups it is expected that higher levels of epoxidation would lead to a higher $\Delta H_{polymerisation}$. For example grapeseed oil [4.75 epoxides, $\Delta H_{polymerisation}$ = 201 Jg^{-1}] releases more energy during polymerisation, than palm oil [1.8 epoxides, $\Delta H_{polymerisation}$ = 58 Jg^{-1}]. It was also

observed that generally the cure temperature was lower for the oils containing the most epoxides.

Repeating the reactions and curing on a larger scale (16g) allowed the materials to be fabricated in dogbone shaped aluminium moulds in accordance to BS EN ISO 527 standard size test pieces (Figure 4.8), the mould was pre-coated with silicone release spray to aid sample removal.

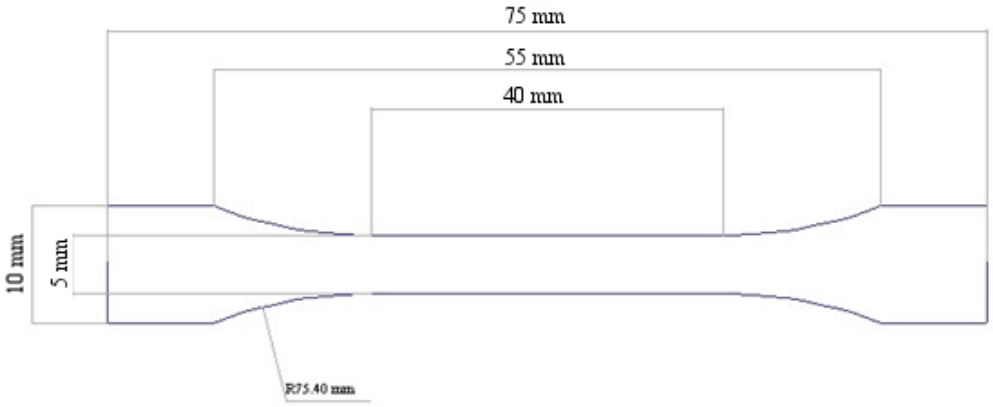

Figure 4.8. Standard size dogbone for tensile testing, conforms to BS EN ISO 527.

The polyesters ranged from brittle hard polymers (for those derived from ESO and EGSO in a 1:1 ratio) to very soft flexible polymers (for lower anhydride ratios and EuO and EPO based samples). They were all of a similar colour, dark yellow to golden brown. Ten pieces were cast for each sample mixture, but not all were fit for testing and some used for crosslinking, swelling and thermal analysis, the tensile testing data was based on an average of at least 5 pieces.

Polyester samples derived from cocoa butter where unsuitable for tensile testing, they lacked the structural integrity needed to be removed intact from the mould, so were excluded from any further investigation.

Tensile testing was performed using a 1 KN load cell and an extension speed of 2mm per minute. The stress strain curves for the five remaining plants oils and Aradur® 917 with an epoxide:anhydride ratio of 1:1 are shown below (Figure 4.9 and Figure 4.10).

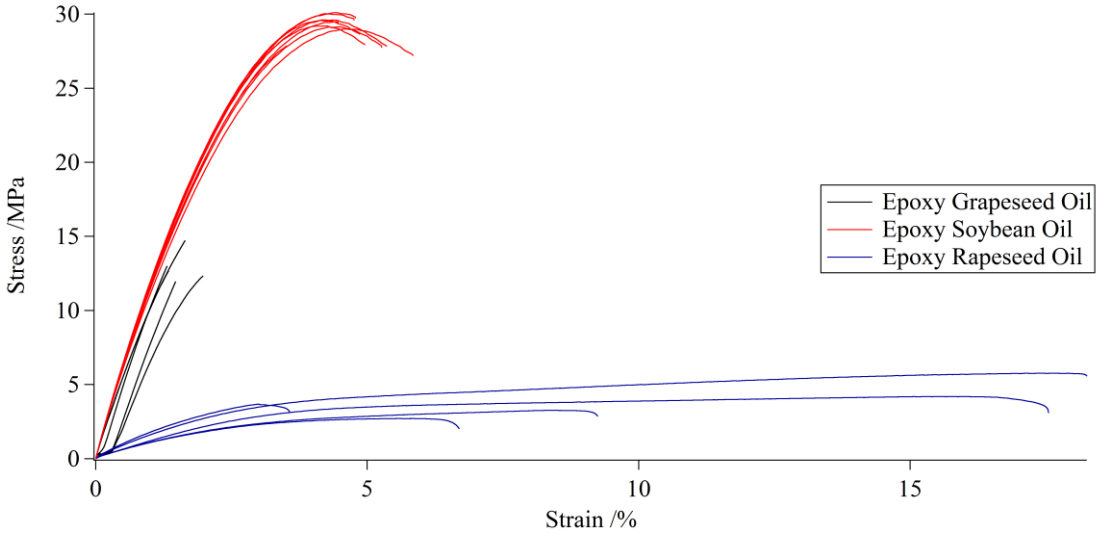

Figure 4.9. Stress Strain curves of polyesters of EGSO, ESBO and ERSO with Aradur® 917 hardener (1:1 ratio). Extension rate 2mm min^{-1} using 1 kN load cell at 20 °C.

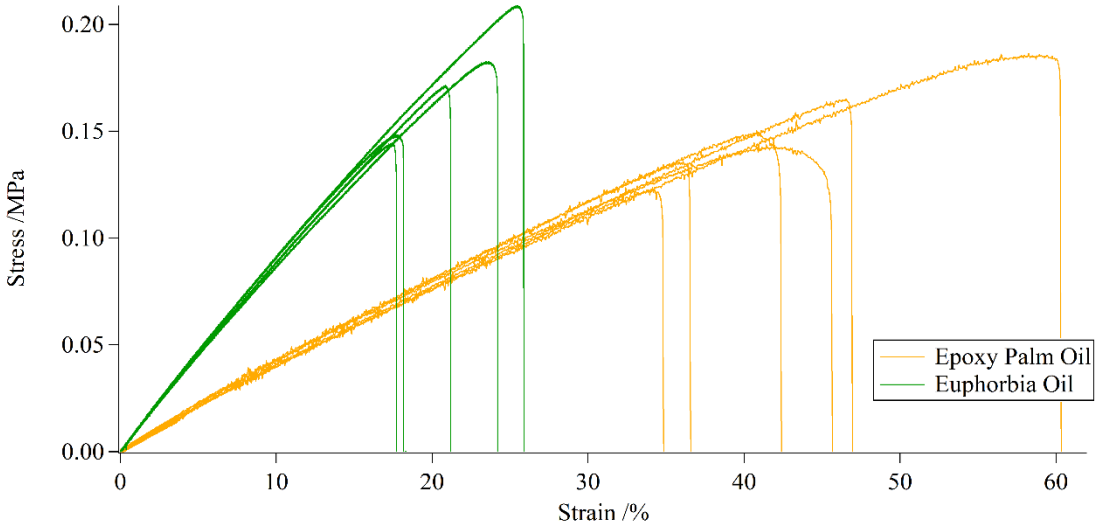

Figure 4.10. Stress Strain curves of polyesters of EPO and EuO with Aradur® 917 hardener (1:1 ratio). Extension rate 2mm min^{-1} using 1 kN load cell at 20 °C.

As can be seen from the stress strain curves and the table below (Table 4.3) the soybean oil based samples showed the greatest tensile strength of around 30 MPa, which decreases to 1.17 and 0.067 MPa with a decreasing amount of hardener. This trend continues with all the oils tested and can be explained as a decrease in hardener leads to a smaller polymer network therefore a lower tensile strength, it has long been recognised that higher molecular weights gives a stronger polymer.[254,255]

Polymer			UTS[a] /MPa	YM[b] /MPa	EB[c] /%
Anhydride	**Epoxide**	**E:A ratio**			
Aradur 917	Epoxy Soybean Oil	1:1	29.33 ±1.48	1090 ±59.4	4.87 ±0.65
		2:1	1.17 ±0.34	10.52 ±1.68	15.2 ±2.44
		4.4:1	0.07 ±0.03	0.75 ±0.26	9.86 ±1.21
	Epoxy Grapeseed Oil	1:1	12.76 ±1.95	1005 ±93.9	1.47 ±0.32
		2:1	0.65 ±0.34	60.08 ±2.98	1.33 ±0.22
		4.75:1	0.06 ±0.02	0.50 ±0.19	13.0 ±1.76
	Epoxy Rapeseed Oil	1:1	3.94 ±1.83	122.1 ±25.2	11.1 ±6.57
		2:1	0.31 ±0.05	4.36 ±0.24	8.54 ±0.95
		3.8:1	0.05 ±0.02	1.22 ±0.31	3.90 ±1.39
	Epoxy Palm Oil	1:1	0.15 ±0.04	0.46 ±0.04	44.5 ±9.15
		2:1	0.05 ±0.01	0.03 ±0.03	105 ±18.07
	Euphorbia Oil	1:1	0.16 ±0.05	0.96 ±0.13	20.6 ±3.84
		2:1	0.07 ±0.02	0.39 ±0.04	23.0 ±3.35

Table 4.3. Tensile testing data (average values) from plant oil and Aradur 917® polyesters. [a] Ultimate Tensile Strength, [b] Youngs Modulus, [c] Elongation at break point. Errors are one standard deviation from the mean.

The variation in tensile strengths between oils (using the same E:A ratio) is approximately parallel to the levels of their epoxide functionality, with soybean and grapeseed showing the highest levels of tensile strength and palm oil and euphorbia oil showing the lowest. It was somewhat surprising that soybean derived materials showed a greater tensile strength than those derived from grapeseed. Consequently, swelling tests were also conducted on the polyester samples to determine the actual crosslinking density and this paralleled the observed tensile strengths. The samples were immersed in toluene for a week to reach an equilibrium swelling size, and the

crosslinking density (υ_c) was calculated using the Flory-Rehner equation,[256] the data is shown in the table below (Table 4.4).

$$M_c = \frac{\nu_s \, \rho_p \left(V_p^{\frac{1}{3}} - V_p/2 \right)}{\ln(1 - V_p) + V_p + \chi V_p^2} \quad \text{and} \quad \upsilon_c = \frac{P_p}{M_c}$$

Polymer			Crosslinking Density, υ_c x 10^{-4} mol/cm^3
Anhydride	**Epoxide**	**E:A ratio**	
Aradur 917	Epoxy Soybean Oil	1:1	35.8
		2:1	19.2
		4.4:1	11.8
	Epoxy Grapeseed Oil	1:1	32.9
		2:1	23.4
		4.75:1	12.8
	Epoxy Rapeseed Oil	1:1	25.7
		2:1	16.4
		3.8:1	9.2
	Epoxy Palm Oil	1:1	2.7
		2:1	0.5
	Euphorbia Oil	1:1	5.2
		2:1	2.4

Table 4.4. Crosslinking density of vegetable oil and Aradur® 917 based polyesters calculated from the Flory-Rehner equation (above table).

Referring to data in Table 4.3 and Table 4.4 it shows that the Young's modulus of the samples is related to crosslinking density, both epoxidised soybean and epoxidised grapeseed (for a 1:1 epoxide:anhydride ratio) have a modulus over 1000 MPa and a crosslinking density of over 30 x 10^{-4} mol/cm^3, whereas euphorbia and epoxidised palm oils have a lot lower crosslinking density (5.21 and 2.69 respectively) and Young's modulus (0.957 and 0.465). The differences in crosslinking density arise from two factors, the first is the amount of hardener used, and the second is the composition of the oil. Epoxidised oils such as EGSO and ESBO had more epoxide groups per molecule (4.75 and 4.4) than ERSO (3.8), EPO

(1.8), and EuO (1.6) so a greater amount of crosslinking was possible, leading to more brittle samples. Why the cross-linking density in grapeseed oil was lower than for soybean oil despite its increased epoxide level is uncertain however.

Thermal properties of the plant oil based polyesters were also studied (Figure 4.11 and Table 4.5). Higher onset of degradation values ($T_{-1\%}$) in all oils were found for samples where the amount of hardener used in a formulation was lowest (e.g. Grapeseed, E:A 1:1 = 224°C, 2:1 = 313°C, 4.75:1 = 324°C). The hardener alone shows an onset of degradation around 200°C, implying the first degradation may correspond to unreacted hardener.[257]

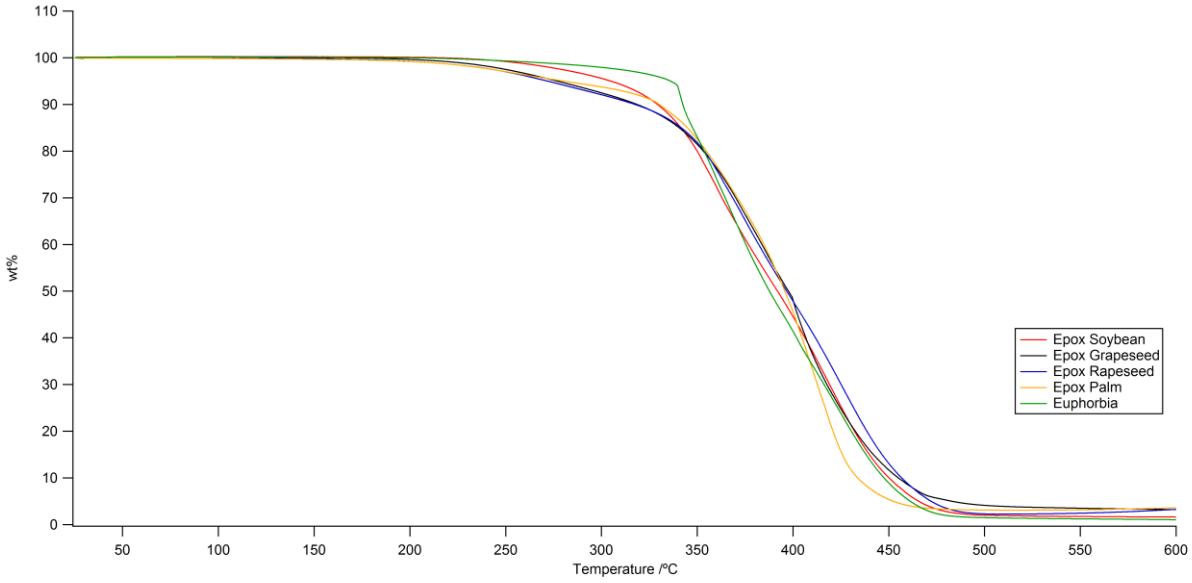

Figure 4.11. TGA analysis of epoxidised plant oil based polyesters with Aradur® 917 with a epoxy:anhydride ratio of 1:1. Heating rate was 10 °C min^{-1} from 25 – 600 °C in air.

Polymer			T_g /°C	$T_{-1\%}$ /°C	$T_{-10\%}$ /°C	$T_{-50\%}$ /°C
Anhydride	**Epoxide**	**E:A ratio**				
Aradur 917	Epoxy Soybean Oil	1:1	6	254	329	392
		2:1	-19	253	334	389
		4.4:1	-25	304	353	405
	Epoxy Grapeseed Oil	1:1	17	224	319	398
		2:1	3	313	359	396
		4.75:1	-17	324	367	411
	Epoxy Rapeseed Oil	1:1	8	209	318	397
		2:1	-1	302	359	416
		3.8:1	-27	312	370	412
	Epoxy Palm Oil	1:1	-33	209	330	396
		2:1	-49	276	348	402
	Euphorbia Oil	1:1	-36	267	343	388
		2:1	-45	318	344	392

Table 4.5. Glass transition and thermal degradation data of epoxidised vegetable oils and Aradur® 917 polymers.

The trend between the different oils themselves at 10% degradation is less obvious to explain. Within the E:A 1:1 series the values roughly approximate the degree of cross-linking (with the exception of the euphorbia oil derived material). Hence, soybean 254°C > grapeseed 224°C > rapeseed 209°C > palm oil~209°C. The hardener is more likely to undergo complete reaction for oils with higher epoxide values. The relatively high value for the euphorbia oil derived material are likely due to the residual alkenes, not present in the other materials. At 50% degradation values are within a relatively small range for all samples (28°C) and within 10°C for the samples prepared with a 1:1 ratio of E:A.

Glass transition temperatures were calculated by DSC, the trend in the data (Table 4.5) is that a lower T_g value is observed when a lower ratio of anhydride is used. This pattern is related to crosslink density and can be observed in the Young's modulus for example grapeseed based polymers; (T_g, Young's Mod, X-link) 1:1 – 17 °C, 1005 MPa, 32.9 x 10^{-4} mol/cm^3, which reduces to 3 °C, 60.1 MPa, 23.4 x 10^{-4} mol/cm^3 at 2:1 and -17 °C, 0.5 MPa, 12.8 x 10^{-4} mol/cm^3 for 4.75:1. A similar

pattern was found for epoxy soybean and is consistent over a range of anhydrides.[260]

The pattern in T_g values between oils similarly follows the crosslink density with lower temperatures for samples with lower epoxide functionality e.g. soybean 1:1 (6 °C), palm 1:1 (-33 °C) and euphorbia 1:1 (-36 °C). Interestingly, soybean oil polymers have relatively low glass transition temperatures being lower than grapeseed and rapeseed oils for all anhydride ratios despite having a higher crosslink density and Young's modulus. The T_g values for all samples were below room temperature so all samples were in an amorphous 'rubbery' state.

4.2.4 Copolymerisation of epoxy oils with methyl-5-norbornene-2,3-dicarboxylic anhydride (methyl nadic anhydride MNA)

One of the most popular anhydrides used for curing epoxy resins is methyl-5-norbornene-2,3-dicarboxylic anhydride or methyl nadic anhydride, MNA (Figure 4.12). Novolac epoxy/NMA polymers which contain terminal epoxides are normally cured at 200°C for 16 hours but the polymers themselves can undergo decomposition *via* a retro Diels-Alder reaction at 240-300°C.[258] We would expect that curing with internal epoxides, such as those in epoxidised vegetable oils, would be slower and require higher temperatures, and thus care must be taken not to decompose the MNA during the curing process.

Figure 4.12. Methyl-5-norbornene-2,3-dicarboxylic anhydride curing agent and 4-methyl imidazole as catalyst.

As before this anhydride was used as a curing agent for the polymerisation of all five epoxidised plant oils (ESBO, EGSO, ERSO, EPO, EuO), and the mechanical and thermal properties were tested as well as measuring the curing temperature. The curing exotherms showed peak curing temperatures of EGSO (203°C), ESBO (206°C), ERSO (210°C), EPO (213°C), EuO (214°C), slightly higher than that reported for the novolac system and paralleling the level of epoxidation as determined previously. During the course of this work, the thermal and mechanical properties of an epoxidised soybean/ NMA polyester were reported. The curing temperature was found to be ~200°C in line with this work.[259]

Dogbones were prepared in an aluminium dogbone mould at 210°C for 1h. The resulting polymers were dark brown in colour and ranged from hard and brittle for EGSO and ESBO in a 1:1 ratio to soft and tacky for EPO, EuO and lower anhydride ratios. The darkening, compared to materials with Aradur are likely due to the higher temperature of curing causing slight decomposition of the anhydride.

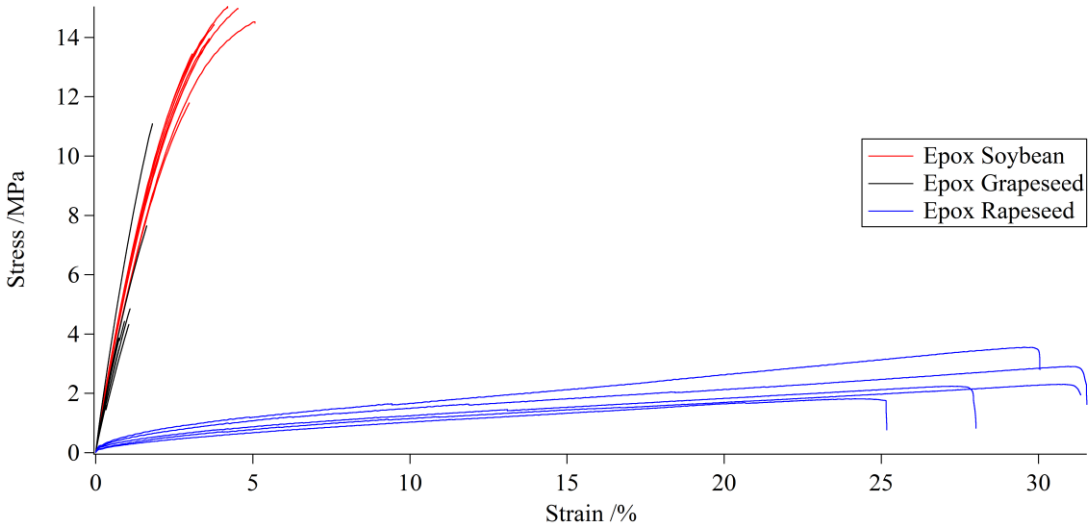

Figure 4.13. Stress Strain curves of EGSO ESBO and ERSO polyesters with MNA hardener (1:1 ratio). Extension rate 2mm min^{-1} using 1 kN load cell at 20 °C.

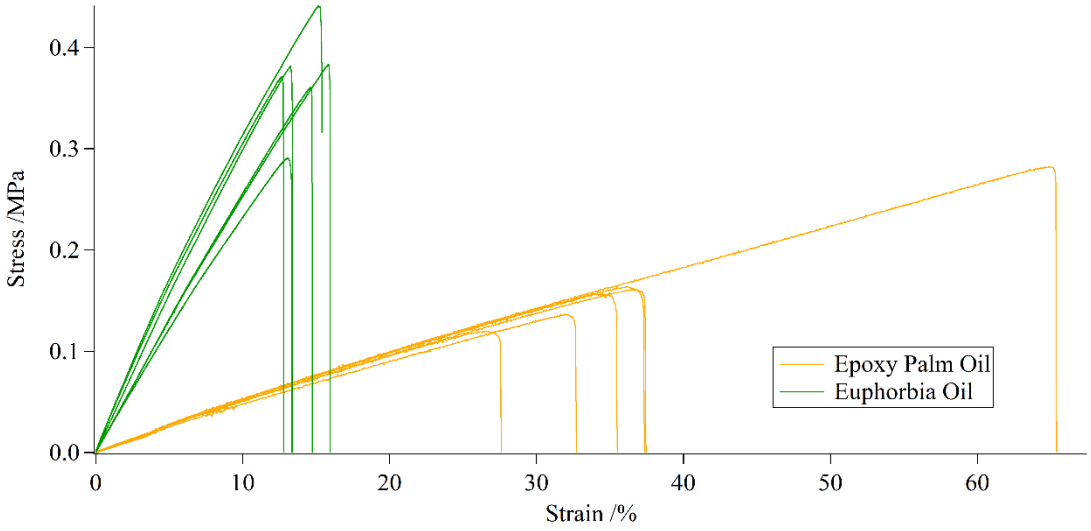

Figure 4.14. Stress Strain curves of EPO and EuO polyesters with MNA hardener (1:1 ratio). Extension rate 2mm min^{-1} using 1 kN load cell at 20 °C.

As can be seen in the stress strain curves (Figure 4.13 and Figure 4.14) and Table 4.6 soybean oil based polymers had the greatest strength at 14 MPa which decreases to 1.06 and 0.12 MPa when the ratio of hardener is reduced. This trend is the same as the Aradur 917 cured samples where the lower amount of hardener produces a smaller polymer network therefore weaker tensile properties. The trend in tensile

strengths between oils follows the same pattern as Aradur 917 cured polymers. At the same E:A ratio the tensile strength relates to epoxide number with soybean and grapeseed producing strong polymers and euphorbia and palm producing weaker samples.

Polymer			UTS /MPa	YM /MPa	EB /%
Anhydride	**Epoxide**	**E:A**			
Methyl nadic anhydride	ESBO	1:1	14.0 ±2.2	533.8 ±38.9	3.79 ±0.53
		2:1	1.06 ±0.29	10.97 ±3.09	13.6 ±2.1
		4.4:1	0.12 ±0.03	0.73 ±0.30	13.1 ±0.9
	EGSO	1:1	5.60 ±1.37	468.9 ±71.6	1.20 ±0.43
		2:1	1.93 ±0.54	30.8 ±12.6	13.95 ±3.45
		4.75:1	0.18 ±0.04	1.22 ±0.10	14.51 ±2.14
	ERSO	1:1	2.51 ±1.04	29.7 ±13.6	29.2 ±2.7
		2:1	0.51 ±0.31	40.0 ±28.6	1.71 ±0.26
		3.8:1	0.03 ±0.01	0.64 ±0.13	4.96 ±0.69
	EPO	1:1	0.17 ±0.05	0.53 ±0.03	34.1 ±4.1
		2:1	0.02 ±0.01	0.02 ±0.01	114 ±11
	EuO	1:1	0.37 ±0.08	2.94 ±0.46	14.3 ±1.3
		2:1	0.11 ±0.03	0.77 ±0.06	18.0 ±1.3

Table 4.6. Tensile data of plant oil polyesters copolymerised with methyl nadic anhydride. [a]Ultimate tensile stress, [b]Young's Modulus, [c]Elongation at break point. Errors are stated as one standard deviation from the mean value.

Methyl nadic anhydride is a larger molecule than methyl tetrahydrophthalic anhydride, not significantly in terms of molecular weight having only one carbon different. However the positon of the extra carbon as a bridge has increased the size from the relatively flat Aradur 917 (Figure 4.15). This increase in bulk was assumed to decrease crosslinking density of MNA cured polymers.

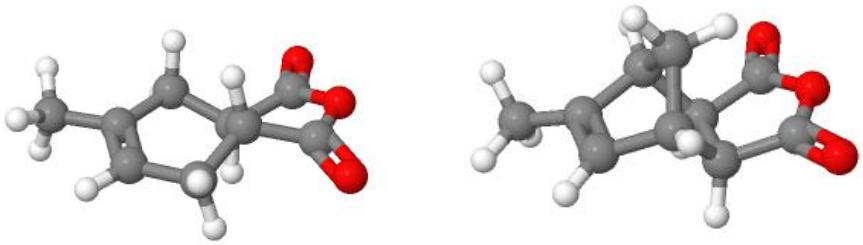

Figure 4.15 Molecular structures of Aradur 917 (left) and MNA (right)

Crosslinking density was measured by immersion in toluene for 1 week and calculated using the Flory-Rehner equation.

Polymer			Crosslinking Density
Anhydride	**Epoxide**	**E:A ratio**	**x 10^{-4} mol/cm^3**
Methyl nadic anhydride	Epoxy Soybean Oil	1:1	23.8 (35.8)
		2:1	14.0 (19.2)
		4.4:1	6.2 (11.8)
	Epoxy Grapeseed Oil	1:1	16.4 (32.9)
		2:1	23.5 (23.4)
		4.75:1	6.0 (12.8)
	Epoxy Rapeseed Oil	1:1	17.4 (25.7)
		2:1	9.6 (16.4)
		3.8:1	3.7 (9.2)
	Epoxy Palm Oil	1:1	1.6 (2.7)
		2:1	0.4 (0.5)
	Euphorbia Oil	1:1	3.3 (5.2)
		2:1	1.7 (2.4)

Table 4.7. Crosslinking density of MNA-plant oil polyesters. Aradur 917 samples in brackets.

The data in Table 4.7 shows a similar general trend as seen in the previous hardener where at the same E:A ratio the oils with greater epoxide functionality have higher crosslinking density such as ESBO 1:1 with 23.8 x10^{-4} mol/cm^3 compared to EPO 1:1 with 1.6 x10^{-4} mol/cm^3. Again the amount of hardener governs crosslinking as the decrease in E:A ratio decreases crosslink density eg rapeseed polymers 1:1 (17.4) 2:1 (9.6) and 3.8:1 (3.7). This trend is reflected in the Young's modulus and tensile strength showing the same patterns, EGSO 1:1 has a tensile strength of 5.6 MPa and

YM = 469 MPa, reducing the ratio to 4.75:1 gives UTS =0.18 and YM = 1.22 or decrease the epoxide functionality with palm oil and UTS = 0.17 and YM = 0.53.

However what is interesting is compared to Aradur 917 copolymerised samples the crosslinking density is considerably less, as low as 50% in some cases (EGSO 1:1 – 16.4 compared to 32.9 and ERSO 3.8:1 3.7 vs 9.2) which can be observed in the tensile data.

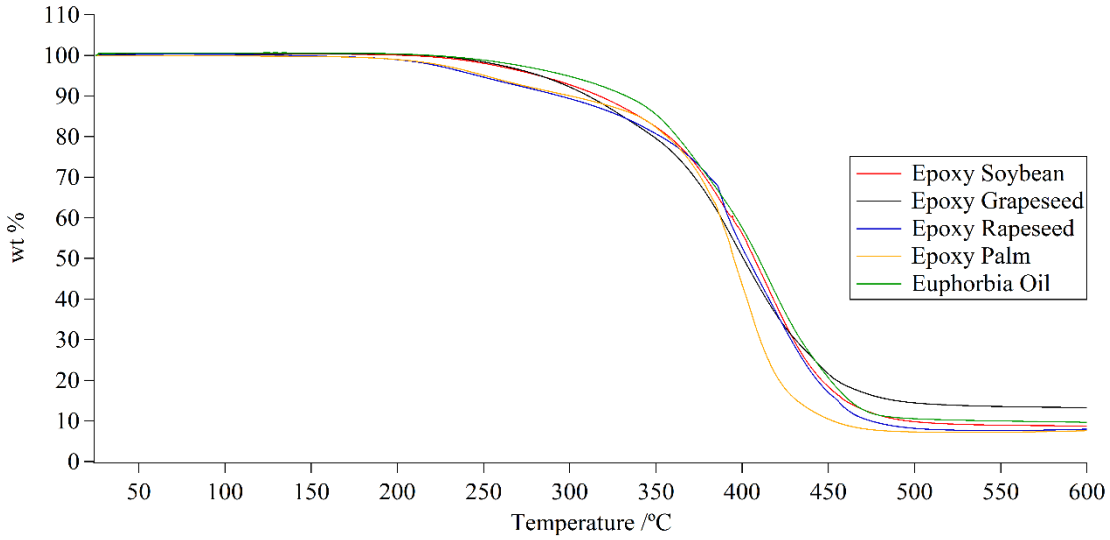

Figure 4.16. TGA analysis of plant oil based polyesters with methyl nadic anhydride hardener (1:1 ratio). Heating rate was 10 °C min^{-1} from 25 – 600 °C in air.

TGA analysis was performed on these polyester samples (Figure 4.16 and Table 4.8). The onset of thermal degradation was higher with lower ratios of anhydride, this was true for all oils (e.g. rapeseed oil 1:1 (198 °C), 2:1 (233 °C) and 3.8:1 (284 °C). Other research has shown methyl nadic anhydride begins to degrade at between 240 °C and 300 °C attributed to a retro Diels-Alder reaction[258] which accounts for the onset of degradation in that range. There was no particular trend between oils and degradation was fairly consistent having a range of only 64 °C at $T_{-10\%}$ which narrows to 25 °C at $T_{-50\%}$.

Polymer			T_g	$T_{-1\%}$	$T_{-10\%}$	$T_{-50\%}$
Anhydride	**Epoxide**	**E:A ratio**	**/°C**	**/°C**	**/°C**	**/°C**
Methyl nadic anhydride	Epoxy Soybean Oil	1:1	54	235	317	407
		2:1	-10	212	309	389
		4.4:1	-19	270	358	410
	Epoxy Grapeseed Oil	1:1	62	241	311	401
		2:1	-23	232	313	399
		4.75:1	-32	258	338	403
	Epoxy Rapeseed Oil	1:1	-12	198	294	403
		2:1	-	233	338	395
		3.8:1	-	284	375	420
	Epoxy Palm Oil	1:1	-29	199	300	395
		2:1	-	259	346	385
	Euphorbia Oil	1:1	-39	246	333	410
		2:1	-53	269	353	401

Table 4.8. Thermal analysis data of MNA copolymerised plant oil polyesters.

The glass transition temperatures were recorded by DSC, methyl nadic anhydride polyesters were consistent with the general trend of lower anhydride ratio giving lower T_g values e.g ESBO 1:1 (54 °C), 2:1 (-10°C) and 4.4:1 (-19 °C) which also follows the trend in crosslinking and Young's modulus. What is to be noted is the significant decrease in values for 1:1 to 2:1 ratios for soybean and grapeseed oil samples (85 °C for EGSO) which is not observed in Aradur 917 cured polymers (max difference 26 °C).

4.2.5 Copolymerisation of Epoxy Oils with Food Safe Anhydride

The previous results indicate that both Aradur® 917 and methyl-5-norbornene-2,3-dicarboxylic anhydride (NMA) when reacted with oils with high epoxide numbers (e.g. EGSO and ESBO) provide strong but brittle polymers (e.g. a 1:1 ratio of ESBO with Aradur® 917 gave a material with a UTS = 29.33 MPa and 4.9% elongation). More flexibility could be achieved either by incorporating a lower level of hardener (e.g. a 2:1 ratio of ESBO, with Aradur® 917, UTS = 1.17 MPa and 15% elongation), or by changing the epoxidised oil to one with a lower epoxide value (e.g. a 1:1 ratio

of EPO, with Aradur® 917, 0.151 MPa and 45% elongation), but in these cases increased flexibility comes at the cost of strength. A common anhydride used for flexible polyesters is dodecenyl succinic anhydride (Figure 4.17), the carbon chain aids flexibility by preventing close packing of molecules and the lowering of the glass transition temperature.[260,261]

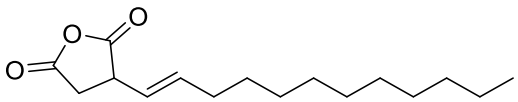

Figure 4.17. Dodecenyl succinic anhydride

A similar anhydride 2-octadecenyl succinic anhydride, (2-OSA) (Figure 4.18) would also allow for flexible polymer but is also safe for food contact[262] and is considered eco-friendly.[263]

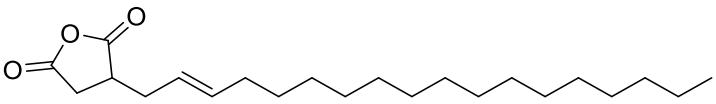

Figure 4.18. 2-Octadecenyl succinic anhydride, (2-OSA).

2-Octadecenyl succinic anhydride (2-OSA) was synthesised from maleic anhydride and 1-octadecene by the ene reaction (Figure 4.19)[264]

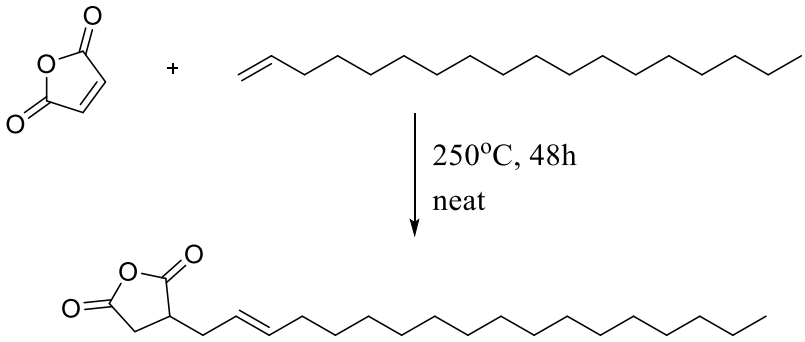

Figure 4.19. Ene reaction of maleic anhydride and 1-octadecene

This anhydride was investigated for its use as a hardener for flexible food contact safe polyesters from epoxidised plant oils and the results compared to the previous two hardeners. As before, the oils were combined in epoxide:anhydride ratios of 1:1, 2:1, and ~4:1 for epoxidised grapeseed, soybean and rapeseed oils and 4-methyl imidazole was used as a catalyst at 1wt% relative to total weight. Cure times and temperature were studied by DSC heating from 25 to 250 °C at 10 °C per minute (Table 4.9).

Polymer			$\Delta H_{polymerisation}$ /Jg^{-1}	Peak Cure Temp /°C
Anhydride	**Epoxide**	**E:A**		
2-Octadecenyl succinic anhydride	Epox Grapeseed Oil	1:1	185	167
	Epox Soybean Oil	1:1	154	172
	Epox Rapeseed Oil	1:1	153	167
	Epox Palm Oil	1:1	72	165
	Euphorbia Oil	1:1	65	170

Table 4.9. DSC data from polymerisation of epoxidised plant oils and 2-octadecenyl succinic anhydride.

The peak cure temperatures (165-172°C) were found to be closer to those measured for Aradur® 917 (138-180°C) than NMA (203-214°C). The actual values did not follow the previously observed trend EGSO<ESBO<ERSO<EPO~EuO, although the

temperature spread was less (2-OSA, ΔPCT = 7°C; Aradur® 917, ΔPCT = 42°C; NMA, ΔPCT = 11°C). As before, the expected trend of $\Delta H_{polymerisation}$ paralleling the epoxide functionality was observed.

Dog bone samples using 2-OSA were formed as previously but curing was carried out at 170°C for 1h in an aluminium mould. The tensile properties are illustrated in Figure 4.20 and Figure 4.21.

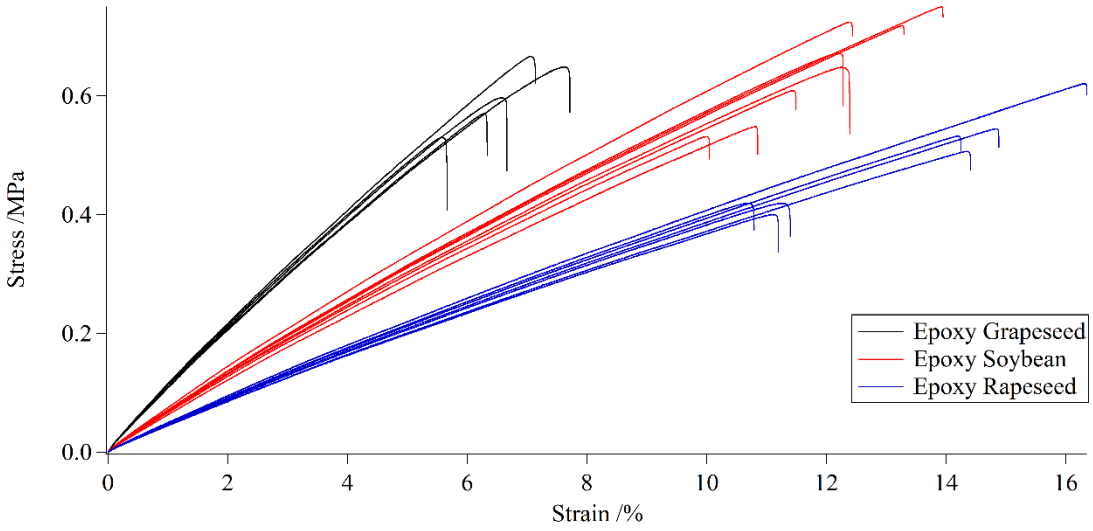

Figure 4.20. Stress strain curves of polyesters of EGSO ESBO and ERSO with 2-octadecenyl succinic anhydride (1:1 ratio). Extension rate 2mm min^{-1} using 1 kN load cell at 20 °C.

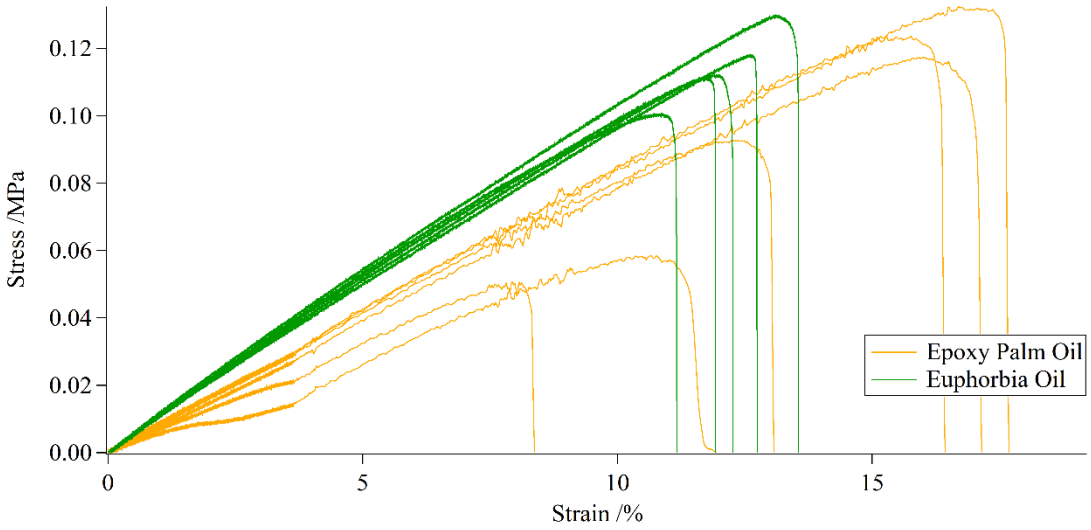

Figure 4.21. Stress strain curves of polyesters of EPO and EuO with 2-octadecenyl succinic anhydride (1:1 ratio). Extension rate 2mm min^{-1} using 1 kN load cell at 20 °C.

Compared to Aradur® 917 and NMA the use of 2-OSA as the hardener has significantly altered the tensile properties (up to 45 times lower) and Young's modulus (up to 167 times lower) with little significant increase in elongation at break, if any. However, the general trends observed previously were recorded. Hence, decreasing the amount of 2-OSA leads to a decrease in the tensile strength (EGSO ratio 1:1, UTS = 0.55; ratio 2:1, UTS = 0.32; ratio 4.75:1, UTS = 0.13) and so does decreasing the epoxide value of the oil (Ratio 1:1 ESBO, UTS = 0.65; EPO, UTS = 0.1). As before this was paralleled in the cross-linking density.

Polymer			UTS[a] /Mpa	YM[b] /Mpa	EB[c] /%
Anhydride	**Epoxide**	**E:A ratio**			
2-Octadecenyl succinic anhydride	Epox Soybean Oil	1:1	0.65 ±0.08	6.52 ±0.32	12.1 ±1.3
		2:1	0.55 ±0.06	7.30 ±0.13	8.75 ±1.17
		4.4:1	0.08 ±0.02	0.87 ±0.15	9.62 ±3.21
	Epox Grapeseed Oil	1:1	0.56 ±0.12	10.5 ±0.4	6.71 ±0.78
		2:1	0.32 ±0.07	9.26 ±0.34	3.68 ±0.96
		4.75:1	0.13 ±0.01	1.77 ±0.55	7.26 ±0.47
	Epox Rapeseed Oil	1:1	0.45 ±0.11	4.42 ±0.15	13.0 ±2.2
		2:1	0.32 ±0.13	4.24 ±0.23	11.1 ±2.5
		3.8:1	0.10 ±0.03	0.77 ±0.04	15.8 ±2.5
	Epox Palm Oil	1:1	0.10 ±0.03	0.74 ±0.13	14.1 ±3.6
		2:1	0.04 ±0.01	0.10 ±0.03	35.5 ±1.9
	Euphorbia Oil	1:1	0.12 ±0.01	1.12 ±0.03	12.3 ±0.9
		2:1	0.08 ±0.01	0.30 ±0.04	36.3 ±3.9

Table 4.10. Tensile testing data (average values) of plant oil and 2-Octadecenyl succinic anhydride polyesters. [a]Ultimate tensile stress, [b]Young's Modulus, [c]Elongation at break point. Errors are stated as one standard deviation from the mean value.

Using 2-OSA has decreased the crosslinking density compared with Aradur® 917 and MNA due to the long aliphatic chain preventing close packing of the polymer network, swelling tests were carried out to prove this. The samples were immersed in toluene for 1 week and the Flory-Rehner equation used to calculated crosslinking density (Table 4.11).

Polymer			Crosslinking Density x10^{-4} mol/cm^3
Anhydride	**Epoxide**	**E:A ratio**	
2-Octadecenyl succinic anhydride	Epox Soybean Oil	1:1	20.2 (35.8)
		2:1	18.8 (19.2)
		4.4:1	7.31 (11.8)
	Epox Grapeseed Oil	1:1	21.7 (32.9)
		2:1	22.2 (23.4)
		4.75:1	4.81 (12.8)
	Epox Rapeseed Oil	1:1	17.8 (25.7)
		2:1	15.4 (16.4)
		3.8:1	7.37 (9.21)
	Epox Palm Oil	1:1	4.49 (2.69)
		2:1	3.11 (0.48)
	Euphorbia Oil	1:1	4.75 (5.21)
		2:1	2.36 (2.37)

Table 4.11. Crosslinking density of epoxidised vegetable oils and 2-OSA polyesters, value with Aradur® 917 are in brackets as a comparison.

These results show that samples made with 2-octadecenyl succinic anhydride do have lower crosslinking density than the other two anhydrides, for example epoxidised soybean oil and anhydrides in a 1:1 epoxide:anhydride ratio have a higher density when cured with Aradur® 917 and methyl-5-norbornene (35.8 and 23.8 respectively) than using 2-OSA (20.2 x 10^{-4} mol/cm^3). This is the case for all the oils and ratios tested apart from epoxidised palm oil where the crosslinking density was higher for 2-octadecenyl using both ratios (4.49 for 1:1 and 3.11 for 2:1) than for the other two anhydrides (2.68 and 0.477 for Aradur 917, 1.62 and 0.395 for MNA). This could be due to greater compatibility, the structure of 2-OSA is more similar to the long saturated chain of palm oil. The other oils have more epoxide groups or C=C bond producing kinks (euphorbia oil) preventing close packing of molecules, palm oil and 2-OSA have greater packing as both are waxy solids at room temperature.

Thermal properties of 2-OSA cured polyesters were also tested (Figure 4.22 and Table 4.12).

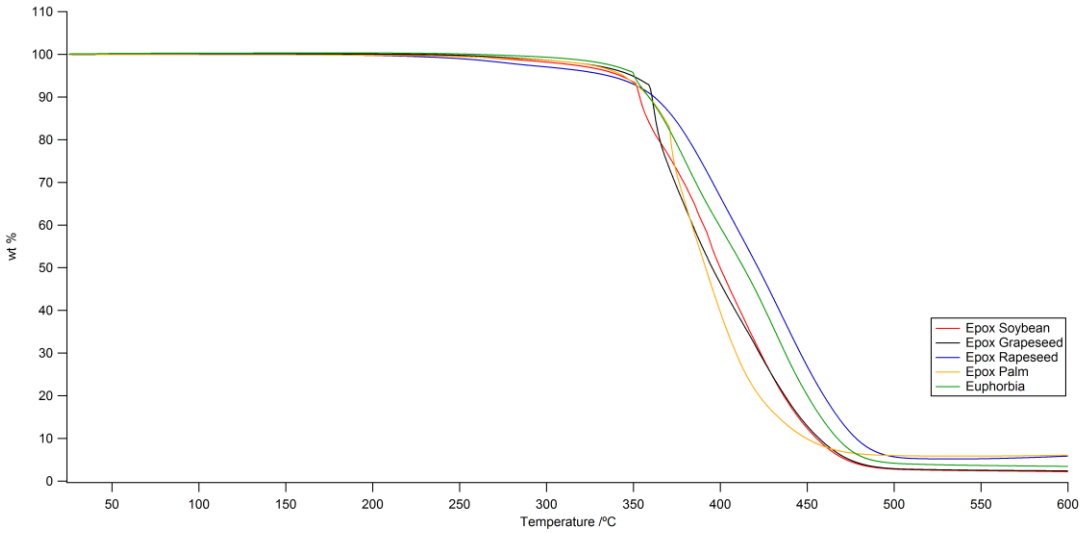

Figure 4.22. TGA analysis of epoxidised vegetable oils and 2-octadecenyl succinic anhydride polymers (1:1 ratio). Heating rate was 10 °C min^{-1} from 25 – 600 °C in air.

The results are similar to the other two anhydrides in that there is no definitive trend between the different oils only that euphorbia oil has the highest onset degradation temperature ($T_{-1\%}$). Also as with thermal results from Aradur® 917 and methyl nadic anhydride there is a wide range of degradation temperatures at 1% weight loss (89°C) which narrows at greater weight loss (20°C at 10% and 30°C at 50%).

Thermal degradation temperatures of polymers cured with 2-OSA are higher in general than MNA and Aradur 917 anhydrides as they exhibit a reverse Diels-Alder reaction upon degradation between 240 and 300 °C.[258] The long chain of 2-OSA puts it closer in structure to fatty acid chains of plant oils, which is observed in an almost single step degradation.

Polymer			$T_{-1\%}$ /°C	$T_{-10\%}$ /°C	$T_{-50\%}$ /°C
Anhydride	**Epoxide**	**E:A ratio**			
2-Octadecenyl succinic anhydride	Epox Soybean Oil	1:1	274	354	400
		2:1	313	360	397
		4.4:1	322	358	395
	Epox Grapeseed Oil	1:1	287	360	395
		2:1	323	366	397
		4.75:1	317	369	413
	Epox Rapeseed Oil	1:1	250	362	422
		2:1	314	370	420
		3.8:1	327	374	420
	Epox Palm Oil	1:1	282	359	392
		2:1	297	363	405
	Euphorbia Oil	1:1	311	359	414
		2:1	339	355	403

Table 4.12. Thermal data of epoxidised vegetable oils and 2-octadecenyl succinic anhydride polymers.

Glass transition temperatures could not be identified from DSC as there was no definitive step change in heat flow. The lack of an obvious transition point is either due to the T_g values of all samples existing below -100 °C (out of machine range) or there is very little energy difference between the amorphous and semi-crystalline states.

Dynamic mechanical thermal analysis (DMTA) can also be employed to measure T_g. A force is applied to a material (stress) and the strain is measured, from this the sample stiffness and energy loss are calculated. The ratio between polymer stiffness (storage modulus) and energy loss (loss modulus) is the tan δ which varies over temperature, the peak of tan δ is the glass transition point.

The glass transition temperatures of 2-OSA cured polyesters were measured, but the values can differ from DSC analysis so Aradur 917 samples were recorded for comparison (Figure 4.23 and Table 4.13).

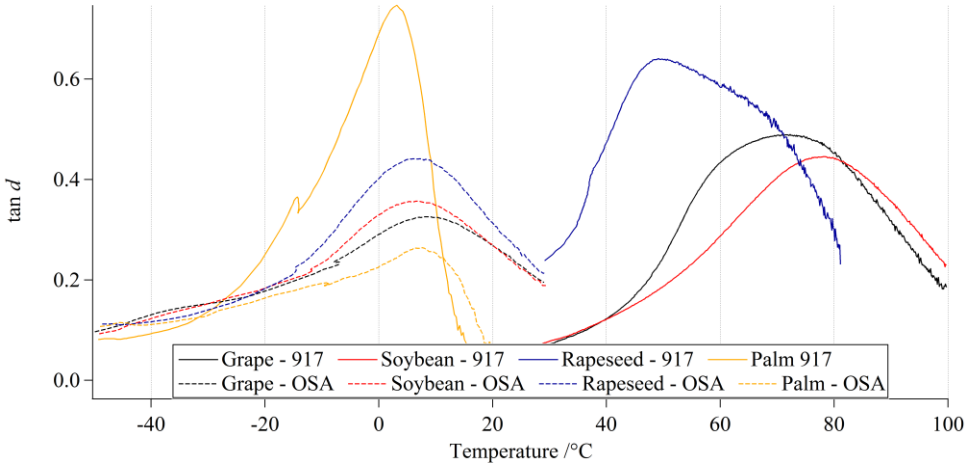

Figure 4.23 Tan δ from DMTA analysis of Aradur 917 and 2-OSA cured polymers (1:1 ratios).

Polymer		T_g - 917 (DSC)	T_g - 917	T_g - 2-OSA
Epoxide	**E:A ratio**	**/ºC**	**/ºC**	**/ºC**
Epoxy Soybean	1:1	6	78	7
	2:1	-19	30	-14
	4.4:1	-25	-10	-33
Epoxy Grapeseed	1:1	17	73	9
	2:1	3	24	-17
	4.75:1	-17	-25	-39
Epoxy Rapeseed	1:1	8	49	6
	2:1	-1	3	-16
	3.8:1	-27	-21	-35
Epoxy Palm	1:1	-33	3	8
	2:1	-49	4	7

Table 4.13. Thermal data of Aradur 917 and 2-OSA cured plan oil polymers data from DMTA and DSC.

Immediately obvious from the results is the considerable difference between T_g values obtained by DSC and DMTA (up to 72 °C) however this is consistent with other research (40 °C DSC and 110 °C DMTA) for epoxy soybean and methyl tetrahydrophthalic anhydride (Aradur 917). These results differ from the other anhydrides as changing the oil does not significantly affect the T_g values e.g. 1:1 E:A

ratio – ESBO (7 °C), EGSO (9 °C), ERSO (6 °C), EPO (8 °C) and 2:1 E:A ratio – ESBO (-14 °C), EGSO (-17 °C), ERSO (-16 °C), EPO (7 °C).

Interestingly samples based on palm oil show a higher T_g for 2-OSA than for Aradur 917. This relatively higher temperature is possibly due to the compatibility of the long alkyl chain of the anhydride and saturated chains in palm oil packing closer similarly to crosslink density.

4.3 Conclusions and Future Work

Anhydride ratio is an important factor when producing crosslinked polyesters from plant oils. The ratio of anhydride to epoxide groups governs the crosslink density which in turn dictates the physical properties such as glass transition temperature, tensile strength and Young's Modulus. Crosslink density is also determined by epoxide functionality as more epoxides per triglyceride produce more crosslinks and greater tensile strength, Young's modulus and a higher T_g.

Thermal degradation is largely independent of epoxide number but is affected by anhydride content. Using more anhydride gives a lower onset of degradation temperature for Aradur 917 and methyl nadic anhydride due to the retro Diels-Alder reaction starting at around 200 °C.

It would appear that if a polyester with maximum strength was required then a high epoxide number is required and to use an anhydride at a ratio of 1:1, e.g. ESBO – Aradur 917 1:1, tensile strength = 29.3 MPa and Young's modulus = 1090 MPa. However these polymers tend to be brittle (elongation = 4.9%).

If a polymer with more flexibility is needed then either less hardener can be used or a more saturated plant oil can be chosen, but this comes as a sacrifice of strength (ESBO – Aradur 917 2:1 elongation = 15% but tensile strength = 1.17 MPa)(ERSO – Aradur 917 1:1 elongation = 11% tensile strength = 3.94 MPa). Alternatively a larger anhydride with a long chain reducing crosslinking can be used but this also affects tensile strength.

Plant oil polyesters copolymerised with cyclic anhydrides seem to occupy two zones on a stress strain chart either high strength ***or*** high flexibility (Figure 4.24).

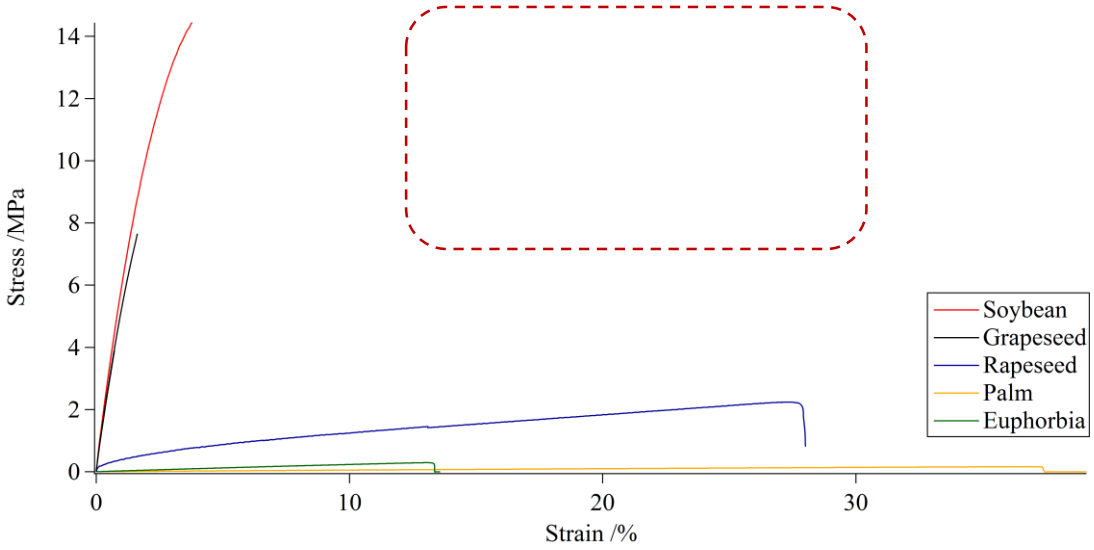

Figure 4.24. Stress Strain chart showing typical curves of plant oil polyesters.

Future studies should focus on the possibility of creating a polymer that has high strength ***and*** high elasticity (dotted area Figure 4.24).

The next chapter will investigate the potential improvements to these plant oil polyesters to gain polymers with strength and flexibility. Avenues to explore will be the addition of solid particles creating composite materials and to blend strong brittle polymers with soft flexible polymers to acquire the properties of both.

5 Nanocomposites and Polymer Blends of Renewable Polyesters from Vegetable Oils

5.1 Introduction

Epoxides are widely used in many industries and can be found in adhesives,[265] resins,[266] or coatings.[267] Epoxide based polymers exhibit useful properties such as chemical resistance, high adhesive strength and electrical insulation, however as found for vegetable oil epoxides in chapter 4 a high level of crosslinking leads to brittle materials, consistent with other epoxides in literature.[268] In the previous chapter where a polyester had high crosslinking, for example epoxy soybean with Aradur 917 1:1 ratio (crosslink density = 35.8 x 10^{-4} mol cm^{-3}), there was a high tensile strength of 29.3 MPa but only little elongation 4.9% before breakage. Whereas a lower crosslinked polymer such as epoxy palm oil with Aradur 917 1:1 ratio (crosslinking = 2.69 x 10^{-4} mol cm^{-3}) was more elastic stretching 44.5% before breakage but the tensile strength was significantly lower at 0.15 MPa.

Some common methods to resist breakage are to create a composite material where a continuous phase (e.g. polymer resin) is reinforced with a material of a different phase (e.g. fibres or particles). For example, glass fibre often used in automotive repair,[269] or carbon fibre[270] as a lightweight alternative to metal in a variety of industries from motor racing[271] to aviation[272] and sports equipment.[273] Recently there has been a rise in using natural fibres in composites such as cellulose[274], hemp[275] and flax.[276] But this area has seen a lot of research especially where plant oil resins are used.

An area of research which has received a lot of interest is nanocomposites, and this is an emerging subject in plant oil based polymers.[277] To be defined as a nanocomposites a material has to be multiphase and at least one phase has to have 1, 2 or three dimensions below 100 nm.[278] Nanocomposites are classified depending on the continuous phase (matrix), the main types being ceramic, metallic and polymeric. Typical fillers used in polymeric nanocomposites can be organoclay discs,[279] nanofibers[280] or particles.[281]

A common material used in nanocomposites is silica as it is relatively cheap, easily produced[282] and can be made in a various shapes and sizes.[281] Silica nanoparticles have generated a lot of research in polymeric composites based on petrochemical polymers, but there is relatively little work on plant oil based silica nanocomposites.[283]

A plant oil polyester reinforced by nano scale particles could potentially be more resistant to breakage while retaining or improving the tensile strength of the original polymer.

5.2 Aims

Investigate the use of nano particles or fillers in plant oil – anhydride polyesters to create nanocomposites which should increase tensile properties such as tensile strength or elongation at break or potentially both compared to those without

5.3 Results and Discussion

5.3.1 Increased Hardener Ratio

Before the addition of any particles we determined if polyester samples without fillers could be improved in terms of tensile strength. The strongest polymer in the previous chapter was prepared with irrespective of the oil or anhydride combination

using a 1:1 ratio of monomers. Vegetable oils with a high percentage of poly unsaturated fatty acids (eg grapeseed oil ~70%) have, in their epoxidised version, a high proportion of epoxides in close proximity to each other. As polymerisation proceeds some of these epoxides experience greater steric hindrance from the crosslinked network, as the degree of polymerisation increases some of these epoxides can become isolated in the network. A small molecule such as an anhydride will have greater mobility and will be able to react with the isolated epoxides, so a greater amount of hardener may lead to fewer unreacted epoxides.

In this section it was investigated whether increasing the amount of anhydride relative to the number of epoxides would increase the strength of plant oil based polyesters used in the previous chapter.

For this investigation both epoxy grapeseed and euphorbia oil were chosen and the hardener was Aradur 917. The hardener was mixed with each oil in a 1:0.8 and 1:0.5 ratio relative to the epoxide number. The polymerisation procedure was the same as described in chapter 4, all reagents were mixed under vacuum and cured at 170 °C for 1 h in a silicone 'dogbone' mould.

Polymer			**UTS[a] /MPa**	**YM[b] /MPa**	**EB[c] /%**
Anhydride	**Epoxide**	**E:A ratio**			
Aradur 917	Epox Grapeseed Oil	1:1	12.8 ±1.0	1005 ±77	1.47 ±0.32
		1:0.8	27.5 ±7.8	1261 ±319	4.36 ±2.09
		1:0.5	3.5 ±1.0	802 ±28	0.59 ±0.26
	Euphorbia Oil	1:1	0.16 ±0.03	0.96 ±0.07	20.6 ±3.8
		1:0.8	0.18 ±0.04	0.62 ±0.07	37.6 ±6.8
		1:0.5	-	-	-

Table 5.1. Tensile data of epoxy grapeseed and euphorbia oils polyesters with increased hardener ratio. [a]Utimate Tensile Stress, [b]Young's Modulus, [c]Elongation at Break Point. Errors are stated as one standard deviation from the mean value.

The epoxy grapeseed oil samples (Table 5.1) showed an increase in tensile strength and Young's modulus when an small excess of anhydride (1:0.8) was used compared to the 1:1 ratio but a severe decrease in strength at the larger 1:0.5 ratio. The euphorbia sample shows much less relative increase in both tensile strength and elasticity with an excess of anhydride. Unfortunately the 1:0.5 ratio sample was not suitable for tensile testing as the test pieces lacked structural integrity (Figure 5.2).

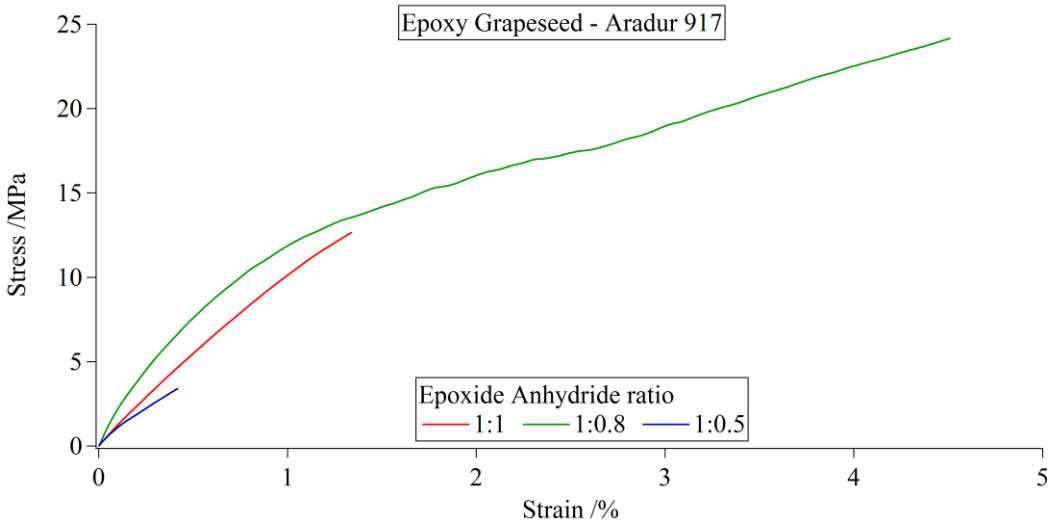

Figure 5.1. Stress - Strain chart of epoxy grapeseed oil polyesters with increased hardener ratio. Extension rate 2mm min^{-1} using 1kN load cell.

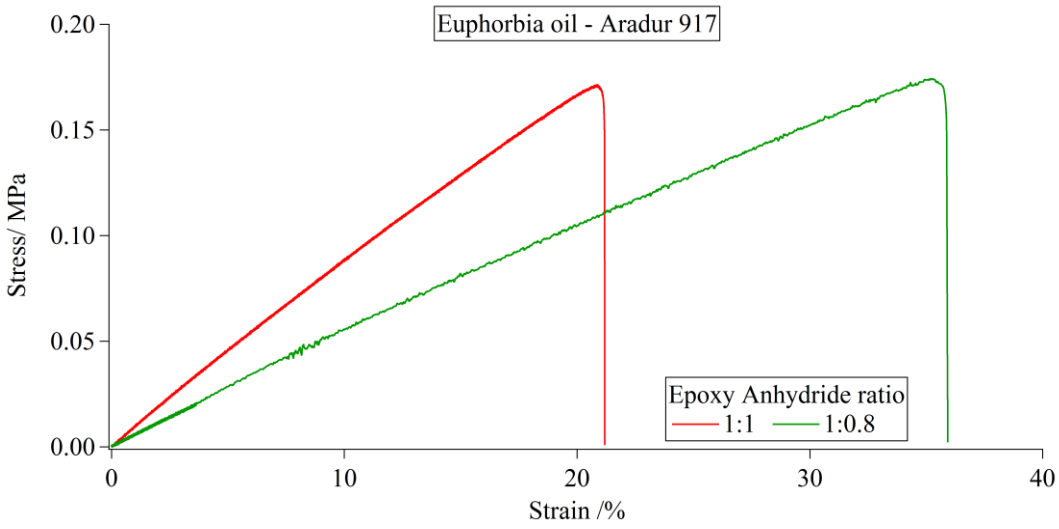

Figure 5.2. Stress - Strain chart of euphorbia oil polyesters with increased hardener ratio. Extension rate 2mm min^{-1} using 1kN load cell.

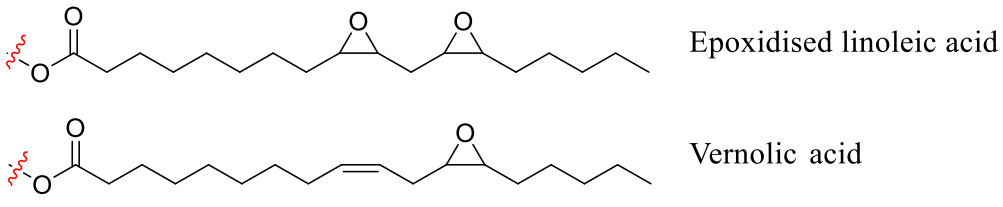

Figure 5.3. Epoxidised linoleic acid and vernolic acid.

It appears that an excess of anhydride increases the tensile strength of epoxy grapeseed samples whereas euphorbia oil samples remain largely unaffected. The increase in strength can be attributed to the steric hindrance argument above. The majority of the fatty acids in grapeseed oil are linoleic acid having epoxides in close proximity whereas in euphorbia oil the main fatty acid is vernolic acid which only contains one epoxide (Figure 5.3).

Conversely in petrochemical epoxides an excess of epoxide is reported to give more complete polymerisation due to competing polyether formation from epoxide-epoxide reactions.[284,285] However it is reported that the highly polyunsaturated linseed oil, upon reaction with cyclic anhydrides, does not form competing polyether links and an excess of anhydride gives a higher flexural modulus (stiffness) consistent with the higher Young's modulus of the 0.8:1 ratio we reported.[286]

It appears that a slight excess of anhydride is beneficial for increasing tensile properties of plant oil epoxide based polyesters and is more effective for greater unsaturated oils. Further investigation to optimise the exact excess required would be useful.

5.3.2 Addition of Silica Particles

The inclusion of silica nanoparticles has shown great interest recently forming nanocomposites and increasing tensile strength compared to the neat resin.[287]

Typically this research is centred on bisphenol epoxides. Nano silica particles have shown to increase tensile strength of a bisphenol-F epoxy resin from 50 MPa for the neat resin to 70 MPa as a composite.[288] Two sizes of silica particle were studied, 12 nm and 100 nm, but size had little difference on tensile properties. Silica nano particles can increase tensile strength of the bisphenol-A system in inclusions as low as 5 vol%.[289] The increase in strength of epoxy – silica composites is attributed to covalent bonds between the particles and the polymer network, silica was shown to ring open epoxy polymers at the same cure temperature as our epoxy-anhydride system (170 °C), which shows potential for our polyesters to form composites.

Although silica nanocomposites have attracted much interest in petrochemical based epoxy resins (typically bisphenol based polymers), relatively little work is produced with silica particles and bio-based epoxides. In epoxy soybean oil / cyanate ester polymers, silica nanoparticles have shown to increase tensile strength from 59 to 70 MPa.[290] For polyurethanes based on castor oil and hexamethylene diisocyanate, silica nanoparticles gave an increase in tensile strength from 4 to 9 MPa, no increase in elongation at break point was observed.[291]

Silica nanoparticles can be created *in situ* by silane coupling agents. Epoxy silane coupling agents (3-glycidyloxypropyl)trimethoxysilane (GPTMS) and 2-(3,4-epoxycyclohexyl)ethyl trimethoxysilane (ECTMS), (Figure 5.4) were used in the formation of nanocomposites with epoxy soybean and epoxy linseed oils.[292]

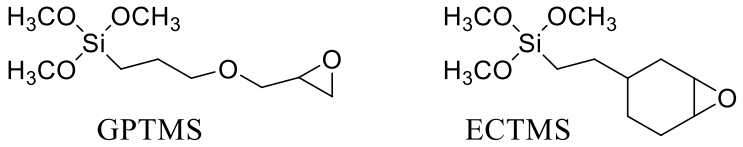

Figure 5.4. Epoxy silane coupling agents used in the formation of silica nanoparticles.

The composites from these silane coupling agents were found to increase tensile stress of epoxy soybean and epoxy linseed oils (1 to 6 MPa and 15.7 to 19.7 respectively).

The addition of nano silica particles has the potential to increase the tensile strength of the plant oil – anhydride polyesters described in chapter 4.

A sample of hollow silica particles were provided. They were synthesised by the Stober process[282] using tetraethyl orthosilicate (TEOS) in ethanol and ammonia. Ellipsoidal calcium carbonate was used as a substrate to grow the silica from. This governs the shape of the shell. The particles were soaked in 0.5M acetic acid to remove the calcium core and yield hollow silica shells (Figure 5.5).

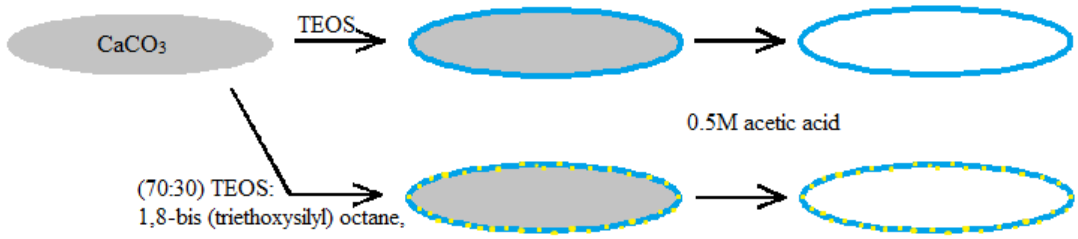

Figure 5.5. Synthesis of hollow silca particles from a calcium carbonatesubstrate.

As SiO_2 is hydrophilic (contact angle = $0< \theta <90°$)[293] and our renewable vegetable oil based polyesters are hydrophobic (contact angles $\sim 100< \theta <115$) it was thought the two would not mix efficiently. As a consequence, another batch of particles was produced with some surface alkyl content. These were formed by growing the shells from a 70:30 mixture of TEOS and 1,8-bis (triethoxysilyl) octane (

Figure 5.6).

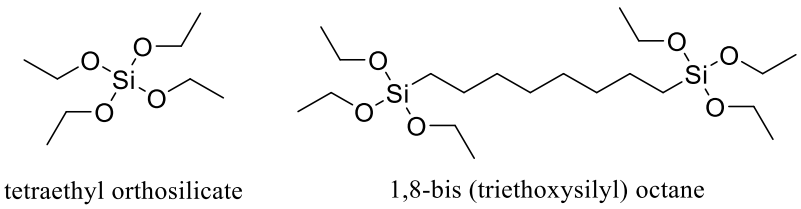

Figure 5.6. Tetraethyl orthosilicate (TEOS) and 1,8-bis (triethoxysilyl) octane used in the formation of hollow silica particles.

Both types of hollow silica particles were used as fillers in epoxy soybean and epoxy grapeseed oil polyesters with Aradur 917 (1:1). The hollow particles were mixed with the resin mixture at 1, 2 and 5 vol%, volume was used due to the extreme low density of the powder.The mixtures were stirred under vacuum overnight to remove any trapped air introduced by the powder when mixed with the resin. The samples were cured at 170 °C for 1 h at ambient pressure.

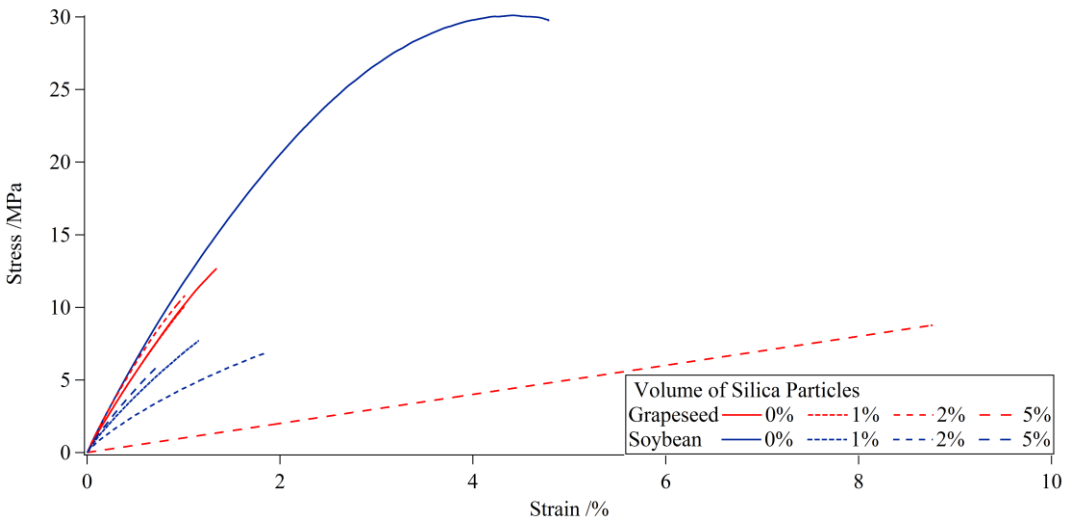

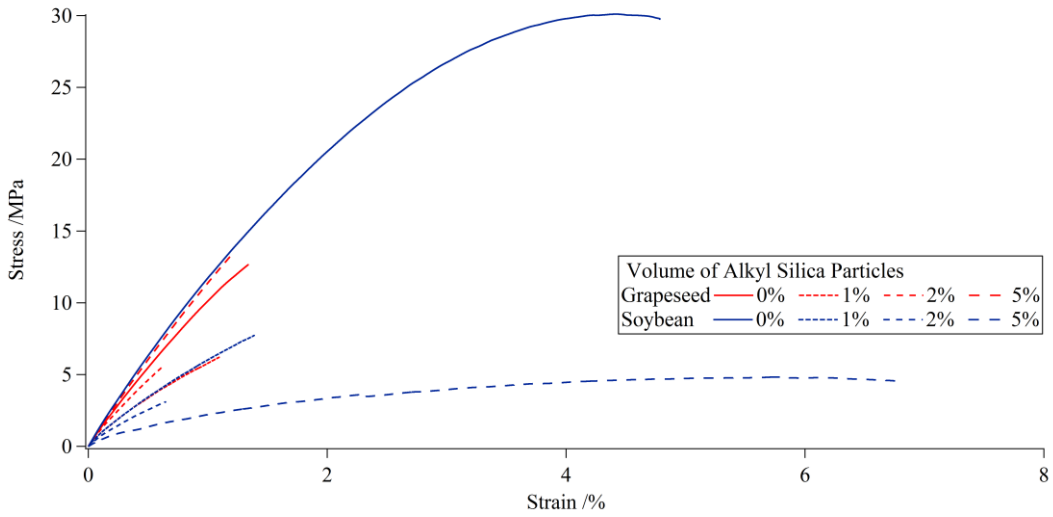

Figure 5.7. Stress Strain charts of original and alkyl functionalised silica nanocomposites with epoxy soybean and grapeseed oils. Extension rate 2mm min^{-1} using 1kN load cell.

Composite Sample			UTS /Mpa	YM /Mpa	EB /%
Particles	**Epoxide**	**vol %**			
None	Epoxy Grapeseed Oil	0	12.8 ±1.0	1005 ±77	1.47 ±0.32
	Epoxy Soybean Oil	0	29.3 ±0.7	1090 ±27	4.87 ±0.65
OH terminated SiO2	Epoxy Soybean Oil	1	7.6 ±0.7	619 ±35	1.13 ±0.06
		2	6.7 ±0.7	376 ±15	2.41 ±0.70
		5	6.10±1.1	632 ±159	0.96 ±0.32
	Epoxy Grapeseed Oil	1	10.5 ±1.0	981 ±63	1.01 ±0.11
		2	10.8 ±1.5	986 ±50	1.03 ±0.22
		5	9.0 ±1.0	1000 ±27	0.82 ±0.10
Octyl functionalised SiO2	Epoxy Soybean Oil	1	7.9 ±1.8	513 ±25	1.62 ±0.69
		2	3.0 ±0.6	321 ±113	0.77 ±0.08
		5	5.2 ±1.0	130 ±15	3.05 ±1.40
	Epoxy Grapeseed Oil	1	5.8 ±1.1	517 ±32	0.98 ±0.21
		2	5.7 ±1.3	717 ±268	0.63 ±0.07
		5	12.8 ±1.9	1134 ±43	1.08 ±0.19
Calcium carbonate	Epoxy Grapeseed Oil	1	7.2 ±1.8	688 ±130	0.92 ±0.12
		2	9.9 ±1.1	861 ±113	1.10 ±0.14
		5	10.4 ±1.1	1064 ±90	0.90 ±0.08

Table 5.2. Tensile data of epoxy grapeseed oils polyesters with silica nanopoarticles. Errors reported as one standard deviation from the mean.

As can be seen from the results (Figure 5.7, Table 5.2) there was a significant decrease in tensile strength on addition of silica or calcium carbonate. For soybean

and OH terminated SiO_2 this decrease was greatest with the largest amount of particles added. This pattern was not as expected, the greater amounts of silica should have provided greater tensile strength. It has been previously reported that particles not bonding to the polymer network do not provide an increase in tensile properties even decreasing strength in some cases due to creation of voids in the network.[294] Poor adhesion of particles to the network means that they can't carry the external load applied to the sample and strength relies solely on the polymer.[295] It is also important that particles used in composites are more resilient than the polymer matrix, hollow silica spheres were found to split upon breakage of the sample in a BADGE – phthalic anhydride system.[296] Calcium carbonate particles (used as a scaffold for the silica production) were included into epoxy grapeseed samples at 1, 2 and 5 vol%, this stronger particle would not covalently bond to epoxides but has shown to hydrogen bond.[297] The results show an increase in tensile strength with increased particle loading consistent with common theories, but the tensile strength is not a high as pure resin due to lack of particle bonding, consistent with our findings.

In summary the use of these particles are not suitable for use as nanocomposites with this epoxy – anhydride system, the reason are two-fold, weak hollow shells that break apart upon tensile stress and poor bonding of the particles to the polymer network. One aspect to explore is functionalization of the silica particles with epoxy containing silane coupling agents. One such agent (3-glycidyloxypropyl)trimethoxysilane has shown to increase tensile strength by 40% compared to pure SiO_2 in bisphenol systems.[298]

5.3.3 Addition of Polyaromatic Hydrocarbon

Since it was first isolated in 2004[299] graphene has received an explosion in interest across many areas in academia and industry due to some interesting properties it is 200 times stronger than steel with a tensile strength of 130 GPa,[300] flexible[301] and electrically conductive.[302] Graphene has shown to increase mechanical properties of a range of polymer composites such as PVA,[303] PMMA[304] and epoxy resins[305] and can show dramatic improvement in properties at very low loadings (0.05 wt%)[304]

Graphene oxide is a single sheet molecule similar to graphene but also having oxygen containing groups such as epoxides, carbonyls and hydroxyls. Graphene oxide has also been used in the manufacture of composite materials from plant oil feed stocks.[306] The oxygen containing groups are shown to covalently bond to epoxidised methyl oleate through ring opening forming ester and ether linkages.

Graphene oxide can be synthesised in a bottom-up approach in a relatively environmentally friendly method starting from glucose or glycerol,[307] showing a potentially green route to graphene synthesis.

An environmentally produced analogue of graphene used as a filler in a plant oil derived polymer shows potential as an interesting new route to green bio-based composites.

A sample of a polyaromatic hydrocarbon (PAH) was provided, this was synthesised from pyrene and glycidol in 80% sulfuric acid under nitrogen atmosphere at 100°C forming a black solid that was collected washed with water and dried. The reaction was terminated by oxidation which produced a mixture of polyaromatic

hydrocarbons with oxygen containing groups on the surface that were analogous to graphene oxide however a lot smaller at only 5 -10 fused rings in size (Figure 5.8).

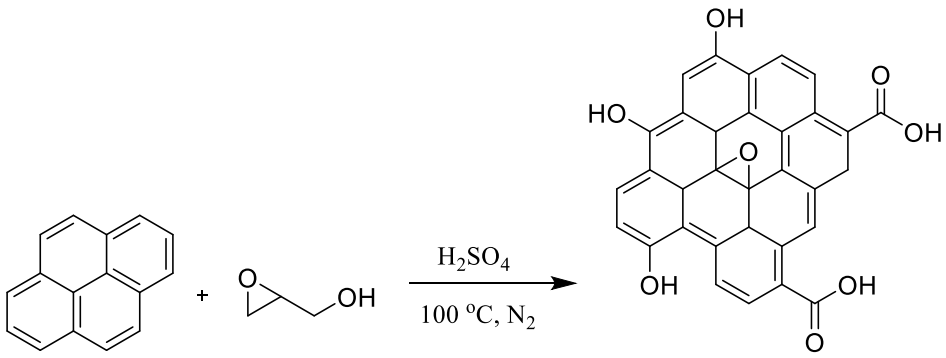

Figure 5.8. Synthesis of a poly aromatic hydrocarbon PAH.

Using polyaromatic hydrocarbons such as this in a plant oil – anhydride polymer would act as a model to assess the potential of graphene or graphene oxide in bio-based polymer composites.

The polyester for this experiment was based on epoxy grapeseed oil and had Aradur 917 as the harder in a 1:1 ratio, the PAH model was mixed with this resin at 1, 2 and 5 wt% and the standard mixing and curing processes were followed.

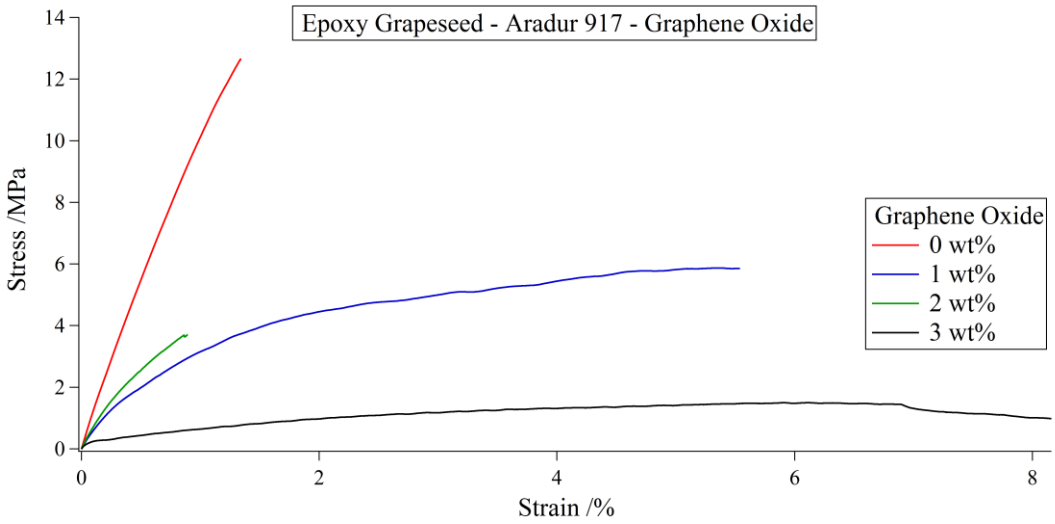

Figure 5.9. Stress Strain chart of PAH reinforced grapeseed polyesters. Extension rate 2mm min^{-1} using 1kN load cell.

The results show a general trend as the amount of PAH is increased the tensile strength and Young's modulus decrease (Table 5.3) at 0 wt% UTS = 12.76 MPa and YM = 1005 MPa which decreases to 1.53 MPa and 55.9 MPa respectively. A large effect in properties was observed even at 1 wt% PAH similarly to other research with graphene composites at low loadings.[304] Also an increase in elongation from 1.5 to 8.3% was observed consistent with the decrease in Young's modulus.

	UTS /Mpa	**YM /Mpa**	**EB /%**
PAH wt%			
0.0	12.8 ±1.0	1005 ±76	1.47 ±0.32
1	5.6 ±1.6	191 ±43	3.11 ±2.64
2	3.9 ±1.0	337 ±115	1.01 ±0.12
5	1.5 ±0.6	56 ±28	8.34 ±1.58

Table 5.3. Tensile data of graphene oxide polyester composites. Errors stated as one standard deviation fom the mean.

The decrease in tensile properties with increasing PAH amounts can be attributed to inefficient bonding to the polymer network, as observed earlier in the case of silica nanoparticles, potentially acting as a barrier between epoxide and anhydride groups decreasing polymerisation efficiency.

It has been shown that in bisphenol-F systems inclusion of graphene oxide nanoplatelets can decrease tensile strength from 77.6 to 35.5 MPa with an increase of graphene oxide from 0 to 6 wt%.[308] A decrease in tensile properties has also been observed in bio-based systems with graphene oxide introducing a 'soft segment' to the polymer network. Tensile strength in this composite was reduced from 8.8 to 4.3, (0 – 0.8 wt%) Young's modulus decreased from 12.4 to 2.4 and an increase in elongation was observed 115 to 266%.[309]

It appears that the addition of polyaromatic hydrocarbon has decreased tensile strength and Young's modulus while increasing elongation which is likely due to poor bonding of the filler to the polymer network.

In both cases with the addition silica and aromatic hydrocarbon the tensile strength of the composite was less than that of the parent polymer. The theory for this is down to less covalent bonding of the filler to the epoxide possibly due to less reactivity of an internal epoxide of a fatty acid chain compared to the terminal epoxides of the petrochemical bisphenol systems.

5.3.4 Addition of Styrene Oxide

It appears the addition of solid particles do not interact well with plant oil epoxides and the resulting composites are weaker in terms of tensile strength and Young's modulus.

To increase the strength of plant oil polyesters without the addition of particles the polymer backbone need to be made tougher. Many high strength polymers have aromatic sections in their polymer network such as polyaramids,[310] polysulfones[311] or polystyrene[312]

Styrene oxide (epoxidised styrene) has shown to be a useful monomer for producing semi-aromatic polyesters when copolymerised with cyclic anhydrides. The reaction can be initiated by enzymes[313] or metal catalysts[314,315] However little work has been produced investigating tensile properties of these polyesters especially with 2-octadecenyl succinic anhydride (2-OSA)

The addition of styrene oxide to a plant oil polyester such as our system should increase tensile strength through the addition of aromatic groups, although not in

the polymer backbone the aromatic groups may add strength through π-interactions.

Epoxy grapeseed oil was mixed with styrene oxide in ratios of 100:0, 80:20, 60:40, 40:60, 20:80 and were copolymerised with 2-OSA, (1 eq per number of epoxides). When these samples were cured at 170 °C bubbles were observed in the solid material, this could be because the curing temperature was near the boiling point of styrene oxide (194 °C) and some styrene oxide vapour may have been liberated. To overcome bubble formation the samples were degassed in a vacuum oven at 80 °C and polymerised over 16 h. Dynamic Scanning Calorimetry (DSC) measurements were recorded to determine whether the reaction was complete. As can be seen by the results (Figure 5.10) there are no exothermic peaks indicating complete polymerisation had occurred. The polymer samples were used for tensile testing without any further curing at higher temperatures.

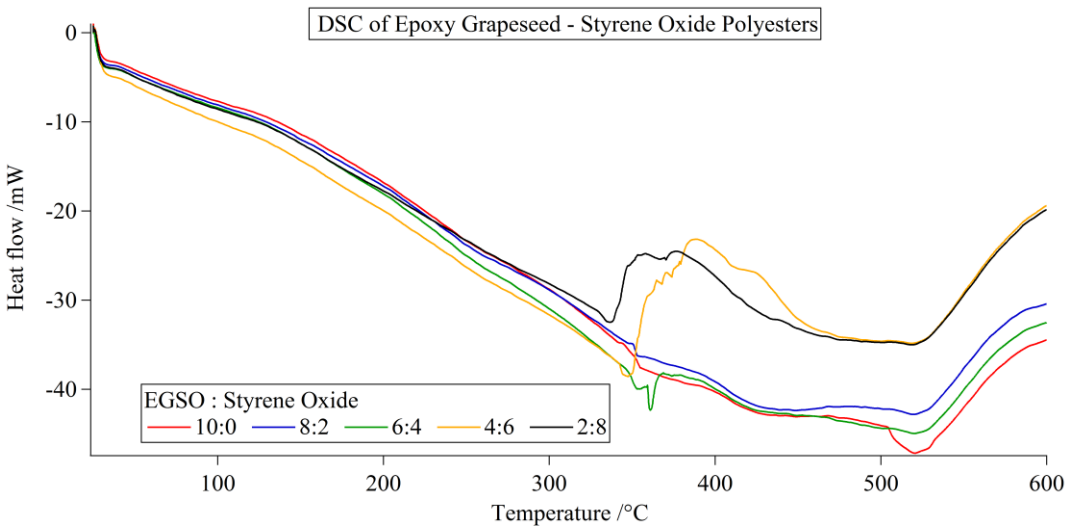

Figure 5.10. DSC chart of styrene oxide - EGSO polyesters cured at 80 °C. Heating rate was 10 °C min^{-1} under an ambient atmosphere.

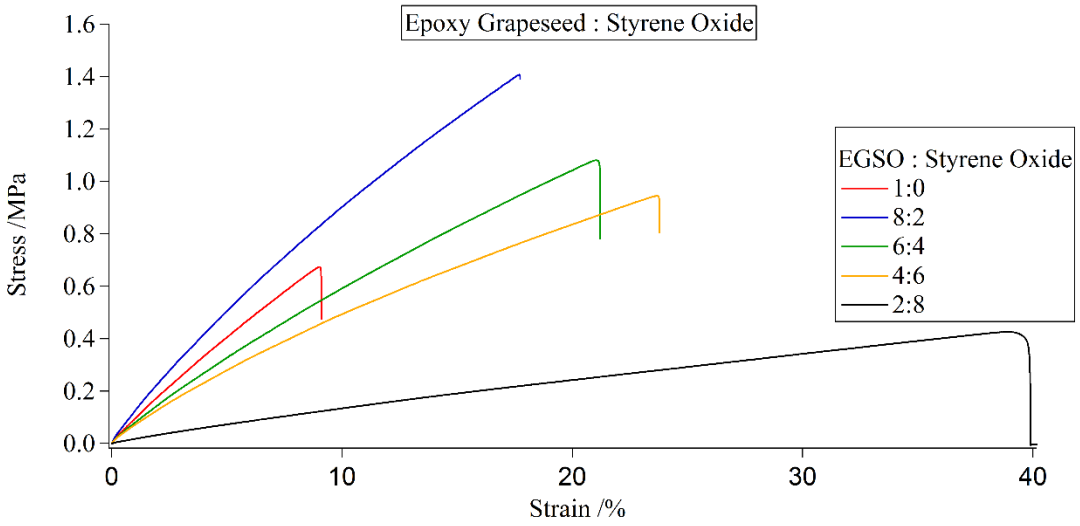

Figure 5.11. Stress Strain chart of styrene oxide - epoxy grapeseed oil polyesters. Extension rate 2mm min^{-1} using 1kN load cell.

The control sample without styrene oxide had tensile properties (tensile strength = 0.56 MPa, elongation =9.3%, Young's Modulus = 7.15 MPa) very similar to the same material prepared from the previous chapter (UTS = 0.56, EB = 6.7%, YM = 10.5 MPa). The two samples should be identical in structure as the same reagents in the same ratios were used but the different curing regimes are responsible for the slight differences.

The data shows that styrene oxide is a useful addition to plant oil polyesters improving both elasticity and tensile strength. As the amount of styrene oxide is increased so is the elasticity ranging from 9.3 % with only EGSO to 40.6 % with a 20:80 mixture. The tensile strength is only improved with lower quantities of styrene oxide, without styrene oxide the samples break at an average of 0.56 MPa which increases to 1.46 MPa with 20% addition. However increasing the amount of styrene oxide above 20% decreases the strength of the polymer to a point that after 60% the sample is weaker than without any at all, but is more elastic.

The addition of small amounts of styrene oxide ~20% increases the tensile strength due to the addition of pendant aromatic groups which could possibly form π – π interactions and strengthen the polymer network. However at higher concentrations the tensile strength is reduced and elongation increases due to a reduced amount of crosslinking.

The thermal properties of these samples was analysed by TGA (Figure 5.12), as can be seen in the results at low styrene oxide concentrations a single step degradation profile is observed. However at higher (>60 %) a two stage profile is evident, the first stage of degradation can be attributed to styrene oxide homopolymer degradation. Thermal degradation of polystyrene has shown to begin at around 270 °C and finish at 425 °C which is slightly higher than our findings, the weight loss is through liberation of aromatic hydrocarbons such as styrene, ethyl benzene and cumene, which is possible in our system.[316]

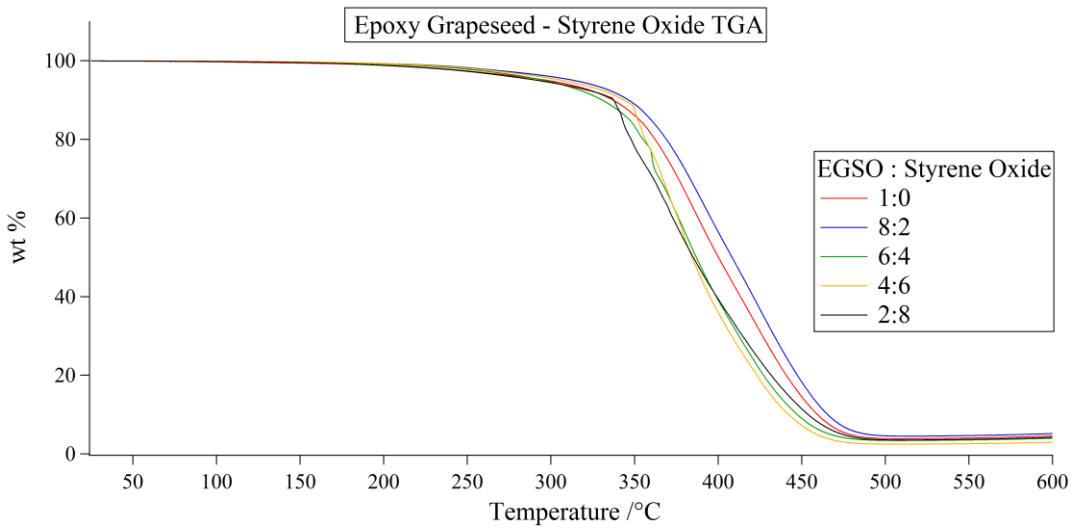

Figure 5.12. TGA data of styrene oxide - EGSO polyesters. Heating rate was 10 °C min^{-1} under an ambient atmosphere

Polymer		T_{-1} /°C	T_{-10} /°C	T_{-50} /°C
Epox Grapeseed	**Styrene Oxide**			
1.0	0.0	192	337	400
0.8	0.2	222	347	409
0.6	0.4	210	331	387
0.4	0.6	219	344	385
0.2	0.8	191	338	385

Table 5.4. Thermal data of styrene oxide - EGSO polyesters.

The addition of styrene oxide at low concentrations has shown an increase in both tensile stress and elongation of polymers. After a ratio of 80:20 EGSO:styrene oxide there was a linear decrease in strength and increase in elasticity, attributed to a greater amount of amorphous linear chains compared with a crosslinked network formed by grapeseed oil.

5.3.5 Epoxy Grapeseed and Euphorbia Blends

Another approach to strengthen a polymer instead of hard particles or fibres is to use soft or elastic components. A hard particle upon the formation of a crack would allow the crack to permeate through the sample but an elastic section would absorb the energy by deforming and dissipate the crack.[317]

Our results have shown that polyesters based on euphorbia oil have shown elastic properties but the lacking tensile strength whereas polymers based on epoxidised grapeseed oil were high in strength but were brittle. Blending the two oils would be beneficial as the highly crosslinked grapeseed oil would provide high strength and the elastic euphorbia oil would prevent crack permeation.

Epoxy grapeseed oil and euphorbia oil were blended in ratios of 100:0, 80:20, 60:40, 40:60, 20:80 and 0:100. Aradur 917 was used as the hardener in a 1:1 ratio relative to the total number of epoxides, which varied depending on EGSO:EuO ratio, and samples were cured at 170 °C for 1 h in an aluminium mould.

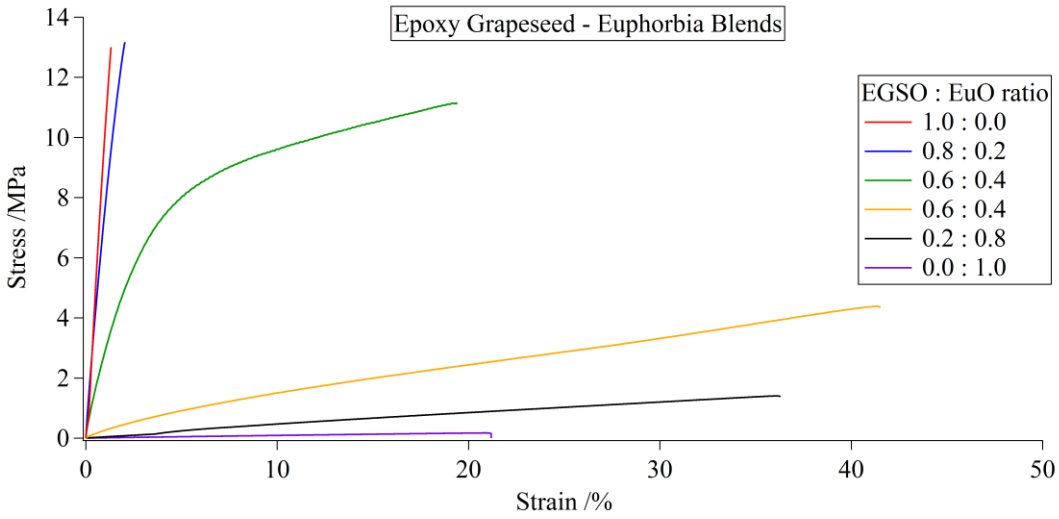

Figure 5.13. Stress Strain chart of epoxy grapeseed - euphorbia oil blends. Extension rate 2mm min^{-1} using 1kN load cell.

The results show a general trend where the flexibility increases and tensile stress decreases as the ratio of euphorbia oil increases (Figure 5.13). Previous samples had either high strength ***or*** elasticity and showed relatively little of the other property, however the sample made from a 0.6:0.4 ratio of oils had characteristics of both. This sample took an average of 10.7 MPa to break, only 2MPa less than pure grapeseed, but could stretch almost 20% of its original length before breakage (Table 5.5).

Polymer		**UTS /Mpa**	**YM /Mpa**	**EB /%**
Epox Grapeseed	**Euphorbia Oil**			
1.0	0.0	12.8 ±1.0	1005 ±77	1.5 ±0.3
0.8	0.2	12.9 ±4.7	671 ±49	2.3 ±1.8
0.6	0.4	10.7 ±0.4	258 ±17	19.1 ±4.3
0.4	0.6	2.8 ±2.3	15 ±12	42.4 ±1.3
0.2	0.8	1.6 ±0.3	4.1 ±0.1	40.5 ±6.0
0.0	1.0	0.2 ±0.1	0.9 ±0.1	20.6 ±3.8

Table 5.5. Tensile data of epoxy grapeseed - euphorbia oil blends. Errors reported as one standard deviation fom the mean.

The trend in elasticity follows the same pattern as crosslinking density. This relationship was identified in the previous chapter, but this data shows that

crosslinking can be controlled by blending oils allowing for fine tuning of polymer properties.

The maximum tensile strength was not improved by this method but an increase in elasticity would reduce the brittleness and allow for use in a wider range of applications.

5.4 Conclusions and future work

In this chapter we have investigated different approaches of modifying plant oil – anhydride polyesters.

The addition of solid particles, hollow silica and polyaromatic hydrocarbons reduced the tensile properties of the polyesters. This reduction of strength is attributed to poor bonding of the particles to the polymer network, possibly due to lower reactivty of the internal epoxides compared with terminal epoxides of typical epoxy resins based on bisphenol. Furthermore with hollow silica particles the weakness was also explained by the breakage of the shells upon external stress, the shells essentially acting as voids in the polymer matrix.

In an effort to increase tensile strength by copolymerisation with styrene oxide was more positive, at lower concentrations the tensile stress and elasticity were increased. After 20% relative to EGSO there was a linear decease in tensile strength and an increase in elongation. The increase in strength was due to the presence of aromatic side groups potentially providing π interactions, whereas the decrease in strength at higher concentrations was thought to be from lower crosslinking due to increased single epoxide monomers.

Epoxy grapeseed oil blended with euphorbia oil in varied ratios was shown to be a attractive method of tailoring physical properties of the polymer. A greater amount

of EGSO produced strong but brittle polymers whereas more euphorbia content produced more elastic polymers. Interestingly a sample of 60% EGSO showed similar tensile strength to pure EGSO (~11 MPA) and flexibility similar to that of pure euphorbia oil (~20%) obtaining the properties of both oils in one polymer.

6 Experimental

6.1 Instruments

^{1}H and ^{13}C NMR were recorded with Bruker DPX-300 Hz and DPX-400 Hz machines, chemical shifts are quoted in parts per million and coupling constants J are quoted in Hz. The infra-red spectra were recorded as solid state on Perkin-Elmer Avatar 320 FTIR spectrometer with absorption maxima recorded in wavenumbers (cm^{-1}). TGA/DSC data were recorded by Metler Toledo DSC1-Star machines using 40 μL standard aluminium pans. Tensile testing was performed on an Instron machine, using a 1 KN load cell and an extension rate of 2mm min^{-1}. GPC was performed on an Agilent 390-MDS with autosampler using PLgel 5.0 μm bead size guard column and two 5.0 μm bead size PLgel mixed D columns using a refractive index detector. $CHCl_3$ was the eluent and system calibrated with polymethylmethacrylate. Profilometry was performed on a WYKO profilometer and analysed using WYKO vision 4.10 software. SEM was performed on a Zeiss Supra 55-VP FEGSEM with EDAX genesis. The oven used for curing polymer samples was a Carbolite RHF-1600.

6.2 Materials

The starting materials used in this project were obtained from commercial suppliers and used as received without any further purification. Liquid coating samples, pre-coated samples and ECCS sheet metal were provided by the sponsors Cooper Coated Coil.

6.3 Analysis Techniques

Tensile Testing

Tensile testing was performed on an Instron machine and following standard BS EN ISO 527. The samples tested were polymerised in an aluminium 'dog bone' mould and were 75 x 10 x 3 mm in total, the gauge section (where the stress is applied to) had a 5 x 3 mm cross section and was 55 mm long. The testing was performed at an extension of 2mm per minute using a 1KN load cell.

Crosslinking Density

Crosslinking density was measured by immersing the samples in toluene until an equilibrium is reached between the solvent expanding the polymer and the crosslinks preventing this, to calculate the crosslinking density the Flory-Rehner equation was used.

$$M_c = \frac{\nu_s \, \rho_p \left(V_p^{\frac{1}{3}} - V_p/2 \right)}{\ln(1 - V_p) + V_p + \chi V_p^2} \quad \text{and} \quad \upsilon_c = \frac{\rho_P}{M_c}$$

where

$$1 + Q = \frac{1}{Vp}$$

and

$$Q = \frac{(\omega_0 - \omega_1)\rho_p}{\omega_0 \rho_s}$$

For these equations measurements of polymer density, initial weight of sample and weight of swelled sample were required. Polymer density was calculated by weight

divided by volume (from water displacement). For swelling samples of size 10 x 10 x 3 mm were placed into 15 mL of toluene at room temperature for 1 week, with gentle swirling daily.

6.4 Experimental Techniques for Non-Stick Coatings (Chapter 2)

6.4.1 Analytical Techniques for Commercial Samples

Centrifugation. Liquid coating samples (~ 6 g) were centrifuged on a Sigma 4-15 machine at 7830 rpm for 30 min. Solid particles dispersed in fresh NMP (10 mL) and centrifuged again (7830 rpm, 30 min) solid particles were dried in vacuum oven at 60 °C until constant weight.

Easy Clean – 5.718 g sample used, 3.953 g recovered - 30.9% solid content.

Single Coat – 5.944 g sample used, 3.983 g recovered – 33.0% solid content.

Base Coat – 5.785 g sample used, 3.056 g recovered – 47.2% solid content.

Top Coat – 5.933g sample used, 3.595 g recovered – 39.4% solid content.

Isolation of Polymer Binders. Supernatant from centrifugation was distilled under vacuum at 60 °C for 1.5 h.

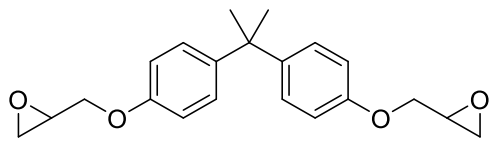

Easy Clean. White solid. ^{1}H NMR (300 MHz, $CDCl_3$) δ 7.11 (d, *J* = 8.2 Hz, 4H, Ar-H), 6.80 (d, *J* = 8.4 Hz, 4H, Ar-H), 4.09 (br s, 4H, OCH_2CHO), 3.41 – 3.32 (m, 2H, OCH_2CHOCH_2), 2.37 (t, *J* = 8.2 Hz, 2H, $CHOCH_2$), 2.07 – 1.93 (m, 2H, $CHOCH_2$), 1.61 (s, 6H, $C(CH_3)_2$).

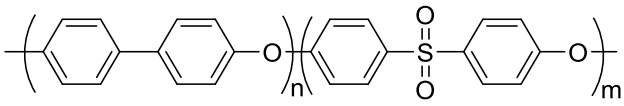

Single Coat. Colourless solid. ^{1}H NMR (300 MHz, $CDCl_3$) δ 7.93 (d, *J* = 8.6 Hz, 4H, SO_2Ar-H), 7.87 (d, *J* = 6.7 Hz, 2H, OAr-H), 7.09 (d, *J* = 8.8 Hz, 4H, Ar-Ar-H), 7.04 (d, *J* = 8.5 Hz, 2H, OAr-H).

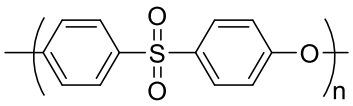

Base Coat and Top Coat. Colourless solid. ^{1}H NMR (300 MHz, $CDCl_3$) δ 7.93 (d, *J* = 8.6 Hz, 4H, SO_2Ar-H), 7.09 (d, *J* = 8.7 Hz, 4H. OAr-H).

SEM and EDAX analysis. Samples were secured to aluminium stubs by double sided carbon tape and analysis was performed on a Zeiss Supra 55-VP FEGSEM with EDAX Genesis and EBSD system.

Profilometry. Coated samples were cut to 50 mm x 50 mm pieces were scratched with a scalpel exposing the substrate. Coating thickness was analysed by a WYKO profilometer and Vision 4.10 software.

Drop Shape Analysis. DSA analysis was performed on a Kruss DSA-100 machine, droplets were ~5 μL of water unless otherwise stated, droplets were placed at random locations on the surface and an average result taken of >5 measurements.

6.4.2 Epoxidation of Vegetable Oils

General procedure proposed by Hignett.[] Tungsten powder (1.53 g, 8.32 mmol, 0.03 eq) and water (20 mL) were mixed followed by the dropwise addition of hydrogen peroxide (30% w/w, 10 mL), the mixture was heated to 50 °C until the tungsten dissolved. Adogen 464 (2 g) was added to the chosen triglyceride (eg soybean oil,

250 g, 0.284 mol, 1 eq) and heated to 60 °C. To the tungsten solution H_3PO_4 (1.36 g, 13.9 mmol, 0.05 eq) was added and this acidic catalyst mixture was added to the oil followed by water (380 mL) and H_2O_2 (336 mL, 30%, total 3.124 mol, 11 eq) and stirred rapidly to ensure complete emulsion. The reaction was left stirring at 60 °C for 6 h, completion was checked by ^{1}H NMR. The reaction was allowed to cool and was diluted with chloroform (500 mL) and the layers separated. The aqueous hase was washed with chloroform (100 mL) and the combined organic extracts washed with water (2 x 300 mL), brine (100 mL) and dried over anhydrous $MgSO_4$, solvent was removed *in vacuo* to yield a golden oil, 248.2 g, (91%).

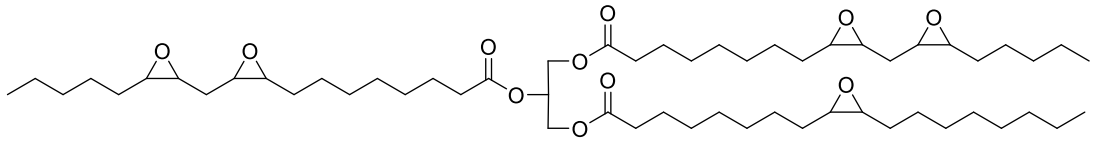

Epoxidised Soybean Oil. Golden oil, 248.2 g (91%). ^{1}H NMR (300 MHz, $CDCl_3$) δ 5.18 – 5.10 (m, 1H, C<u>H</u>O), 4.18 (dd, *J* = 11.9, 4.3 Hz, 2H, C<u>H</u>$_2$O), 4.02 (dd, *J* = 11.9, 5.9 Hz, 2H,C<u>H</u>$_2$O), 2.96 (ddd, *J* = 12.7, 10.6, 6.2 Hz, 4H, $CH_2CHOC\underline{H}CH_2C\underline{H}OCHCH_2$), 2.84 (s, 3H, $CH_2C\underline{H}OCHCH_2CHOC\underline{H}CH_2$), 2.76 (s, 2H, $CH_2C\underline{H}OCHCH_2$), 2.19 (t, *J* = 7.4 Hz, 6H, O=CC<u>H</u>$_2$CH$_2$), 1.68 – 1.57 (m, 4H, $CH_2CHOCHC\underline{H}_2CHOCHCH_2$), 1.49 (s, 6H, $O{=}CCH_2C\underline{H}_2CH_2$), 1.42 – 1.34 (m, 18H, C<u>H</u>$_2$CHOCHC<u>H</u>$_2$, C<u>H</u>$_2$CH$_3$), 1.21 (s, 20H, C<u>H</u>$_2$CH$_2$), 1.13 (s, 20H, C<u>H</u>$_2$CH$_2$), 0.77 (q, *J* = 7.0 Hz, 9H, $CH_2C\underline{H}_3$). ^{13}C NMR (75 MHz, $CDCl_3$) δ 173.00, 172.61 (<u>C</u>=O), 68.82 (H<u>C</u>-O), 61.97 (H$_2$<u>C</u>-O), 57.04 - 56.50 ($CH_2\underline{C}HOCHCH_2CHO\underline{C}HCH_2$), 54.20, 54.05 ($CH_2CHO\underline{C}HCH_2\underline{C}HOCHCH_2$), 34.01, 33.85 ($O{=}C\underline{C}H_2CH_2$), 31.76 - 22.48 ($\underline{C}H_2CH_2$), 13.90 ($CH_2\underline{C}H_3$). IR (cm^{-1}): 2923, 2854 (ν_{CH_2/CH_3}), 1740, ($\nu_{C=O}$), 1461 (ν_{CH_2/CH_3}). 823 ($\nu_{C\text{-}O\ epox}$). ESI-MS: calcd for

$C_{57}H_{100}O_{11}Na$ - $[M+Na]^+$ (983.72): found *m/z* 983.7(100%), 984.7(63), 985.7(21), 986.7(4).

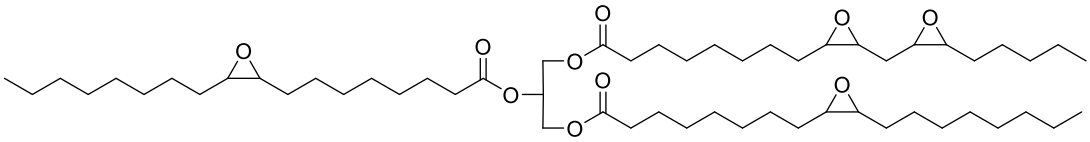

Epoxidised Rapeseed Oil. Yellow Oil, ^1H NMR (300 MHz, $CDCl_3$) δ 5.26 – 5.17 (m, 1H, C<u>H</u>O), 4.25 (dd, *J* = 11.9, 4.3 Hz, 2H, C<u>H</u>$_2$O), 4.09 (dd, *J* = 11.9, 5.9 Hz, 2H, C<u>H</u>$_2$O), 3.18 – 2.98 (m, 2H, $CH_2CHOC\underline{H}CH_2C\underline{H}OCHCH_2$), 2.93 (s, 2H, $CH_2C\underline{H}OCHCH_2CHOC\underline{H}CH_2$), 2.85 (s, 4H, $CH_2C\underline{H}OC\underline{H}CH_2$), 2.27 (t, *J* = 7.5 Hz, 6H, O=CC<u>H</u>$_2$CH$_2$), 1.76 – 1.65 (m, 2H, $CH_2CHOCHC\underline{H}_2CHOCHCH_2$), 1.57 (s, 6H, O=C $CH_2C\underline{H}_2CH_2$), 1.44 (s, 18H, C<u>H</u>$_2$CHOCHCH$_2$CHOCHC<u>H</u>$_2$, C<u>H</u>$_2$CH$_3$), 1.28 (s, 25H, C<u>H</u>$_2$CH$_2$), 1.23 (s, 15H, C<u>H</u>$_2$CH$_2$), 1.20 (s, 8H, C<u>H</u>$_2$CH$_2$), 0.83 (t, *J* = 6.7 Hz, 9H, $CH_2C\underline{H}_3$). ^{13}C NMR (75 MHz, $CDCl_3$) δ 172.58, 172.17 (<u>C</u>=O), 68.25 (<u>C</u>H-O), 61.45 (<u>C</u>H$_2$-O), 56.58, 56.02 ($CH_2\underline{C}HO\underline{C}HCH_2$), 53.71, 53.55 ($CH_2CHO\underline{C}HCH_2\underline{C}HOCHCH_2$), 33.34 (O=C<u>C</u>H$_2$), 31.21 - 24.14 (<u>C</u>H$_2$CH$_2$), 22.02 (<u>C</u>H$_2$CH$_2$), 13.47 ($CH_2\underline{C}H_3$). IR (cm^{-1}): 2925, 2855 (ν_{CH_2/CH_3}), 1738 ($\nu_{C=O}$ acid), 1462 (ν_{CH_2/CH_3}), 824 (ν_{epox}). ESI-MS: calcd for $C_{57}H_{102}O_{10}Na$ - $[M+Na]^+$ (969.74): found *m/z* 969.7(100%), 970.7(60), 971.7(26), 972.7(8).

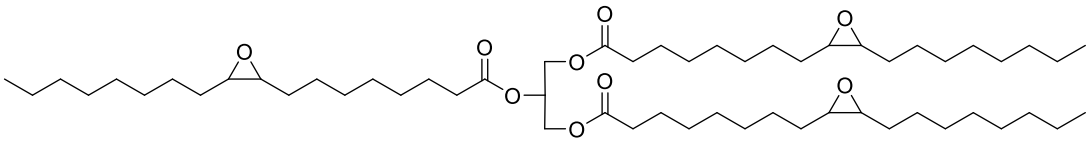

Epoxidised High Oleic Sunflower Oil. Green tinted oil, 305.2 g (96%). ^1H NMR (400 MHz, $CDCl_3$) δ 5.30 – 5.22 (m, 1H, C<u>H</u>O), 4.31 (dd, *J* = 11.9, 4.1 Hz, 2H, C<u>H</u>$_2$O), 4.14 (dd, *J* = 11.9, 6.0 Hz, 2H, C<u>H</u>$_2$O), 3.72 – 3.61 (m, 1H, <u>H</u>CO), 3.14 – 2.86 (m, 4H, $CH_2C\underline{H}OCHCH_2$), 2.31 (t, *J* = 7.4 Hz, 6H, O=CC<u>H</u>$_2$CH$_2$), 1.61 (s, 6H,

O=CCH$_2$CH$_2$CH$_2$), 1.50 (s, 12H, CHOCHCH$_2$), 1.42 – 1.20 (m, 60H, CH$_2$CH$_2$), 0.88 (t, *J* = 6.5 Hz, 9H, CH$_2$CH$_3$). ^{13}C NMR (101 MHz, $CDCl_3$) δ 173.04, 172.64 (C=O), 72.57, 68.84 (HC-O), 61.96 (H$_2$C-O), 57.11 (CH$_2$CHOCHCH$_2$), 33.82 - 22.53 (CH$_2$CH$_2$), 13.97 (CH$_2$CH$_3$). IR (cm^{-1}): 2923, 2853 (ν_{CH_2/CH_3}), 1741 ($\nu_{C=O}$ ester), 1461 (ν_{CH_2/CH_3}), 824 (ν_{epox}). ESI-MS: calcd for $C_{57}H_{104}O_9Na$ - $[M+Na]^+$ (955.76): found *m/z* 955.8(100%), 956.8(62), 957.8(19).

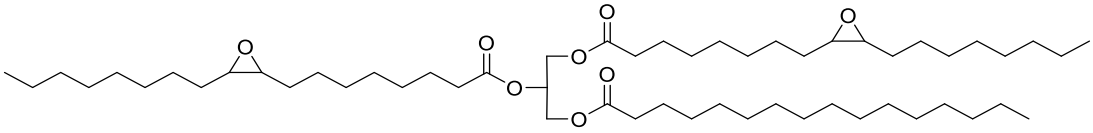

Epoxidised Palm Oil. Cream solid, 253.5 g (98%). ^{1}H NMR (400 MHz, $CDCl_3$) δ 5.25 – 5.13 (m, 1H, CHO), 4.23 (dd, *J* = 11.9, 4.3 Hz, 2H, CCH$_2$O), 4.07 (dd, *J* = 11.9, 5.9 Hz, 2H, CH$_2$O), 3.09 – 2.74 (m, 4H, CH$_2$CHOCHCH$_2$), 2.24 (t, *J* = 7.5 Hz, 6H, O=CCH$_2$CH$_2$), 1.61 – 1.49 (m, 6H, O=CCH$_2$CH$_2$CH$_2$), 1.42 (s, 8H, CHOCH$_2$CH$_2$), 1.33 – 1.12 (m, 68H, CH$_2$CH$_2$), 0.81 (dd, *J* = 7.3, 6.2 Hz, 9H, CH$_2$CH$_3$). ^{13}C NMR (101 MHz, $CDCl_3$) δ 173.29, 172.81 (C=O), 68.90 (HC-O), 62.07 (H$_2$C-O), 57.22 (CH$_2$CHOCHCH$_2$), 34.05 (O=CCH$_2$), 31.93 - 26.62 (CH$_2$CH$_2$), 24.86 (O=CCH$_2$CH$_2$CH$_2$), 22.66 (CH$_2$CH$_3$), 14.11 (CH$_2$CH$_3$). IR (cm^{-1}): 2921, 2852 (ν_{CH_2/CH_3}), 1742 ($\nu_{C=O}$ ester), 1459 (ν_{CH_2/CH_3}), 825 (ν_{epox}). ESI-MS: calcd for $C_{55}H_{102}O_8Na$ - $[M+Na]^+$ (913.75): found *m/z* 913.7(100%), 914.7(61), 915.7(23), 916.7(4).

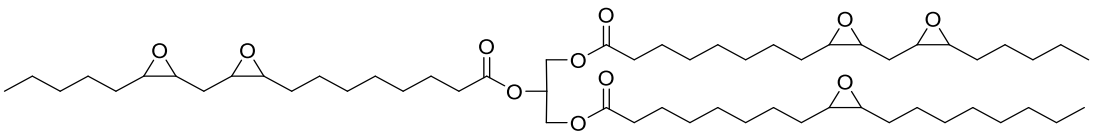

Epoxidised Euphorbia Oil. Green tinted oil. ^{1}H NMR (400 MHz, $CDCl_3$) δ 5.29 – 5.23 (m, 1H, C<u>H</u>O), 4.30 (dd, *J* = 11.9, 4.2 Hz, 2H, C<u>H$_2$</u>O), 4.14 (dd, *J* = 11.9, 5.9 Hz, 2H, C<u>H$_2$</u>O), 3.15 – 3.04 (m, 4H, $CH_2CHOC\underline{H}CH_2C\underline{H}OCHCH_2$), 2.98 (s, 4H, $CH_2C\underline{H}OCHCH_2CHOC\underline{H}CH_2$), 2.90 (s, 1H, $CH_2C\underline{H}OCHCH_2$), 2.31 (t, *J* = 7.4 Hz, 6H, O=CC<u>H$_2$</u>CH$_2$), 1.76 (ddd, *J* = 15.6, 13.4, 7.0 Hz, 4H, $CH_2CHOCHC\underline{H_2}CHOCHCH_2$), 1.61 (s, 6H, $O{=}CCH_2C\underline{H_2}CH_2$), 1.51 (dt, *J* = 21.4, 10.5 Hz, 18H, C<u>H$_2$</u>CHOCHC<u>H$_2$</u>, C<u>H$_2$</u>CH$_3$), 1.33 (s, 40H, C<u>H$_2$</u>CH$_2$), 0.89 (t, *J* = 11.7 Hz, 9H, $CH_2C\underline{H_3}$). ^{13}C NMR (101 MHz, $CDCl_3$) δ 172.99 (<u>C</u>=O), 68.90 (H<u>C</u>-O), 62.08 (H$_2$<u>C</u>-O), 57.21 - 56.72 ($CH_2\underline{C}HOCHCH_2CHO\underline{C}HCH_2$), 54.34, 54.17 ($CH_2CHO\underline{C}HCH_2\underline{C}HOCHCH_2$), 34.11, 33.96 ($O{=}C\underline{C}H_2CH_2$), 31.83 - 22.55 ($\underline{C}H_2CH_2$), 14.09, 13.97 ($CH_2\underline{C}H_3$). IR (cm^{-1}): 2925, 2855 (ν_{CH_2/CH_3}), 1740 ($\nu_{C=O}$ acid), 1461 (ν_{CH_2/CH_3}), 824 (ν_{epox}). ESI-MS: calcd for $C_{57}H_{100}O_{11}Na$ - $[M+Na]^+$ (983.72): found *m/z* 983.6(100%), 984.6(67), 985.6(28), 986.8(10).

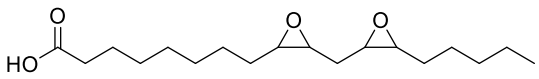

Epoxidised Linoleic Acid. Linoleic acid (100g, 0.357mol) dissolved in toluene (50mL) and heated to 60ºC, Amberlite (25g) and acetic acid (10.7g, 0.179mol, 0.5eq) were added. Hydrogen peroxide 35% (52.04g, 0.536mol, 1.5eq) was added dropwise over 10 minutes and the reaction was left stirring at 60ºC overnight in air. After 16 hours the reaction mixture was partitioned between water and $CHCl_3$ (500mL of each). The aqueous layer was washed with $CHCl_3$ (150mL), the combined organic layers were washed with water (500mL), brine (150mL) and dried over $MgSO_4$. The solvents were removed *in vacuo* to yield a green tinted oil, 96.37g (86.4%). ^{1}H NMR (400 MHz, $CDCl_3$) δ 3.16 – 3.05 (m, 2H, $CH_2CHOC\underline{H}CH_2C\underline{H}OCHCH_2$), 3.02 – 2.95 (m, 2H, $CH_2C\underline{H}OCHCH_2CHOC\underline{H}CH_2$),

2.34 (t, *J* = 7.5 Hz, 2H, O=CC$\underline{H_2}$CH$_2$), 1.84 – 1.70 (m, 1H, CH$_2$CHOCHC$\underline{H_2}$CHOCHCH$_2$), 1.68 – 1.59 (m, 2H, O=CCH$_2$C$\underline{H_2}$CH$_2$), 1.56 – 1.43 (m, 6H, C$\underline{H_2}$CHOCHC$\underline{H_2}$, C$\underline{H_2}$CH$_3$), 1.35 (s, 12H, C$\underline{H_2}$CH$_2$), 0.90 (t, *J* = 6.7 Hz, 3H, CH$_2$C$\underline{H_3}$). ^{13}C NMR (101 MHz, CDCl$_3$) δ 179.50 (O=$\underline{C}$CH$_2$), 57.45 (CH$_2\underline{C}$HOCHCH$_2$CHO$\underline{C}$HCH$_2$), 56.73 (CH$_2$CHO$\underline{C}$HCH$_2\underline{C}$HOCHCH$_2$), 40.89 (O=C$\underline{C}$H$_2$CH$_2$), 34.03 – 20.57 ($\underline{C}$H$_2$CH$_2$), 17.27 ($\underline{C}$H$_2$CH$_3$), 13.96 (CH$_2\underline{C}$H$_3$). IR (cm^{-1}): 2924, 2854 (ν_{CH_2/CH_3}), 1709 ($\nu_{C=O}$ acid), 1461 (ν_{CH_2/CH_3}), 824 (ν_{epox}). ESI-MS: calcd for C$_{18}$H$_{32}$O$_4$Na - [M+Na]$^+$ (335.22): found *m/z* 335.2(100%), 336.2(22), 337.2(2).

6.4.3 Industry Coating Surface Tests.

Tests were performed at the industrial sponsors to analyse the physical properties of a coatings surface.

Cross Hatch, BS EN ISO 2409:2013. Measures the adhesive properties of a coating. A grid of 100 1 mm x 1 mm squares are scored into the surface exposing the substrate. Adhesive tape is applied to the area and removed rapidly, the tape is placed on white paper to assess any removal of coating

Flexibility, BS EN 13523-7:2001. Determines flexibility of the coating. The test piece is bent through 180°, tape is applied to the fold and removed sharply, the tape is placed on white paper and any removal of coating is examined. The first fold (denoted 0T) has the smallest radius so is a larger stress on the coating, if a coating fails this the piece is bent again over the same area where the thickness is now double so the fold radius is larger (1T).

Erichsen, BS EN ISO 1520:2006. Measures adhesion to a substrate. The area where a cross hatch test has been performed is clamped onto a metal ring where a rod

pushed through and deforms the sample into a dome 8 mm in height. Tape is used to inspect for any removal of coating.

Pencil Hardness, BS EN 13523-4:2001. Measures hardness of the coatings surface, conforms to EN 13523-4:2001. Pencils of different lead hardness's are pushed across the surface at a 45° angle. The hardest lead that doesn't damage the surface determines the degree of hardness e.g. 2H.

6.4.4 Renewable Polymer Binder

General Coating Procedure. Samples of electrolytic chrome coated steel (ECCS) were cut to 75 mm x 100 mm in size and were 0.29 mm in thickness. Sharp edges were filed to ensure a flat surface. The coating formulation of ~2g was poured in a line along the top edge of the ECCS piece and the coating was drawn down using a wire wound coating bar producing a ~12μm film. The coating was cured in a Carbolite oven at 400 °C for 60 s, removed and allowed to cool naturally.

Alternatively UV curing was employed which is described below.

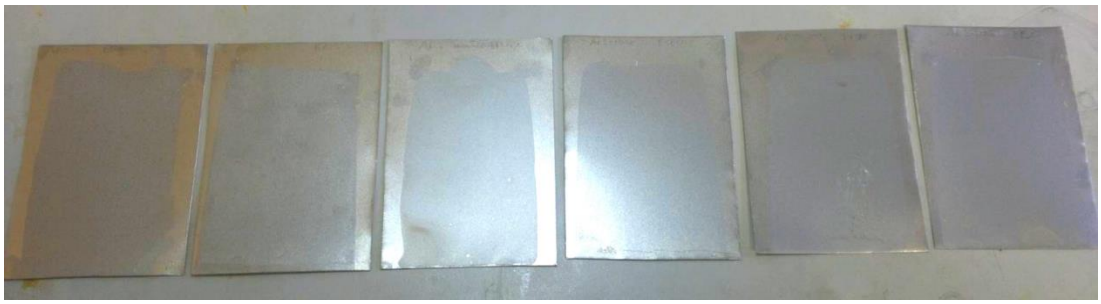

UV cured coatings. Coating were cured on a UV weather station typically used to accelerate aging of paint samples, power was 0.45 W/m^2 and the samples were cured until were dry to the touch. **Epoxy linoleic acid** (1g, 3.2 mmol) and triarylhexafluoro antimonite salts (TAS, 50% solution in propylene carbonate)(0.06 g, 3 wt%) were mixed and coated onto ECCS (12 μm) and cured under a UV light (0.45 W/m^2) for 30 min. X-Hatch (XH) = 100%, Flexibility (Flex) = Pass, Pencil hardness (PH) = F.

Epoxy palm oil (1g, 1.1 mmol) and TAS (0.06 g, 3 wt%) were mixed and coated onto ECCS (12 μm) and cured under a UV light (0.45 W/m^2) for 15 min. XH = 80%, Flex = Pass, PH = F. **Epoxy sunflower oil** (1g, 1.1 mmol) and TAS (0.06 g, 3 wt%) were mixed and coated onto ECCS (12 μm) and cured under a UV light (0.45 W/m^2) for 5 min. XH = 100%, Flex = Pass, PH = HB. **Epoxy rapeseed oil** (1g, 1 mmol) and TAS (0.06 g, 3 wt%) were mixed and coated onto ECCS (12 μm) and cured under a UV light (0.45 W/m^2) for 25 min. XH = 100%, Flex = Pass, PH = HB. **Epoxy soybean oil** (1g, 1 mmol) and TAS (0.06 g, 3 wt%) were mixed and coated onto ECCS (12 μm) and cured under a UV light (0.45 W/m^2) for 10 min. XH = 25%, Flex = Fail, PH = F-H. **Epoxy euphorbia oil** (1g, 1 mmol) and TAS (0.06 g, 3 wt%) were mixed and coated onto ECCS (12 μm) and cured under a UV light (0.45 W/m^2) for 5 min. XH = Fail, Flex = Fail, PH = 2H-3H.

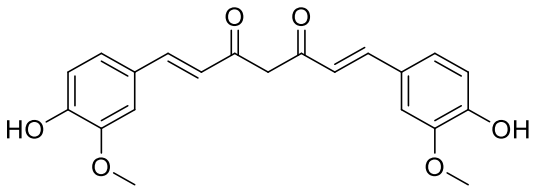

Isolation of Curcumin. Turmeric (15 g) placed in soxhlet tube and extracted with DCM (100 mL) at 50 °C over 2 h. Solvent concentrated on a rotary evaporator to ~10 mL and triturated with hexane (2 x 10 mL). the solid was removed *via* suction filtration to yield orange solid, 204 mg. Solid purified by column chromatography using DCM:MeOH (99:1, R_f = 0.26) to yield 98 mg of bright orange product.

UV + Photosensitzer curing. Epoxy sunflower oil (1 g, 1.1 mmol), TAS (0.02 g, 1wt%) and curcumin (0.001 g, 0.1 wt%) were mixed and coated onto ECCS using a 12 μm coating bar. The sample was cured under UV light (0.45 W/m^2) for 5 min. XH = 100%, Flex = Patchy, PH = 4H. **Epoxy soybean oil** (1 g, 1.0 mmol), TAS

(0.02 g, 1wt%) and curcumin (0.001 g, 0.1 wt%) were mixed and coated onto ECCS using a 12 μm coating bar. The sample was cured under UV light (0.45 W/m^2) for 5 min. XH = 100%, Flex = Fail, PH =5H. **Epoxy euphorbia oil** (1 g, 1.0 mmol), TAS (0.02 g, 1wt%) and curcumin (0.001 g, 0.1 wt%) were mixed and coated onto ECCS using a 12 μm coating bar. The sample was cured under UV light (0.45 W/m^2) for 5 min. XH = 100%, Flex = Patchy, PH = 3H.

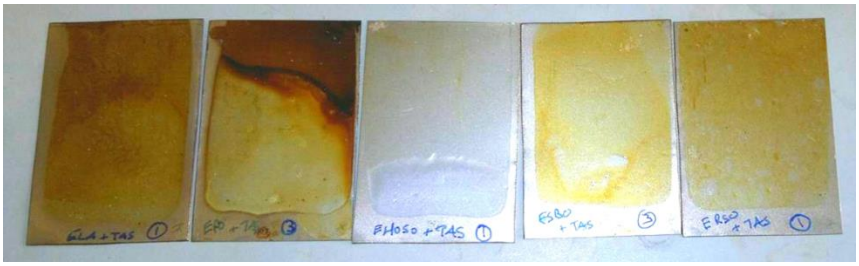

Thermally cured coatings. Epoxy linoleic acid (2g, 6.4 mmol) and TAS (0.12 g, 3 wt%) were mixed and coated onto ECCS (12 μm) and cured at 400 °C for 60 s. XH = 100%, Flex = Pass, PH = <HB. **Epoxy palm oil** (2g, 2.2 mmol) and TAS (0.12 g, 3 wt%) were mixed and coated onto ECCS (12 μm) and cured at 400 °C for 60 s. XH = 100%, Flex = Pass, PH = <HB. **Epoxy sunflower oil** (2g, 2.1 mmol) and TAS (0.12 g, 3 wt%) were mixed and coated onto ECCS (12 μm) and cured at 400 °C for 60 s. XH = 100%, Flex = Pass, PH = HB-F. **Epoxy rapeseed oil** (2g, 2.1 mmol) and TAS (0.12 g, 3 wt%) were mixed and coated onto ECCS (12 μm) and cured at 400 °C for 60 s. XH = 100%, Flex = Pass, PH = <F. **Epoxy soybean oil** (2g, 2.0 mmol) and TAS (0.12 g, 3 wt%) were mixed and coated onto ECCS (12 μm) and cured at 400 °C for 60 s. XH = 100%, Flex = Pass, PH = <F.

6.4.5 Addition of Solid Particles

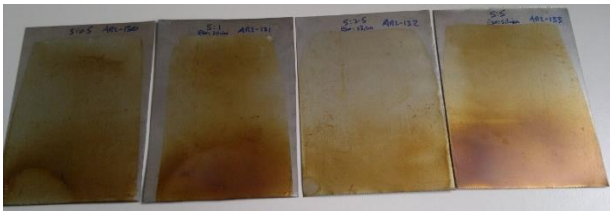

Addition of Fumed Silica. Epoxy soybean oil (**ESBO,** 10 mL) and fumed silica (1 mL) were mixed and degassed under vacuum for 10 min. 1 g of this sample taken and mixed with TAS (50% solution)(0.06 g, 3 wt%) and coated onto ECCS with a 12 μm coating bar and cured at 400 °C for 60 s, XH = 100%, Flex = Pass, PH = 4H, Erichsen (ER) = 100%. **ESBO** (5 mL) and fumed silica (1 mL) were mixed and degassed under vacuum for 10 min. 1 g of this sample taken and mixed with TAS (50% solution)(0.06 g, 3 wt%) and coated onto ECCS with a 12 μm coating bar and cured at 400 °C for 60 s, XH = 100%, Flex = Pass, PH = 5H, ER = 100%. **ESBO** (5 mL) and fumed silica (2.5 mL) were mixed and degassed under vacuum for 10 min. 1 g of this sample taken and mixed with TAS (50% solution)(0.06 g, 3 wt%) and coated onto ECCS with a 12 μm coating bar and cured at 400 °C for 60 s, XH = 100%, Flex = Pass, PH = 5H, ER = 100%. **ESBO** (5 mL) and fumed silica (5 mL) were mixed and degassed under vacuum for 10 min. 1 g of this sample taken and mixed with TAS (50% solution)(0.06 g, 3 wt%) and coated onto ECCS with a 12 μm coating bar and cured at 400 °C for 60 s, XH = 100%, Flex = Pass, PH = 5H, ER = 100%.

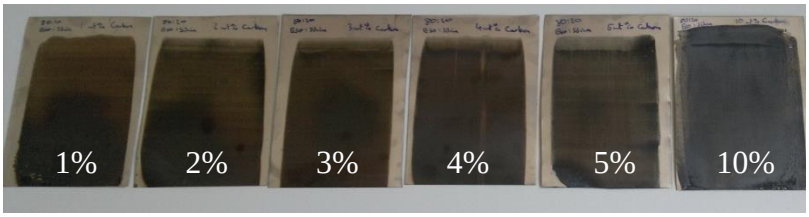

Addition of Carbon Black. 1%, a sample (0.99 g) of ESBO/SiO_2 (5:1 vol) was mixed with carbon black (0.01 g, 1 wt%) and TAS (0.06g 3 wt%), coated into ECCS

(12 μm) and cured at 400 °C for 60 s, PH = >5H, Flex = Fail, XH = 100%, ER = 100%. **2%,** a sample (0.98 g) of ESBO/SiO_2 (5:1 vol) was mixed with carbon black (0.02 g, 2 wt%) and TAS (0.06g 3 wt%), coated into ECCS (12 μm) and cured at 400 °C for 60 s, PH = >5H, Flex = Pass, XH = 100%, ER = 100%. **3%,** a sample (0.97 g) of ESBO/SiO_2 (5:1 vol) was mixed with carbon black (0.03 g, 3 wt%) and TAS (0.06g 3 wt%), coated into ECCS (12 μm) and cured at 400 °C for 60 s, PH = >5H, Flex = Patchy, XH = 100%, ER = 100%. **4%,** a sample (0.96 g) of ESBO/SiO_2 (5:1 vol) was mixed with carbon black (0.04 g, 4 wt%) and TAS (0.06g 3 wt%), coated into ECCS (12 μm) and cured at 400 °C for 60 s, PH = >5H, Flex = Fail, XH = 100%, ER = 100%. **5%,** a sample (0.95 g) of ESBO/SiO_2 (5:1 vol) was mixed with carbon black (0.05 g, 5 wt%) and TAS (0.06g 3 wt%), coated into ECCS (12 μm) and cured at 400 °C for 60 s, PH = >5H, Flex = Fail, XH = 100%, ER = <100%. **10%,** a sample (0.90 g) of ESBO/SiO_2 (5:1 vol) was mixed with carbon black (0.1 g, 10 wt%) and TAS (0.06g 3 wt%), coated into ECCS (12 μm) and cured at 400 °C for 60 s, PH = >5H, Flex = Fail, XH = 100%, ER = <100%.

Addition of PTFE. A mixture of ESBO/SiO_2 (10:2 mL) was produced, from this samples were taken and mixed with carbon black PTFE and TAS initiator. The formulations were mixed in the following ratios (ESBO/SiO_2 : carbon black : PTFE : TAS). **1% PTFE** (0.96g : 0.03g : 0.01g : 0.06g), **2% PTFE** (0.95g : 0.03g : 0.02g : 0.06g), **3% PTFE** (0.94g : 0.03g : 0.03g : 0.06g), **4% PTFE** (0.93g : 0.03g : 0.04g : 0.06g), **5% PTFE** (0.92g : 0.03g : 0.05g : 0.06g), **10% PTFE** (0.87g : 0.03g : 0.10g : 0.06g), **20PTFE** (0.77g : 0.03g : 0.2g : 0.06g). All samples were cured at 400 °C for 60 s on ECCS. The samples were unsuitable for industry surface testing.

6.4.6 Sulfonic acid initiators

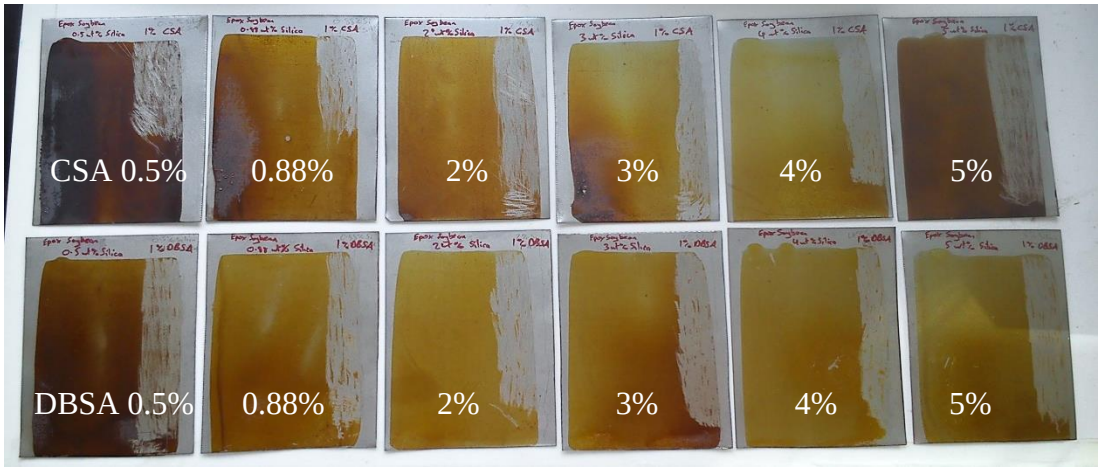

Camphor sulfonic acid (CSA). 0.5% SiO_2, ESBO (0.97 g), fumed silica (0.01g) and CSA (0.02g) were mixed, coated onto ECCS (12 μm) and cured (400 °C, 60 s). Flex = Pass, PH = >5H, XH = 100%, ER = 100%. **0.88% SiO_2,** ESBO (0.9624 g), fumed silica (0.0176g) and CSA (0.02g) were mixed, coated onto ECCS (12 μm) and cured (400 °C, 60 s). Flex = Pass, PH = >5H, XH = 100%, ER = 100%. **2% SiO_2,** ESBO (0.94 g), fumed silica (0.04g) and CSA (0.02g) were mixed, coated onto ECCS (12 μm) and cured (400 °C, 60 s). Flex = Pass, PH = >5H, XH = 100%, ER = 100%. **3% SiO_2,** ESBO (0.92 g), fumed silica (0.06g) and CSA (0.02g) were mixed, coated onto ECCS (12 μm) and cured (400 °C, 60 s). Flex = Pass, PH = 4H, XH = 90%, ER = 100%. **4% SiO_2,** ESBO (0.90 g), fumed silica (0.08g) and CSA (0.02g) were mixed, coated onto ECCS (12 μm) and cured (400 °C, 60 s). Flex = Patchy, PH = H, XH = 100%, ER = 100%. **5% SiO_2,** ESBO (0.88 g), fumed silica (0.10g) and CSA (0.02g) were mixed, coated onto ECCS (12 μm) and cured (400 °C, 60 s). Flex = Pass, PH = >5H, XH = 100%, ER = 100%.

Dodecylbenzene sulfonic acid (DBSA). 0.5% SiO_2, ESBO (0.97 g), fumed silica (0.01g) and DBSA (0.02g) were mixed, coated onto ECCS (12 μm) and cured (400 °C, 60 s). Flex = Pass, PH = 3H, XH = 100%, ER = 100%. **0.88% SiO_2,** ESBO (0.9624 g), fumed silica (0.0176g) and DBSA (0.02g) were mixed, coated onto

ECCS (12 μm) and cured (400 °C, 60 s). Flex = Patchy, PH = H, XH = 100%, ER = 100%. **2% SiO_2,** ESBO (0.94 g), fumed silica (0.04g) and DBSA (0.02g) were mixed, coated onto ECCS (12 μm) and cured (400 °C, 60 s). Flex = Pass, PH = 3H, XH = 100%, ER = 100%. **3% SiO_2,** ESBO (0.92 g), fumed silica (0.06g) and DBSA (0.02g) were mixed, coated onto ECCS (12 μm) and cured (400 °C, 60 s). Flex = Pass, PH = 3H, XH = 100%, ER = 100%. **4% SiO_2,** ESBO (0.90 g), fumed silica (0.08g) and DBSA (0.02g) were mixed, coated onto ECCS (12 μm) and cured (400 °C, 60 s). Flex = Pass, PH = H, XH = 95%, ER = 100%. **5% SiO_2,** ESBO (0.88 g), fumed silica (0.10g) and DBSA (0.02g) were mixed, coated onto ECCS (12 μm) and cured (400 °C, 60 s). Flex = Patchy, PH = H, XH = 100%, ER = 100%.

Solvent Addition and Rheometry. Samples of ESBO (1.88 g), DBSA (0.02 g), fumed silica (0.04 g) and carbon black (0.06 g) were mixed and propyl acetate added – **7.5 vol %** (0.15 mL), **10 vol%** (0.20 mL), **15 vol%** (0.30 mL), **20 vol%** (0.40 mL), and **25 vol%** (0.50 mL). Rheometry was performed on ~1g sample at 25 °C and shear rate ranged from 0 to 800 s^{-1}, viscosity was measured in Pa.s.

Larger Scale Formulation. ESBO (95 g, 0.99 mol), DBSA (1g, 1wt%), fumed silica (2g, 2wt%), carbon black (3g, 3wt%) and propyl acetate (10 ml, 10 vol%) were mixed. The coating was performed at the sponsors' premises but followed our standard procedure using a 12 μm bar and curing at 400 °C for 60 s on ECCS approximately 200mm x 300mm. Flex = Pass, PH = 5H, XH = 100%, ER = 100%.

'Real World' Tests. Two tests to assess a coatings end use performance were implemented, one cooking and one cleaning, the coated sample was folded at the edges to form a tray. **Cooking,** a piece of beef steak was placed on the surface and the sample placed in a domestic oven at 200 °C for 1 h. After the cooking time it was

removed and the coating assess on the food release properties. **Cleaning,** after cooking the test piece was immersed in household detergent solution for 20 min, followed by scrubbing with souring pad and a wash cycle in a domestic dishwasher. The coating was assessed for cleanliness and coating removal after each cleaning process. Both of these tests were subjective and had no numerical value.

Addition of Linoleic acid. Epoxidised linoleic acid (ELA) was added in 1, 2 and 5 wt% replacing Epoxy soybean oil (ESBO). **1wt% ELA,** ESBO (1.88 g), ELA (0.02 g), fumed silica (0.04 g), carbon black (0.06 g) and propyl acetate (0.2 mL) were mixed, coated onto ECCS (12 μm) and cured (400 °C, 60 s). **2wt% ELA,** ESBO (1.86 g), ELA (0.04 g), fumed silica (0.04 g), carbon black (0.06 g) and propyl acetate (0.2 mL) were mixed, coated onto ECCS (12 μm) and cured (400 °C, 60 s). **5wt% ELA,** ESBO (1.80 g), ELA (0.1 g), fumed silica (0.04 g), carbon black (0.06 g) and propyl acetate (0.2 mL) were mixed, coated onto ECCS (12 μm) and cured (400 °C, 60 s).

6.5 Experimental for Hydrosilylation (Chapter 3)

6.5.1 The Hydrosilylation Reaction

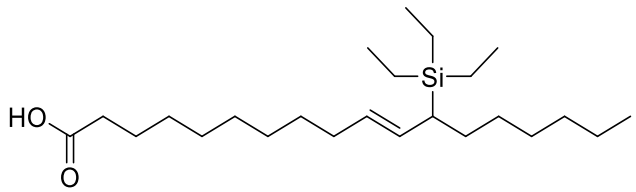

Synthesis of Compound 3.1

Linoleic acid (0.28 g, 1 mmol) and triethylsilane (0.233 g, 2 mmol, 2 eq) were mixed in an N_2 atmosphere and heated to 40 °C. Karstedts catalyst was added (1 drop) and

the reaction stirred for 4 h at 40 °C. To finish the reaction cyclohexane (1 mL) and propylene carbonate (1 mL) were added and the phases allowed to separate, the top phase (cyclohexane) was collected and solvent removed by rotary evaporation. Green tinted oil, 0.25g, (63%) ^{1}H NMR (300 MHz, $CDCl_3$) δ 5.42-5.25 (m, 2H, $CH_2CHCHCHSi$), 2.26 (t, *J* = 7.4 Hz, 2H, $O{=}CCH_2CH_2$), 1.93 (br s, 3H, $CH_2CHCHCHSi$), 1.56 (quin, *J* = 6.9 Hz, 2H, $O{=}CCH_2CH_2CH_2$), 1.22 (s, 20H, CH_2CH_2), 0.93 (t, *J* = 7.8 Hz, 9H, $SiCH_2CH_3$), 0.84 (t, *J* = 6.7 Hz, 3H, CH_2CH_3), 0.72 (q, *J* = 7.9 Hz, 6H, $SiCH_2CH_3$), 0.52 – 0.39 (m, 1H, CH_2CHSi). ^{13}C NMR (101 MHz, $CDCl_3$) δ 173.37 ($C{=}O$), 129.35 129.31 ($CHSiCHCHCH_2$), 72.39, 69.58, 34.84 ($O{=}CCH_2$), 31.64-24.18 (CH_2CH_2), 21.72 (CH_2CH_3), 13.09 (CH_2CH_3), 5.46 ($SiCH_2CH_3$), 3.53 ($SiCH_2CH_3$). IR (cm^{-1}): 2956.1 (ν_{CH}), 2922.6 (ν_{CH_2}), 2876.4 (ν_{CH_3}), 1717.1 ($\nu_{C=O}$) 1257.8 (ν_{C-Si}). ESI-MS: *m/z* 419.3 $[M+Na]^+$, 435.3 $[M+K]^+$.

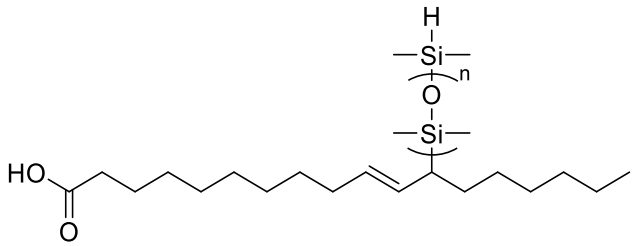

Synthesis of Compound 3.2

Linoleic acid (0.224 g, 0.8 mmol) and DMS-H11 (0.84 g, 0.8 mmol, 1 eq) were mixed in an N_2 atmosphere with rapid stirring to form an emulsion. The mixture was heated to 40 °C and Karstedts catalyst (1 drop) was added, the reaction was stirred at 40 °C for 4 h. To finish the reaction cyclohexane (1 mL) and propylene carbonate (1 mL) were added and the phases allowed to separate, the top phase (cyclohexane) was collected and solvent removed by rotary evaporation. Pale cream oil, 0.516g, (48%).

^{1}H NMR (400 MHz, $CDCl_3$) δ 5.36 – 5.23 (m, 2H, $CH_2C\underline{H}C\underline{H}CHSi$), 2.22 (t, *J* = 7.5 Hz, 2H, $O{=}CC\underline{H_2}CH_2$), 1.97 – 1.86 (m, 3H, $C\underline{H_2}CHCHCHSi$), 1.51 (d, *J* = 6.5 Hz, 2H, $O{=}CCH_2C\underline{H_2}$), 1.20 (br s, *J* = 7.2 Hz, 20H, $C\underline{H_2}CH_2$), 0.80 (t, *J* = 6.4 Hz, 3H, $CH_2C\underline{H_3}$), 0.21 (s, 6H, $CHSi(C\underline{H_3})_2O$), 0.04 – -0.08 (m, 90H, $Si(C\underline{H_3})O$). ^{13}C NMR (101 MHz, $CDCl_3$) δ 172.58 ($O{=}\underline{C}CH_2$), 129.69 129.38 ($CH_2\underline{C}H\underline{C}HCHSi$), 34.88 ($O{=}C\underline{C}H_2$), 33.60 - 23.88 ($\underline{C}H_2CH_2$), 21.64 ($\underline{C}H_2CH_3$), 13.06 ($CH_2\underline{C}H_3$), -0.01 ($Si(\underline{C}H_3)_2O$). IR ($cm^{-1}$): 2962.7 ($\nu_{CH}$), 2923.5 ($\nu_{CH_2}$), 2852.3 ($\nu_{CH_3}$), 2246.2 ($\nu_{Si\text{-}H}$), 1719.8 ($\nu_{C=O\ ester}$), 1254.3 ($\nu_{Si\text{-}CH_3}$), 1009.2 ($\nu_{Si\text{-}O}$).

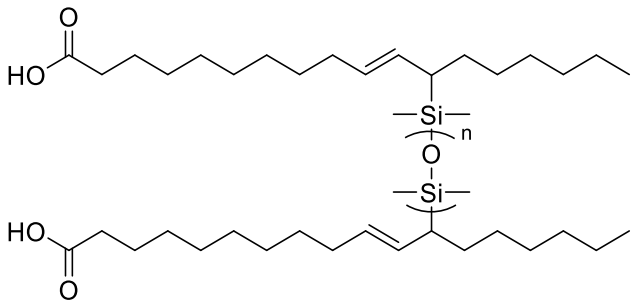

Synthesis of Compound 3.3

Linoleic acid (0.56 g, 2mmol) and DMS-H11 (1.05 g, 1 mmol, 0.5 eq) were mixed with rapid stirring to create an emulsion in an N_2 atmosphere and heated to 40 °C. Karstedts catalyst (1 drop) was added and the reaction was stirred at 40 °C for 4 h. Propylene carbonate and cyclohexane were added and allowed to separate, the top layer (cyclohexane) was collected and solvent removed by rotary evaporation. 1.402 g, (87%). ^{1}H NMR (400 MHz, $CDCl_3$) δ 5.37 – 5.20 (m, 4H, $CH_2C\underline{H}C\underline{H}CHSi$), 2.22 (t, *J* = 7.6 Hz, 4H, $O{=}CC\underline{H_2}$), 2.01 – 1.87 (m, 8H, $C\underline{H_2}CHCHCHSiC\underline{H_2}$), 1.52 (q, *J* = 6.9 Hz, 4H, $O{=}CCH_2C\underline{H2}$), 1.23 (s, 22H, $CH_2C\underline{H_2}$, $CH_2C\underline{H}Si$), 1.18 (s, 16H, $CH_2C\underline{H_2}$), 0.80 (t, *J* = 6.4 Hz, 6H, $CH_2C\underline{H_3}$), 0.03 (s, 12H, $CH_2CHSi(C\underline{H_2})_2$) , -0.00 (s, 66H, $OSi(C\underline{H_2})_2$). ^{13}C NMR (101 MHz, $CDCl_3$) δ 172.56 ($O{=}\underline{C}CH_2$), 129.15 128.84 ($CH_2\underline{C}H\underline{C}HCHSi$), 34.87 ($O{=}CH_2\underline{C}H_2$), 32.93 - 23.88 ($\underline{C}H_2CH_2$), 21.65

($\underline{C}H_2CH_3$), 13.06 ($CH_2\underline{C}H_3$), -0.01 ($Si(\underline{C}H_3)_2O$). IR (cm^{-1}): 2960.9 (ν_{CH}), 2925.9 (ν_{CH_2}), 2855.1 (ν_{CH_3}), 1722.6 ($\nu_{C=O\ ester}$), 1257.9 ($\nu_{Si\text{-}CH_3}$), 1012.9 ($\nu_{Si\text{-}O}$).

Synthesis of Compound 3.4

Grapeseed oil (0.881 g, 1 mmol) and DMS-H11 (1.05 g, 1 mmol, 1 eq) were mixed under an N_2 atmosphere and heated to 40 °C. Karstedts catalyst (1 drop) was added and the reaction stirred at 40 ° for 4 h. Propylene carbonate and cyclohexane were added and allowed to separate, the top layer (cyclohexane) was collected and solvent removed by rotary evaporation. Product was a green tinted oil, 1.874 g, (97%). ^{1}H NMR (400 MHz, $CDCl_3$) δ 5.36 – 5.18 (m, 5H, $CH_2C\underline{H}C\underline{H}CH_2$), 5.22 – 5.14 (m, 1H, $OCH_2C\underline{H}OCH_2O$), 4.63 (s, 1H, Si-H), 4.22 (dd, *J* = 11.9, 4.2 Hz, 2H, $OC\underline{H_2}CHOC\underline{H_2}O$), 4.07 (dd, *J* = 11.9, 5.9 Hz, 2H, $OC\underline{H_2}CHOC\underline{H_2}O$), 2.64 (t, *J* = 5.5 Hz, 1H, $CHCHC\underline{H_2}CHCH$), 2.23 (t, *J* = 7.5 Hz, 6H, $OCC\underline{H_2}$), 2.09 – 1.85 (m, 12H, $C\underline{H_2}CHCHCH_2$), 1.53 (br s, 6H, $OCCH_2C\underline{H_2}$), 1.21 (br s, 38H, $C\underline{H_2}CH_2$), 1.18 (s, 20H, $C\underline{H_2}CH_2$), 0.80 (t, *J* = 6.3 Hz, 9H, $CH_2C\underline{H_3}$), -0.00 (s, 82H, $OSi(C\underline{H_3})_2O$). ^{13}C NMR (101 MHz, $CDCl_3$) δ 172.19 171.78 ($O\underline{C}CH_2$), 133.69 ($\underline{C}HCHCH_2CH\underline{C}H_2$), 129.69 ($CH_2\underline{C}H\underline{C}HCHSi$), 124.57 ($CH\underline{C}HCH_2\underline{C}HCHC$), 67.88 ($OCH_2\underline{C}HOCH_2O$), 61.06 ($O\underline{C}H_2CHO\underline{C}H_2O$), 33.00 ($OC\underline{C}H_2$), 31.91 - 23.85 ($\underline{C}H_2CH_2$), 21.66 ($\underline{C}H_2CH_3$), 18.42 ($CH_2\underline{C}HSi$), 13.07 ($CH_2\underline{C}H_3$), -0.01 ($OSi(\underline{C}H_3)_2O$). IR ($cm^{-1}$): 2960.3 ($\nu_{CH}$), 292.8 ($\nu_{CH_2}$), 2854.0 ($\nu_{CH_3}$), 1745.5 ($\nu_{C=O\ ester}$), 1258.0 ($\nu_{Si\text{-}CH_3}$), 1014.7 ($\nu_{Si\text{-}O}$). Reaction was repeated and left for 5 days, an insoluble gel had formed **3.4**.

Synthesis of Compound 3.5

Grapeseed oil (0.881 g, 1 mmol) and DMS-H11 (1.05 g, 1 mmol, 1 eq) were mixed under an N_2 atmosphere and heated to 100 °C. Karstedts catalyst (1 drop) was added

and the reaction stirred at 100 ° for 18 h forming an insoluble gel after 1 h but reaction left to fully cure overnight.

6.5.2 Silicone and Plant Oil Rubbers

General Procedure for Silicone/Plant oil Rubber 3.6 – 3.14. The plant oil and silane were mixed under an N_2 atmosphere and heated to 100 °C, 1 drop of Karstedts catalyst was added and the reaction left for 18h. High speed stirring was used to create an emulsion as oils and silane not miscible. Generally the reaction gelled after 1 h but left overnight to ensure complete reaction.

3.6, Grapeseed oil (0.881 g, 1 mmol) and DMS-H11 (1.05 g, 1 mmol).

3.7, Grapeseed oil (0.102 g, 0.116 mmol) and DMS-H25 (2.0 g, 0.116 mmol).

3.8, Grapeseed oil (1.06 g, 1.2 mmol) and HMS-991 (0.16 g, 0.1 mmol).

3.9, Soybean oil (0.881 g, 1 mmol) and DMS-H11 (0.105 g, 1 mmol).

3.10, Soybean oil (0.102 g, 0.116 mmol) and DMS-H25 (2.0 g, 0.116 mmol).

3.11, Soybean oil (0.106 g, 1.2 mmol) and HMS-991 (0.16 g, 0.1 mmol).

3.12, Rapeseed oil (0.883 g 1 mmol) and DMS-H11 (1.05 g, 1 mmol).

3.13, Rapeseed oil (1.03 g, 0.116 mmol) and DMS-H25 (2.0 g, 0.116 mmol).

3.14, Rapeseed oil (1.06 g, 1.2 mmol) and HMS-991 (0.16 g 0.1 mmol).

6.5.3 Synthesis of Silicone / Epoxy Fatty Acid Hybrids

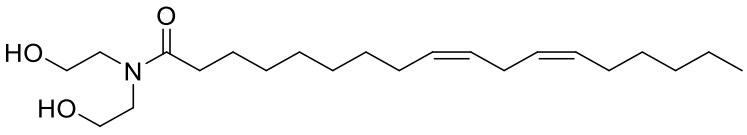

Synthesis of Compound 3.15

Linoleic acid (30 g, 0.107 mol) dissolved in THF (150 mL), N-methyl morpholine (12.9 g, 0.118 mol, 1.1 eq) added and mixture stirred for 5 min. Ethyl chloroformate

(11.3 g, 0.118 mol, 1.1 eq) added dropwise and the reaction mixture stirred for 30 min forming a white precipitate which was filtered and washed with THF (30 mL). The filtrate was added dropwise to a solution of diethanolamine (11.3 g, 0.116 mol, 1.1 eq), trimethylamine (16.4 g, 0.116 mol, 1.1 eq) in DMF (150 mL) and left to react for 4 h. The reaction was quenched with HCl (50 mL, 2 M) and product extracted with diethyl ether (400 mL). The organic phase was washed with water (4 x 400 mL), brine (100 mL) and dried with anhydrous $MgSO_4$, removal of solvent by rotary evaporation yielded golden oil, 35.17 g (89%), product was used without further purification. ^{1}H NMR (300 MHz, $CDCl_3$) δ 5.38 – 5.20 (m, 4H, $CH_2CHCHCH_2$), 4.48 (b s, 2H, OH), 3.71 (dt, *J* = 11.1, 4.8 Hz, 4H, NCH_2CH_2OH), 3.44 (dt, *J* = 10.4, 5.1 Hz, 4H, NCH_2CH_2OH), 2.71 (t, *J* = 6.0 Hz, 2H, $CHCHCH_2CHCH$), 2.32 (t, *J* = 7.8 Hz, 2H, $O=CCH_2CH_2$), 1.99 (q, *J* = 6.5 Hz, 4H, $CH_2CHCHCH_2CHCHCH_2$), 1.55 (quin, *J* = 6.9 Hz, 2H, $O=CCH_2CH_2CH_2$), 1.25 (s, 14H, CH_2CH_2), 0.83 (t, *J* = 6.8 Hz, 3H, CH_2CH_2). ^{13}C NMR (75 MHz, $CDCl_3$) δ 174.96 ($O=CCH_2$), 129.57 129.39 ($CH_2CHCHCH_2CHCHCH_2$), 127.38 127.25 ($CH_2CHCHCH_2CHCHCH_2$), 60.51 60.03 (OCH_2CH_2N), 51.63 49.92 (NCH_2CH_2O), 32.97 ($O=CCH_2$), 30.8 - 24.67 (CH_2CH_2), 21.93 (CH_2CH_3), 13.44 (CH_2CH_3). IR (cm^{-1}): 3354.9 (ν_{OH}), 3008.2 (ν_{CH}), 2923.6 (ν_{CH_2}), 2853.8 (ν_{CH_3}), 1615.7 ($\nu_{C=O\ amide}$), 1464.9 ($\nu_{C=C}$). ESI-MS: calcd for $C_{22}H_{45}NO_3H$ (367.31), $C_{22}H_{45}NO_3Na$ (390.30), $C_{22}H_{45}NO_3K$ (406.27) found *m/z* 368.3(18%) $[M+H]^+$, 390.3(100%), 391.3(25), 392.3(9) $[M+Na]^+$, 406.3(26%), 407.3(7) $[M+K]^+$.

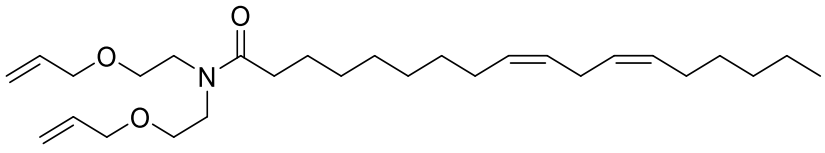

Synthesis of Compound 3.16

The fatty amide (compound **3.15**, 35 g, 0.097 mol) was dissolved in dry THF (200 mL) under a nitrogen atmosphere and cooled to -78 °C, NaH (5.17 g, 0.213 mol, 2.2 eq) was added and the reaction left stirring for 30 min. Allyl bromide (25.82 g, 0.213 mol, 2.2 eq) was added dropwise and the reaction was left to warm to room temperature overnight. To quench the reaction HCl was added (50 mL, 2M) and the product was extracted with diethyl ether (400 mL). The organic layer was washed with water (3 x 400 mL), brine (50 mL) and dried with anhydrous $MgSO_4$. Solvent was removed by rotary evaporation to yield a green tinted oil, 38.8 g (89%). Product was purified by passing through a silica plug under suction using petroleum ether:ethyl acetate (4:1) as the eluent. 34.01g (78%).^{1}H NMR (300 MHz, $CDCl_3$) δ 5.85 – 5.69 (m, 2H, $OCH_2C\underline{H}CH_2$), 5.33 – 5.19 (m, 4H, $CH_2C\underline{H}C\underline{H}CH_2C\underline{H}C\underline{H}CH_2$), 5.19 – 5.10 (m, 2H, $OCH_2CHC\underline{H}_2$), 5.10 – 5.01 (m, 2H, $OCH_2CHC\underline{H}_2$), 3.91 – 3.82 (m, 4H, $OC\underline{H}_2CHCH_2$), 3.54 – 3.40 (m, 8H, $NC\underline{H}_2C\underline{H}_2O$), 2.67 (t, *J* = 5.9 Hz, 2H, $CHCHC\underline{H}_2CHCH$), 2.28 (t, *J* = 7.5 Hz, 2H, $O{=}CC\underline{H}_2$), 1.95 (q, *J* = 6.5 Hz, 4H, $C\underline{H}_2CHCHCH_2CHCHC\underline{H}_2$), 1.53 (quin, *J* = 6.9 Hz, 2H, $O{=}CCH_2C\underline{H}_2$), 1.22 (s, 14H, $C\underline{H}_2CH_2$), 0.79 (t, *J* = 6.8 Hz, 3H, $CH_2C\underline{H}_3$). ^{13}C NMR (75 MHz, $CDCl_3$) δ 173.05 ($O{=}\underline{C}CH_2$), 134.04 133.71 ($OCH_2\underline{C}HCH_2$), 129.42 ($\underline{C}HCHCH_2CH\underline{C}H$), 127.23 ($CH\underline{C}HCH_2\underline{C}HCH_2$), 116.26 115.97 ($OCH_2CH\underline{C}H_2$), 71.48 71.19 ($O\underline{C}H_2CHCH_2$), 67.59 ($NCH_2\underline{C}H_2O$), 48.32 45.84 ($N\underline{C}H_2CH_2$), 32.34 ($O{=}C\underline{C}H_2$), 30.83 - 21.88 ($\underline{C}H_2CH_2$), 13.39 ($CH_2\underline{C}H_3$). IR ($cm^{-1}$): 3079.5 ($\nu_{CH}$), 2924.1 ($\nu_{CH_2}$), 2853.2 ($\nu_{CH_3}$), 1645.6 ($\nu_{C=O\ amide}$), 1463.9 ($\nu_{C=C}$), 1101.1 ($\nu_{C-O}$). ESI-MS: calcd for $C_{28}H_{49}NO_3H$ (448.38), $C_{22}H_{45}NO_3Na$ (470.36) found *m/z* 448.4(28%), 449.4(9) $[M+H]^+$, 470.3(100%), 471.3(31), 472.3(7) $[M+Na]^+$.

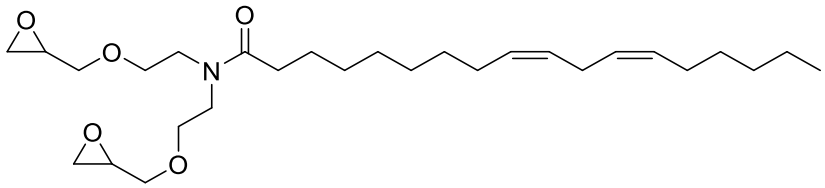

Synthesis of Compound 3.17

Fatty amide (compound **3.15**), epichlorohydrin (2.30 g, 32.6 mmol, 6 eq), NaOH (1.30 g, 32.6 mmol, 6 eq), tetrabutyl ammonium bromide (0.08 g, 0.2 mmol, 0.05 eq) and water (0.146g, 8.16 mmol, 1.5 eq) were mixed and heated to 40 °C. After 4 h DCM (20 mL) was added and the solid was removed by Buchner filtration, the residue was washed with DCM and solvent removed from the filtrate by rotary evaporation. Excess epichlorohydrin was removed by distillation under reduced pressure and the residue was purified by column chromatography (DCM:MeOH 24:1) to yield a golden oil 1.584 g (61%). ^{1}H NMR (300 MHz, $CDCl_3$) δ 5.37 – 5.25 (m, 4H, $CH_2CHCHCH_2CHCHCH_2$), 3.70 (ddd, *J* = 14.1, 11.6, 2.5 Hz, 2H, OCH_2CHOCH_2), 3.57 (d, *J* = 5.1 Hz, 4H, NCH_2CH_2O), 3.52 (d, *J* = 5.3 Hz, 4H, NCH_2CH_2O), 3.29 (ddd, *J* = 11.4, 5.9, 1.6 Hz, 2H, OCH_2CHOCH_2), 3.10 – 3.02 (m, 2H, $OCH_2CHCHOCH_2$), 2.71 (dd, *J* = 10.8, 5.5 Hz, 4H, OCH_2CHOCH_2, $CHCHCH_2CHCH$), 2.57 – 2.50 (m, 2H, OCH_2CHOCH_2), 2.31 (t, *J* = 7.5 Hz, 2H, $O{=}CCH_2$), 1.97 (q, *J* = 6.3 Hz, 4H, $CH_2CHCHCH_2CHCHCH_2$), 1.56 (t, *J* = 6.6 Hz, 2H, $O{=}CCH_2CH_2$), 1.25 (s, 14H, CH_2CH_2), 0.83 (t, *J* = 6.4 Hz, 3H, CH_2CH_3). ^{13}C NMR (75 MHz, $CDCl_3$) δ 173.03 ($C{=}O$), 129.54 129.45 ($CHCHCH_2CHCH$), 127.33 127.27 ($CHCHCH_2CHCH$), 71.24 71.05 (NCH_2CH_2O), 69.19 68.87 (OCH_2CHOCH_2), 50.09 50.06 (OCH_2CHOCH_2), 48.20 45.73 (NCH_2CH_2O), 43.55 43.30 OCH_2CHOCH_2, 32.44 ($O{=}C$), 30.86 - 24.64 (CH_2CH_2), 21.93 (CH_2CH_3), 13.44 ($CHCH_3$). IR (cm^{-1}): 3005.9 (ν_{CH}), 2923.6 (ν_{CH_2}), 2853.8 (ν_{CH_3}), 1642.0 ($\nu_{C=O}$

$_{amide}$), 1463.3 ($\nu_{C=C}$), 1107.3 ($\nu_{C\text{-}O\ ether}$), 842.3 ($\nu_{C\text{-}O\ epox}$). ESI-MS: calcd for $C_{28}H_{49}NO_5Na$ (479.36) found *m/z* 502.3 (100%), 503.3(34), 504.3(7).

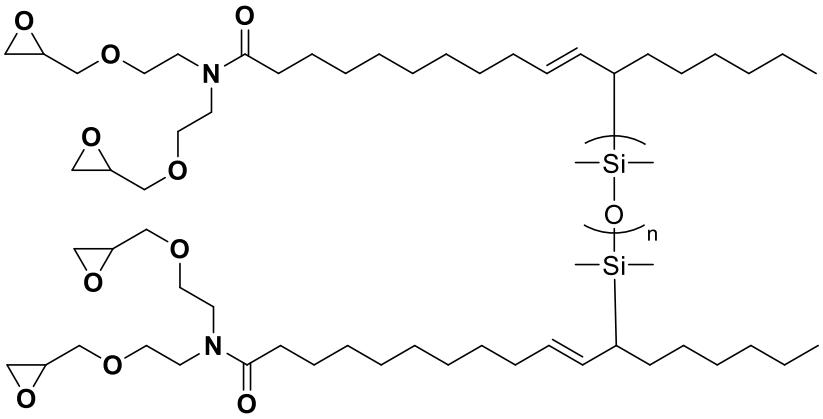

Synthesis of Compound 3.18

The epoxidised fatty amide (compound **3.17**, 0.5 g, 1.04 mmol) and DMS-H11 (0.547, 0.521 mmol. 0.5 eq) were mixed with rapid stirring creating an emulsion and heated to 40 °C. Karstedts catalyst was added and the reaction stirred for 5 days. Reaction mixture diluted with DCM (10 mL) and passed through a silica plug to remove the catalyst. Solvent was removed by rotary evaporation to yield a colourless oil, 0.5481 g (52%). ^{1}H NMR (400 MHz, $CDCl_3$) δ 5.45 – 5.20 (m, 4H, SiCHC$\underline{H}$C$\underline{H}$CH$_2$), 3.69 (dd, *J* = 19.5, 11.7 Hz, 4H, OC$\underline{H_2}$CHOCH$_2$), 3.56 (d, *J* = 4.5 Hz, 8H, NCH$_2$C$\underline{H_2}$O), 3.51 (d, *J* = 6.1 Hz, 8H, NC$\underline{H_2}$CH$_2$O), 3.27 (d, *J* = 9.0 Hz, 4H, OC$\underline{H_2}$CHOCH$_2$), 3.05 (s, 4H, OCH$_2$C$\underline{H}$OCH$_2$), 2.72 (s, 4H, OCH$_2$CHOC$\underline{H_2}$), 2.52 (s, 4H, OCH$_2$CHOC$\underline{H_2}$), 2.30 (t, *J* = 6.5 Hz, 4H, O=CC$\underline{H_2}$), 1.97 (q, *J* = 6.8 Hz, 4H, C$\underline{H_2}$CHCHCHSi), 1.55 (s, 6H, O=CCH$_2$C$\underline{H_2}$, SiC$\underline{H}$CHCH), 1.24 (s, 40H, C$\underline{H_2}$CH$_2$), 0.82 (s, 6H, CH$_2$C$\underline{H_3}$), 0.11 (s, 12H, CHSi(C$\underline{H_3}$)O), -0.00 (s, 90H, OSi(C$\underline{H_3}$)O). ^{13}C NMR (75 MHz, $CDCl_3$) δ 161.44 (O=$\underline{C}$CH$_2$), 129.70 127.91 (CH$_2\underline{C}$H$\underline{C}$HCHSi), 72.52 (O$\underline{C}$H$_2$CH$_2$N), 69.63 (O$\underline{C}$H$_2$CHOCH$_2$), 49.70 (OCH$_2\underline{C}$HOCH$_2$), 47.81 (OCH$_2\underline{C}$H$_2$N), 43.10 (OCH$_2$CHO$\underline{C}$H$_2$), 33.60 (O=C$\underline{C}$H$_2$), 32.02 - 24.32 ($\underline{C}$H$_2$CH$_2$),

18.38 ($CH_2\underline{C}H_3$), -0.01 ($Si(\underline{C}H_3)_2O$). IR (cm^{-1}): 3005.9 (ν_{CH}), 2926.1 (ν_{CH_2}), 2856.0 (ν_{CH_3}), 2246.2 (ν_{Si-H}) 1629.9 ($\nu_{C=O\ amide}$), 1465.1 ($\nu_{C=C}$), 1101.2 ($\nu_{C-O\ ether}$), 909.5 838.7 ($\nu_{C-O\ epox}$).

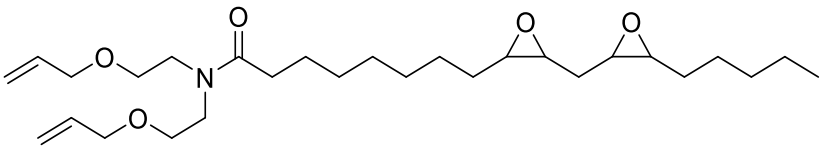

Synthesis of Compound 3.19

The fatty amide (compound **3.16**, 2.0g, 4.5 mmol) was dissolved in DCM (20 mL), peracetic acid (1.74g, 8.9 mmol, 2 eq) was added and the reaction mixture was stirred at room temperature. The reaction was followed by ^{1}H NMR analysing samples periodically up to 4 h and then at 20 h. After 20 h the reaction was diluted with DCM (30 mL), washed with water (3 x 50 mL), brine (20 mL) and dried with anhydrous $MgSO_4$. The solvent was removed by rotary evaporation to yield a colourless oil, 2.05g (96%). ^{1}H NMR (300 MHz, $CDCl_3$) δ 5.80 (dtdd, *J* = 15.9, 10.5, 5.5, 3.3 Hz, 2H, $OCH_2C\underline{H}CH_2$), 5.23 – 5.14 (m, 2H, $OCH_2CHC\underline{H}_2$), 5.14 – 5.05 (m, 2H, $OCH_2CHC\underline{H}_2$), 3.89 (td, *J* = 3.9, 1.9 Hz, 4H, $OC\underline{H}_2CHCH_2$), 3.56 – 3.44 (m, 8H, $NC\underline{H}_2C\underline{H}_2O$), 3.09 – 2.97 (m, 2H, $CH_2CHOC\underline{H}CH_2C\underline{H}OCHCH_2$), 2.95 – 2.87 (m, 2H, $CH_2C\underline{H}OCHCH_2CHOC\underline{H}CH_2$), 2.31 (t, *J* = 7.8 Hz, 2H, $O{=}CC\underline{H}_2$), 1.66 (t, *J* = 6.2 Hz, 2H,), 1.55 (t, *J* = 5.8 Hz, 2H, $CH_2CHOCHC\underline{H}_2CHOCHCH_2$), 1.44 (s, 6H, $O{=}CCH_2C\underline{H}_2$, $C\underline{H}_2CH_3$), 1.27 (s, 12H, $C\underline{H}_2CH_2$), 0.83 (t, *J* = 6.9 Hz, 3H, $CH_2C\underline{H}_3$). ^{13}C NMR (75 MHz, $CDCl_3$) δ 173.01 ($O{=}\underline{C}$), 134.04 133.74 ($OCH\underline{C}HCH_2$), 116.41 116.13 ($OCH_2CH\underline{C}H_2$), 71.54 71.30 ($O\underline{C}H_2CHCH_2$), 68.17 67.59 ($NCH\underline{C}H_2O$), 56.40 56.11 ($CH_2\underline{C}HOCHCH_2CHO\underline{C}HCH_2$), 53.73 53.58 ($CH_2CHO\underline{C}HCH_2CHO\underline{C}HCH_2$), 48.32 45.87 ($N\underline{C}H_2CH_2O$), 32.39 ($O{=}C\underline{C}H_2$), 31.03 - 24.60 ($\underline{C}H_2CH_2$), 21.93 ($\underline{C}H_2CH_3$), 13.36 ($CH_2\underline{C}H_3$). IR ($cm^{-1}$): 3079.5 ($\nu_{CH}$),

2925.2 (ν_{CH_2}), 2854.7 (ν_{CH_3}), 1643.6 ($\nu_{C=O\ amide}$), 1463.3 ($\nu_{C=C}$), 1101.5 (ν_{C-O}). ESI-MS: calcd for $C_{28}H_{49}NO_5H$ (480.37) found *m/z* 480.4(100%), 481.4(30%).

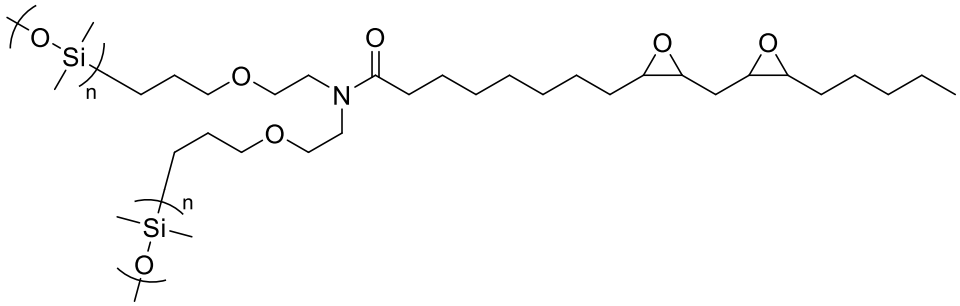

Synthesis of Compound 3.20

The epoxidised fatty amide (compound **3.19**, 2.0 g, 4.16 mmol) and DMS-H11 (4.3 g, 4.16 mmol, 1 eq) were mixed with rapid stirring to create an emulsion and heated to 100 °C. Karstedts catalyst (1 drop) was added, a clear solution formed after 1 h, but the reaction was stirred overnight to ensure completion. The reaction mixture was dissolved in DCM (20 mL) and passed through a silica column to remove the catalyst. Solvent was removed by rotary evaporation to yield a golden oil 5.48g (87%). Product was purified by column chromatography using DCM and methanol (5% v/v). ^{1}H NMR (300 MHz, $CDCl_3$) δ 5.91 – 5.85 (m, 0.26H, OC<u>H</u>CH_2), 5.53 – 5.43 (m, 0.26H, OCHC<u>H</u>$_2$), 5.42 – 5.34 (m, 0.26H, OCHC<u>H</u>$_2$), 3.57 – 3.46 (m, 8H, OC<u>H</u>$_2$$CH_2$N, OCH_2C<u>H</u>$_2$N), 3.33 (t, *J* = 6.9 Hz, 4H, OC<u>H</u>$_2$$CH_2CH_2$Si), 3.12 – 3.00 (m, 2H, CH_2C<u>H</u>OCHCH_2CHOC<u>H</u>CH_2), 2.98 – 2.85 (m, 2H, CH_2CHOC<u>H</u>CH_2C<u>H</u>OCHCH_2), 2.34 (t, *J* = 7.5 Hz, 2H, OCC<u>H</u>$_2$), 1.69 (t, *J* = 7.0 Hz, 2H, CHOCHC<u>H</u>$_2$CHOCH), 1.65 – 1.43 (m, 10H, OCH_2C<u>H</u>$_2$, C<u>H</u>$_2$CHOCHCH_2CHOCHC<u>H</u>$_2$, OCH_2C<u>H</u>$_2$$CH_2$Si), 1.31 (s, 14H, C<u>H</u>$_2$$CH_2$), 0.91 – 0.82 (m, 3H, CH_2C<u>H</u>$_3$), 0.52 – 0.43 (m, 4H. OCH_2CH_2C<u>H</u>$_2$Si), 0.04 (s, 132H, Si(C<u>H</u>$_3$)$_2$O). ^{13}C NMR (75 MHz, $CDCl_3$) δ 163.67 (O=<u>C</u>CH_2), 72.91 (O<u>C</u>$H_2CH_2CH_2$Si), 68.18 (O<u>C</u>H_2CH_2N), 55.99 (<u>C</u>HOCHCH_2CHO<u>C</u>H), 53.29

(CHO<u>C</u>HCH$_2$<u>C</u>HOCH), 45.42 (OCH$_2$<u>C</u>H$_2$N), 33.62 (OC<u>C</u>H$_2$CH$_2$), 32.04 (OCH$_2$<u>C</u>H$_2$CH$_2$Si), 30.62 - 24.23 (<u>C</u>H$_2$CH$_2$), 22.44 (<u>C</u>H$_2$CH$_3$), 13.11 (CH$_2$<u>C</u>H$_3$), 0.12 (CH$_2$Si(<u>C</u>H$_3$)$_2$O), -0.01 (OSi(<u>C</u>H$_3$)$_2$O). IR (cm^{-1}): 2960.7 (ν_{CH_2}), 2858.4 (ν_{CH_3}), 1646.8 ($\nu_{C=O\ amide}$), 1257.4 (ν_{C-O}) 1011.6 (ν_{Si-O}), 863.2 ($\nu_{C-O\ epox}$).

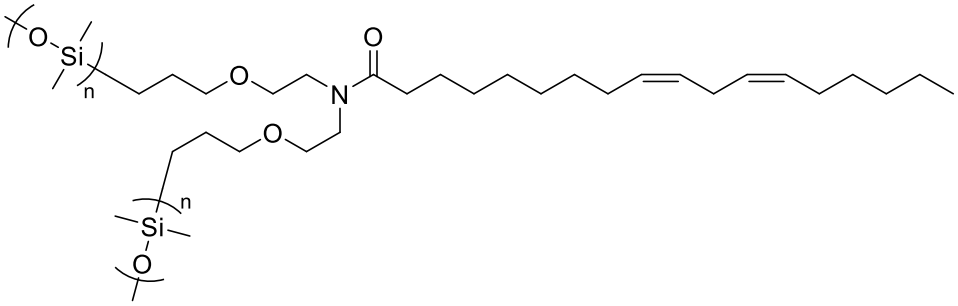

Synthesis of Compound 3.21

The fatty amide (compound **3.16**, 0.522 g, 1.166 mmol) was mixed with DMS-H11 (1.224 g, 1.166 mmol, 1 eq) with rapid stirring to create an emulsion and heated to 100 °C. Karstedts catalyst (1 drop) was added and the reaction was stirred for 1 h, DCM (10 mL) was added and the solution passed through a silica plug to remove the catalyst. Solvent was removed by rotary evaporation to yield a green tinted oil. ^{1}H NMR (300 MHz, CDCl$_3$) δ 5.43 – 5.24 (m, 3H, CH$_2$C<u>H</u>C<u>H</u>CH$_2$), 3.52 (s, 8H, OC<u>H$_2$</u>C<u>H$_2$</u>N), 3.34 (t, *J* = 6.4 Hz, 4H, OC<u>H$_2$</u>CH$_2$CH$_2$Si), 2.74 (t, *J* = 6.2 Hz, 1H, CHCHC<u>H$_2$</u>CHCH), 2.34 (t, *J* = 7.2 Hz, 2H, OCC<u>H$_2$</u>), 2.12 – 1.88 (m, 4H, C<u>H$_2$</u>CHCHC<u>H$_2$</u>), 1.63 – 1.48 (m, 6H, OCCH$_2$C<u>H$_2$</u>, OCH$_2$C<u>H$_2$</u>CH$_2$Si), 1.28 (s, 14H, C<u>H$_2$</u>CH$_2$), 0.85 (t, *J* = 5.5 Hz, 3H, CH$_2$C<u>H$_3$</u>), 0.52 – 0.44 (m, 3H, OCH$_2$CH$_2$C<u>H$_2$</u>Si), 0.04 (s, 132H, OSi(C<u>H$_3$</u>)$_2$O).

6.5.4 Silicone Additives in Non-stick Coating

Silicone additives **3.18** and **3.20** were combined with coating samples from chapter 2 (section 6.4.6, with 2wt% linoleic acid), the silicone replaced ESBO to keep solid

content constant. **3.22 0wt% (control)**, ESBO (1.86 g), ELA (0.04 g), fumed silica (0.04 g), carbon black (0.06 g) and propyl acetate (0.2 mL) were mixed, coated onto ECCS (12 μm) and cured (400 °C, 60 s). PH = 6H, XH = 100%, Flex = 1T Pass. **3.23** (1% 3.18), ESBO (1.84 g), ELA (0.04 g) and 3.18 (0.02 g) fumed silica (0.04 g), carbon black (0.06 g) and propyl acetate (0.2 mL) were mixed, coated onto ECCS (12 μm) and cured (400 °C, 60 s). PH = 6H, XH = 100%, Flex = 0T Pass. **3.24** (2% 3.18), ESBO (1.82 g), ELA (0.04 g) and 3.18 (0.04 g) fumed silica (0.04 g), carbon black (0.06 g) and propyl acetate (0.2 mL) were mixed, coated onto ECCS (12 μm) and cured (400 °C, 60 s). PH = 6H, XH = 100%, Flex = 0T Pass. **3.25** (5% 3.18), ESBO (1.76 g), ELA (0.04 g) and 3.18 (0.1 g) fumed silica (0.04 g), carbon black (0.06 g) and propyl acetate (0.2 mL) were mixed, coated onto ECCS (12 μm) and cured (400 °C, 60 s). PH = 5H, XH = 100%, Flex = 1T Pass. **3.26** (1% 3.20), ESBO (1.84 g), ELA (0.04 g) and 3.20 (0.02 g) fumed silica (0.04 g), carbon black (0.06 g) and propyl acetate (0.2 mL) were mixed, coated onto ECCS (12 μm) and cured (400 °C, 60 s). PH = 6H, XH = 100%, Flex = 0T Pass. **3.27** (2% 3.20), ESBO (1.82 g), ELA (0.04 g) and 3.20 (0.04 g) fumed silica (0.04 g), carbon black (0.06 g) and propyl acetate (0.2 mL) were mixed, coated onto ECCS (12 μm) and cured (400 °C, 60 s). PH = 6H, XH = 100%, Flex = 0T Pass. **3.28** (5% 3.20), ESBO (1.76 g), ELA (0.04 g) and 3.20 (0.1 g) fumed silica (0.04 g), carbon black (0.06 g) and propyl acetate (0.2 mL) were mixed, coated onto ECCS (12 μm) and cured (400 °C, 60 s). PH = 5H, XH = 95%, Flex = 1T Pass.

6.6 Experimental procedures for Epoxide – Anhydride (Chapter 4)

6.6.1 General procedure for epoxidation of vegetable oils

Epoxidation method proposed by Petrovic[107] and performed on a 200 – 400 g scale. The vegetable oil (e.g. grapeseed oil, 400 g, 0.454 mol) was dissolved in toluene (1000 mL) and heated to 80 °C. Acetic acid (13.62, 0.5 eq) and Amberlite® (100 g, 25 wt%) were added followed by dropwise addition of hydrogen peroxide solution (35%, 352 mL, 8 eq). The reaction was stirred overnight at 80 °C in air. After completion the reaction was washed with water (3 x 500 mL), NaCl (saturated, 2 x 100 mL) and dried using $MgSO_4$. The solvent was removed under vacuum to yield a green tinted oil (421.8 g, 96.6%).

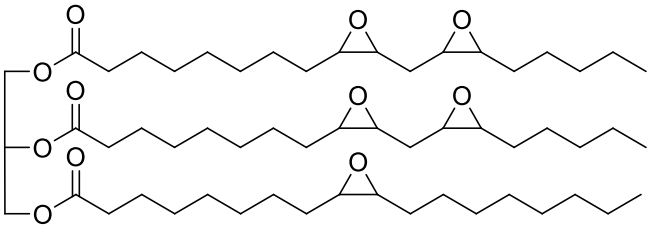

Epoxidised Soybean Oil. Yellow/green tinted oil, 314.7 g (96.3%). ^{1}H NMR (300 MHz, $CDCl_3$) δ 5.31 – 5.21 (m, 1H, C<u>H</u>O), 4.31 (dd, *J* = 11.9, 4.2 Hz, 2H, C<u>H$_2$</u>O), 4.14 (dd, *J* = 11.9, 5.9 Hz, 2H, C<u>H$_2$</u>O), 3.22 – 3.02 (m, 4H, $CH_2CHOC\underline{H}CH_2C\underline{H}OCHCH_2$), 2.97 (s, 3H, $CH_2C\underline{H}OCHCH_2CHOC\underline{H}CH_2$), 2.89 (s, 2H, $CH_2C\underline{H}OC\underline{H}CH_2$), 2.32 (t, *J* = 7.7 Hz, 6H, O=CC<u>H$_2$</u>CH$_2$), 1.75 (dt, *J* = 15.1, 6.3 Hz, 4H, $CH_2CHOCHC\underline{H_2}CHOCHCH_2$), 1.62 (s, 6H, $O{=}CCH_2C\underline{H_2}CH_2$), 1.50 (d, *J* = 4.1 Hz, 18H, C<u>H$_2$</u>CHOCHCH$_2$CHOCHC<u>H$_2$</u>, C<u>H$_2$</u>CH$_3$), 1.34 (s, 22H, C<u>H$_2$</u>CH$_2$), 1.26 (s, 20H, C<u>H$_2$</u>CH$_2$), 0.89 (t, *J* = 6.9 Hz, 9H, CH$_2$C<u>H$_3$</u>). ^{13}C NMR (75 MHz, $CDCl_3$) δ 173.00, 172.61(<u>C</u>=O), 68.82 (<u>C</u>H-O), 61.97 (<u>C</u>H$_2$-O), 57.04 - 56.50 ($CH_2\underline{C}HOCHCH_2CHO\underline{C}HCH_2$), 54.20, 54.05 ($CH_2CHO\underline{C}HCH_2\underline{C}HOCHCH_2$), 34.01, 33.85 ($O{=}C\underline{C}H_2$), 31.76 - 24.69 (<u>C</u>H$_2$CH$_2$), 22.48 (<u>C</u>H$_2$CH$_3$), 13.90 (<u>C</u>H$_3$). IR (cm^{-1}): 2923, 2854 (ν_{CH_2/CH_3}), 1741 ($\nu_{C=O}$), 823 (ν_{epox}). ESI-MS: calcd for

$C_{57}H_{100}O_{11}Na$ - $[M+Na]^+$ (983.72): found *m/z* 983.7(100%), 984.7(63), 985.7(21), 986.7(4).

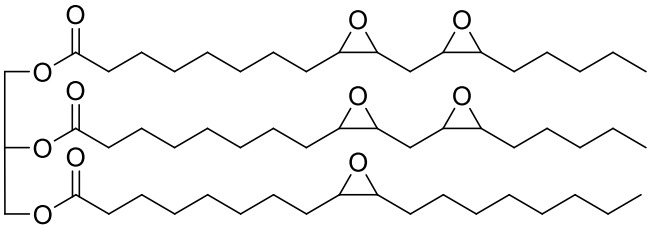

Epoxidised Grapeseed Oil. Green tinted oil, 421.8 g (96.6%). ^{1}H NMR (400 MHz, $CDCl_3$) δ 5.29 – 5.23 (m, 1H, C<u>H</u>O), 4.30 (dd, *J* = 11.9, 4.3 Hz, 2H, C<u>H$_2$</u>O), 4.15 (dd, *J* = 11.9, 5.9 Hz, 2H, C<u>H$_2$</u>O), 3.15 – 3.04 (m, 4H, $CH_2CHOC\underline{H}CH_2C\underline{H}OCHCH_2$), 3.01 – 2.94 (m, 4H, $CH_2C\underline{H}OCHCH_2CHOC\underline{H}CH_2$), 2.89 (s, 1H, $CH_2C\underline{H}OC\underline{H}CH_2$), 2.32 (t, *J* = 7.5 Hz, 6H, O=CC<u>H$_2$</u>CH$_2$), 1.80 – 1.76 (m, 1H, $CH_2CHOCHC\underline{H_2}CHOCHCH_2$), 1.73 (t, *J* = 6.0 Hz, 3H, $CH_2CHOCHC\underline{H_2}CHOCHCH_2$), 1.62 (s, 6H, O=CCH$_2$C<u>H$_2$</u>CH$_2$), 1.56 – 1.43 (m, 18H, C<u>H$_2$</u>CHOCHCH$_2$CHOCHC<u>H$_2$,</u> C<u>H$_2$</u>CH$_3$), 1.34 (d, *J* = 2.2 Hz, 30H, <u>C</u>H$_2$CH$_2$), 1.26 (s, 12H, <u>C</u>H$_2$CH$_2$), 0.89 (t, *J* = 7.3 Hz, 9H, CH$_2$C<u>H$_3$</u>). ^{13}C NMR (75 MHz, $CDCl_3$) δ 172.46, 172.06 (<u>C</u>=O), 68.22 (<u>C</u>H-O), 61.39 (<u>C</u>H$_2$-O), 56.48 - 55.94 ($CH_2\underline{C}HOCHCH_2CHO\underline{C}HCH_2$), 53.63, 53.48 ($CH_2CHO\underline{C}HCH_2\underline{C}HOCHCH_2$), 33.43, 33.27 (O=C<u>C</u>H$_2$), 31.17 - 24.09 (<u>C</u>H$_2$CH$_2$), 21.89(<u>C</u>H$_2$CH$_3$), 13.32 (<u>C</u>H$_3$). IR (cm^{-1}) 2924, 2854 (ν_{CH_2/CH_3}), 1740 ($\nu_{C=O}$), 822 (ν_{epox}). ESI-MS: calcd for $C_{57}H_{100}O_{11}Na$ - $[M+Na]^+$ (983.72): found *m/z* 983.7(100%), 984.7(62), 985.7(22), 986.7(6).

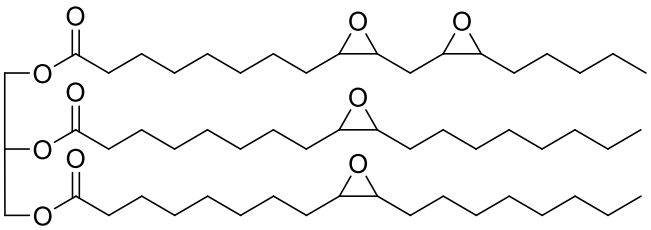

Epoxidised Rapeseed Oil. Cream waxy solid, 203.1 g (94.9%). ^{1}H NMR (300 MHz, $CDCl_3$) δ 5.26 – 5.17 (m, 1H, C<u>H</u>O), 4.25 (dd, *J* = 11.9, 4.3 Hz, 2H, C<u>H$_2$</u>O), 4.09 (dd, *J* = 11.9, 5.9 Hz, 2H, C<u>H$_2$</u>O), 3.18 – 2.98 (m, 2H, $CH_2CHOC\underline{H}CH_2C\underline{H}OCHCH_2$), 2.93 (s, 2H, $CH_2C\underline{H}OCHCH_2CHOC\underline{H}CH_2$), 2.85 (s, 4H, $CH_2C\underline{H}OC\underline{H}CH_2$), 2.27 (t, *J* = 7.5 Hz, 6H, O=CC<u>H$_2$</u>CH$_2$), 1.76 – 1.65 (m, 2H, $CH_2CHOCHC\underline{H_2}CHOCHCH_2$), 1.57 (s, 6H, O=C $CH_2C\underline{H_2}CH_2$), 1.44 (s, 18H, $C\underline{H_2}CHOCHCH_2CHOCHC\underline{H_2}$, $C\underline{H_2}CH_3$), 1.28 (s, 25H, $C\underline{H_2}CH_2$), 1.23 (s, 15H, $C\underline{H_2}CH_2$), 1.20 (s, 8H, $C\underline{H_2}CH_2$), 0.83 (t, *J* = 6.7 Hz, 9H, $CH_2C\underline{H_3}$). ^{13}C NMR (75 MHz, $CDCl_3$) δ 172.58, 172.17 (<u>C</u>=O), 68.25 (<u>C</u>H-O), 61.45 (<u>C</u>H$_2$-O), 56.58, 56.02 ($CH_2\underline{C}HO\underline{C}HCH_2$), 53.71, 53.55 ($CH_2CHO\underline{C}HCH_2\underline{C}HOCHCH_2$), 33.34 (O=C<u>C</u>H$_2$), 31.21 - 24.14 (<u>C</u>H$_2$CH$_2$), 22.02 (<u>C</u>H$_2$CH$_2$), 13.47 ($CH_2\underline{C}H_3$). IR (cm^{-1}) 2923, 2854 (ν_{CH_2/CH_3}), 1741 ($\nu_{C=O}$), 824 (ν_{epox}). ESI-MS: calcd for $C_{57}H_{102}O_{10}Na$ - $[M+Na]^+$ (969.74): found *m/z* 969.7(100%), 970.7(60), 971.7(26), 972.7(8).

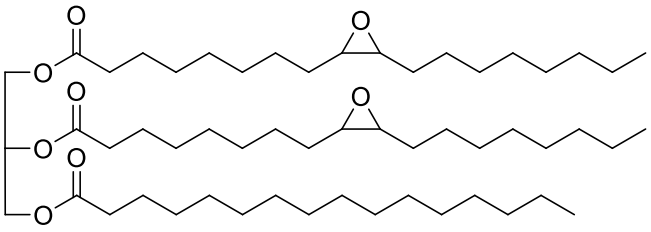

Epoxidised Palm Oil. Cream waxy solid, 246.8 g (95.4%). ^{1}H NMR (400 MHz, $CDCl_3$) δ 5.22 – 5.15 (m, 1H, C<u>H</u>O), 4.23 (dd, *J* = 11.9, 4.3 Hz, 2H, C<u>H$_2$</u>O), 4.07 (dd, *J* = 11.9, 5.9 Hz, 2H, C<u>H$_2$</u>O), 3.07 – 2.76 (m, 4H, $CH_2C\underline{H}OC\underline{H}CH_2$), 2.24 (t, *J* = 7.5 Hz, 6H, O=CC<u>H$_2$</u>CH$_2$), 1.59 – 1.50 (m, 6H, O=C$CH_2C\underline{H_2}$), 1.42 (s, 8H, $C\underline{H_2}CHOCHC\underline{H_2}$), 1.31 – 1.15 (m, 64H, $C\underline{H_2}CH_2$), 0.81 (t, *J* = 6.8 Hz, 9H, $CH_2C\underline{H_3}$). ^{13}C NMR (101 MHz, $CDCl_3$) δ 173.29, 172.81 (O=<u>C</u>), 68.90 (<u>C</u>H-O), 62.07 (<u>C</u>H$_2$-O), 57.22 - 57.16 ($CH_2\underline{C}HO\underline{C}HCH_2$), 54.34 - 54.18 ($CH_2CHOC\underline{H}CH_2C\underline{H}OCHCH_2$), 34.05 (O=C<u>C</u>H$_2$), 31.93 - 24.86 (<u>C</u>H$_2$CH$_2$), 22.69

($\underline{C}H_2CH_3$), 14.11 ($CH_2\underline{C}H_3$). IR (cm^{-1}) 2921, 2852 ($\nu_{CH2/CH3}$), 1742 ($\nu_{C=O}$), 841 (ν_{epox}). ESI-MS: calcd for $C_{55}H_{102}O8Na$ - $[M+Na]^+$ (913.75): found *m/z* 913.7(100%), 914.7(61), 915.7(23), 916.7(4).

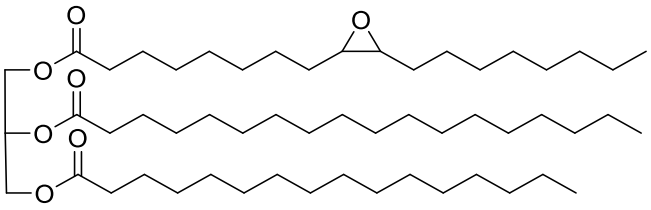

Epoxidised Cocoa Butter. Cream waxy solid, 194.1 g (96.1%). ^{1}H NMR (400 MHz, $CDCl_3$) δ 5.30 – 5.22 (m, 1H, C$\underline{H}$O), 4.30 (dd, *J* = 11.9, 4.2 Hz, 2H, C$\underline{H_2}$O), 4.14 (dd, *J* = 11.9, 5.9 Hz, 2H, C$\underline{H_2}$O), 2.89 (s, 2H, $CH_2C\underline{H}OC\underline{H}CH_2$), 2.31 (t, *J* = 7.5 Hz, 6H, O=CC$\underline{H_2}CH_2$), 1.67 – 1.55 (m, 6H, O=C$CH_2C\underline{H_2}$), 1.49 (s, 6H, C$\underline{H_2}CH_3$), 1.33 (s, 10H, C$\underline{H_2}CH_2$), 1.28 (s, 18H, C$\underline{H_2}CH_2$), 1.26 (s, 42H, C$\underline{H_2}CH_2$), 0.88 (t, *J* = 5.9 Hz, 9H, $CH_2C\underline{H_3}$). ESI-MS: calcd for $C_{55}H_{104}O_7Na$ - $[M+Na]^+$ (899.77): found *m/z* 899.7(100%), 900.7(63), 901.7(24), 902.7(7).

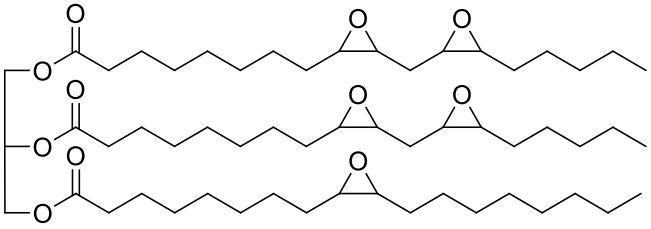

6.6.2 Epoxidation of grapeseed oil without solvent.

Grapeseed oil (10.0 g, 11.3 mmol) was heated to 80 °C. Acetic acid (0.341 g 5.6 mmol) and Amberlite (2.5 g 25 wt%) were added followed by the dropwise addition of hydrogen peroxide solution (35%, 8.819 mL, 8 eq). The reaction was stirred at 80 °C and was monitored by ^{1}H NMR spectrometry (disappearance of alkene peaks at 5.4 ppm and appearance of epoxide peaks at 2.8 – 3.1 ppm). After 6 hours the reaction was complete and was diluted with $CHCl_3$ (100 mL). The reaction mixture

was washed with water (3 x 100 mL), NaCl solution (sat. 20 mL), dried over $MgSO_4$ and the solvent was removed under vacuum to yield a green tinted oil 9.36 g, (86.1%). ^{1}H NMR (400 MHz, $CDCl_3$) δ 5.26 (p, *J* = 5.2 Hz, 1H, C<u>H</u>O), 4.30 (dd, *J* = 11.9, 4.3 Hz, 2H, C<u>H$_2$</u>O), 4.15 (dd, *J* = 11.9, 5.9 Hz, 2H, C<u>H$_2$</u>O), 3.15 – 3.03 (m, 4H, $CH_2CHOC\underline{H}CH_2C\underline{H}OCHCH_2$), 3.01 – 2.93 (m, 4H, $CH_2C\underline{H}OCHCH_2CHOC\underline{H}CH_2$), 2.89 (s, 1H, $CH_2C\underline{H}OC\underline{H}CH_2$), 2.32 (t, *J* = 7.5 Hz, 6H, O=CCHC<u>H$_2$</u>), 1.84 – 1.76 (m, 1H, CHOCHC<u>H$_2$</u>CHOCH), 1.73 (t, *J* = 6.1 Hz, 3H, CHOCHC<u>H$_2$</u>CHOCH), 1.62 (s, 6H, $O{=}CCHCH_2C\underline{H_2}$), 1.56 – 1.42 (m, 18H, C<u>H$_2$</u>CHOCHCH$_2$CHOCHC<u>H$_2$</u>, C<u>H$_2$</u>CH$_3$), 1.34 (s, 28H, C<u>H$_2$</u>CH$_2$), 1.26 (s, 12H, C<u>H$_2$</u>CH$_2$), 0.90 (t, *J* = 7.9 Hz, 9H, $CH_2\underline{CH_3}$).

6.6.3 General procedure for polymerisation of epoxy vegetable oils and cyclic anhydrides.

Polymerisation performed on a 16 g scale. The epoxidised vegetable oil and 4-methyl imidazole were combined and heated to 40 °C to aid dissolving of imidazole. The mixture was degassed for 10 minutes under high vacuum and fast stirring. The anhydride was added in varying amounts to give the required epoxide:anhydride mol ratio and the mixture was further degassed for 20 minutes. The reaction mixture was poured into an aluminium ‘dog bone’ mould lined with silicone release spray and heated at 170 °C for 1 h.

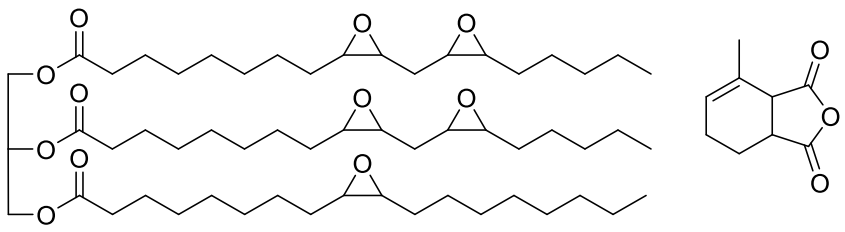

Epoxidised Soybean Oil and Aradur 917 (1:1). ESBO (9.0 g, 9.4 mmol) and Aradur 917 (6.84 g, 41.2 mmol, 4.4 eq) and 4-methyl imidazole (0.1584 g, 1wt%)

cured at 170 °C for 1 h forming an orange-brown rigid polymer. IR (cm^{-1}): 2924, 2854 (ν_{CH_2/CH_3}), 1730 ($\nu_{C=O}$), 1455 (ν_{C-H}) 1158, 1107 (ν_{C-O}). Ultimate tensile stress – 29.33 MPa, Youngs modulus – 1090 MPa, elongation at break – 4.87%, Crosslinking density – 35.8 $x10^4$ mol/cm^3, Sol content 6.55%, Swelling ratio – 1.45, Contact angle (θ_{water}) 105.8.

Epoxidised Soybean Oil and Aradur 917 (2:1). ESBO (12.0 g, 12.5 mmol) and Aradur 917 (4.56 g, 27.4 mmol, 2.2 eq) and 4-methyl imidazole (0.1656 g, 1wt%) cured at 170 °C for 1 h forming an orange-brown slightly flexible polymer. IR (cm^{-1}): 2924, 2854 (ν_{CH_2/CH_3}), 1729 ($\nu_{C=O}$), 1454 (ν_{C-H}) 1162, 1072 (ν_{C-O}). Ultimate tensile stress – 1.17 MPa, Youngs modulus – 10.52 MPa, elongation at break – 15.2%, Crosslinking density – 19.16 $x10^4$ mol/cm^3, Sol content 11.74%, Swelling ratio – 2.03, Contact angle (θ_{water}) 105.4.

Epoxidised Soybean Oil and Aradur 917 (4.4:1). ESBO (12.0 g, 12.5 mmol) and Aradur 917 (2.074 g, 12.5 mmol, 1 eq) and 4-methyl imidazole (0.1407 g, 1wt%) cured at 170°C for 1 h forming an orange-brown flexible polymer. IR (cm^{-1}): 2923, 2854 (ν_{CH_2/CH_3}), 1738 ($\nu_{C=O}$), 1459 (ν_{C-H}) 1157, 1095 (ν_{C-O}). Ultimate tensile stress – 0.067 MPa, Youngs modulus – 0.746 MPa, elongation at break – 9.86%, Crosslinking density – 11.85 $x10^4$ mol/cm^3, Sol content 29.15%, Swelling ratio – 2.68, Contact angle (θ_{water}) 103.1.

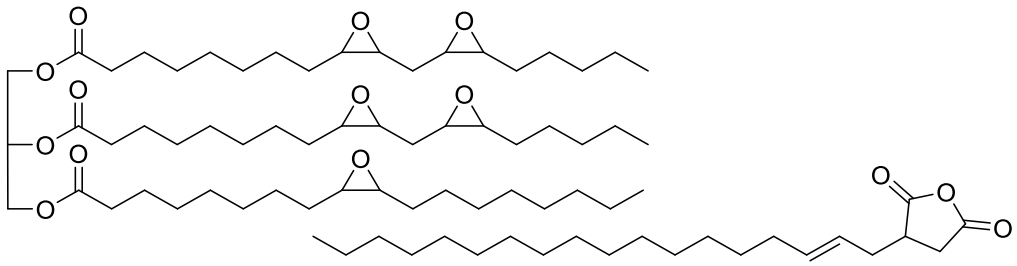

Epoxidised Soybean Oil and 2-Octadecenyl succinic anhydride (1:1). ESBO (6.0 g, 6.2 mmol) and 2-octadecenyl succinic anhydride (9.62 g, 27.4 mmol, 4.4 eq) and 4-methyl imidazole (0.1563 g, 1wt%) cured at 170 °C for 1 h forming a dark brown flexible polymer. IR (cm^{-1}): 2921, 2851 (ν_{CH_2/CH_3}), 1736 ($\nu_{C=O}$), 1463 (ν_{C-H}) 1155, 1101 (ν_{C-O}). Ultimate tensile stress – 0.651 MPa, Youngs modulus – 6.517 MPa, elongation at break – 12.1%, Crosslinking density – 20.24 $x10^4$ mol/cm^3, Sol content 19.94%, Swelling ratio – 2.78, Contact angle (θ_{water}) 106.7.

Epoxidised Soybean Oil and 2-Octadecenyl succinic anhydride (2:1). ESBO (9.0 g, 9.4 mmol) and 2-octadecenyl succinic anhydride (7.22 g, 2.6 mmol, 2.2 eq) and 4-methyl imidazole (0.1622 g, 1wt%) cured at 170 °C for 1 h forming a dark brown flexible polymer. IR (cm^{-1}): 2921, 2852 (ν_{CH_2/CH_3}), 1737 ($\nu_{C=O}$), 1464 (ν_{C-H}) 1154, 1100 (ν_{C-O}). Ultimate tensile stress – 0.550 MPa, Youngs modulus – 7.299 MPa, elongation at break – 8.75%, Crosslinking density – 18.79 $x10^4$ mol/cm^3, Sol content 7.19%, Swelling ratio – 2.06, Contact angle (θ_{water}) 106.3.

Epoxidised Soybean Oil and 2-Octadecenyl succinic anhydride (4.4:1). ESBO (12.0 g, 12.5 mmol) and 2-octadecenyl succinic anhydride (4.375 g, 12.5 mmol, 1 eq) and 4-methyl imidazole (0.1638 g, 1wt%) cured at 170 °C for 1 h forming a dark brown very flexible polymer. IR (cm^{-1}): 2921, 2852 (ν_{CH_2/CH_3}), 1737 ($\nu_{C=O}$), 1463 (ν_{C-H}) 1157, 1099 (ν_{C-O}). Ultimate tensile stress – 0.0.076 MPa, Youngs modulus – 0.867 MPa, elongation at break – 9.62%, Crosslinking density – 7.31 $x10^4$ mol/cm^3, Sol content 15.97%, Swelling ratio – 2.61, Contact angle (θ_{water}) 111.8.

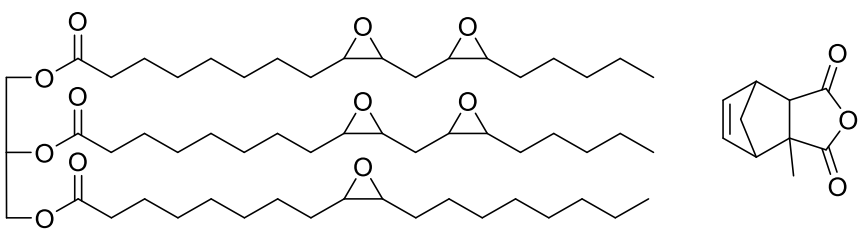

Epoxidised Soybean Oil and Methyl-5-norbornene-2,3-dicarboxylic anhydride (1:1). ESBO (9.0 g, 9.4 mmol) and methyl-5-norbornene-2,3-dicarboxylic anhydride (7.34 g, 41.2 mmol, 4.4 eq) and 4-methyl imidazole (0.1634 g, 1wt%) cured at 170 °C for 1 h forming a dark brown rigid polymer. IR (cm^{-1}): 2923, 2854 (ν_{CH_2/CH_3}), 1738 ($\nu_{C=O}$), 1459 (ν_{C-H}) 1159, 1108 (ν_{C-O}). Ultimate tensile stress – 8.03 MPa, Youngs modulus – 326.2 MPa, elongation at break – 4.17%, Crosslinking density – 30.94 $x10^4$ mol/cm^3, Sol content 6.56%, Swelling ratio – 1.60, Contact angle (θ_{water}) 106.4.

Epoxidised Soybean Oil and Methyl-5-norbornene-2,3-dicarboxylic anhydride (2:1). ESBO (11.5 g, 12.0 mmol) and methyl-5-norbornene-2,3-dicarboxylic anhydride (4.68 g, 26.3 mmol, 2.2 eq) and 4-methyl imidazole (0.1618 g, 1wt%) cured at 170 °C for 1 h forming a dark brown slightly flexible polymer. IR (cm^{-1}): 2923, 2854 (ν_{CH_2/CH_3}), 1737 ($\nu_{C=O}$), 1460 (ν_{C-H}) 1161, 1108 (ν_{C-O}). Ultimate tensile stress – 1.055 MPa, Youngs modulus – 10.97 MPa, elongation at break – 13.6%, Crosslinking density – 19.28 $x10^4$ mol/cm^3, Sol content 10.3%, Swelling ratio – 2.24, Contact angle (θ_{water}) 109.3.

Epoxidised Soybean Oil and Methyl-5-norbornene-2,3-dicarboxylic anhydride (4.4:1). ESBO (13.5 g, 14 mmol) and methyl-5-norbornene-2,3-dicarboxylic anhydride (2.50 g, 14 mmol, 1 eq) and 4-methyl imidazole (0.160 g, 1wt%) cured at 170 °C for 1 h forming a dark brown flexible polymer. IR (cm^{-1}): 2923, 2854 (ν_{CH_2/CH_3}), 1738 ($\nu_{C=O}$), 1461 (ν_{C-H}) 1156, 1093 (ν_{C-O}). Ultimate tensile stress – 0.118 MPa, Youngs modulus – 0.73 MPa, elongation at break – 13.1%, Crosslinking density – 9.53 $x10^4$ mol/cm^3, Sol content 29.36%, Swelling ratio – 2.71, Contact angle (θ_{water}) 112.7.

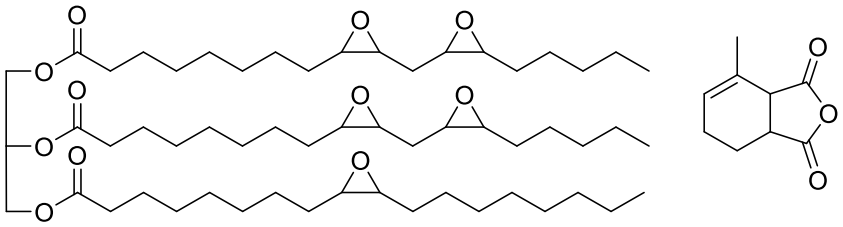

Epoxidised Grapeseed Oil and Aradur 917 (1:1). EGSO (9.0 g, 9.4 mmol) and Aradur 917 (7.39g, 44.5 mmol, 4.75 eq) and 4-methyl imidazole (0.1639 g, 1wt%) cured at 170 °C for 1 h forming an orange rigid polymer. IR (cm^{-1}): 2924, 2856 (ν_{CH_2/CH_3}), 1737 ($\nu_{C=O}$), 1453 (ν_{C-H}) 1085, 1016 (ν_{C-O}). Ultimate tensile stress – 12.76 MPa, Youngs modulus – 1005 MPa, elongation at break – 1.47%, Crosslinking density – 32.91 $x10^4$ mol/cm^3, Sol content 5.91%, Swelling ratio – 1.94, Contact angle (θ_{water}) 105.8.

Epoxidised Grapeseed Oil and Aradur 917 (2:1). EGSO (11.5 g, 12 mmol) and Aradur 917 (4.72 g, 28.4 mmol, 2.38 eq) and 4-methyl imidazole (0.1622 g, 1wt%) cured at 170 °C for 1 h forming an orange flexible polymer. IR (cm^{-1}): 2923, 2854 (ν_{CH_2/CH_3}), 1736 ($\nu_{C=O}$), 1458 (ν_{C-H}) 1160, 1103 (ν_{C-O}). Ultimate tensile stress – 0.653 MPa, Youngs modulus – 60.1 MPa, elongation at break – 1.33%, Crosslinking density – 23.42 $x10^4$ mol/cm^3, Sol content 18.01%, Swelling ratio – 1.82, Contact angle (θ_{water}) 106.9.

Epoxidised Grapeseed Oil and Aradur 917 (4.75:1). EGSO (13.5 g, 14 mmol) and Aradur 917 (2.33 g, 14 mmol, 1 eq) and 4-methyl imidazole (0.1583 g, 1wt%) cured at 170 °C for 1 h forming an orange flexible polymer. IR (cm^{-1}): 2924, 2854 (ν_{CH_2/CH_3}), 1738 ($\nu_{C=O}$), 1461 (ν_{C-H}) 1158, 1100 (ν_{C-O}). Ultimate tensile stress – 0.064 MPa, Youngs modulus – 0.504 MPa, elongation at break – 13.0%, Crosslinking density – 12.76 $x10^4$ mol/cm^3, Sol content 40.88%, Swelling ratio – 2.34, Contact angle (θ_{water}) 115.0.

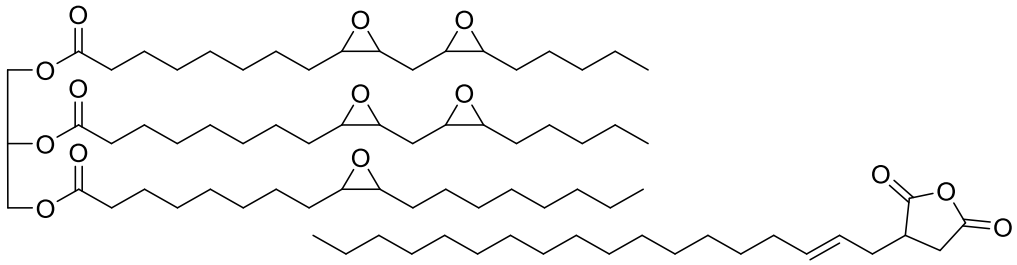

Epoxidised Grapeseed Oil and 2-Octadecenyl succinic anhydride (1:1). EGSO (6.0 g, 6.2 mmol) and 2-octadecenyl succinic anhydride (10.39 g, 29.6 mmol, 4.75 eq) and 4-methyl imidazole (0.1639 g, 1wt%) cured at 170 °C for 1 h forming a dark brown flexible polymer. IR (cm^{-1}): 2962 (ν_{CH_2/CH_3}), 1740 ($\nu_{C=O}$), 1468 (ν_{C-H}) 1150, 1091 (ν_{C-O}). Ultimate tensile stress – 0.559 MPa, Youngs modulus – 10.5 MPa, elongation at break – 6.71%, Crosslinking density – 21.68 $x10^4$ mol/cm^3, Sol content 10.49%, Swelling ratio – 1.9, Contact angle (θ_{water}) 109.5.

Epoxidised Grapeseed Oil and 2-Octadecenyl succinic anhydride (2:1). EGSO (9.0 g, 9.4 mmol) and 2-octadecenyl succinic anhydride (7.79 g, 22.2 mmol, 2.38 eq) and 4-methyl imidazole (0.1679 g, 1wt%) cured at 170 °C for 1 h forming a dark brown flexible polymer. IR (cm^{-1}): 2921, 2852 (ν_{CH_2/CH_3}), 1737 ($\nu_{C=O}$), 1461 (ν_{C-H}) 1089, 1020 (ν_{C-O}). Ultimate tensile stress – 0.317 MPa, Youngs modulus – 9.264 MPa, elongation at break – 3.68%, Crosslinking density – 22.24 $x10^4$ mol/cm^3, Sol content 7.63%, Swelling ratio – 1.9, Contact angle (θ_{water}) 105.5.

Epoxidised Grapeseed Oil and 2-Octadecenyl succinic anhydride (4.75:1). EGSO (12.0 g, 12.5 mmol) and 2-octadecenyl succinic anhydride (4.375 g, 12.5 mmol, 1 eq) and 4-methyl imidazole (0.1638 g, 1wt%) cured at 170 °C for 1 h forming a dark brown flexible polymer. IR (cm^{-1}): 2922, 2853 (ν_{CH_2/CH_3}), 1739 ($\nu_{C=O}$), 1461 (ν_{C-H}) 1149, 1087 (ν_{C-O}). Ultimate tensile stress – 0.132 MPa, Youngs modulus – 1.771 MPa, elongation at break – 7.26%, Crosslinking density – 4.81

x10^4 mol/cm^3, Sol content 42.68%, Swelling ratio – 3.01, Contact angle (θ_{water}) 111.0.

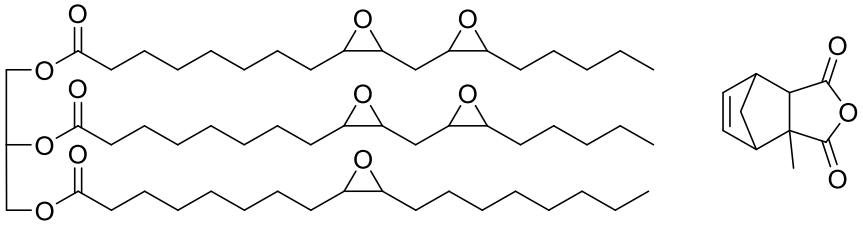

Epoxidised Grapeseed Oil and Methyl-5-norbornene-2,3-dicarboxylic anhydride (1:1). EGSO (9.0 g, 9.4 mmol) and methyl-5-norbornene-2,3-dicarboxylic anhydride (7.92 g, 44.4 mmol, 4.75 eq) and 4-methyl imidazole (0.1692 g, 1wt%) cured at 170 °C for 1 h forming a dark brown rigid polymer. IR (cm^{-1}): 2923, 2854 (ν_{CH_2/CH_3}), 1736 ($\nu_{C=O}$), 1457 (ν_{C-H}) 1154, 1093 (ν_{C-O}). Ultimate tensile stress – 6.491 MPa, Youngs modulus – 233.7 MPa, elongation at break – 5.23%, Crosslinking density – 22.23 x10^4 mol/cm^3, Sol content 4.27%, Swelling ratio – 1.69, Contact angle (θ_{water}) 107.6.

Epoxidised Grapeseed Oil and Methyl-5-norbornene-2,3-dicarboxylic anhydride (2:1). EGSO (11 g, 11.4 mmol) and methyl-5-norbornene-2,3-dicarboxylic anhydride (4.84 g, 27.2 mmol, 2.38 eq) and 4-methyl imidazole (0.1584 g, 1wt%) cured at 170 °C for 1 h forming a dark brown slightly flexible polymer. IR (cm^{-1}): 2924, 2854 (ν_{CH_2/CH_3}), 1737 ($\nu_{C=O}$), 1457 (ν_{C-H}) 1156, 1102 (ν_{C-O}). Ultimate tensile stress – 1.931 MPa, Youngs modulus – 30.81 MPa, elongation at break – 13.95%, Crosslinking density – 30.50 x10^4 mol/cm^3, Sol content 12.92%, Swelling ratio – 1.85, Contact angle (θ_{water}) 104.5.

Epoxidised Grapeseed Oil and Methyl-5-norbornene-2,3-dicarboxylic anhydride (4.75:1). EGSO (13.0 g 13.5 mmol) and methyl-5-norbornene-2,3-

dicarboxylic anhydride (2.41 g, 13.5 mmol, 1 eq) and 4-methyl imidazole (0.1541 g, 1wt%) cured at 170 °C for 1 h forming a dark brown flexible polymer. IR (cm^{-1}): 2922, 2853 (ν_{CH_2/CH_3}), 1736 ($\nu_{C=O}$), 1459 (ν_{C-H}) 1162, 1092 (ν_{C-O}). Ultimate tensile stress – 0.177 MPa, Youngs modulus – 1.218 MPa, elongation at break – 14.51%, Crosslinking density – 9.33 $x10^4$ mol/cm^3, Sol content 31.057%, Swelling ratio – 3.07, Contact angle (θ_{water}) 112.7.

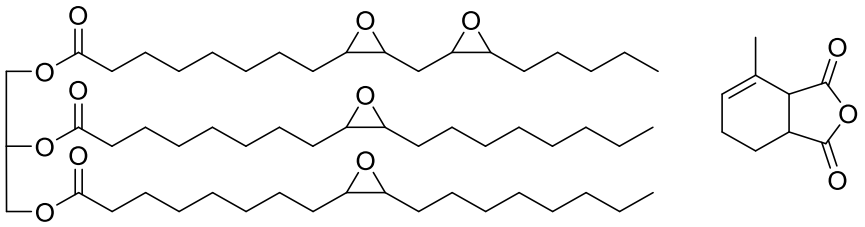

Epoxidised Rapeseed Oil and Aradur 917 (1:1). ERSO (10 g, 10.55 mmol) and Aradur 917 (6.67 g, 41.0 mmol, 3.8 eq) and 4-methyl imidazole (0.1667 g, 1wt%) cured at 170 °C for 1 h forming an orange-brown slightly flexible polymer. IR (cm^{-1}): 2924, 2854 (ν_{CH_2/CH_3}), 1730 ($\nu_{C=O}$), 1456 (ν_{C-H}) 1159, 1094 (ν_{C-O}). Ultimate tensile stress – 3.94 MPa, Youngs modulus – 122.1 MPa, elongation at break – 11.06%, Crosslinking density – 25.74 $x10^4$ mol/cm^3, Sol content 3.73%, Swelling ratio – 1.87, Contact angle (θ_{water}) 87.0.

Epoxidised Rapeseed Oil and Aradur 917 (2:1). ERSO (12 g, 12.66 mmol) and Aradur 917 (3.99 g, 24.0 mmol, 1.9 eq) and 4-methyl imidazole (0.160 g, 1wt%) cured at 170 °C for 1 h forming an orange-brown flexible polymer. IR (cm^{-1}): 2924, 2854 (ν_{CH_2/CH_3}), 1735 ($\nu_{C=O}$), 1457 (ν_{C-H}) 1156, 1097 (ν_{C-O}). Ultimate tensile stress – 0.306 MPa, Youngs modulus – 4.356 MPa, elongation at break – 8.54%, Crosslinking density – 16.38 $x10^4$ mol/cm^3, Sol content 18.28%, Swelling ratio – 2.03, Contact angle (θ_{water}) 102.3.

Epoxidised Rapeseed Oil and Aradur 917 (3.8:1). ERSO (13.5 g, 14.25 mmol) and Aradur 917 (2.37 g, 14.25 mmol, 1 eq) and 4-methyl imidazole (0.1590 g, 1wt%) cured at 170 °C for 1 h forming an orange-brown flexible polymer. IR (cm^{-1}): 2916, 2849 (ν_{CH_2/CH_3}), 1732 ($\nu_{C=O}$), 1472, 1464 (ν_{C-H}) 1092, 1021 (ν_{C-O}). Ultimate tensile stress – 0.045 MPa, Youngs modulus – 1.219 MPa, elongation at break – 3.9%, Crosslinking density – 9.21 $x10^4$ mol/cm^3, Sol content 38.44%, Swelling ratio – 2.46, Contact angle (θ_{water}) 110.1.

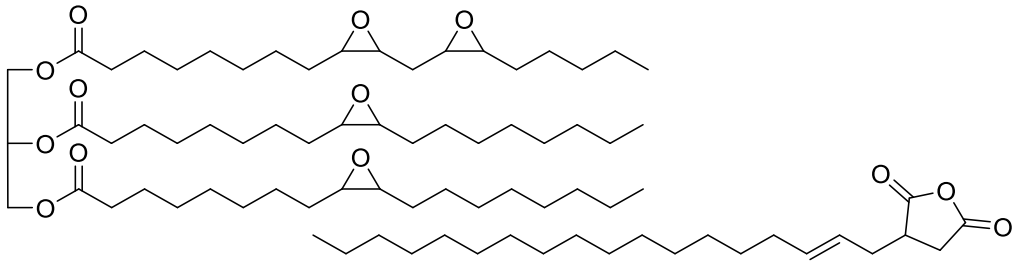

Epoxidised Rapeseed Oil and 2-Octadecenyl succinic anhydride (1:1). ERSO (7.0 g, 7.4 mmol) and 2-octadecenyl succinic anhydride (9.8 4g, 28.1 mmol, 3.8 eq) and 4-methyl imidazole (0.1684 g, 1wt%) cured at 170 °C for 1 h forming a dark brown flexible polymer. IR (cm^{-1}): 2920, 2851 (ν_{CH_2/CH_3}), 1733 ($\nu_{C=O}$), 1464 (ν_{C-H}) 1095, 1020 (ν_{C-O}). Ultimate tensile stress – 0.451 MPa, Youngs modulus – 4.421 MPa, elongation at break – 13.0%, Crosslinking density – 17.77 $x10^4$ mol/cm^3, Sol content 17.17%, Swelling ratio – 2.1, Contact angle (θ_{water}) 95.9.

Epoxidised Rapeseed Oil and 2-Octadecenyl succinic anhydride (2:1). ERSO (9.0 g, 9.5 mmol) and 2-octadecenyl succinic anhydride (6.327 g, 18.0 mmol, 1.9 eq) and 4-methyl imidazole (0.1533 g, 1wt%) cured at 170 °C for 1 h forming a dark brown flexible polymer. IR (cm^{-1}): 2918, 2850 (ν_{CH_2/CH_3}), 1733 ($\nu_{C=O}$), 1464 (ν_{C-H}) 1094, 1021 (ν_{C-O}). Ultimate tensile stress – 0.315 MPa, Youngs modulus – 4.239

MPa, elongation at break – 11.1%, Crosslinking density – 15.4 x10^4 mol/cm^3, Sol content 7.61%, Swelling ratio – 2.14, Contact angle (θ_{water}) 104.1.

Epoxidised Rapeseed Oil and 2-Octadecenyl succinic anhydride (3.8:1). ERSO (12 g, 12.66 mmol) and 2-octadecenyl succinic anhydride (4.44 g, 12.66 mmol, 1 eq) and 4-methyl imidazole (0.1644 g, 1wt%) cured at 170 °C for 1 h forming a dark brown flexible polymer. IR (cm^{-1}): 2916, 2849 (ν_{CH_2/CH_3}), 1732 ($\nu_{C=O}$), 1464 (ν_{C-H}) 1170, 1094 (ν_{C-O}). Ultimate tensile stress – 0.103 MPa, Youngs modulus – 0.765 MPa, elongation at break – 15.8%, Crosslinking density – 7.37 x10^4 mol/cm^3, Sol content 26.28%, Swelling ratio – 2.71, Contact angle (θ_{water}) 109.5.

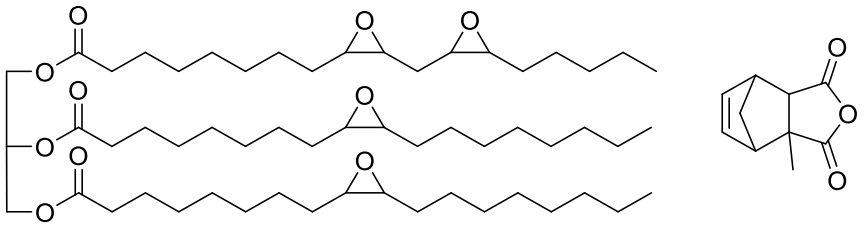

Epoxidised Rapeseed Oil and Methyl-5-norbornene-2,3-dicarboxylic anhydride (1:1). ERSO (9.5 g, 10 mmol) and methyl-5-norbornene-2,3-dicarboxylic anhydride (6.79 g, 38.1 mmol, 3.8 eq) and 4-methyl imidazole (0.1629 g, 1wt%) cured at 170 °C for 1 h forming a dark brown rigid polymer. IR (cm^{-1}): 2920, 2852 (ν_{CH_2/CH_3}), 1731 ($\nu_{C=O}$), 1457 (ν_{C-H}) 1168, 1107 (ν_{C-O}). Ultimate tensile stress – 2.514 MPa, Youngs modulus – 29.74 MPa, elongation at break – 29.2%, Crosslinking density – 17.36 x10^4 mol/cm^3, Sol content 20.95%, Swelling ratio – 1.73, Contact angle (θ_{water}) 80.1.

Epoxidised Rapeseed Oil and Methyl-5-norbornene-2,3-dicarboxylic anhydride (2:1). ERSO (11.5 g, 12.1 mmol) and methyl-5-norbornene-2,3-dicarboxylic anhydride (4.11 g, 23 mmol, 1.9 eq) and 4-methyl imidazole (0.1561 g, 1wt%) cured

at 170 °C for 1 h forming a dark brown flexible polymer. IR (cm^{-1}): 2917, 2850 (ν_{CH_2/CH_3}), 1733 ($\nu_{C=O}$), 1463 (ν_{C-H}) 1079, 1019 (ν_{C-O}). Ultimate tensile stress – 0.507 MPa, Youngs modulus – 39.99 MPa, elongation at break – 1.71%, Crosslinking density – 9.58 $x10^4$ mol/cm^3, Sol content 25.57%, Swelling ratio – 2.17, Contact angle (θ_{water}) 100.7.

Epoxidised Rapeseed Oil and Methyl-5-norbornene-2,3-dicarboxylic anhydride (3.8:1). ERSO (13 g, 13.7 mmol) and methyl-5-norbornene-2,3-dicarboxylic anhydride (2.44 g, 13.7 mmol, 1 eq) and 4-methyl imidazole (0.1544 g, 1wt%) cured at 170 °C for 1 h forming a dark brown flexible polymer. IR (cm^{-1}): 2918, 2850 (ν_{CH_2/CH_3}), 1734 ($\nu_{C=O}$), 1464 (ν_{C-H}) 1082, 1019 (ν_{C-O}). Ultimate tensile stress – 0.027 MPa, Youngs modulus – 0.641 MPa, elongation at break – 4.96%, Crosslinking density – 3.72 $x10^4$ mol/cm^3, Sol content 30.27%, Swelling ratio – 2.93, Contact angle (θ_{water}) 108.1.

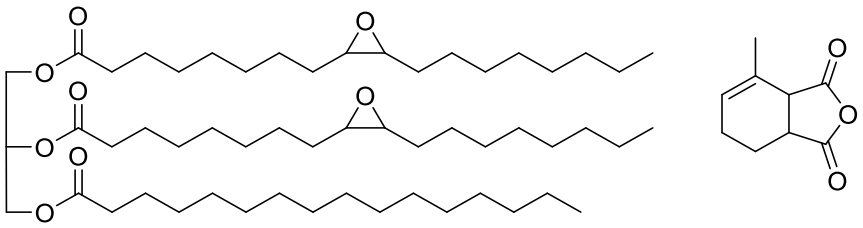

Epoxidised Palm Oil and Aradur 917 (1:1). EPO (11.5 g, 12.9 mmol) and Aradur 917 (3.86 g, 23.2 mmol, 1.8 eq) and 4-methyl imidazole (0.1536 g, 1wt%) cured at 170 °C for 1 h forming a yellow soft polymer. IR (cm^{-1}): 2919, 2851 (ν_{CH_2/CH_3}), 1734 ($\nu_{C=O}$), 1456 (ν_{C-H}) 1259, 1069, 1018 (ν_{C-O}). Ultimate tensile stress – 1.51 MPa, Youngs modulus – 0.465 MPa, elongation at break – 20.6%, Crosslinking density – 2.69 $x10^4$ mol/cm^3, Sol content 22.25%, Swelling ratio – 3.97, Contact angle (θ_{water}) 113.2.

Epoxidised Palm Oil and Aradur 917 (2:1). EPO (13 g, 14.6 mmol) and Aradur 917 (2.181 g, 13.1 mmol, 0.9 eq) and 4-methyl imidazole (0.1518 g, 1wt%) cured at 170 °C for 1 h forming a yellow soft polymer. IR (cm^{-1}): 2920, 2851 (ν_{CH_2/CH_3}), 1736 ($\nu_{C=O}$), 1457 (ν_{C-H}) 1259, 1075, 1020 (ν_{C-O}). Ultimate tensile stress – 0.047 MPa, Youngs modulus – 0.033 MPa, elongation at break – 23.0%, Crosslinking density – 0.477 $x10^4$ mol/cm^3, Sol content 54.14%, Swelling ratio – 7.27, Contact angle (θ_{water}) 117.2.

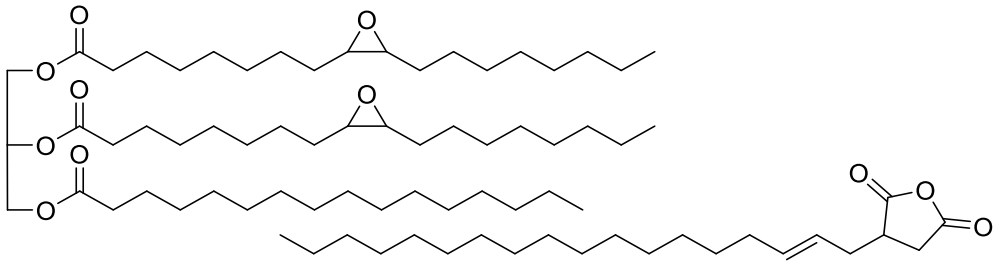

Epoxidised Palm Oil and 2-Octadecenyl succinic anhydride (1:1). EPO (9.0 g, 10.1 mmol) and 2-octadecenyl succinic anhydride (6.37 g, 18.2 mmol, 1.8 eq) and 4-methyl imidazole (0.1537 g, 1wt%) cured at 170 °C for 1 h forming a dark brown flexible polymer. IR (cm^{-1}): 2921, 2852 (ν_{CH_2/CH_3}), 1736 ($\nu_{C=O}$), 1459 (ν_{C-H}) 1260, 1084, 1022 (ν_{C-O}). Ultimate tensile stress – 0.096 MPa, Youngs modulus – 0.741 MPa, elongation at break – 12.3%, Crosslinking density – 4.49 $x10^4$ mol/cm^3, Sol content 14.1%, Swelling ratio – 3.27, Contact angle (θ_{water}) 109.4

Epoxidised Palm Oil and 2-Octadecenyl succinic anhydride (2:1). EPO (11.5 g, 12.9 mmol) and 2-octadecenyl succinic anhydride (4.07 g, 11.6 mmol, 0.9 eq) and 4-methyl imidazole (0.1557 g, 1wt%) cured at 170 °C for 1 h forming a dark brown flexible polymer. IR (cm^{-1}): 2921, 2852 (ν_{CH_2/CH_3}), 1739 ($\nu_{C=O}$), 14564 (ν_{C-H}) 1260, 1089, 1022 (ν_{C-O}). Ultimate tensile stress – 0.043 MPa, Youngs modulus – 0.101

MPa, elongation at break – 36.3%, Crosslinking density – 3.11 x10^4 mol/cm^3, Sol content 39.87%, Swelling ratio – 3.83, Contact angle (θ_{water}) 112.8.

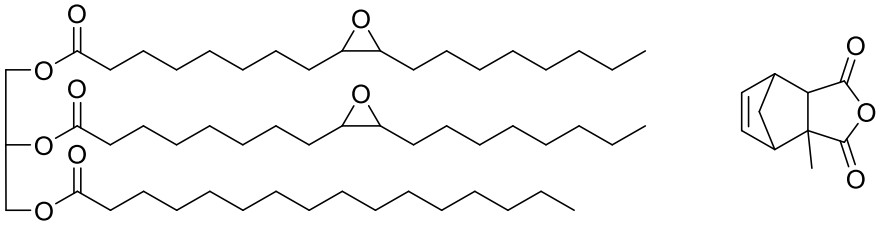

Epoxidised Palm Oil and Methyl-5-norbornene-2,3-dicarboxylic anhydride (1:1). EPO (11.25 g, 12.6 mmol) and methyl-5-norbornene-2,3-dicarboxylic anhydride (4.04 g, 22.7 mmol, 1.8 eq) and 4-methyl imidazole (0.1530 g, 1wt%) cured at 170 °C for 1 h forming a dark brown soft polymer. IR (cm^{-1}): 2919, 2851 (ν_{CH_2/CH_3}), 1737 ($\nu_{C=O}$), 1457 (ν_{C-H}) 1259, 1081, 1020 (ν_{C-O}). Ultimate tensile stress – 0.173 MPa, Youngs modulus – 0.526 MPa, elongation at break – 14.3%, Crosslinking density – 1.62 x10^4 mol/cm^3, Sol content 21.93%, Swelling ratio – 3.76, Contact angle (θ_{water}) 113.3.

Epoxidised Palm Oil and Methyl-5-norbornene-2,3-dicarboxylic anhydride (2:1). EPO (13 g, 14.6 mmol) and methyl-5-norbornene-2,3-dicarboxylic anhydride (2.34 g, 13.1 mmol, 0.9 eq) and 4-methyl imidazole (0.1534 g, 1wt%) cured at 170 °C for 1 h forming a dark brown soft polymer. IR (cm^{-1}): 2919, 2851 (ν_{CH_2/CH_3}), 1738 ($\nu_{C=O}$), 1457 (ν_{C-H}) 1259, 1064, 1016 (ν_{C-O}). Ultimate tensile stress – 0.024 MPa, Youngs modulus – 0.024MPa, elongation at break – 18.0%, Crosslinking density – 0.395 x10^4 mol/cm^3, Sol content 66.75%, Swelling ratio – 8.63, Contact angle (θ_{water}) 112.2.

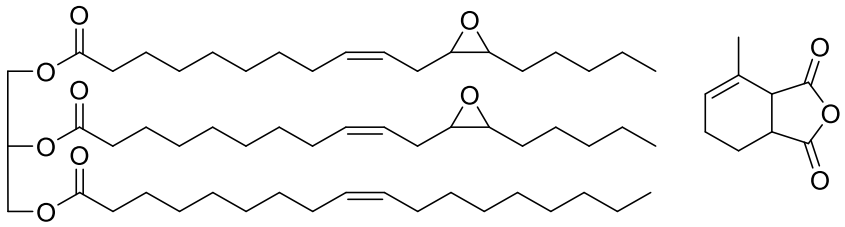

Euphorbia Oil and Aradur 917 (1:1). EuO (12 g, 13.1 mmol) and Aradur 917 (3.49 g, 21 mmol, 1.6 eq) and 4-methyl imidazole (0.1549 g, 1wt%) cured at 170 °C for 1 h forming a yellow soft polymer. IR (cm^{-1}): 2923, 2853 (ν_{CH_2/CH_3}), 1735 ($\nu_{C=O}$), 1456 (ν_{C-H}) 1092, 1020 (ν_{C-O}). Ultimate tensile stress – 0.161 MPa, Youngs modulus – 0.957 MPa, elongation at break – 44.5%, Crosslinking density – 5.22 $x10^4$ mol/cm^3, Sol content 15.88%, Swelling ratio – 3.37, Contact angle (θ_{water}) 109.0.

Euphorbia Oil and Aradur 917 (2:1). EuO (14 g, 15.3 mmol) and Aradur 917 (2.038 g, 12.2 mmol, 0.8 eq) and 4-methyl imidazole (0.1603 g, 1wt%) cured at 170 °C for 1 h forming a yellow soft polymer. IR (cm^{-1}): 2922, 2854 (ν_{CH_2/CH_3}), 1738 ($\nu_{C=O}$), 1456 (ν_{C-H}) 1161, 1089 (ν_{C-O}). Ultimate tensile stress – 0.074 MPa, Youngs modulus – 0.387 MPa, elongation at break – 104.9%, Crosslinking density – 2.37 $x10^4$ mol/cm^3, Sol content 20.58%, Swelling ratio – 4.84, Contact angle (θ_{water}) 110.1.

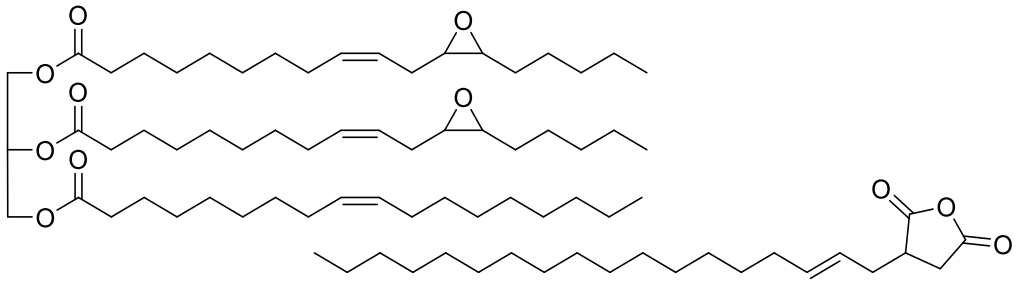

Euphorbia Oil and 2-Octadecenyl succinic anhydride (1:1). EuO (10 g, 10.9 mmol) and 2-octadecenyl succinic anhydride (6.14 g, 17.5 mmol, 1.6 eq) and 4-methyl imidazole (0.1614 g, 1wt%) cured at 170 °C for 1 h forming a dark brown

flexible polymer. IR (cm^{-1}): 2921, 2852 (ν_{CH_2/CH_3}), 1737 ($\nu_{C=O}$), 1463 (ν_{C-H}) 1093, 1022 (ν_{C-O}). Ultimate tensile stress – 0.115 MPa, Youngs modulus – 1.117 MPa, elongation at break – 14.1%, Crosslinking density – 4.75 $x10^4$ mol/cm^3, Sol content 9.9%, Swelling ratio – 9.85, Contact angle (θ_{water}) 100.4

Euphorbia Oil and 2-Octadecenyl succinic anhydride (2:1). EuO (12.5 g, 13.7 mmol) and 2-octadecenyl succinic anhydride (3.84 g, 11 mmol, 0.8 eq) and 4-methyl imidazole (0.1634 g, 1wt%) cured at 170 °C for 1 h forming a dark brown flexible polymer. IR (cm^{-1}): 2922, 2852 (ν_{CH_2/CH_3}), 1738 ($\nu_{C=O}$), 1459 (ν_{C-H}) 1086, 1020 (ν_{C-O}). Ultimate tensile stress – 0.084 MPa, Youngs modulus – 0.30 MPa, elongation at break – 35.5%, Crosslinking density – 2.36 $x10^4$ mol/cm^3, Sol content 25.13%, Swelling ratio – 4.53, Contact angle (θ_{water}) 97.5.

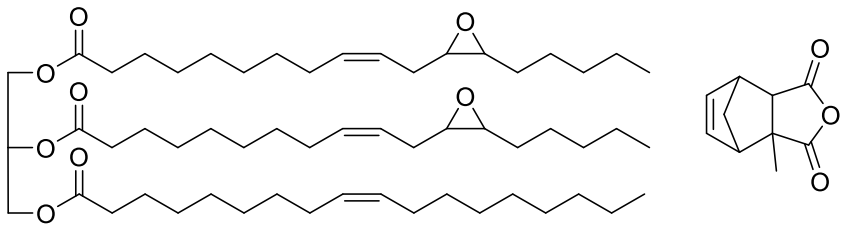

Euphorbia Oil and Methyl-5-norbornene-2,3-dicarboxylic anhydride (1:1). EuO (12 g, 13.1 mmol) and methyl-5-norbornene-2,3-dicarboxylic anhydride (3.74 g, 21 mmol, 1.6 eq) and 4-methyl imidazole (0.1574 g, 1wt%) cured at 170 °C for 1 h forming a dark brown soft polymer. IR (cm^{-1}): 2925, 2855 (ν_{CH_2/CH_3}), 1736 ($\nu_{C=O}$), 1460 (ν_{C-H}) 1097, 1023 (ν_{C-O}). Ultimate tensile stress – 0.372 MPa, Youngs modulus – 0.2.94 MPa, elongation at break – 34.1%, Crosslinking density – 5.63 $x10^4$ mol/cm^3, Sol content 34.75%, Swelling ratio – 4.89, Contact angle (θ_{water}) 108.9.

Euphorbia Oil and Methyl-5-norbornene-2,3-dicarboxylic anhydride (2:1). EuO (13 g, 14.2 mmol) and methyl-5-norbornene-2,3-dicarboxylic anhydride (2.03 g,

11.4 mmol, 0.8 eq) and 4-methyl imidazole (0.1503 g, 1wt%) cured at 170 °C for 1 h forming a dark brown soft polymer. IR (cm^{-1}): 2925, 2854 (ν_{CH_2/CH_3}), 1736 ($\nu_{C=O}$), 1461 (ν_{C-H}) 1063, 1090 (ν_{C-O}). Ultimate tensile stress – 0.113 MPa, Youngs modulus – 0.778 MPa, elongation at break – 113.5%, Crosslinking density – 3.28 $x10^4$ mol/cm^3, Sol content 21.58%, Swelling ratio – 3.89, Contact angle (θ_{water}) 109.0.

6.7 Experimental data for Modifications to Plant oil Polyesters (Chapter 5).

6.7.1 Increased Hardener Ratio

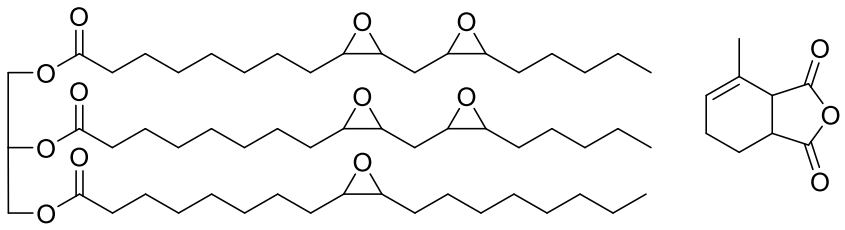

Epoxidised Grapeseed Oil and Aradur 917 (0.8:1). EGSO (8.0 g, 8.3 mmol) and Aradur 917 (8.21 g, 49.4 mmol, 5.94 eq) and 4-methyl imidazole (0.1621 g, 1wt%) cured at 170 °C for 1 h forming an orange rigid polymer. Ultimate tensile stress – 27.46 MPa, Youngs modulus – 1261 MPa, elongation at break – 4.36 %, Contact angle 116.2 (θ_{water})

Epoxidised Grapeseed Oil and Aradur 917 (0.5:1). EGSO (6.0 g, 6.24 mmol) and Aradur 917 (9.85 g, 59.3 mmol, 9.5 eq) and 4-methyl imidazole (0.1585 g, 1wt%) cured at 170 °C for 1 h forming a brittle yellow polymer. Ultimate tensile stress – 3.46 MPa, Youngs modulus – 802 MPa, elongation at break – 0.59 %, Contact angle 110.4 (θ_{water}) .

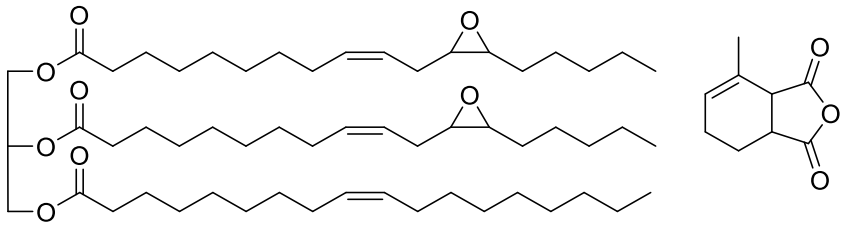

Euphorbia Oil and Aradur 917 (0.8:1). EuO (11.5 g, 12.6 mmol) and Aradur 917 (4.18 g, 25.2 mmol, 2 eq) and 4-methyl imidazole (0.1568 g, 1wt%) cured at 170 °C for 1 h forming an yellow slightly flexible polymer. Ultimate tensile stress – 0.186 MPa, Youngs modulus – 0.624 MPa, elongation at break – 37.57 %, Contact angle 120.7 (θ_{water})

Euphorbia Oil and Aradur 917 (0.5:1). EuO (10.0 g, 10.95 mmol) and Aradur 917 (5.82 g, 35.0 mmol, 3.2 eq) and 4-methyl imidazole (0.1582 g, 1wt%) cured at 170 °C for 1 h forming an yellow brittle polymer Tensile data not recorded due to lack of structural integrity. Contact angle 114.8 (θ_{water})

6.7.2 Addition of Silica Nanoparticles

Synthesis of Silica Particles.

The particles used in this section were synthesised by another party and were used as received. Ellipsoidal precipitated calcium carbonate was suspended in a solution of ethanol and ammonium hydroxide, to this tetraethyl orthosilicate (TEOS) was added over 12 h and the mixture allowed to react for a total of 24 h. The particles were washed by centrifugation and re-suspension in clean ethanol. To remove the calcium carbonate the particles were immersed in 0.5M acetic acid which produced hollow ellipsoidal silica shells. For the alkyl functionalised silica, a mixture of TEOS and 1,8-bis (triethoxysilyl) octane in a 70:30 ratio was used. The silica particles were dried overnight in a vacuum oven and stored in a drying oven until required.

General Procedure for Addition of Silica Particles

The epoxidised oil (ESBO or EGSO) and Aradur 917 were mixed in a raito of 1 mol epoxide group to 1 mol anhydride. The silica (or calcium) particles were added according at the vol % required and the mixture stirred under vacuum overnight. Imidazole catalyst was added (1wt%) and the mixture stirred under vacuum for 15 min then poured into a silicone 'dog-bone' mould and samples were cured at 170 °C for 1 h.

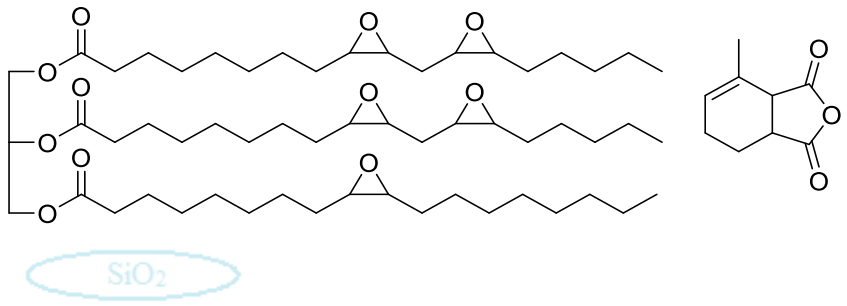

Epoxidised Grapeseed Oil and Aradur 917 (1:1) with hollow silica shells (1 vol%). EGSO (9.0 g, 9.36 mmol), Aradur 917 (7.39 g, 44.5 mmol, 4.75 eq) and hollow silica particles (0.15 mL, 1 vol%) stirred under vacuum. 4-methyl imidazole added (0.164 g, 1 wt%) and sample cured at 170 °C for 1 h in silicone mould forming a golden brown rigid polymer. Ultimate tensile stress – 10.45 MPa, Youngs modulus – 980.5 MPa, elongation at break – 1.01%.

Epoxidised Grapeseed Oil and Aradur 917 (1:1) with hollow silica shells (2 vol%). EGSO (9.0 g, 9.36 mmol), Aradur 917 (7.39 g, 44.5 mmol, 4.75 eq) and hollow silica particles (0.3 mL, 2 vol%) stirred under vacuum. 4-methyl imidazole added (0.164 g, 1 wt%) and sample cured at 170 °C for 1 h in silicone mould forming a golden brown rigid polymer. Ultimate tensile stress – 10.77 MPa, Youngs modulus – 985.6 MPa, elongation at break – 1.03%.

Epoxidised Grapeseed Oil and Aradur 917 (1:1) with hollow silica shells (5 vol%). EGSO (9.0 g, 9.36 mmol), Aradur 917 (7.39 g, 44.5 mmol, 4.75 eq) and hollow silica particles (0.75 mL, 5 vol%) stirred under vacuum. 4-methyl imidazole added (0.164 g, 1 wt%) and sample cured at 170 °C for 1 h in silicone mould forming a golden brown rigid polymer. Ultimate tensile stress – 8.99 MPa, Youngs modulus – 1001 MPa, elongation at break – 0.82%.

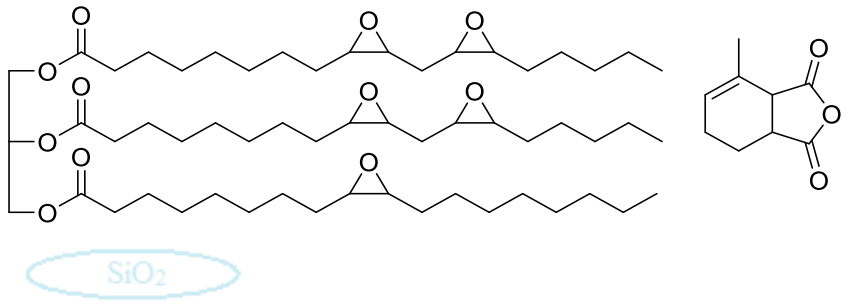

Epoxidised Soybean Oil and Aradur 917 (1:1) with hollow silica shells (1 vol%). ESBO (9 g, 9.36 mmol), Aradur 917 (6.84 g, 41.2 mmol, 4.4 eq) and hollow silica particles (0.16 mL, 1 vol%) stirred under vacuum. 4-methyl imidazole added (0.158 g, 1 wt%) and sample cured at 170 °C for 1 h in silicone mould forming a golden brown rigid polymer. Ultimate tensile stress – 7.634 MPa, Youngs modulus – 619.7 MPa, elongation at break – 1.13%.

Epoxidised Soybean Oil and Aradur 917 (1:1) with hollow silica shells (2 vol%). ESBO (9 g, 9.36 mmol), Aradur 917 (6.84 g, 41.2 mmol, 4.4 eq) and hollow silica particles (0.32 mL, 1 vol%) stirred under vacuum. 4-methyl imidazole added (0.158 g, 1 wt%) and sample cured at 170 °C for 1 h in silicone mould forming a golden brown rigid polymer. Ultimate tensile stress – 6.743 MPa, Youngs modulus – 376.4 MPa, elongation at break – 1.83%.

Epoxidised Soybean Oil and Aradur 917 (1:1) with hollow silica shells (5 vol%). ESBO (9 g, 9.36 mmol), Aradur 917 (6.84 g, 41.2 mmol, 4.4 eq) and hollow silica particles (0.80 mL, 5 vol%) stirred under vacuum. 4-methyl imidazole added (0.158 g, 1 wt%) and sample cured at 170 °C for 1 h in silicone mould forming a golden brown rigid polymer. Ultimate tensile stress – 6.012 MPa, Youngs modulus – 632.3 MPa, elongation at break – 0.96 %.

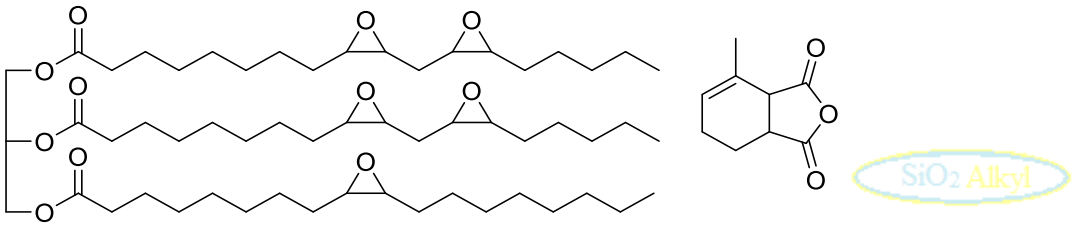

Epoxidised Grapeseed Oil and Aradur 917 (1:1) with hollow silica shells – Octyl functionalised (1 vol%). EGSO (9.0 g, 9.36 mmol), Aradur 917 (7.39 g, 44.5 mmol, 4.75 eq) and hollow silica particles (0.15 mL, 1 vol%) stirred under vacuum. 4-methyl imidazole added (0.164 g, 1 wt%) and sample cured at 170 °C for 1 h in silicone mould forming a golden brown rigid polymer. Ultimate tensile stress – 5.752 MPa, Youngs modulus – 517.0 MPa, elongation at break – 0.98%.

Epoxidised Grapeseed Oil and Aradur 917 (1:1) with hollow silica shells – Octyl functionalised (2 vol%). EGSO (9.0 g, 9.36 mmol), Aradur 917 (7.39 g, 44.5 mmol, 4.75 eq) and hollow silica particles (0.3 mL, 2 vol%) stirred under vacuum. 4-methyl imidazole added (0.164 g, 1 wt%) and sample cured at 170 °C for 1 h in silicone mould forming a golden brown rigid polymer. Ultimate tensile stress – 5.73 MPa, Youngs modulus – 717.1 MPa, elongation at break – 0.63%.

Epoxidised Grapeseed Oil and Aradur 917 (1:1) with hollow silica shells – Octyl functionalised (5 vol%). EGSO (9.0 g, 9.36 mmol), Aradur 917 (7.39 g, 44.5 mmol,

4.75 eq) and hollow silica particles (0.75 mL, 5 vol%) stirred under vacuum. 4-methyl imidazole added (0.164 g, 1 wt%) and sample cured at 170 °C for 1 h in silicone mould forming a golden brown rigid polymer. Ultimate tensile stress – 12.82 MPa, Youngs modulus – 1134 MPa, elongation at break – 1.08%.

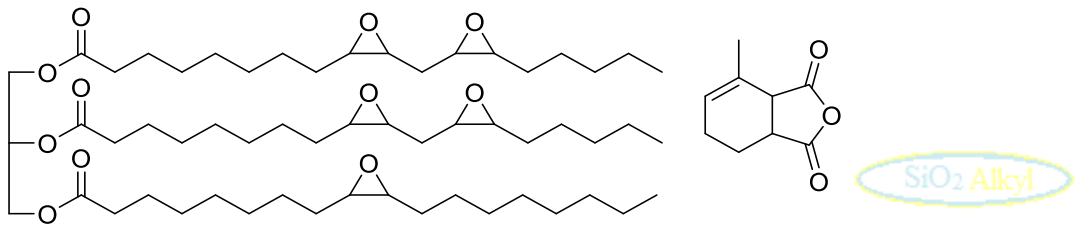

Epoxidised Soybean Oil and Aradur 917 (1:1) with hollow silica shells – octyl functionalised (1 vol%). ESBO (9 g, 9.36 mmol), Aradur 917 (6.84 g, 41.2 mmol, 4.4 eq) and hollow silica particles (0.16 mL, 1 vol%) stirred under vacuum. 4-methyl imidazole added (0.158 g, 1 wt%) and sample cured at 170 °C for 1 h in silicone mould forming a golden brown rigid polymer. Ultimate tensile stress – 7.919 MPa, Youngs modulus – 513.4 MPa, elongation at break – 1.62%.

Epoxidised Soybean Oil and Aradur 917 (1:1) with hollow silica shells – octyl functionalised (2 vol%). ESBO (9 g, 9.36 mmol), Aradur 917 (6.84 g, 41.2 mmol, 4.4 eq) and hollow silica particles (0.32 mL, 2 vol%) stirred under vacuum. 4-methyl imidazole added (0.158 g, 1 wt%) and sample cured at 170 °C for 1 h in silicone mould forming a golden brown rigid polymer. Ultimate tensile stress – 2.959 MPa, Youngs modulus – 321.4 MPa, elongation at break – 0.77%.

Epoxidised Soybean Oil and Aradur 917 (1:1) with hollow silica shells – octyl functionalised (5 vol%). ESBO (9 g, 9.36 mmol), Aradur 917 (6.84 g, 41.2 mmol, 4.4 eq) and hollow silica particles (0.80 mL, 5 vol%) stirred under vacuum. 4-methyl imidazole added (0.158 g, 1 wt%) and sample cured at 170 °C for 1 h in silicone

mould forming a golden brown rigid polymer. Ultimate tensile stress – 5.163 MPa, Youngs modulus – 130.9 MPa, elongation at break – 4.98%.

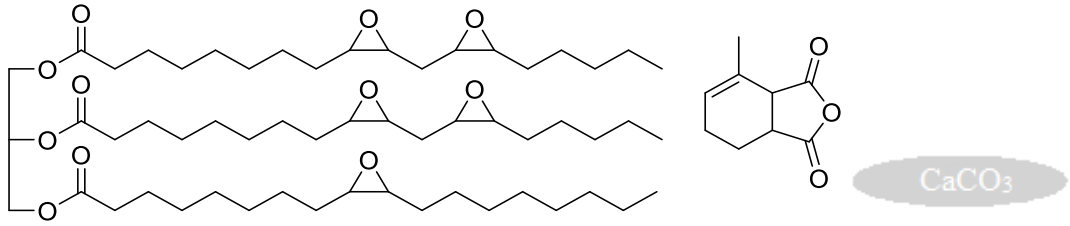

Epoxidised Grapeseed Oil and Aradur 917 (1:1) with solid calcium carbonate precipitate (1 vol%). EGSO (9.0 g, 9.36 mmol), Aradur 917 (7.39 g, 44.5 mmol, 4.75 eq) and calcium particles (0.15 mL, 1 vol%) stirred under vacuum. 4-methyl imidazole added (0.164 g, 1 wt%) and sample cured at 170 °C for 1 h in silicone mould forming a golden brown rigid polymer. Ultimate tensile stress – 7.147 MPa, Youngs modulus – 687.7 MPa, elongation at break – 0.92%.

Epoxidised Grapeseed Oil and Aradur 917 (1:1) with solid calcium carbonate precipitate (2 vol%). EGSO (9.0 g, 9.36 mmol), Aradur 917 (7.39 g, 44.5 mmol, 4.75 eq) and calcium particles (0.30 mL, 2 vol%) stirred under vacuum. 4-methyl imidazole added (0.164 g, 1 wt%) and sample cured at 170 °C for 1 h in silicone mould forming a golden brown rigid polymer. Ultimate tensile stress – 9.913 MPa, Youngs modulus – 861.7 MPa, elongation at break – 1.10%.

Epoxidised Grapeseed Oil and Aradur 917 (1:1) with solid calcium carbonate precipitate (5 vol%). EGSO (9.0 g, 9.36 mmol), Aradur 917 (7.39 g, 44.5 mmol, 4.75 eq) and calcium particles (0.75 mL, 5 vol%) stirred under vacuum. 4-methyl imidazole added (0.164 g, 1 wt%) and sample cured at 170 °C for 1 h in silicone mould forming a golden brown rigid polymer. Ultimate tensile stress – 10.37 MPa, Youngs modulus – 1064 MPa, elongation at break – 0.90%.

6.7.3 Nanocomposites with Polyaromatic Hydrocarbon.

Synthesis of Polyaromatic Hydrocarbon (PAH)

The sample of graphene was provided. It was synthesised from pyrene and glycidol in an 80% sulphuric acid solution at 100 °C under a nitrogen atmosphere. This produced a polyaromatic hydrocarbon 5 to 10 fused rings in size.

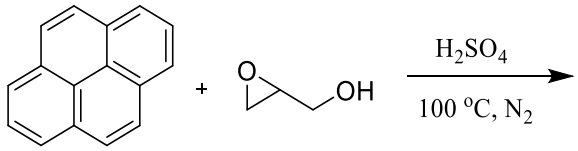

Epoxidised Grapeseed Oil and Aradur 917 (1:1) with 1wt% PAH. EGSO (9.0 g, 9.4 mmol), Aradur 917 (7.39 g, 44.5 mmol, 4.75 eq), graphene oxide (0.164 g, 1wt%) and 4-methyl imidazole (0.1639 g, 1wt%) cured at 170 °C for 1 h forming an dark brown brittle polymer. Ultimate tensile stress – 5.63 MPa, Youngs modulus – 191 MPa, elongation at break – 3.10%.

Epoxidised Grapeseed Oil and Aradur 917 (1:1) with 2wt% PAH. EGSO (9.0 g, 9.4 mmol), Aradur 917 (7.39 g, 44.5 mmol, 4.75 eq), graphene oxide (0.328 g, 2wt%) and 4-methyl imidazole (0.1639 g, 1wt%) cured at 170 °C for 1 h forming an dark brown brittle polymer. Ultimate tensile stress – 3.92 MPa, Youngs modulus – 337 MPa, elongation at break – 1.01%.

Epoxidised Grapeseed Oil and Aradur 917 (1:1) with 1wt% PAH. EGSO (9.0 g, 9.4 mmol), Aradur 917 (7.39 g, 44.5 mmol, 4.75 eq), graphene oxide (0.82 g, 5wt%) and 4-methyl imidazole (0.1639 g, 1wt%) cured at 170 °C for 1 h forming an dark brown brittle polymer. Ultimate tensile stress – 1.53 MPa, Youngs modulus – 55.9 MPa, elongation at break – 8.34%.

6.7.4 Copolymerisation with Styrene Oxide

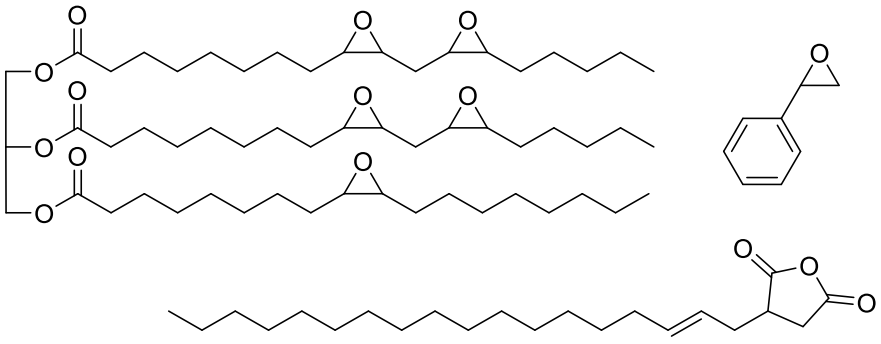

Epoxidised Grapeseed Oil and Styrene oxide (1:0) with 2-Octadecenyl succinic anhydride. EGSO (5.49 g, 5.7 mmol, 0.8 eq), and 2-Octadecenyl succinic anhydride (9.51 g, 27.1 mmol, 4.75 eq) and 4-methyl imidazole (0.150 g, 1wt%) were cured at 80 °C for 16 h. The resulting polymer was golden brown and flexible. Ultimate tensile stress – 0.557 MPa, Youngs modulus – 7.15 MPa, elongation at break – 9.343%, Crosslinking density – 21.68 $x10^4$ mol/cm^3, Sol content 11.59%, Swelling ratio – 2.17, Contact angle (θ_{water}) 93.0.

Epoxidised Grapeseed Oil and Styrene oxide (0.8:0.2) with 2-Octadecenyl succinic anhydride. EGSO (5.30 g, 5.5 mmol, 0.8 eq), styrene oxide (0.166 g, 1.4 mmol, 0.2 eq) and 2-Octadecenyl succinic anhydride (9.67 g, 27.6 mmol, 4 eq) and 4-methyl imidazole (0.1513 g, 1wt%) were cured at 80 °C for 16 h. The resulting polymer was golden brown and flexible. Ultimate tensile stress – 1.457 MPa, Youngs modulus – 10.65 MPa, elongation at break – 18.33%, Crosslinking density – 25.13 $x10^4$ mol/cm^3, Sol content 15.54%, Swelling ratio – 2.6, Contact angle (θ_{water}) 90.9.

Epoxidised Grapeseed Oil and Styrene oxide (0.6:0.4) with 2-Octadecenyl succinic anhydride. EGSO (4.93 g, 5.1 mmol, 0.6 eq), styrene oxide (0.411 g, 3.4 mmol, 0.4 eq) and 2-Octadecenyl succinic anhydride (9.735 g, 27.8 mmol, 3.25 eq)

and 4-methyl imidazole (0.1507 g, 1wt%) were cured at 80 °C for 16 h. The polymer was golden brown and flexible. Ultimate tensile stress – 0.931 MPa, Youngs modulus – 5.48 MPa, elongation at break – 22.5%, Crosslinking density – 11.58 $x10^4$ mol/cm^3, Sol content 19.94%, Swelling ratio – 2.8, Contact angle (θ_{water}) 97.4.

Epoxidised Grapeseed Oil and Styrene oxide (0.4:0.6) with 2-Octadecenyl succinic anhydride. EGSO (4.37 g, 4.5 mmol, 0.4 eq), styrene oxide (0.819 g, 6.8 mmol, 0.6 eq) and 2-Octadecenyl succinic anhydride (9.937 g, 28.3 mmol, 2.5 eq) and 4-methyl imidazole (0.1515 g, 1wt%) were cured at 80 °C for 16 h. The polymer was golden brown and flexible. Ultimate tensile stress – 0.949 MPa, Youngs modulus – 6.04 MPa, elongation at break – 21.85%, Crosslinking density – 10.39 $x10^4$ mol/cm^3, Sol content 22.24%, Swelling ratio – 2.95, Contact angle (θ_{water}) 104.0.

Epoxidised Grapeseed Oil and Styrene oxide (0.2:0.8) with 2-Octadecenyl succinic anhydride. EGSO (3.205g, 3.33 mmol, 0.2 eq), styrene oxide (1.602 g, 13.33 mmol, 0.8 eq) and 2-Octadecenyl succinic anhydride (10.223 g, 29.2 mmol, 1.75 eq) and 4-methyl imidazole (0.1503 g, 1wt%) were cured at 80 °C for 16 h. The resulting polymer was golden brown and flexible. Ultimate tensile stress – 0.431 MPa, Youngs modulus – 1.54 MPa, elongation at break – 40.65%, Crosslinking density – 8.21 $x10^4$ mol/cm^3, Sol content 36.28%, Swelling ratio – 3.52, Contact angle (θ_{water}) 112.2.

Epoxidised Grapeseed Oil and Styrene oxide (0:1.0) with 2-Octadecenyl succinic anhydride. Styrene oxide (0.3876 g, 3.23 mmol, 1 eq) and 2-Octadecenyl succinic anhydride (1.130 g, 3.23 mmol, 1 eq) and 4-methyl imidazole (0.0152 g,

1wt%) were cured at 80 °C for 16 h. This formed a sticky oil unsuitable for tensile testing.

6.7.5 Grapeseed and Euphorbia Blends

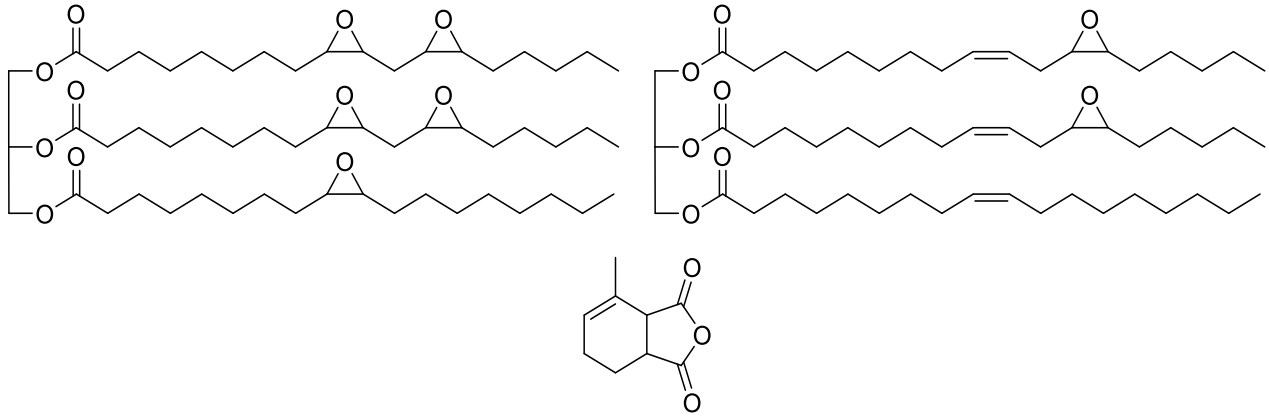

Epoxidised Grapeseed Oil and Euphorbia Oil (0.8:0.2) with Aradur 917. EGSO (7.325 g, 7.62 mmol, 0.8 eq), EuO (1.74 g, 1.9 mmol, 0.2 eq), Aradur 917 (6.52 g, 39.2 mmol, 4.12 eq) and 4-methyl imidazole (0.1558 g, 1wt%) were cured at 170 °C for 1 h to yield a golden brown rigid polymer. IR (cm^{-1}): 2924, 2854 (ν_{CH_2/CH_3}), 1731 ($\nu_{C=O}$), 1457 (ν_{C-H}) 1259, 1158, 1094, 1017 (ν_{C-O}). Ultimate tensile stress – 12.9 MPa, Youngs modulus – 671 MPa, elongation at break – 2.3%, Crosslinking density – 32.24 $x10^4$ mol/cm^3, Sol content 20.16%, Swelling ratio – 1.85, Contact angle (θ_{water}) 97.2.

Epoxidised Grapeseed Oil and Euphorbia Oil (0.6:0.4) with Aradur 917. EGSO (5.678 g, 5.9 mmol, 0.6 eq), EuO (3.654 g, 4.0 mmol, 0.4 eq), Aradur 917 (5.8 g, 34.9 mmol, 3.5 eq) and 4-methyl imidazole (0.1572 g, 1wt%) were cured at 170 °C for 1 h to yield a golden brown slightly flexible polymer. IR (cm^{-1}): 2924, 2854 (ν_{CH_2/CH_3}), 1732 ($\nu_{C=O}$), 1456 (ν_{C-H}) 1260, 1160, 1093 (ν_{C-O}). Ultimate tensile stress – 10.7 MPa, Youngs modulus – 258 MPa, elongation at break – 19.1%, Crosslinking density – 28.86 $x10^4$ mol/cm^3, Sol content 9.91%, Swelling ratio – 1.92, Contact angle (θ_{water}) 110.7.

Epoxidised Grapeseed Oil and Euphorbia Oil (0.4:0.6) with Aradur 917. EGSO (4.273 g, 4.44 mmol, 0.4 eq), EuO (6.089 g, 6.67 mmol, 0.6 eq), Aradur 917 (5.281 g, 31.8 mmol, 2.86 eq) and 4-methyl imidazole (0.1563 g, 1wt%) were cured at 170 °C for 1 h to yield a golden brown flexible polymer. IR (cm^{-1}): 2925, 2854 (ν_{CH_2/CH_3}), 1733 ($\nu_{C=O}$), 1456 (ν_{C-H}) 1260, 1158, 1085 (ν_{C-O}). Ultimate tensile stress – 2.8 MPa, Youngs modulus – 15 MPa, elongation at break – 42.4%, Crosslinking density – 21.29 $x10^4$ mol/cm^3, Sol content 7.99%, Swelling ratio – 1.64, Contact angle (θ_{water}) 108.9.

Epoxidised Grapeseed Oil and Euphorbia Oil (0.2:0.8) with Aradur 917. EGSO (2.262 g, 2.35 mmol, 0.2 eq), EuO (8.597 g, 9.41 mmol, 0.8 eq), Aradur 917 (4.36 g, 26.2 mmol, 2.23 eq) and 4-methyl imidazole (0.1522 g, 1wt%) were cured at 170 °C for 1 h to yield a golden brown soft polymer. IR (cm^{-1}): 2924, 2854 (ν_{CH_2/CH_3}), 1734 ($\nu_{C=O}$), 1456 (ν_{C-H}) 1260, 1160, 1095 (ν_{C-O}). Ultimate tensile stress – 1.6 MPa, Youngs modulus – 4.1 MPa, elongation at break – 40.5%, Crosslinking density – 14.49 $x10^4$ mol/cm^3, Sol content 7.93%, Swelling ratio – 1.75, Contact angle (θ_{water}) 113.4.

References

1. N. Abas, A. Kalair, N. Khan, *Futures.,* 2015, **69,** 31-49.
2. R. Sawangkeaw, S. Ngampraser, *Renew. Sust. Energ. Rev.,* 2013, **25,** 97-108.
3. R. C. Brown, T. R. Brown, *Biochemical Processing of Carbohydrate-Rich Biomass, in Biorenewable Resources: Engineering New Products from Agriculture,* Wiley, USA, 2nd Ed, 2014.
4. D. D. Perez, C. Dupont, A. Guillemain, *Waste. Biomass. Valorization.,* 2015, **6,** 515-526.
5. R. Mckendry, *Bioresour. Technol.,* 2002. **83,** 37-46.
6. B. Hu, K. Wang, L. Wu, M. Antonietti, *Adv. Mater.,* 2010, **22,** 813-828.
7. F. Giglio, *Open. J. Civil. Eng.,* 2013, **3,** 82-84.
8. R. M. Rowel, *J. Polym. Environ.,* 2007, **15,** 229-235.
9. R. L. Wu, X. L. Wang, L. Fang, H. Z. Li, *Bioresour. Technol.,* 2009, **100,** 2569-2574.
10. H. T. Sahin, M. B. Arslan, *Int. J. Mol. Sci.,* 2008, **9,** 78-88.
11. D. Klemm, B, Heublein, H. P. Fink, A, Bohn, *Angew. Chem. Int. Ed.,* 2005, **44,** 3358-3393.
12. S. Paunonem, *Bioresources.,* 2005, **8,** 3098-3121.
13. P. Hedenberg, P. Gatenholm, *J. Appl. Polym. Sci.,* 1995, **56,** 641-651.
14. G. Siquerra, A. P. Matthew, K. Oksman, *Compos. Sci. Technol.,* 2011, **71,** 1886-1892.
15. J. L. Wen, Y. C. Sun, F. Xu, R. C. Sun, *J. Agric. Food. Chem.,* 2010, **58,** 11372-11383.
16. B. Ru, G. Dai, W. Sun, K. Qui, J. Zhou, *Bioresource. Technol.,* 2015, **190,** 211-218.
17. J. González, J. M. Cruz, H. Domínguez, J. C. Parajó, *Food. Chem.,* 2004, **84,** 243-251.
18. J. Hartman, A. C. Albertsson, M. S. Lindblad, J. Sjöberg, *J. Appl. Polym. Sci.,* 2006, **100,** 2985-2991.
19. D. Melandri, A. D. Angelis, V. Reiner, *Burns.,* 2006, **32,** 964-972.
20. X. Peng, J. Ren, R. Sun, *Biomacromol.,* 2010, **11,** 3519-3524.
21. J. Zhang, H. Xiao, N. Li, Q. Ping, Y. Zhang, *J. Appl. Polym. Sci.,* 2015, **132,** 42441.
22. M. P. Pandey, C. S. Kim, *Chem. Eng. Technol.,* 2011, **34,** 29-41.
23. S. Laurichesse, L. Avérous, *Prog. Polym. Sci.,* 2004, **39,** 1268-1290.
24. M. Alekhina, J. Erdmann, A. Ebert, A. M. Stepman, H. Sixta, *J. Mater. Sci.,* 2015, **50,** 6395-6406.
25. S. Doi, J. H. Clark, D. J. Macquarrie, *Chem. Comm.,* 2002, 2632.
26. P. S. Shuttleworth, V. Budarin, J. H. Clark, *J. Mater. Chem.* 2009, **19,** 8589.
27. Z. Zhang, D. J. Macquarrie, J. H. Clark, A. S. Matharu, *RSC. Adv.* 2014, **4,** 41947-41955.
28. M. M. Ibrahim, A. Dufrense, W. K. El-Zawawy, F. A. Ayblevor, *Bioresour. Technol.* 2010, **101,** 3534.
29. R. Hallmann, B. Cooper, *Methods of Isolating Polyhydroxyl Alkanoates* US08313935, 2012.
30. J. R. Xavier, S. T. Babusha, G. Johnsy, *Appl. Biochem. Biotech.* 2015, **176,** 1498-1510.

31. H. Ren, Z. Liu, Z. Zhuan, *Bioresour.* 2015, **10,** 432-447.
32. M. Singh, P. Kumar, S. Ray. V. E. Kalia, *Indian. J. Microbiol.*, 2015, **55,** 235-249.
33. Y. H. Yang, S. K. Bhatia, Y. H. Shim, J. M. Jeon, *Bioprocess. Biosyst. Eng.*, 2015, **35,** 1479-1484.
34. R. Duarah, N. Karak, *RSC. Adv.*, 2015, **5,** 64456-64465.
35. A. R. Solanki, B. V. Kamath, S. Thakore, *J. Appl. Polym. Sci.*, 2015, **138,** 42223.
36. F. D. Gunstone, *The Chemistry of Oils and Fats: Sources, Composition, Properties and Uses*; Blackwell Pub., 2004.
37. R. Mythili, P. Venkatachalam, P. Subramanian, D. Uma, *Int. J. Energ. Res.* 2014, **38,** 1233-1259.
38. F. R. Ma, M. A. Hanna, *Bioresource. Technol.* 1999, **70,** 1-15.
39. B. Fillion, B. I. Morsi, *Ind. Eng. Chem. Res.* 2000, **39,** 2157-2168.
40. J. Edvardsson, P. Rautanen, A. Littorin, M. Larsson, *J. Am. Oil. Chem. Soc.* 2001, **79,** 319-327.
41. M. R. Kessler, R. Ding, C. Zhang, *Macromol. Rapid. Commun.* 2014, **35,** 1068-1074.
42. A. J. Clark, S. S. Hoong, *Polym. Chem.* 2014, **5,** 3238-3244.
43. The Statistics Portal website, accessed 07/09/2015. http://www.statista.com/statistics/263937/vegetable-oils-global-consumption.
44. N. A. Porter, D. G. Wujek, *J. Am. Chem. Soc.*, 1984, **106,** 2626-2629.
45. G. Knothe, M. O. Bagby, D. Weisleder, R. E. Peterson, *J. Am. Oil. Chem. Soc.*, 1995, **72,** 703-706.
46. L. E. Gast, W. Schneider, J. C. Cowan, *J. Am. Oil. Chem. Soc.*, 1966, **43,** 418.
47. L. Perreux, A. Loupy, F. Volatron, *Tetrahedron.*, 2002, **58,** 2155.
48. A. Khalafi-Nezhad, B. Mokhtari, M. N. R. Soltani, *Tetrahedron. Lett.*, 2003, **44,** 7325.
49. C. Ferroud, M. Godart, S. Ung, *Tetrahedron. Lett.*, 2008, **49,** 3004.
50. R. Aravindan, P. Anubmathi, T. Vinthagiri, *Indian. J. Biotechnol.*, 2007, **6,** 141-158.
51. L. Vayesse, E. Dubreucq, J. L. Pirat, *J. Biotechnol.*, 1997, **53,** 41-46.
52. R. J. González-Paz, G. Lligdas, J. C. Ronda, M. Galia, *Macromol. Biosci.*, 2012, **12,** 1697-1705.
53. C. G. Almeida, I. F. de Souza, R. A. Sousa, M. L. Hyaric, *Cat. Comm.*, 2013, **42,** 25-29.
54. V. S. Rana, A. M. Blazques, *JLST.*, 2008, **40,** 65-66.
55. A. P. More, R. A. Kute, S. T. Mhaske, *Pig. Res. Technol.*, 2014, **43,** 285-292.
56. U. V. Inekwe, M. O. Odey, B. Gauje, *Ann. Bio. Res.*, 2012, **3,** 4860-4864.
57. H. Noureddini, V. Medikonduru, *J. Am. Oil. Chem. Soc.*, 1997, **74,** 419.
58. A. Kayacier, R. K. Singh, *J. Food. Process. Pres.*, 2003, **27,** 1-8.
59. S. L. Cooper, N. A. Kocaoglu-Vurma, B. Tharp, *J. Food. Sci.*, 2013, **78,** 811-816.
60. A. Demirbas, *Eng. Source. Part-A.*, 2010, **32,** 628.
61. I. Lee, L. Johnson, E. Hammond, *J. Am. Oil. Chem. Soc.*, 1995, **72,** 1155.
62. A. M. Fureby, L. Tian, P. Adlercreutz, *Enzyme. Microb. Tech.*, 1997, **20,** 198-206.
63. K. Tangkam, N. Webster, B. Wiege, *Grasas. Aceites.*, 2008, **59,** 245-253.
64. N. Tippayawong, P. Sittisun, *Sci. Iran.*, 2012, **19,** 1324-1328.
65. W. Norman, British Patent 1 515, 1902.

66. M. J. H. Keijbets, G. Ebbenhorsteller, J. Ruisch, *J. Am. Oil. Chem. Soc.,* 1985, **62,** 720-724.
67. H. Sakurai, J. Pokorny, *Eur. J. Lipid. Sci. Technol.,* 2003, **105,** 769-778.
68. D. S. Cap, *Cosmetic Product Including Vegetable Oil Blend,* US 08709453, 2014.
69. K. Rezaei, T. Wang, L. A. Johnson, *J. Am. Oil. Chem. Soc.,* 2002, **79,** 1241-1247.
70. S. McArdle, T. Curtin, J. J. Leahy, *Appl. Catal. A-Gen.,* 2010, **382,** 332-338.
71. H. N. Cheng, M. W. Rau, M. K. Dowd, M. W. Easson, B. D. Condon, *J. Am. Oil. Chem. Soc.,* 2014, **91,** 1461.
72. M. Sanchez, F. Jhan, D. E. Boldrini, G. M. Tonetto, *Chem. Eng. J.,* 2011, **187,** 355-361,
73. A. V. Romanenko, I. N. Voropaev, R. M. Adullina, *Solid. Fuel. Chem.,* 2014, **48,** 356-363.
74. M. B. Fernandez, G. M. Tonetto, G. H. Crapiste, *J. Food. Eng.,* 2007, **82,** 199-208.
75. G. Darsow, US 5861521, 1999.
76. S. Filip, R. Fink, J. Hribar, *Food. Technol. Biotech.,* 2010, **48,** 135-142.
77. S. Vega-Lopez, N. R. Matthan, L. M. Ausman, *Atherosclerosis.,* 2009, **207,** 208-212.
78. D. Singh, M. E. Rezac, P. H. Pfromm, *J. Am. Oil. Chem. Soc.,* 2009, **86,** 93-101.
79. J. Mallégol, J. Lemaire, J. L. Gardette, *J. Am. Oil. Chem. Soc.,* 2009, **76,** 967-976.
80. D. B. Min, E. Choe, *Comp. Rev. Food. Sci. Food. Safety.,* 2006, **5,** 169-186.
81. I. Aidos, S. Lourenco, A. van der Padt, *J. Food. Sci.,* 2002, **67,** 3314-3320.
82. J. Mallégol, J. Lemaire, J. L. Gardette, *Prog. Org. Coat.,* 2000, **39,** 107.
83. G. Booth, D. E. Delatte, S. F Thames, *Ind. Crop. Prod.,* 2007, **25,** 257-265.
84. V. R. Chitareddy, R. E. Oshel, K. M. Doll, *J. Am. Oil. Chem. Soc.,* 2012, **89,** 1749-1762.
85. E. Bowman, R. van Gorkum, *J. Coat. Technol. Res.,* 2007, **4,** 491.
86. Y. Wang, G. W. Padua, *J. Appl. Pol. Sci.,* 2010, **115,** 2565-2572.
87. Q. Wang, Y. Wang, W. E. Artz, *J. Agri. Food. Chem.,* 2008, **56,** 3043-3048.
88. D. Astruc, *New. J. Chem.,* 2005, **29,** 42-56.
89. S. Z. Erhan, M. O. Bagby, T. C. Nelsen, *J. Am. Oil. Chem. Soc.,* 1997, **74,** 703-706.
90. P. B. van Dam, M. C. Mittelmeijer, C. Boelhouwer. *J. Am. Oil. Chem. Soc.,* 1974, **51,** 389.
91. P. Schwab, M. B. France, J. W. Ziller, R. H. Grubbs, *Angew. Chem. Int. Ed. Engl.,* 1995, **34,** 2039-2041.
92. M. D. Refuik, R. C. Larok, Q. Tian, *J. Am. Oil. Chem. Soc.,* 1999, **73,** 93-98.
93. M. B. Dinger, J. C. Mol, *Adv. Synth. Catal.,* 2002, **344,** 671.
94. K. B. Wagener, J. M. Boncella, J. G. Nel, *Macromol. Chem. Phys.,* 1990, **191,** 365.
95. Q. Tian, R. Larock, *J. Am. Oil. Chem. Soc.,* 2002, **79,** 479-488.
96. U. Biermann, J. O. Metzger, M. A. R. Meier, *Macromol. Chem. Phys.,* 2010, **211,** 854-862.
97. T. Saurabh, M. Patnaik, S. L. Bhagt, V. C. Renge, *Int. J. Adv. Eng. Tech.,* 2011, **2,** 491-501.

98. A. Campanella, C. Fontanini, M. A. Baltanes, *Chem. Eng. J.,* 2008, **144,** 466-475.
99. S. F. Cai, L. S. Wang, C. L. Fan, *Molecules.,* 2009, **14,** 2935-2946.
100. C. Aouf, E. Durand, J. Lecomte, *Green. Chem.,* 2014, **16,** 1740-1754.
101. P. D. Bartlett, *Rec. Chem. Prog.* 1950, **11,** 47.
102. K. Miyazaki, *Method for Purifying an Epoxidation Product.* US4423239A, 1982.
103. S. Dinda, A. V. Patwardhan, V. V. Goud. N. C. Pradhan, *Bioresour. Technol.,* 2008, **99,** 3737-3744.
104. P. P. Meyer, N. Techaphattana, S. Maundawee, *Thammasat. Int. J. Sci. Technol.,* 2008, **13,** 1-5.
105. P. Lathi, B. Mattiasson, *Appl. Catal. B-Environ.,* 2007, **69,** 207-212.
106. R. P. Wool, *Polymers and Composite Resins from Plant Oils, Biobased Polymers and Composites*, 2005, ISBN:978-12-763952-9.
107. Z. S. Petrović, A. Zlatanic, C. C. Lava, S. S. Fišer, *Eur. J. Lipid. Sci. Technol.,* 2002, **104,** 293-299.
108. V. V. Goud, A. V. Patwardhan, S. Dinda, N. C. Pradhan, *Eur. J. Lipid. Sci. Technol.,* 2007, **107,** 575-584.
109. A. Campanella, M. A. Baltanás, M. C. Capel-Sánchez, J. M. Campus-Martin, J. L. G. Fierro, *Green. Chem.,* 2004, **6,** 330-334.
110. C. Venturello, E. Almeri, M. Ricci, *J. Org. Chem.,* 1983, **48,** 3831-3833.
111. K. A. Jørgensen, *Chem. Rev.* 1989, **89,** 431-458.
112. U. Törnvall, C. Orellana-Coca, R. H. Kaul. D. Adlercreutz, *Enzyme. Microb. Tech.,* 2007, **40,** 447-451.
113. S. Sun, X. Ke. L. Cui, G. Yang, Y. Bi, F. Song, X. Xu, *Ind. Crop. Prod.,* 2011, **33,** 676-682.
114. M. R. Klaas, S. Warwel, *J. Am. Oil. Chem. Soc.,* 1996, **73,** 1453-1457.
115. R. C. S. Schneider, L. R. S. Lara, T. B. Bitencourt, *J. Braz. Chem. Soc.,* 2009, **20,** 1473-1477.
116. B. K. Sharma, A. Adhvaryu, Z. Liu, S. Z. Erhan, *J. Am. Oil. Chem. Soc.,* 2006, **83,** 129-136.
117. H. Dai, L. Yang, B. Lin, G. Wang, G. Shi, *J. Am. Oil. Chem. Soc.,* 2009, **86,** 261-267.
118. B. K. Sharma, A. Adhvaryu, S. Z. Erhan, *J. Agri. Food. Chem.,* 2006, **54,** 9866-9872.
119. C. Lee, T. Ooi, C. Kuah, S. Ahmad, *J. Am. Oil. Chem. Soc.,* 2007, **84,** 945-952.
120. A. Guo, Y. Cho, Z. S. Petrović, *J. Polym. Sci. Pol. Chem.,* 2000, **38,** 3900-3910.
121. K. Hariyoti, A. Jayasooriyamu, *J. Oil. Palm. Res.,* 2015, **27,** 39-56.
122. R. Auvergne, S. Caillol, G. David, J. P. Pascault, *Chem. Rev.,* 2014, **114,** 1082-1115.
123. J. V. Crivello, R. Narayan, *Chem. Mater.,* 1992, **4,** 692-699.
124. S. J. Park, F. L. Jin, J. R. Lee, J. Shin, *Eur. Polym. J.,* 2005, **41,** 231-237.
125. G. Lligdas, J. C. Ronda, M. Galia, U. Biermann, J. O. Metzger, *J. Polym. Sci. Pol. Chem.,* 2006, **44,** 634-645.
126. Z. Liu, S. Z. Erhan, *J. Am. Oil. Chem. Soc.,* 2010, **87,** 437-444.
127. A. J. Clark, S. S. Hoong, *Polym. Chem.* 2014, **5,** 3238-3244.
128. A. Guo, I. Javni, Z. Petrović, *J. Appl. Polym. Sci.,* 2000, **77,** 467-473.
129. I. Javin, W. Zhang, Z. S. Petrović, *J. Appl. Polym. Sci.,* 2003, **88,** 2912-2916.

130. C. S. Wang, L. T. Yang, B. L. Ni, G. Shi, *J. Appl. Polym. Sci.*, 2009, **114,** 125-131.
131. F. I. Altuna, L. H. Espósito, R. A. Ruseckaite, P. M. Stefani, *J. Appl. Polym. Sci.*, 2011, **120,** 789-798.
132. H. Miyagawa, M. Misra, L. T. Drzal, *Polym. Eng. Sci.*, 2005, **45,** 487-495.
133. J. D. Earls, J. E. White, L. C. López, *Polymer.*, 2007, **48,** 712-719.
134 T. Takahashi, K. Hirayama, N. Teramoto, M. Shibata, *J. Appl. Polym. Sci.*, 2008, **108,** 1596-1602.
135. R. van Gorkum, E. Bouwman, *Coordin. Chem. Rev.*, 2005, **249,** 1709-1728.
136. T. Learner, *The Conservator.*, 2000, **24,** 96-103.
137. P. A. Sørensen, S. Kiil, K. Dom-Johansen, C. E. Weinell, *J. Coat. Technol. Res.*, 2009, **6,** 135-176.
138. M. D. Soucek, T. Khattab, J. Wu, *Prog. Org. Coat.*, 2012, **73,** 435-454.
139. E. F. Assanvo, S. Baruah, *Prog. Org. Coat.*, 2015, **86,** 25-32.
140. P. Gogoi, M. Boruah, S. Sharma, S. K. Dolui, *ACS. Sustainable. Chem. Eng.*, 2015, **3,** 261-268.
141. T. H. Xie, J. Lin, *J. Phys. Chem.*, 2007, **111,** 9968-9974.
142. P. Parkin, R. G. Palgrave, *J. Mater. Chem.*, 2005, **15,** 1689-1695.
143. R. W. Andrews, A. Pollard, J. M. Pearce, *Sol. Energy. Mater. Sol. Cell.*, 2013, **113,** 71-78.
144. C. Wang, X. He, *J. Appl. Surf. Sci.*, 2006, **252,** 8348-8351.
145. S. Banerjee, D. D. Dionysiou, S. C. Pillai, *Appl. Cat. B-Environ.*, 2015, **176,** 396-428.
146. N. P. Mellot, C. Durucan, E. G. Parate, M. Guglielmi, *Thin. Solid. Film.*, 2006, **502,** 112-120.
147. S. K. Lee, S. McIntyre, A. Mills, *J. Photochem. A-Chem.*, 2004, **162,** 203.
148. A. Abbott, P. D. Abel, D. W. Arnold, A. Milne, *Sci. Total. Environ.*, 2000, **258,** 5-19.
149. S. Kiil, C. E. Weinell, M. S. Pedersen, K. D. Johansen, *Chem. Eng. Res.*, 2002, **80,** 45-52.
150. M. Berglin, N. Lönn, P. Gatenholm, *Biofouling*, 2003, **19,** 63-69.
151. R. F. Brady, *Prog. Org. Coat.*, 2001, **43,** 188-192.
152. R. F. Brady, I. S. Singer, *Biofouling.*, 2000, **15,** 73-81.
153. G. W. Critchlow, R. E. Litchfield, I. Sutherland, *Int. J. Adhes. Adhes.*, 2006, **26,** 577-599.
154. M. J. Sorel, *Franklin. I.* 1838, **13,** 52-56.
155. P. Kajitvichyanukul, J. Ananpattarachai, S. Pongpom, *Sci. Technol. Adv. Mater.*, 2005, **6,** 352-358.
156. R. Menini, Z. Ghalmi, M. Farzaneh, *Cold. Reg. Sci. Technol.*, 2011, **65,** 65-69.
157. F. T. Lynch, A. Khodadoust, *Prog. Aerosp. Sci.*, 2001, **37,** 669-767.
158. E. Almedia, *Prog. Org. Coat.*, 2007, **59,** 2-20.
159. J. J. Licari (2003). Coating Materials for Electronic Applications; Polymers, Processes, Reliability, Testing. P 227. ISBN: 978-0-8155-1492-3.
160. G. Gugler, R. Beer, M. Mauron, *Chem. Eng. Process.*, 2011, **50,** 462-465.
161. Cooper Coated Coil company website, http://www.coopercoated.com/what-is-coil-coating.html (accessed 01/08/15)
162. T. Chung-Jyi, M. F. Leitzmann, W. C. Willet, *Am. J. Clin. Nutr.*, 2007, **85,** 518-522.
163. R. Jiang, J. Ma, A. Ascherio, *Am. J. Clin. Nutr.*, 2004, **79,** 70-75.

164. A. P. Serro, C. Completo, R. Colaco, *Surf. Coat. Tech.,* 2009, **203,** 3701-3707.
165. W. A. Groll, Stick Resistant Coating for Cookware. US 6360,423. **2002.**
166. F. Ganachaud, *Polym. Degrad. Stabil.,* 2009, **94,** 465-495.
167. R. Plunkett, Tetrafluoroethylene Polymers. US 2230,654. **1941.**
168.https://www.chemours.com/Teflon_Industrial/en_US/tech_info/techinfo_compare.html accessed 27/08/15.
169. D. A. Ellis, S. A. Mabury, J. W. Martin, D.C. G. Muir, *Nature.,* 2001, **412,** 321-324.
170. A. B. Newton, J. B. Rose, *Polymer.,* 1972, **13,** 465-474.
171. H. P. Tannenbaum *Fluoropolymer Non-Stick Coatings,* US 6,761,964 B2, **2004.**
172. Y. L. Shizuoka, *Process for Improving the Corrosion Resistance of a Non-stick Coating on a Substrate.* US 2007/0036900, **2007.**
173. K. Shimizu, F. Sasaki, Y. Watanabe, *Brilliant Black Pigments,* WO 20012/076110 A1, **2012.**
174. J. O. Metzger, U. Biermann, W. Friedt, *Angew. Chem. Int. Ed.,* 2000, **39,** 2206-2224
175. D. V. Palaskar, A. Boyer, E. Cloutet, *J. Polym. Sci. Pol. Chem.,* 2012, **50,** 1766-1782.
176. S. R. Coles, G. Barker, A. J. Clark, *Macromol, Biosci.,* 2008, **8,** 526-532.
177. J. V. Crivello, U. Bulut, *J. Polym. Sci. Pol. Chem.,* 2006, **44,** 6750-6764.
178. C. Decker, T. N. T. Viet, H. P. Thi, *Polym. Int.,* 2001, **50,** 986-997.
179. UK government website. *Environmental Risk Reduction Strategy and Analysis of Advantages and Drawbacks for Hexavalent Chromium.* Accessed 11/08/15 https://www.gov.uk/government/uploads/system/uploads/attachment_data/file/183155/hexavalent060203.pdf.
180. J. Wijenberg, Z. Portegies, *Method for electrodeposition of chromium containing coatings from trivalent chromium based electrolytes.* WO2014079911 A2, **2014.**
181. J. Blumm, A. Linderman, M. Meyer, *Int. J. Thermophys.,* 2010, **31,** 1919-1927.
182. J. L. G. Coq, H. E. Seymus, *Coating composition of poly(arylene sufide) polytetrafluoroethylene and barium or calcium sulfate.* CA1210184 A1, **1986.**
183. D. Quéré, *Physica. A.* 2002, **131,** 32-46.
184. A. J. Clark, S. S. Hoong, *Polym. Chem*., 2014, **5,** 3238-3244.
185. S. S. Hoong, PhD Thesis, University of Warwick, 2013.
186. The statistics portal website, accessed 23/08/15. http://www.statista.com/statistics/263933/production-of-vegetable-oils-worldwide-since-2000/.
187. H. Meerwien, D. Delfs, *Angew. Chem.,* 1960, **72,** 927-934.
188. J. V. Crivello, U. Bulut, *J. Polym. Sci. Pol. Chem.,* 2005, **43,** 5217-5231.
189. A. Chemtob, C. Croutxe´-Barghorn, O. Soppera, S. Rigolet, *Macromol. Chem. Phys.,* 2009, **210,** 1127–1137.
190. D. H. Campbell, J. E. Echols, W. H. Ohrbom, *Scratch resistant clearcoats containing surface reactive microparticles and method therefore.* US5853809 A. **1998.**
191. W. Zhang, A. A. Dehghani-Sanij, R. S. Blackburn, *Prog. Nat. Sci.,* 2008, **18,** 801–805.
192. Wacker Chemie AG company website, accessed 04/08/2015 http://www.wacker.com/cms/en/products/product/product.jsp?product=9323.

193. C. B. Ferrer, M. C. Garrigós, A. Jiménez, *Polym. Degrad. Stabil.,* 2010, **95,** 2207-2212.
194. European Food Safety Authority website - http://www.efsa.europa.eu/en/efsajournal/pub/2592.htm, accessed 04/08/15
195. F. H. Allen, O. Kennard, D. G. Watson, L. Brammer, *J. Chem. Soc. Perkin. Trans. II.,* 1987, S1-S19.
196. Z. Lozada, *J. Appl. Pol. Sci.,* 2009, **113,** 2252-2260.
197. C. P. Wong, J. Lu, K. S. Moon, B. K. Kim, *Polymer.,* 2007, **48,** 1510-1516.
198. D. Khastgir, B. G. Soares, M. Celestino, M. Magioli, V. X. Moreira, *Synthetic. Mat.,* 2010, **160,** 1981-1986.
199. Euopean food contact materials database, accessed 12/08/15. https://webgate.ec.europa.eu/sanco_foods/main/index.cfm?event=substance.view&identifier=658.
200. K. Kosswig, *Surfactants* in *Ulmans Encyclopaedia of Industrial Chemistry,* Wiley, 2005.
201. Euopean food contact materials database, accessed 12/08/15. https://webgate.ec.europa.eu/sanco_foods/main/index.cfm?event=substance.view&identifier=658.
202. I. Matos, I. S. Fonseca *et al, Appl. Catal. A-Gen.,* 2012, **439-440,** 24-30.
203. A. Benazzouz, L. Moity, J. M. Aubry, *Ind. Eng. Chem. Res.,* 2013, **52,** 16585-16597.
204. A. Marrion (2004) The Chemistry and Physics of Coatings, 2nd Ed, P. 39. ISBN:0-85404-656-9.
205. R. Simič, M. Kalin, *Appl. Surf. Sci.,* 2013, **283,** 460-470.
206. A. Bubat, W. Scholz, *Chimia,.* 2002, **5,** 230-209.
207. Dow Corning company website. Accessed 17/08/15. http://www.dowcorning.com/content/pressure/pressureadhesive/
208. O. I. Strube, J. Birkmann, B. Huesgen, *Polym-Plast. Technol.,* 2014, **52,** 1327-1332.
209. L. Sommer, E. Pietrusza, F. Whitmore. *J. Am. Chem. Soc.* 1947, **69,** 188.
210. M. Green, J. L. Spencer, G. A. Stone, C. A. Tsipis. *J. Chem. Soc., Dalton Trans.,* 1977, **16,** 1525-1529.
211. M. F. Lappert, T. A. Nile. *J. Organomet. Chem.* 1975, **102,** 543 – 550.
212. K. Yamamoto, T. Hayashi, M. Kumada. *J. Organomet. Chem.* 1972, **46,** 65 – 67.
213. M. V. Jiménez, L. A. Oro. *Organometallics.* 2008, **27,** 224 – 234.
214. R. Takeuchi, N. Tanouchi. *J. Chem. Soc. Perkin. Trans.* 1994, **1,** 2909 – 2913.
215. L. Liu, X. Li, H. Dong, C. Wu. *J. Organomet. Chem.* 2013, **745-46,** 454 – 459.
216. S. V. Maifeld, M. N. Tran, D. Lee. *Tetrahedron. Lett.* 2005, **46,** 105 – 108.
217. D. Chung, G. Tae, *J. Ind. Eng. Chem.,* 2007, **13,** 571-577.
218. S. E. Denmark, Z. Wang. *Org. Lett.* 2001, **3,** 1073 – 1076.
219. L. N. Lewis, J. Stein, Y. Gao, R. E. Colborn, G. Hutchins. *Platinum. Metals. Rev.* 1997, **41,** 66 – 75.
220. J. Stein, L. N. Lewis, K. A. Smith, K. X. Lettko. *J. Inorg. Organomet. P.* 1991, **1,** 325 – 334.
221. N. Saghian, D. Gertner. *J. Am. Oil. Chem. Soc.* 1974, **51,** 363 – 367.
222. A. E.Kadib, A. Castel, F. Delpech, P. Rivière. *Chem. Phys. Lipids.* 2007, **148,** 112 – 120.

223. G. Lligadas, J. C. Ronda, M. Galià, V. Cádiz. *Biomacromol.* 2006, **7,** 2420 – 2426.
224. A. Behr, F. Naendrup, D. Obst. *Adv. Synth. Catal.* 2002, **344,** 1142 – 1145.
225. A. Behr, F. Naendrup, D. Obst. *Eur. J. Lipid. Sci. Technol.* 2002, **104,** 161 – 166.
226. G. Camino, S. M. Lomakin, M. Lazzari, *Polymer.*, 2001, **42,** 2395-2402.
227. M. A. Semsarzadeh, A. H. Navarchian, *J. Appl. Polym. Sci.* 2003, **90,** 963-972.
228. S. Hamdani, C. Longuet, D. Perrin, F. Ganachaud, *Polym. Degrad. Stabil.* 2009, **94,** 465-495.
229. H. S. Rho, H. S. Back, D. H. Kim, I. S. Kim. *Bull. Korean. Chem. Soc.* 2006, **27,** 584-586.
230. G. L. Anderson, S. D. Stanley, G. L. Young, R. A. Brown, K. B. Evans, L. A. Wurth, *J. Adhesion.*, 2010, **86,** 1159-1177.
231. X. Pan, P. Sengupta, D. C. Webster, *Biomacromol.*, 2011, **15,** 2416-2428.
232. J. Rösch, R. Mülhaupt, *Polym. Bull.*, 1993, **31,** 679-685.
233. A. Ručigaj, B. Alič, M. Krajnc, U. Šebenik, *Eur. Polym. J.*, 2014, **52,** 105-116.
234. S. B. Kamel, H. Dawson, Y. Kakuda, *J. Am. Oil. Chem. Soc.* 1985, **62,** 881-883.
235. A. Srivastava, R. Prasad, *Renew. Sust. Energ. Rev.* 2000, **4,** 111-133.
236. P. Fantozzi, A. A. Betschart, *J. Am. Oil. Chem. Soc.* 1979, **56,** 457-459.
237. United Nations Food and Agriculture Organisation. http://faostat3.fao.org/faostat-gateway/go/to/browse/Q/QC/E. (accessed 12/08/2014).
238. C. Cai, H. Dai, R. Chen, C. Su, X. Xu, S. Zhang, L. Yang, *Eur. J. Lipid Sci Tech*. 2008, **110,** 341-346.
239. A. J. Clark, S. S. Hoong, *Polym. Chem.*, 2014, **5,** 3238-3244.
240. I. Franek, P. Czub, *Polimery-W.*, 2013, **58,** 135-139.
241. S. N. Mustapha, A. R. Rahmat, A. Arsad, *Mater. Res. Innov.*, 2014, **18,** 326-330.
242. www.palmoilresearch.org/statistics.html. Accessed 14/08/15.
243. World Cocoa Foundation website accessed 30/08/2015. http://www.unitedcacao.com/index.php/en/corporate-profile/global-cocoa-market.
244. The Statistics Portal website accessed 30/08/2015. http://www.statista.com/statistics/238849/global-chocolate-consumption/.
245. R. D. O'Brien, *Fats and Oils: Formulating and Processing for Applications*, CRC Press, FL USA, 2nd Ed, 2003, 14-39.
246. R. C. Larock, D. D. Andjelovic, M. Valverde, P. Henna, F. Li, *Polymer*, 2005, **46,** 9674-9685.
247. S. S. Hoong, PhD Thesis, University of Warwick, 2013.
248. R. Wang, M. A. Hanna, B. A. Song, S. Yang, *Bioresour. Technol.*, 2011, **102,** 1194-1199.
249. Z. S. Petrovic, *Polym. Rev.* 2008, **48,** 109-.
250. L. G. Angelini, E. Moscheni, G. Colonna, P. Belloni, E. Bonari, *Ind. Crop. Prod.* 1997, **6,** 313-323.
251. D. S. Martini, B. A. Braga, D. Samios, *Polymer.* 2009, **50,** 2919-2925.
252. J. Karger-Kocsis, S. Grishchuk, L. Sorochynska, M. Z. Rong, *Polym. Eng. Sci.* 2013, **54,** 747-755.
253. J. M. España, L. Sánchez-Nacher, T. Boromat, V.Fombuena, R. Balart, *J. Am. Oil. Chem. Soc.*, 2012, **89,** 2067-2075.
254. P. I. Vincent, *Polymer.*, 1960, **1,** 425-444.

255. M. A. Hallam, G. Pollard, I. M. Ward, *J. Mater. Sci. Lett.*, 1987, **6,** 975-976.
256. M. A. Semsarzadeh, A. H. Navarchian, *J. Appl. Polym. Sci.* 2003, **90,** 963-972.
257. S. Montserrat, C. Flaque, M. Calafell, G. Andreu, J. Malek, *Thermochim. Acta.*, 1995, **269,** 213-229.
258. E. S. Freeman, A. J. Becker, *J. Pol. Sci. Part A.*, 1968, **6,** 2829-2851.
259. Y. Chen, L. Yang, J. Wu, L. Ma, D. Finlow, S. Lin, K. Song, *J. Therm. Anal. Calorim.*, 2013, **113,** 939-945.
260. A. Gerbase, C. L. Petzhold, A. P. O. Costa, *J. Am. Oil. Chem. Soc.* 2002, **8,** 797-802.
261. R. Ramaswamy, P. Sasidharan, K. G. Shine, *J. Appl. Polym. Sci.* 1987, **33,** 49-65.
262. FDA List of Indirect Additives Used in Food Contact Substances. http://www.accessdata.fda.gov/scripts/fcn/fcnNavigation.cfm?filter=anhydride&sortColumn=&rpt=iaListing (accessed 26/08/14).
263. M. Ash, I. Ash, *Handbook of Green Chemicals.* Synapse Resource Information Inc. NY USA, 2nd Ed, 2004, 801.
264. F. R. Benn, J. Dwyer, I. Chappell, *J. Chem. Soc. Perkin. Trans. 2.* 1977, **5,** 533-535.

265. H. Dodiuk, S. King, *Prog. Polym. Sci.* 1994, **3,** 439-467.
266. R. A. Dubois, P. S. Sheih, *J. Coat. Technol.*, 1992, **64,** 51-57.
267. N. N. Meis, L. G. J. van der Ven, R. A. van Benthem, *Prog. Org. Coat.*, 2014, **77,** 176-183.
268. J. Liu, H. J. Sue, Z. J. Thompson. *Polymer.*, 2009, **50,** 4683-4689.
269. A. Parvizi, K. W. Garrett, J. E. Bailey, *J. Mater. Sci.*, 1978, **13,** 195-201.
270. J. Summerscales, D. Short, *Composites.*, 1978, **3,** 157-166.
271. L. N. Phillips, *Composites.*, 1969, **1,** 50-51.
272. C. Soutis, *Prog. Aerosp. Sci.*, 2005, **5,** 143-151.
273. C. H. Yeh, US4931247 A, 1990.
274. A. K. Bledzki, J. Gassan, *Prog. Polym. Sci.*, 1999, **2,** 221-274.
275. M. A. Sawpan, K. L. Pickering, A. Fernyhough, *J. Compos. Mater.*, 2013, **47,** 1513-1525.
276. L. Yan, N. Chouw, K. Jayaraman, *Compos. Part B-Eng.*, 2013, **56,** 296-317.
277. M. A. Mosiewicki, M. I. Aranguren, *Eur. Polym. J.*, 2013, **49,** 1243-1256.
278. R. Rustum, R. A. Ronnen, *Mater. Lett.*, 1986, **4,** 323-328.
279. Y. S. Lu, R. C. Larock, *Biomacromol.*, 2006, **7,** 2692-2700.
280. A. Greiner, H. Wendorff, A. L. Yarin, E. Zussman, *Appl. Microbiol. Biot.*, 2006, **71,** 387-393.
281. S. A. F. Bon, T. Chen, *Langmuir.*, 2007, **23,** 9527-9530.
282. W. Stober, A. Fink, E. Bohn, *J. Colloid Interface Sci.*, 1968, **26,** 62-69.
283. T. Tsujimoto, H. Uyama, S. Kobayashi, H. Oikawa, M. Yamahiro. *Metals.*, 2015, **5,** 1136-1147.
284. D. S. Kim, J. K. Lee, E. J. Choi, *Polym-Korea.*, 1999, **23,** 569-579.
285 M. A. Corcuera, I. Mondragon. C. C. Riccard, *J. Appl. Polym. Sci.*, 1997, **64,** 157-166.
286. N. Boquillon, C. Fringant, *Polymer.*, 2000, **41,** 8603-8613.
287. H. Zou, J. Shen, *Chem. Rev.*, 2008, **108,** 3893-3857.
288. Q. Chen, I. Chasiotis, C. Chen, A. Roy, *Compos. Sci. Technol.*, 2008, **68,** 3137-3144.

289. P. Rosso, L. Yee, K. Freidrich, S. Sprenger, *J. Appl. Polym. Sci.,* 2006, **100,** 1849-1855.
290. G. Zhan, X. Tang, Y. Yu, S. Li, *Polym. Eng. Sci.,* 2010, **51,** 426-433.
291. K. M. S. Meera, R. M. Sankar, J. Paul, S. N. Jaisankar, A. B. Mandal, *Phys. Chem. Chem. Phys.* 2014, **16,** 9276-9288.
292. T. Tsujimoto, H. Ugama, S. Kobayashi, *Polym, Degrad. Stabil.,* 2010, **95,** 1399-1405.
293. R. Williams, A. M. Goodman, *App. Phys. Lett.,* 1974, **25,** 531-532.
294. P. Dittanet, R. A. Pearson, *Polymer.,* 2012, **53,** 1890-1905.
295. R. D. Sudduth, *J. Compos. Mater.,* 2006, **40,** 301-331.
296. A. C. Moloney, H. H. Kausch, H. R. Steiger, *J. Mater. Sci.,* 1984, **19,** 1125-1130.
297. R. Demichels, P. Raiteri, J. D. Gale, *J. Crsyt. Growth.,* 2014, **401,** 33-37.
298. A. Afzal, H. M. Kausch, H. R. Stieger, *Mater. Express.,* 2011, **1,** 299-306.
299. K. S. Novoselov, A. K. Geim, *Science.,* 2004, **306,** 666-669.
300. C. Lee, X. Wei, J. W. Kysar, J. Hone, *Science.,* 2008, **321,** 385-388.
301. S. F. Braga, V. R. Coluci, S. Legoas, *Nano. Lett.* 2004, **4,** 881-884.
302. F. V. Kusmartsev, W. M. Wu, M. P. Pierpoint, K. C. Yung, *Prog. Optical. Sci. Photonics.,* 2014, **2,** 191-221.
303. X. Zhao, Q. Zhang, D. Chen, *Macromol.,* 2010, **43,** 2357-2363.
304. T. Ramanathan, A. Abdala, L. C. Brinson, *Nat. Nanotechnol.* 2008, **3,** 327-331.
305. L. C. Tang, Y. J. Wan, D. Yan, *Carbon.,* 2013, **60,** 16-27.
306. B. Kollbe, J. Sung, V. Berry, X. S. Sun, *Adv. Mater.,* 2012, **24,** 2123-2129.
307. L. Tau, X. Li, S. P. Lau, *J. Mater. Chem.,* 2012, **22,** 5676-5783.
308. J. A. King, D. R. Klimek, I. Miskioglu, G. M. Odegard, *J. Appl. Polym. Sci.,* 2013, **128,** 4217-4223.
309. J. Zhang, C. Zhang, S. A. Madbouly, *J. Appl. Polym. Sci.,* 2015, **132,** 41751-41758.
310. T. Amornsakchai, B. Sinpatanapan, *Polymer.,* 1999, **40,** 2993-2999.
311. S. Banerjee, G. Maier, *Chem. Mater.,* 1999, **11,** 2179-2184.
312. W. Y. Su, K. S. Min. R. P. Quick, *Polymer.,* 2001, **42,** 5121-5134.
313. Y. Soeda, T. Okamoto, K. Toshima, S. Matsumura, *Macromol. Biosci.,* 2002, **2,** 429-436.
314. E. H. Nejad, A. Pasoniasari, C. E. Koning, R. Duchateau, *Polym. Chem.,* 2012, **3,** 1308-1313.
315. D. Liu, X. Zhang, L. Zhu, J. Wu, X. Lu, *Catal. Sci. Technol.,* 2015, **5,** 562-571.
316. P. Pfäffi, A. Zitting, H. Vainio, *Scand. J. Work. Environ. Health.* 1978, **4,** 22-27.
317. C. Acebo, X. F. Francos, S. de la Flor, X. Ramis, A. Serra, *Prog. Org. Coat.,* 2015, **85,** 52-59.